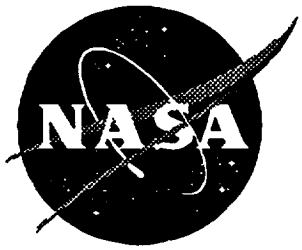
NASA Conference Publication 10190



Computational Materials Research

Edited by
Jeffrey A. Hinkley and Thomas S. Gates
Langley Research Center • Hampton, Virginia

Proceedings of a workshop sponsored by the
National Aeronautics and Space Administration,
Washington, D.C., and held at
The College of William and Mary,
Williamsburg, Virginia
January 4–5, 1996

November 1996

Printed copies available from the following:

NASA Center for AeroSpace Information
800 Elkridge Landing Road
Linthicum Heights, MD 21090-2934
(301) 621-0390

National Technical Information Service (NTIS)
5285 Port Royal Road
Springfield, VA 22161-2171
(703) 487-4650

Table of Contents

Title	Page
Foreword	2
Molecular Modeling of Polyimides	3
Molecular Mechanics and Molecular Dynamics	27
Effect of Molecular Weight on Properties of LaRC™ - SI	50
Molecular Modeling of Novel Piezoelectric Polyimides	77
Monte Carlo Simulation of a Polyimide Melt	98
Equation of State Measurements: Thermal Pressure Coefficient of an Imide-Ketone Model Compound	118
Mechanical Properties from Acoustical Measurements on LaRC™ - SI	124
Predicting Bulk Polymer Properties from Molecular Structure	155
Multiaxial and Time Dependent Response of Rigid Polymers	206
Static and Viscoelastic Testing/ Modeling of LaRC™ - SI	238

Foreword

NASA-Langley's Computational Materials program began in October 1994. The interdisciplinary team representing NASA Centers, universities, and industry met formally for the first time in January 1995 at LaRC.

One year later, with some changes in personnel, the group assembled again, this time at The College of William and Mary, to review the technical progress that had been made and to identify future directions. The present document is a collection of the technical charts presented at that two-day workshop.

The concept of Computational Materials requires model development at size scales ranging from atomic dimensions to the macroscopic, and times ranging from picoseconds to weeks. The LaRC program therefore adopts a hierarchical approach, with careful attention paid to the links between disciplines. This collection of papers is presented in order of increasing scale, as follows:

Workshop Participant	Discipline	Scale
G. D. Smith, U. Missouri-Columbia	Quantum/molecular mechanics	Subatomic to molecular
B. L. Farmer U. Virginia	Molecular mechanics	Molecular
E. J. Siochi Lockheed	Physical chemistry	Molecular
J. A. Young U. Virginia	Molecular dynamics	Molecular assemblies
E. J. Dawnkaski College of William & Mary	Monte Carlo simulation	Molecular assemblies
R. A. Orwoll College of William & Mary	Chemical Thermodynamics	Liquids
T. Yost, J. Cantrell NASA LaRC	Physics	Solids
W. W. Welsh	Chemistry; statistics	Molecular to continuum
W. G. Knauss California Inst. of Tech.	Constitutive models	Continuum
T. S. Gates NASA LaRC	Viscoplasticity	Micromechanics to macroscopic

Molecular Modeling of Polyimides

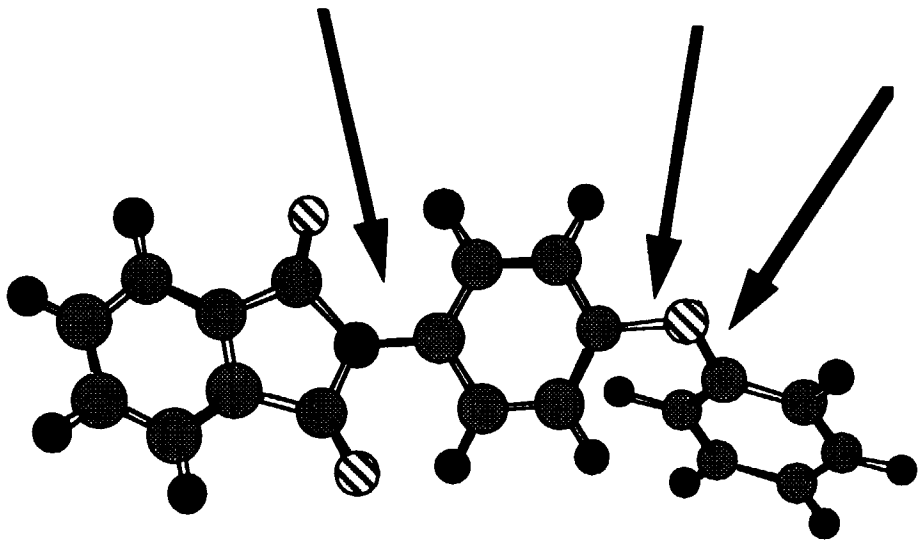
Grant D. Smith

Department of Chemical Engineering
University of Missouri-Columbia

Outline

- Ab initio quantum chemistry studies of a model imide
- Force field for a model imide
- Molecular dynamics simulations of a model imide
- Future work and directions

Structure of the model ether-imide



Bonded parameters

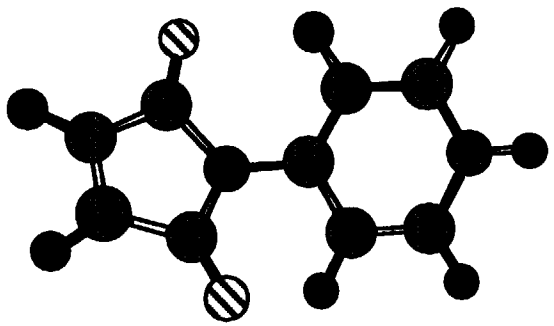
- From 6-31G** SCF optimized geometry

Bond Stretch	Constrained	(Å)
C_i=O (carbonyl)[a]		1.19
C-O (ether)		1.38
C-H		1.07
C=C		1.38
C_i-N		1.43
C- C_i		1.49

Bonded parameters, cont.

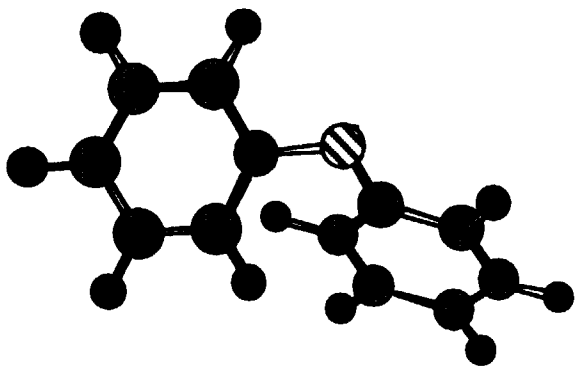
Valence Bend	$E_{ijk} = 0.5\ k_{ijk}(\theta_{ijl} - \theta^\circ_{ijl})^2$	k_{ijk} (kcal/mol rad^2)	θ°_{ijl}
C-C_i-N		144.	1.817
C-C-C_i^b		100.8	1.882
C-C-C_i^c		100.8	2.286
C_i-N-C_i		115.2	1.988
C-C_i-O		144.	2.253
C-C-C		144.	2.094
C-C-H		72.	2.094
C_i-N-C		115.2	2.148
C-O-C		148.6	2.072
C-C-O		100.8	2.094
N-C_i-O		100.8	2.1991
N-C-C		115.2	2.094

Torsional characteristics



6-31G+**

minimum = 52.4 °
perp = 0.38 kcal/mol (9.8)
planar = 3.03 kcal/mol (4.7)



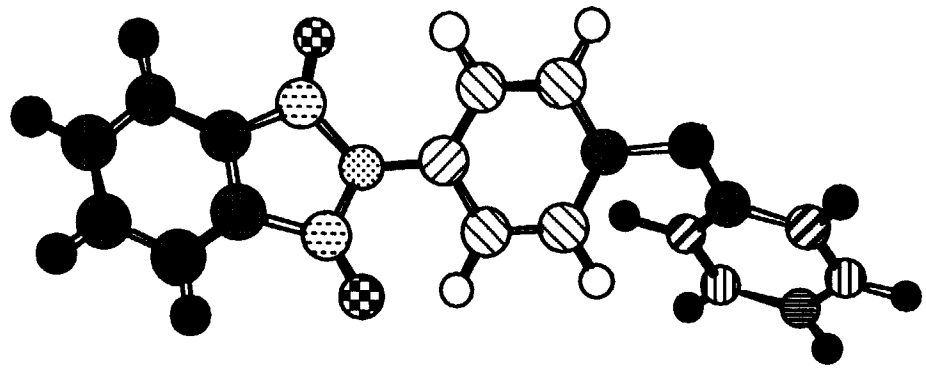
6-31G*

single = 2.5 kcal/mol (3.7)
double =0.0 kcal/mol (1.2)

Partial atomic charges

- Charges were determined from electrostatic potential method--This method involves calculating the electrostatic potential for a grid of points around the moleculed and best reproducing this with a distribution of partial atomic charges

Partial atomic charges, cont.



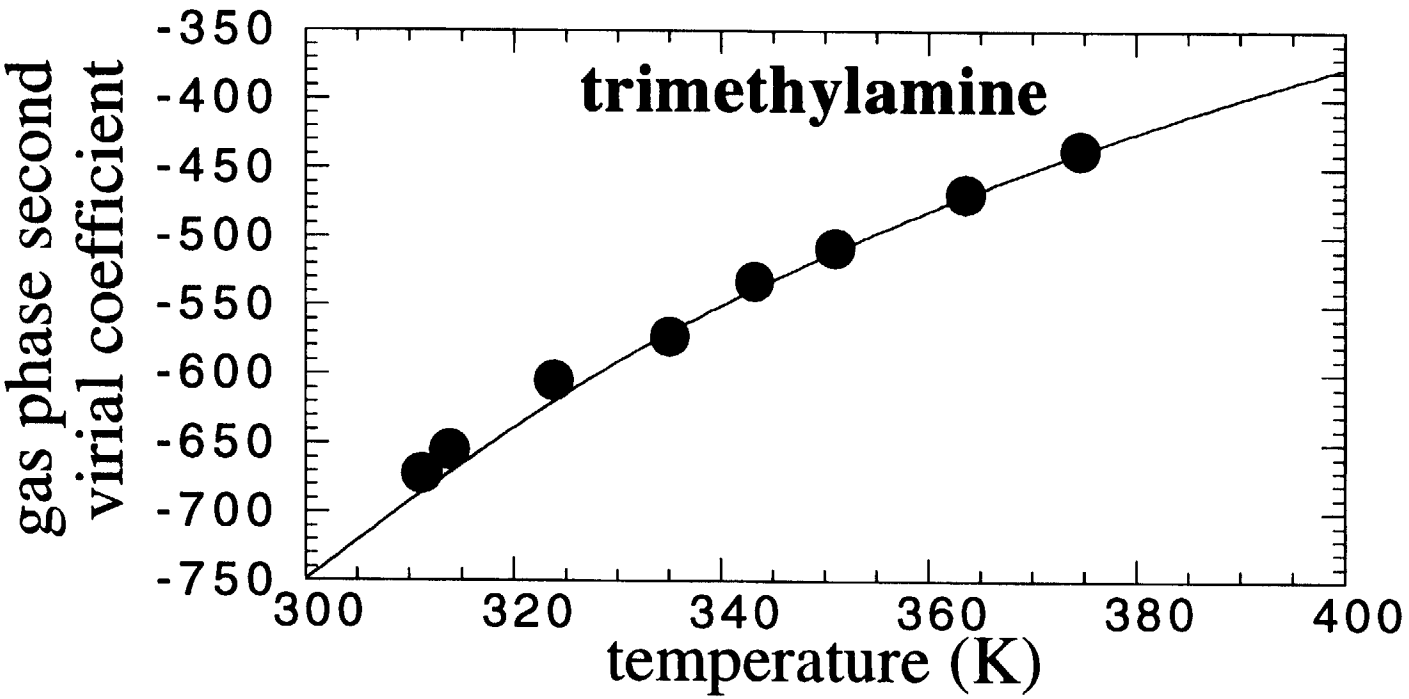
- nitrogen q = -0.4959
- hydrogen q = +0.1566
- hydrogen q = +0.1223
- carbon q = -0.1922
- carbon q = -0.0418
- carbon q = -0.2848
- carbon q = +0.5290
- carbon q = +0.4892
- carbon q = -0.2201
- carbon q = +0.2839
- carbon q = +0.6817
- carbon q = -0.0856
- ether oxygen q = -0.5553
- carbonyl oxygen q = -0.5510

Nonbonded parameters

- Dispersion/repulsion parameters were mostly taken from our previous work
- Extensive quantum chemistry and MD studies of benzene revealed the importance of including hydrogen atoms
- Oxygen parameters were taken from our work with model ethers

Nonbonded parameters, cont.

- Nitrogen Parameters were adjusted to match second virial coefficient data



Nonbonded parameters

Nonbonded Dispersion/Repulsion	$E_{ij} = A_{ij}\exp(-B_{ij}r_{ij}) - C_{ij}/r^6_{ij}$	A_{ij} (kcal/mol)	B_{ij} (Å)	C_{ij} kcal/mol Å^6
C-C		78988.	3.6	519.3
O-O		75845.	4.063	398.9
O-C		77400.5	3.8315	455.1
O-H		13448.4	3.902	99.1
O-N		67926.0	3.922	446.6
C-H		3888.0	3.415	124.416
C-N		69323.6	3.69	509.6
H-H		2384.6	3.74	24.624
H-N		28122.	4.252	127.7
N-N		60833.9	3.780	500.0

Out-of-plane deformation

- Parameters were taken from the empirical force field of Boyd

Out-of-plane deformation	$E_{ijkl} = 0.5k_{ijkl}\delta^2$	k_{ijkl} (kcal/mol rad^2)
C-C*H-C		41.76
C-C*C_i-C		115.2
C-C_i*O-N		115.2
C_i-N*C-C_i		43.2
C-C*N-C		115.2
C-C*O-C		115.2

Molecular dynamics simulations

- 100 ether-imide molecules
- Ewald summation
- 5 fs time step (hydrogen atom positions constrained)
- Box = 36 Å

Density

- Experimental density measurements have been performed from 436 to 473 K.
- At 473 K, a constant volume simulation at experimental density yields a pressure of -700 atmospheres.
- At 473 K, a constant pressure simulation at 1 atmosphere yields a density about 4% greater than experiment.

Thermal expansion

- At 1 atmosphere, thermal expansion over the experimental temperature range is 7.7 X 10^{-4} /K
- The experimental value is 6.8 X 10^{-4}/K

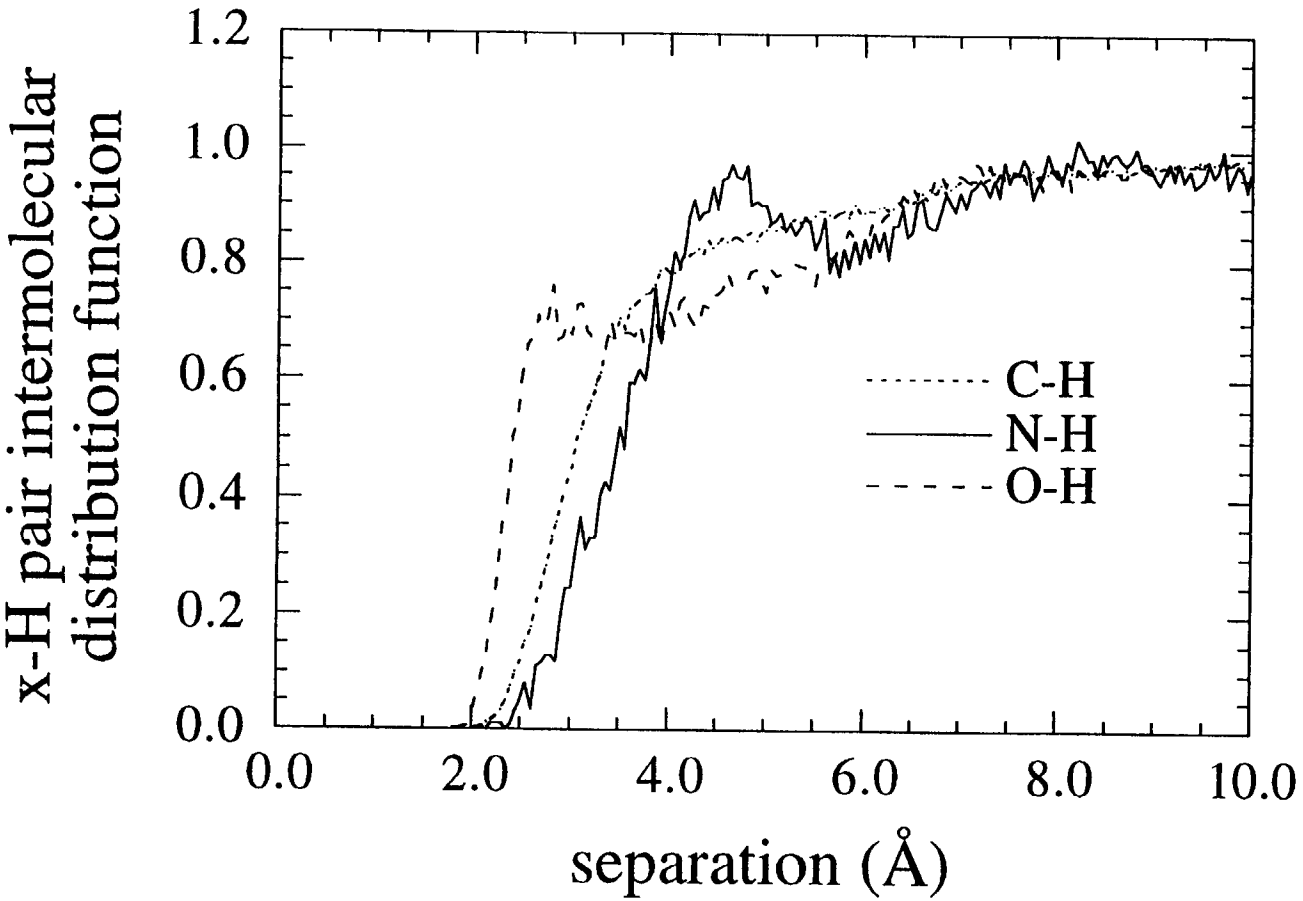
Sensitivity of density to force field parameters

- The density is insensitive to intramolecular parameters
- The density does is not very sensitive to electrostatic interaction*
- We are investigating the sensitivity of the density to nonbonded parameters

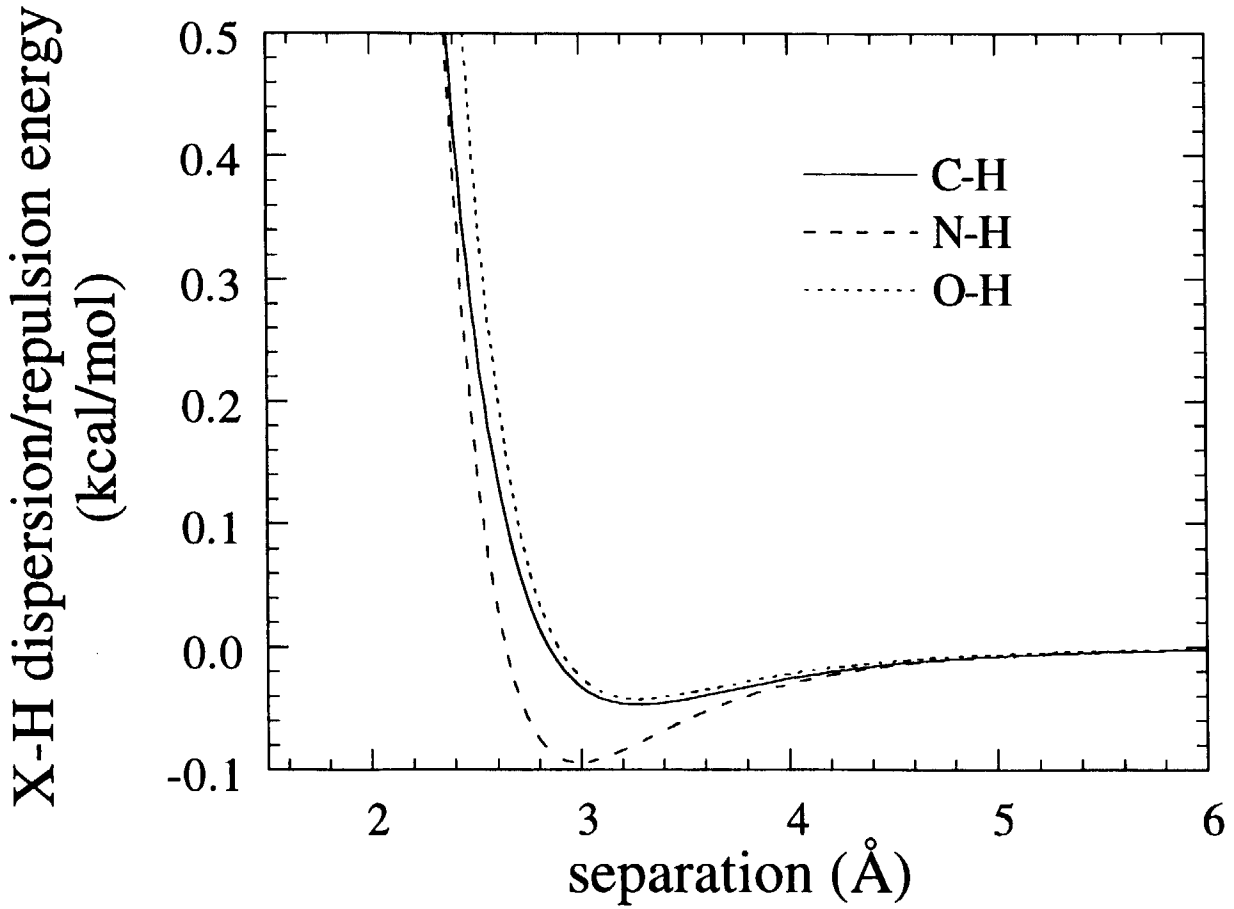
Pair distribution functions

- We have begun looking for important intermolecular interactions by examining pair distribution functions

Pair distribution functions, cont.



Pair distribution functions, cont.



Ongoing work

- PVT measurements of internal energy
- Force field parameterization for ketone-imide
- Fine-tuning of force fields
- MD simulation of model imide liquids

Key issues and future work

- Determine the most interesting chemical modifications to investigate
- Learn how to best interact with people further up the food chain-- including experimentalists and continuum models
- Apply techniques to interface, additives, etc.

Acknowledgments

- Dr. Richard Jaffe, NASA Ames Research Center
- Mr. Steven Shi

Table I

Quantum Chemistry Based Force Field for Ether-Imide

Type	Energy Function	Parameters	
Bond Stretch	Constrained	(Å)	
C_i=O (carbonyl)[a]		1.19	
C-O (ether)		1.38	
C-H		1.07	
C=C		1.38	
C_i-N		1.43	
C- C_i		1.49	
Valence Bend	$E_{ijk} = 0.5\ k_{ijk}(\theta_{ijl} - \theta^\circ_{ijl})^2$	k_{ijk} (kcal/mol rad^2)	θ°_{ijl}
C-C_i-N		144.	1.817
C-C-C_i[b]		100.8	1.882
C-C-C_i[c]		100.8	2.286
C_i-N-C_i		115.2	1.988
C-C_i-O		144.	2.253
C-C-C		144.	2.094
C-C-H		72.	2.094
C_i-N-C		115.2	2.148
C-O-C		148.6	2.072
C-C-O		100.8	2.094
N-C_i-O		100.8	2.1991
N-C-C		115.2	2.094

Torsion	$E_{ijkl} = 0.5[k^2_{ijkl} (1-\cos(2\phi_{ijkl})) + k^4_{ijkl} (1-\cos(4\phi_{ijkl}))]$	k^2_{ijkl} (kcal/mol)	k^4_{ijkl}
C-C-C-C		25.92	0.00
C-C-C-H		0.00	0.00
H-C-C-H		0.00	0.00
C_i-C-C-C		0.00	0.00
C_i-C-C-H		0.00	0.00
C_i-C-C-C_i		0.00	0.00
O-C_i-C-C		0.00	0.00
N-C_i-C-C		0.72	0.00
C-N-C_i-C		0.00	0.00
C-N-C_i-O		14.40	0.00
C-C-O-C		0.86	0.00
C-C-C-O		0.00	0.00
H-C-C-O		0.00	0.00
C-C_i-C-O		0.00	0.00
C_i-N-C_i-O		7.06	0.00
C-C-N-C_i		1.20	0.26
N-C-C-C		0.00	0.00
N-C-C-H		0.00	0.00

William & Mary Computational Materials Workshop

January, 1996

Barry L. Farmer

Retrospective Summary

(including both material presented and insight gained from resulting discussions)

The UVA (on-grounds) effort has focused on exploring the validity of the Tripos force field for computing the interactions between a graphite surface and a polyimide chain. Validation has proceeded along two paths.

The first validation path has involved comparison of calculations using the Tripos force field with the results of semiempirical molecular orbital and *ab initio* calculations for pairs of molecules, e.g. methane, formaldehyde, and trimethyl amine with benzene. The comparisons have not been good. However, rather than point to a deficiency in the empirical (Tripos) force field, the results underscore the inability of the molecular orbital and *ab initio* methods to properly represent dispersion interactions except when very extensive basis sets are employed. Thus the validation of the Tripos force field lies more correctly in the comparisons with experimental data than with the results with the more fundamental computational methods.

The second validation pathway involves calculations of the association between various small molecules (corresponding to representative fragments of polyimides) and a section of a graphitic surface (specifically, a coronene molecule) were made. These were compared with previous computational results based on more elegant treatments of the interaction potential developed to reproduce experimental data. Both the interaction energy *versus* distance curve and the geometry of the minimum energy association calculated using the Tripos force field for benzene on graphite were in good agreement with the previous model and data. In addition,

comparisons of the experimental heats of adsorption of other molecular fragments with graphitic substrates were generally in good agreement with the calculated interaction energies.

Another aspect of the semiempirical molecular orbital and *ab initio* calculations results however is both useful and interesting. Graphite, as a material, is electrically conductive. The effects of this conductivity on graphite's interactions with adsorbing material has apparently not been studied previously in the context of modern computational methods. (This neglect may arise in fact from the inability of molecular orbital calculations to provide a reasonable treatment of dispersion forces). A dipole in the vicinity of a conducting (metal) surface interacts electrostatically with an image dipole as well as through dispersion effects with the substrate atoms. The image interaction is about an order of magnitude smaller than the dispersive ones. This indicates that, overall, "summation of dispersion and repulsive energies" may indeed be a good approximation for computing the interaction energies of adsorbate molecules with graphite. At the same time, ignoring the image interactions may lead to underestimation of the role of the dipolar moieties of the polyimides on the interactions with the graphite substrate. The size of these effects will determine whether we will need to modify the potential function parameters to get a reasonable representation of the behavior of a polyimide on a graphite substrate Since the interaction is electrostatic, the results of semiempirical molecular orbital and *ab initio* calculations should be valid in spite of the inability of these methods to properly account for dispersion interactions.

The calculations to date indicate that the partial charges in the adsorbing molecule and those on the atoms of the "substrate" molecule (benzene, naphthalene, coronene) change to a small extent as the separation distance changes. As expected, the charges on the substrate atoms nearest the adsorbate change individually more than those at greater distances, drawing upon contributions from its own several neighbors. The perturbations in electron distribution extend out from the location of the adsorbate, but they are damped in magnitude.

Figure Captions and Annotations

Note:

Sybyl does molecular mechanics calculations using a classical description of the force field.
Spartan does semiempirical molecular orbital (quantum mechanical) calculations.

1. Title

2. Polyimides of Interest

3. Energy (and partial atomic charge on methane hydrogen) versus separation distance between benzene and methane calculated using Spartan (semiempirical molecular orbital methods).

4. Energy (and partial atomic charge on fluorine) versus separation distance between benzene and perfluoromethane calculated using Spartan (semiempirical molecular orbital methods).

5. Energy (and partial atomic charge on nitrogen) versus separation distance between benzene and thrimethylamine calculated using Spartan (semiempirical molecular orbital methods).

6. Energy (and partial atomic charge on oxygen) versus separation distance between benzene and formaldehyde calculated using Spartan (semiempirical molecular orbital methods).

7. Charges on the formaldehyde carbon and oxygen and three of the benzene carbons as a function of distance between benzene and formaldehyde (calculated using Spartan semiempirical molecular orbital methods).

These date show that the proximity of a polar (carbonyl) group perturbs the distribution of charges in the benzene molecule. What might be the effect of polar groups proximate to delocalized ring systems such as naphthalene, anthracene, coronene, and ultimately, graphite.

8. Charges on the formaldehyde carbon and oxygen and three of the naphthalene carbons in Ring 1 as a function of distance between naphthalene and formaldehyde (calculated using Spartan semiempirical molecular orbital methods). The formaldehyde molecule was centered over Ring 1 of the naphthalene molecule.

9. Charges on the formaldehyde carbon and oxygen and four of the naphthalene carbons in Ring 2 as a function of distance between naphthalene and formaldehyde (calculated using Spartan semiempirical molecular orbital methods). The formaldehyde molecule was centered over Ring 1 of the naphthalene molecule.

10. Charges on the formaldehyde carbon and oxygen and three of the anthracene carbons in Ring 1 as a function of distance between anthracene and formaldehyde (calculated using Spartan semiempirical molecular orbital methods). The formaldehyde molecule was centered over Ring 1 of the anthracene molecule.

11. Charges on the formaldehyde carbon and oxygen and three of the anthracene carbons in Ring 1 as a function of distance between anthracene and formaldehyde (calculated using Spartan semiempirical molecular orbital methods). The formaldehyde molecule was centered over Ring 2 of the anthracene molecule.

12. Charges on the formaldehyde carbon and oxygen and four of the anthracene carbons in Ring 2 as a function of distance between anthracene and formaldehyde (calculated using Spartan semiempirical molecular orbital methods). The formaldehyde molecule was centered over Ring 3 of the anthracene molecule.

These data show that a polar group does induce charge redistribution in rings sharing delocalized electronic structure with the ring closest to the approaching polar functionality. The effect, not surprisingly, dies out with distance. This can be attributed (in part if not totally) to the fact that there is an increasing number of atoms to contribute decreasing amounts of charge (per atom).

How do molecular mechanics (Sybyl) results compare with semiempirical (Spartan) results. Specifically, how do the energy versus distance curves compare?

13. Energy versus separation distance between coronene and methane calculated using Tripos force field and Sybyl for molecular mechanics.

14. Energy versus separation distance between coronene and methane calculated using Spartan semiempirical molecular orbital methods.

15. Energy versus separation distance between coronene and formaldehyde calculated using Tripos force field and Sybyl for molecular mechanics.

16. Energy versus separation distance between coronene and formaldehyde calculated using Spartan semiempirical molecular orbital methods.

The molecular mechanics results and semiempirical molecular orbital results are not in good agreement. Molecular mechanics methods compute van der Waals non-bonded interactions and Coulombic interactions as a matter of course. Semiempirical molecular orbital methods can account mainly for the Coulombic effects. Similarly, even ab initio *methods cannot take into account non-bonded interactions (because they arise from electron correlation effects) unless prohibitively large, delocalized basis sets are used.*

Comparisons with experimental data and other types of calculations in the literature might provide a better measure of the validity of the Tripos force field.

17. Orthogonal views of a benzene molecule proximate to a coronene molecule (representing a section of a graphite sheet).

18. Relative energy as a function of distance between benzene and coronene (in the positions shown in the previous figure).

19. Title and figures from a paper reporting calculations (and comparisons with experimental data) for the absorption of benzene on graphite.

The Sybyl results are in very nice agreement with the results in this paper, both in regard to the minimum energy orientation, the depth of the energy minimum, and the minimum energy separation distance.

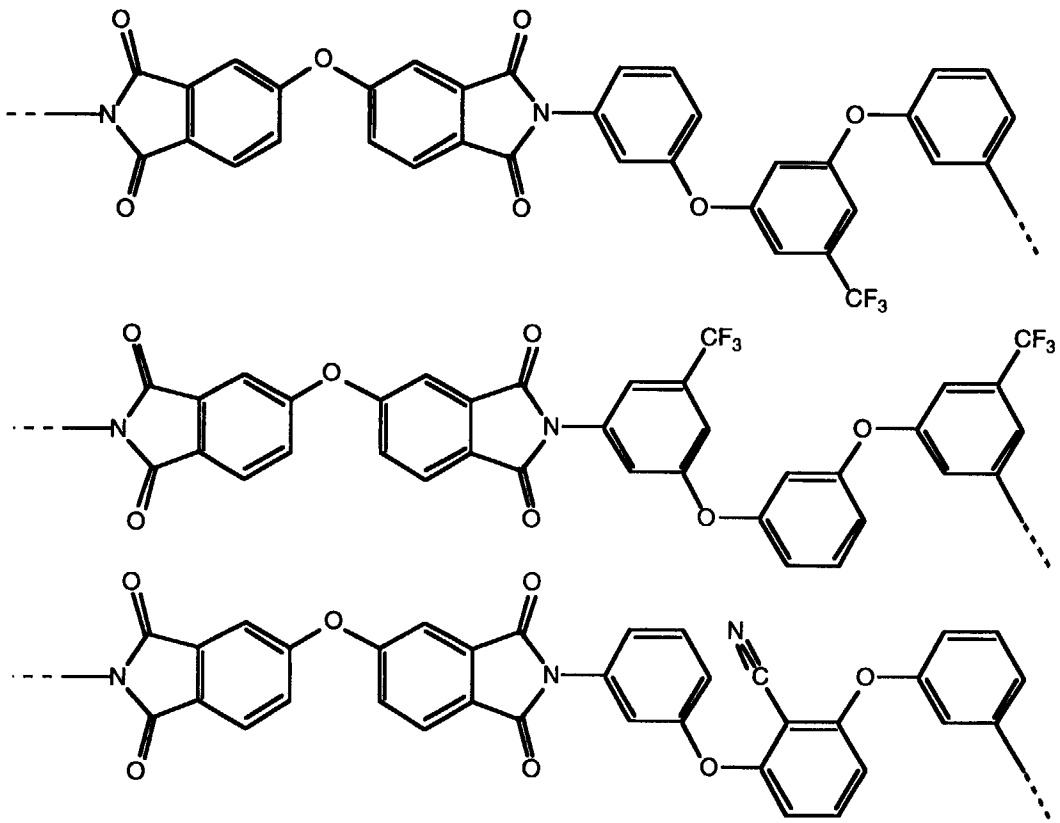
Molecular Mechanics and Molecular Dynamics

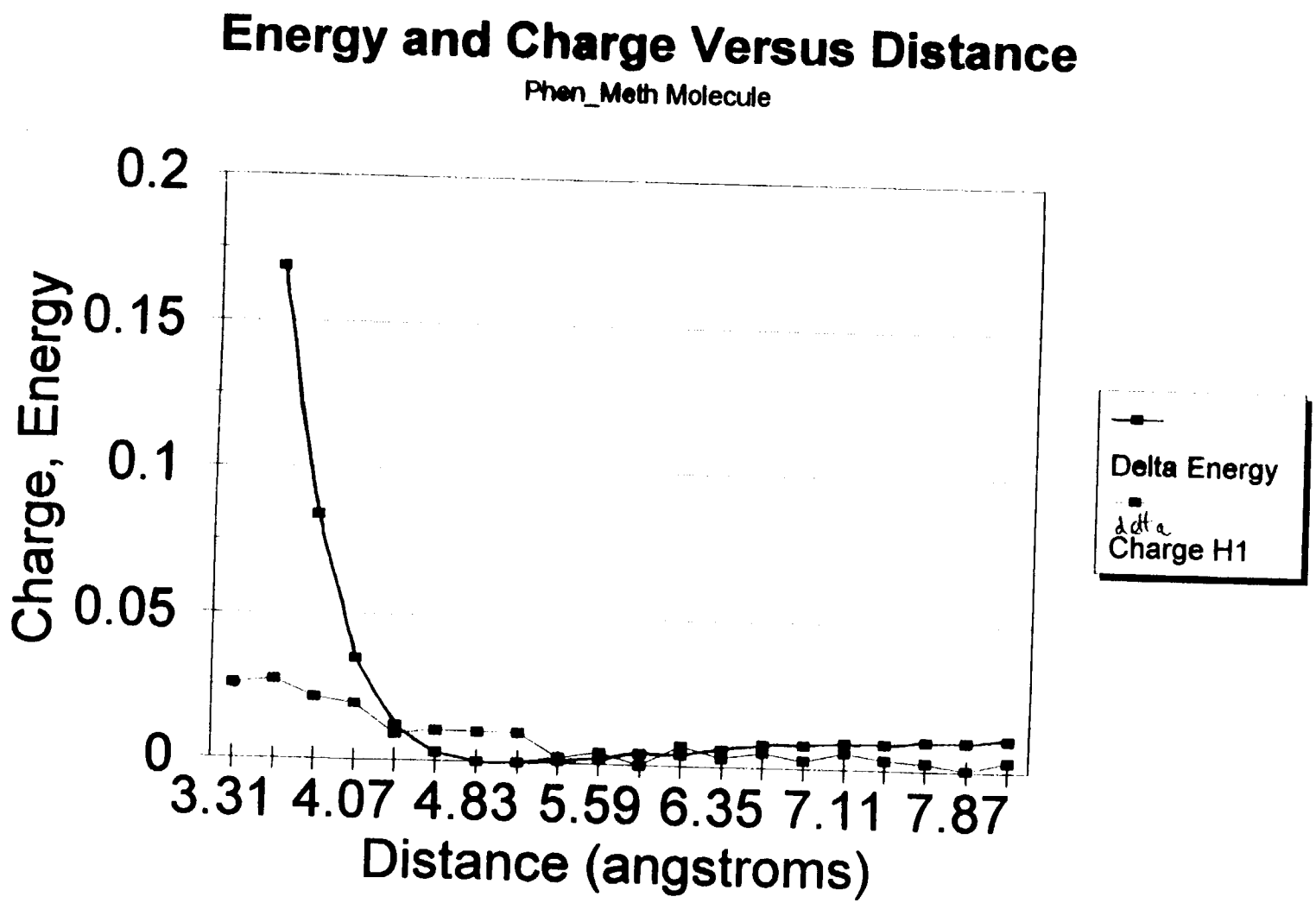
with applications to polyimides as piezoelectric and composite materials

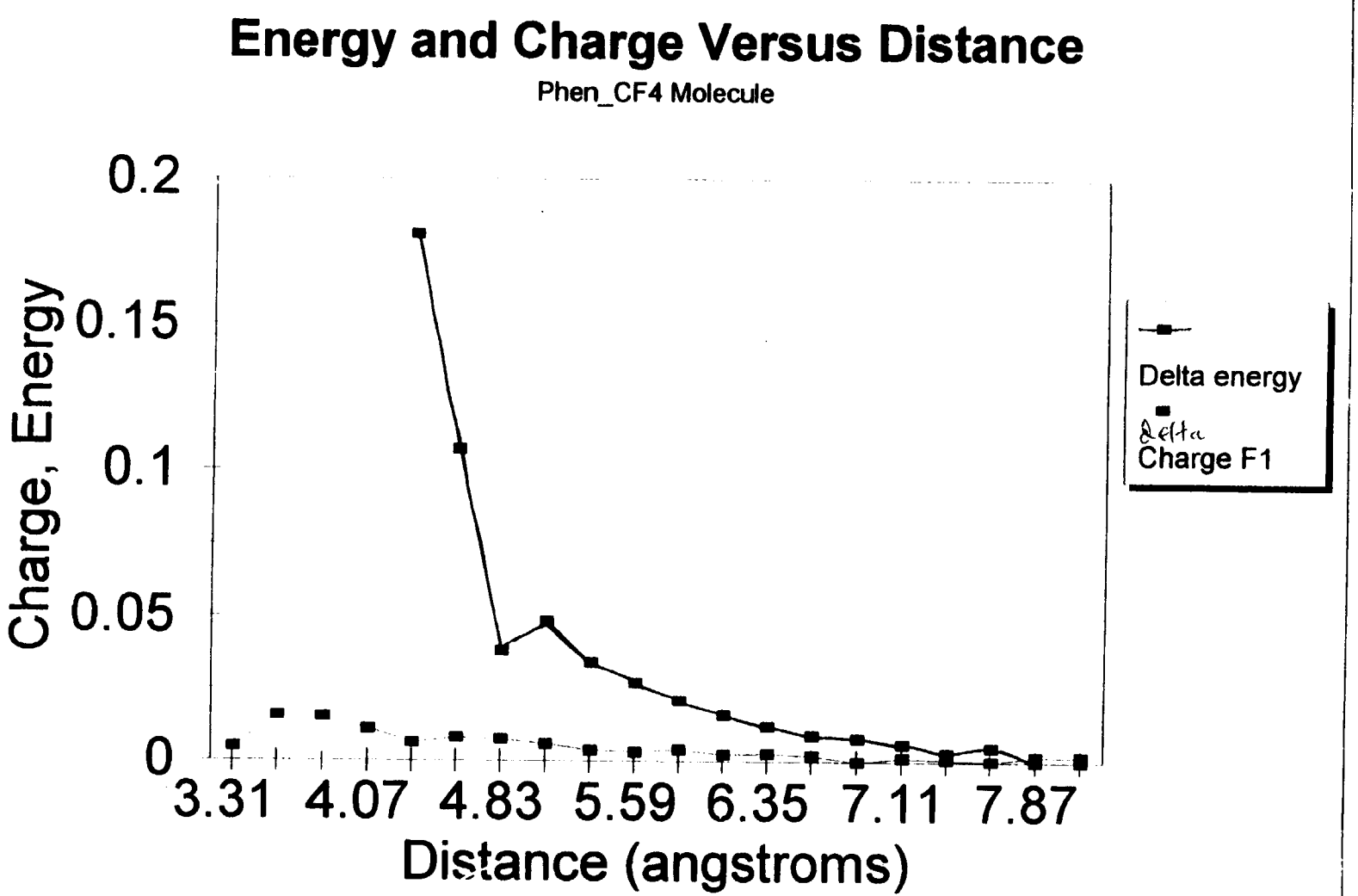
B. L. Farmer

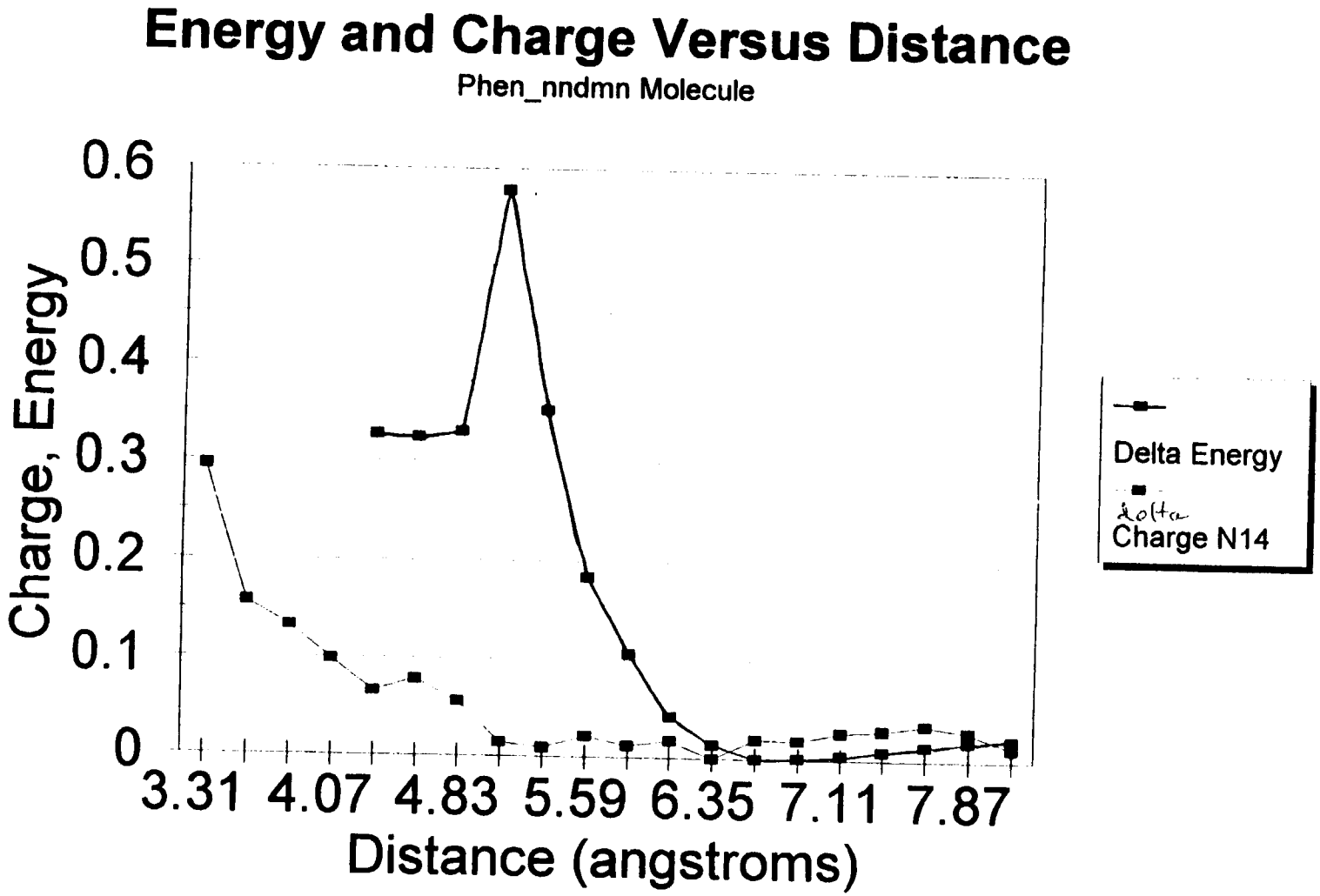
Materials Science and Engineering
University of Virginia

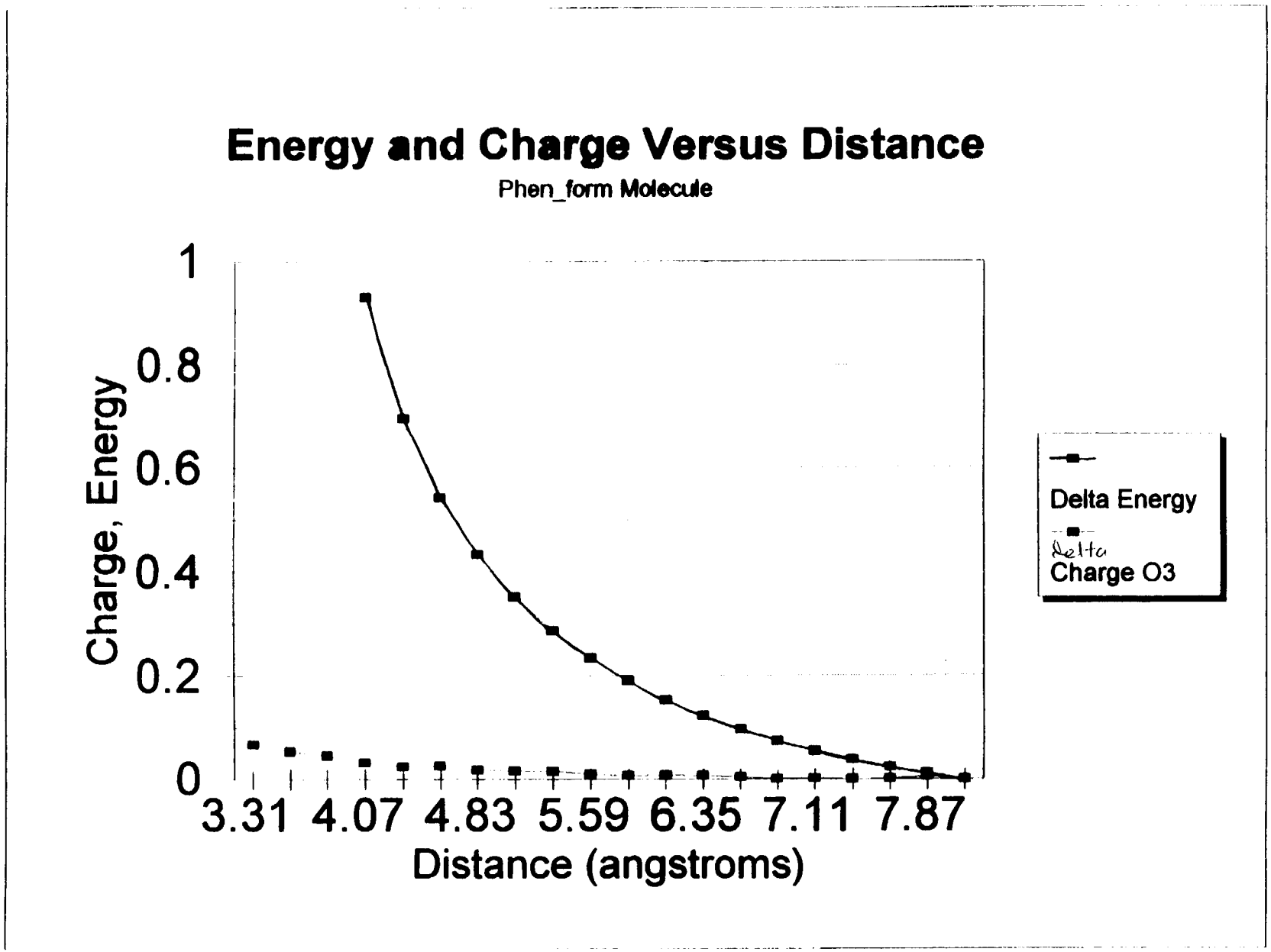
Piezoelectric Polyimides

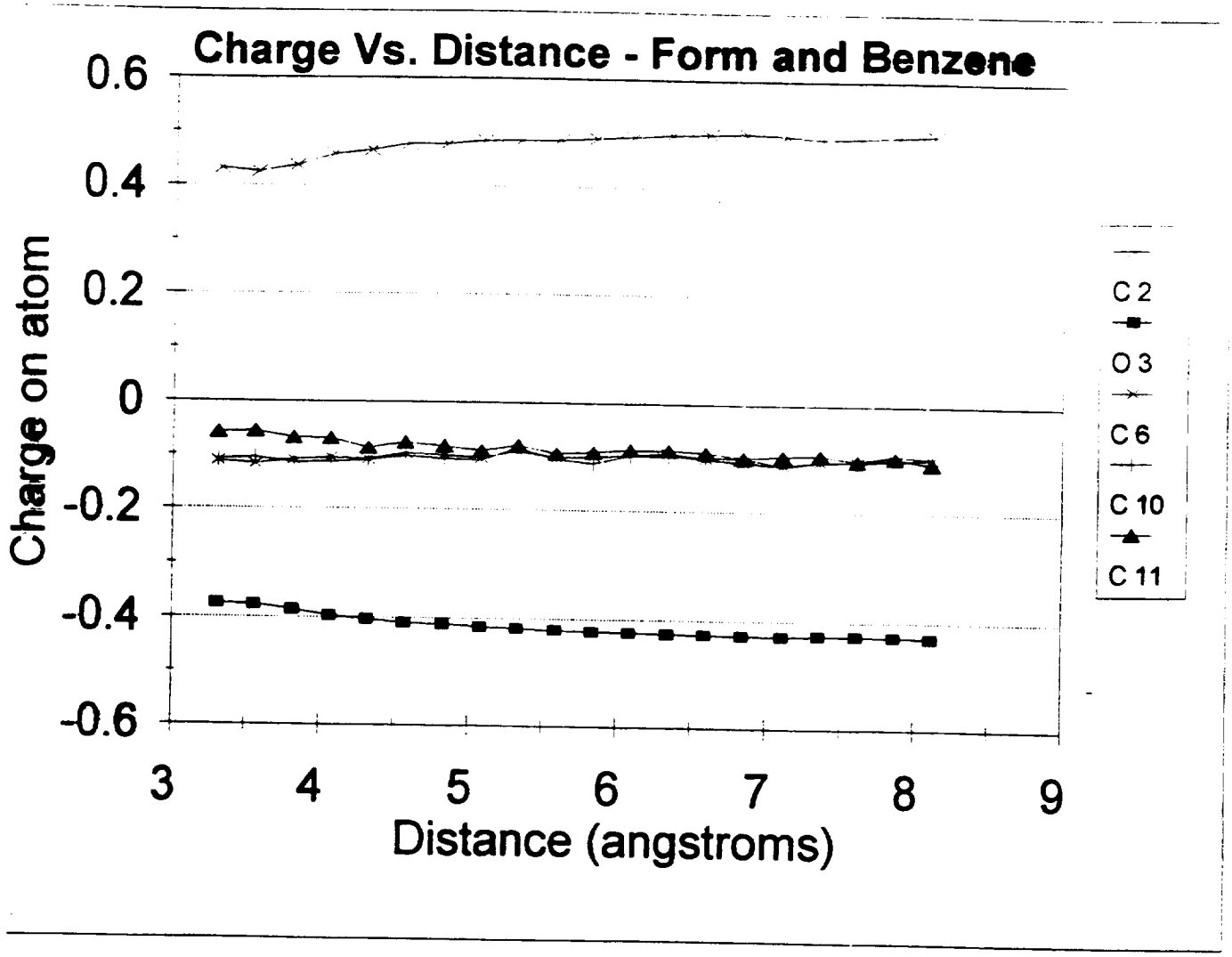


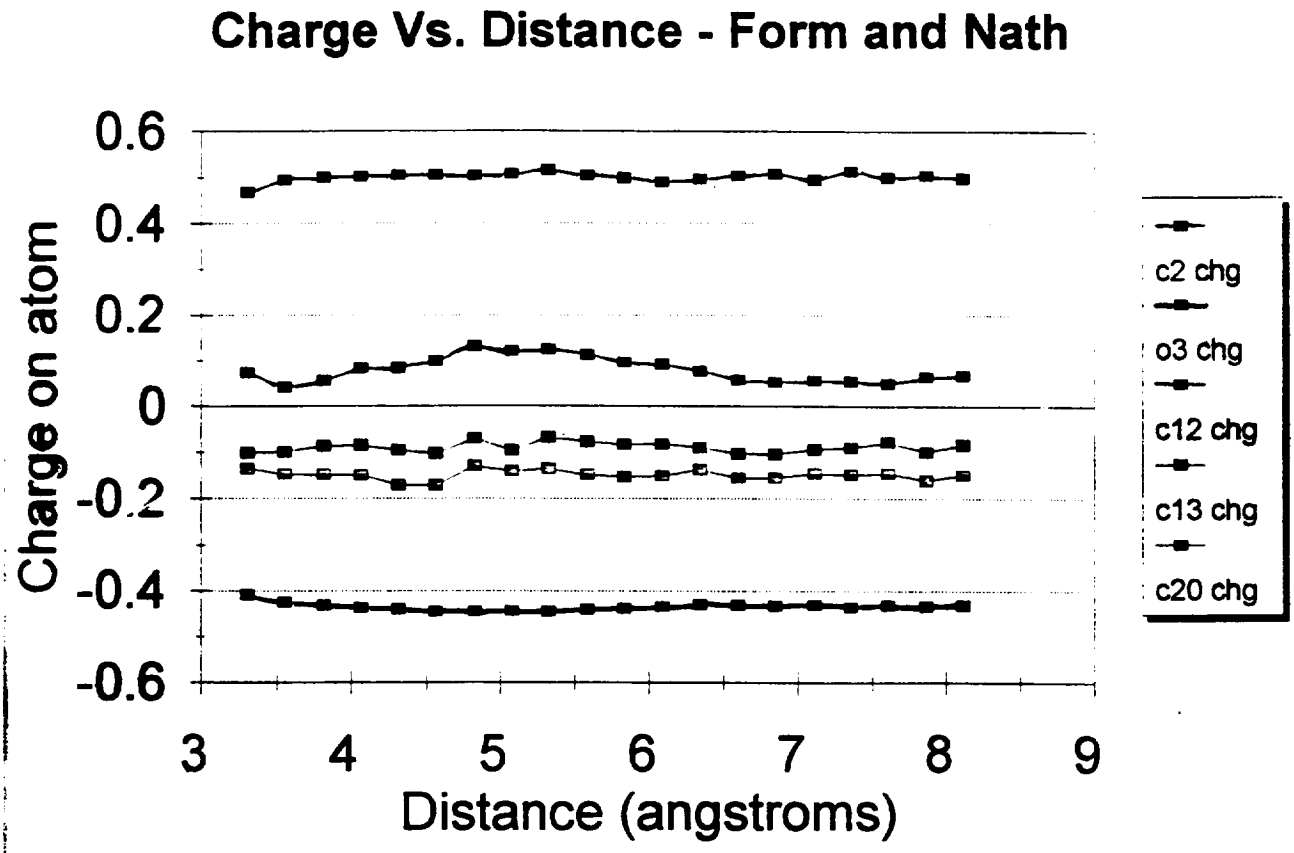

Energy and Charge Versus Distance
Phen_Meth Molecule
Charge, Energy
0.2
0.15
0.1
0.05
0
3.31
4.07
4.83
5.59
6.35
7.11
7.87
Distance (angstroms)
Delta Energy
Charge H1


Energy and Charge Versus Distance
Phen_CF4 Molecule
Charge, Energy
0.2
0.15
0.1
0.05
0
3.31
4.07
4.83
5.59
6.35
7.11
7.87
Distance (angstroms)
Delta energy
Delta Charge F1


Energy and Charge Versus Distance
Phen_nndmn Molecule
Charge, Energy
0.6
0.5
0.4
0.3
0.2
0.1
0
3.31
4.07
4.83
5.59
6.35
7.11
7.87
Distance (angstroms)
Delta Energy
Delta Charge N14

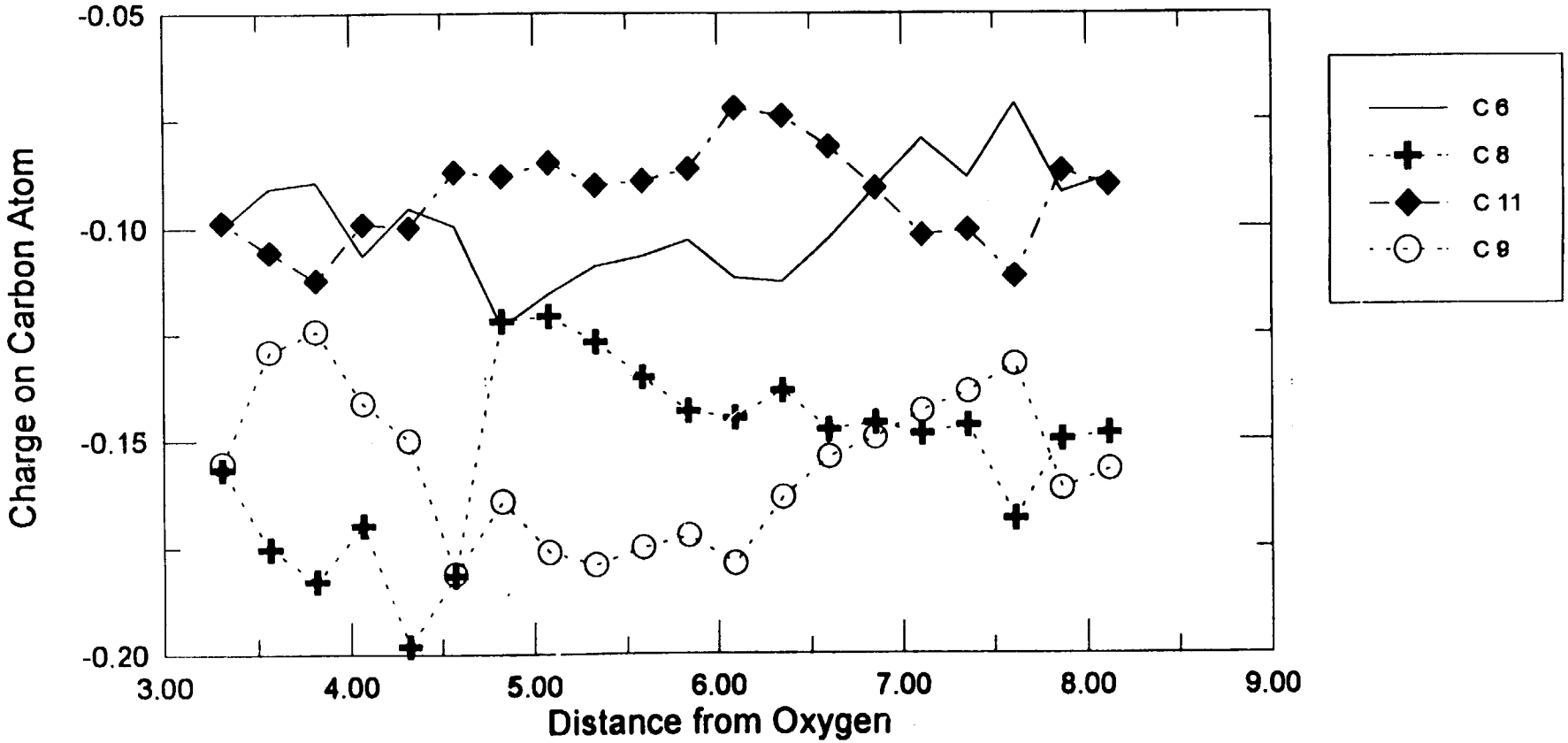

Energy and Charge Versus Distance
Phen_form Molecule
Charge, Energy
1
0.8
0.6
0.4
0.2
0
3.31
4.07
4.83
5.59
6.35
7.11
7.87
Distance (angstroms)
Delta Energy
Delta Charge O3

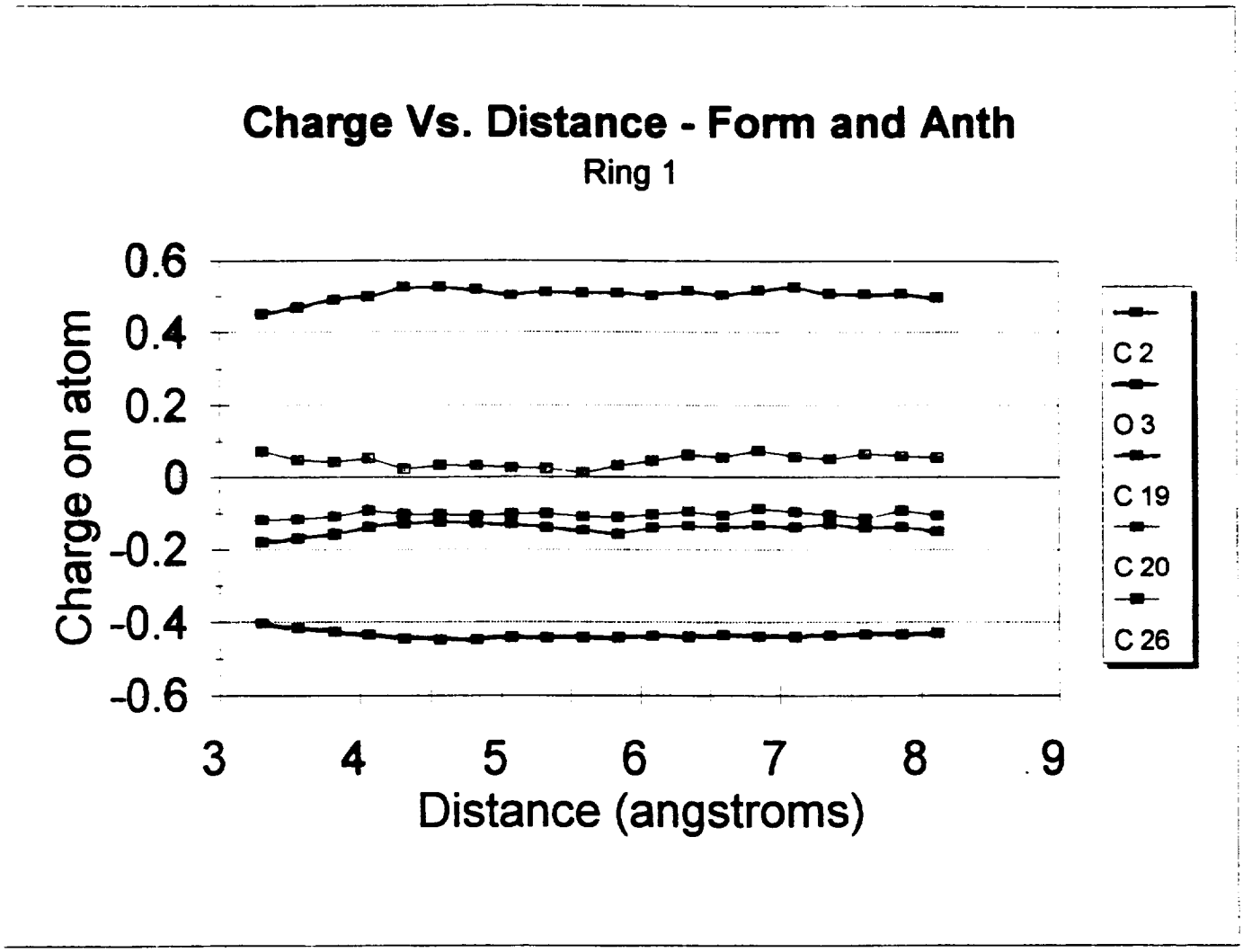

Charge Vs. Distance - Form and Benzene
0.6
0.4
0.2
0
-0.2
-0.4
-0.6
Charge on atom
3
4
5
6
7
8
9
Distance (angstroms)
C 2
O 3
C 6
C 10
C 11

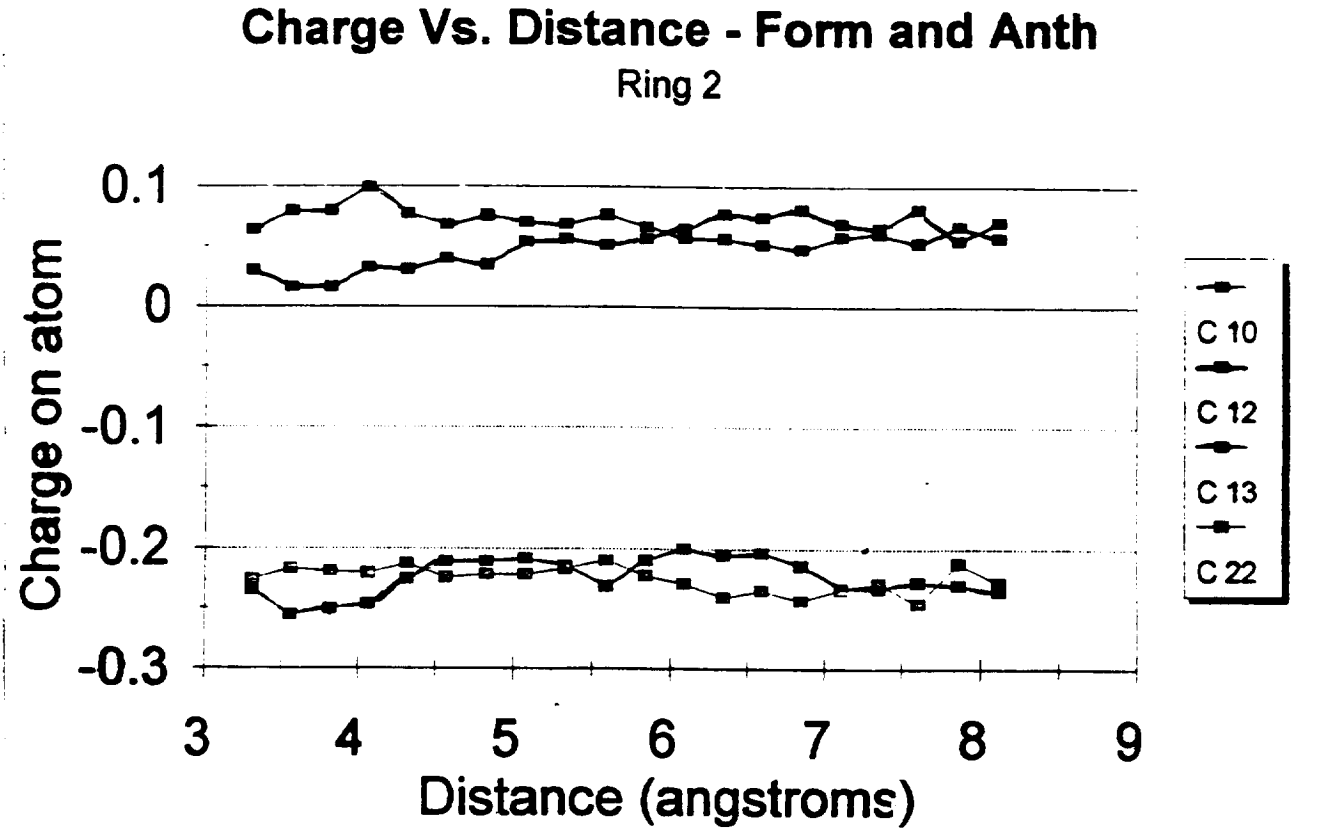

Charge Vs. Distance - Form and Nath
0.6
0.4
0.2
0
-0.2
-0.4
-0.6
Charge on atom
3
4
5
6
7
8
9
Distance (angstroms)
c2 chg
o3 chg
c12 chg
c13 chg
c20 chg

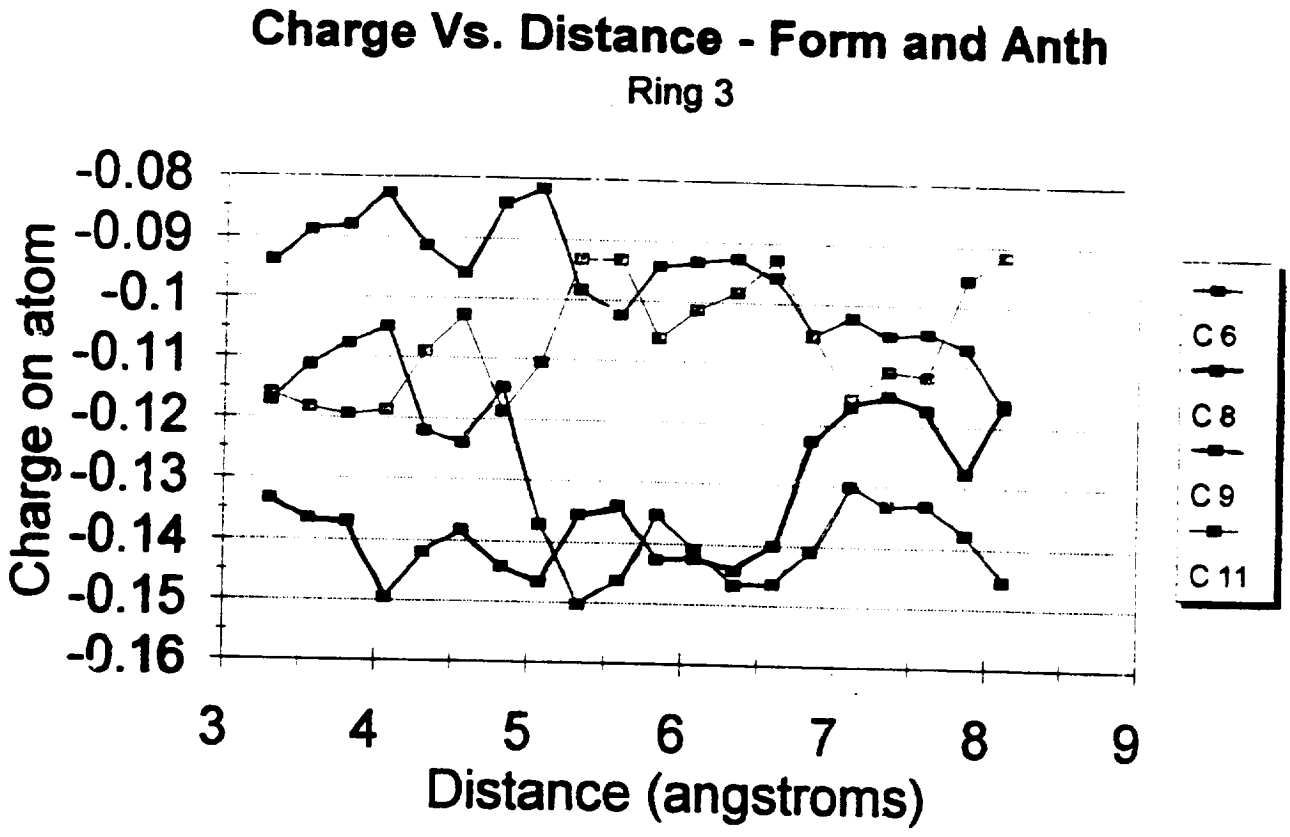
Charge on Carbon Atoms Versus Distance From Oxygen

Formaldehyde and Naphthalene

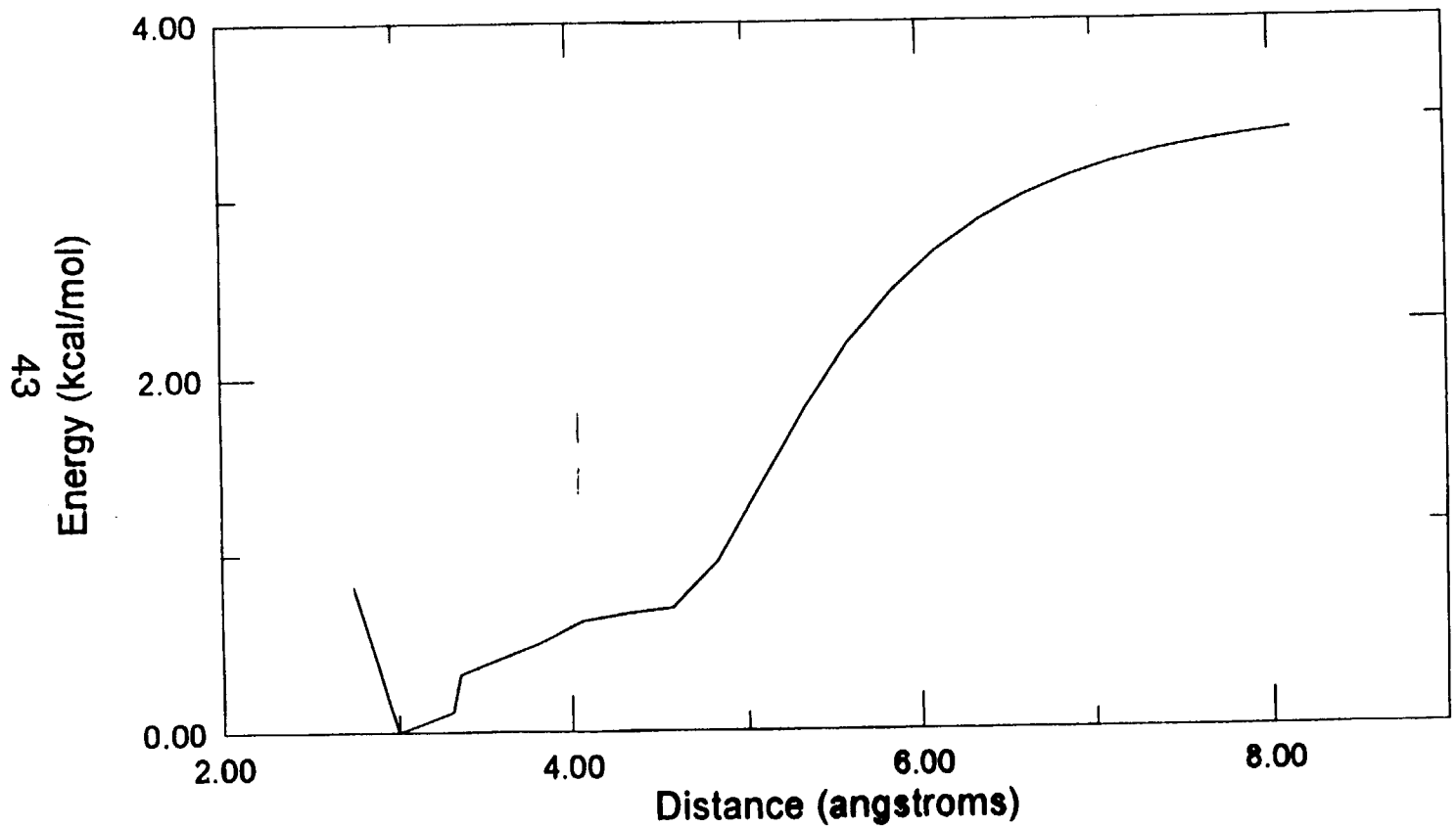



Charge Vs. Distance - Form and Anth
Ring 1
0.6
0.4
0.2
0
-0.2
-0.4
-0.6
Charge on atom
3
4
5
6
7
8
9
Distance (angstroms)
C 2
O 3
C 19
C 20
C 26

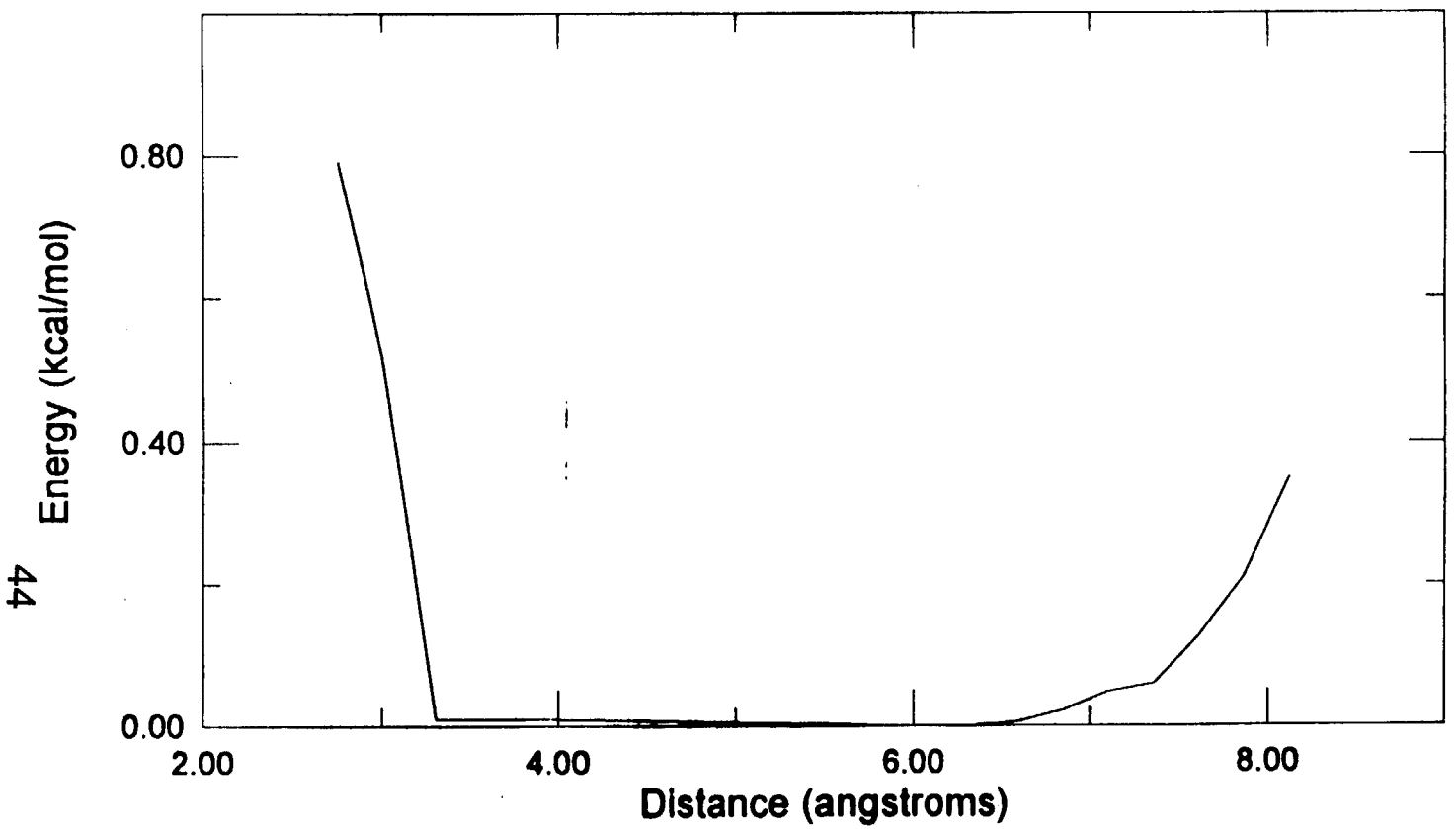

Charge Vs. Distance - Form and Anth
Ring 2
0.1
0
-0.1
-0.2
-0.3
Charge on atom
3
4
5
6
7
8
9
Distance (angstroms)
C 10
C 12
C 13
C 22


Charge Vs. Distance - Form and Anth
Ring 3
Charge on atom
-0.08
-0.09
-0.1
-0.11
-0.12
-0.13
-0.14
-0.15
-0.16
3
4
5
6
7
8
9
Distance (angstroms)
C 6
C 8
C 9
C 11

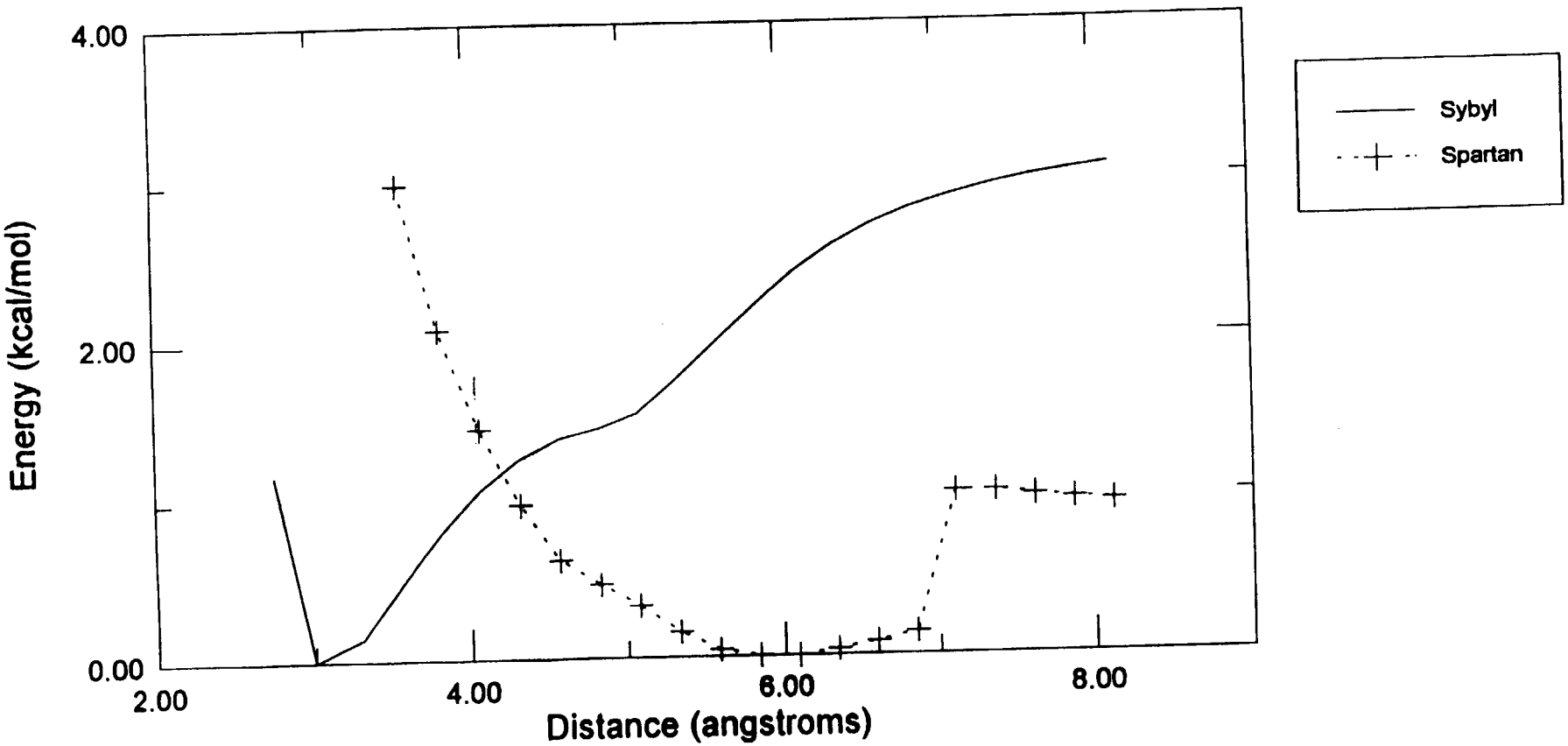
Energy Calculated by Sybyl Versus Distance
Methane and Coronene Molecule



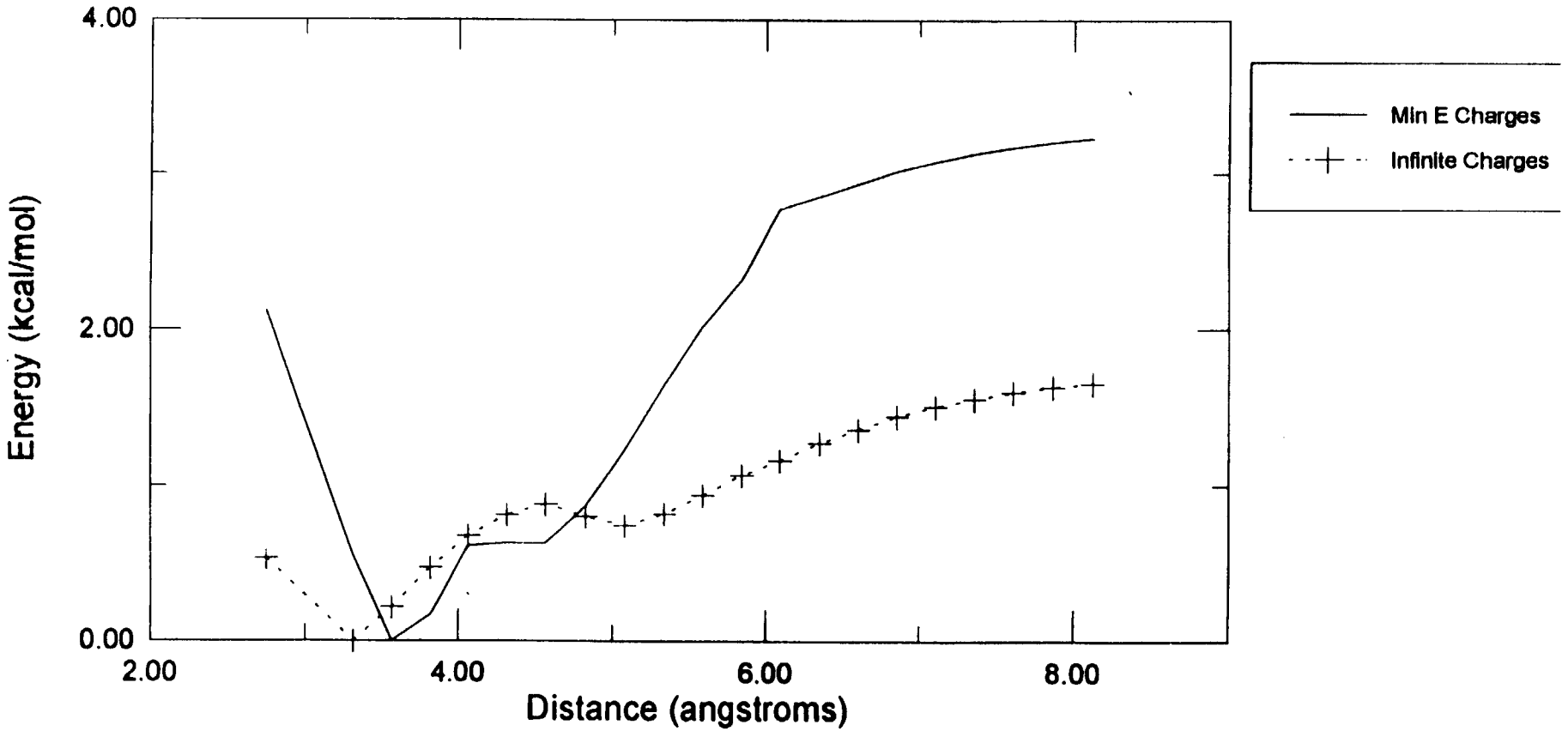
Energy Calculated by Spartan Versus Distance
Methane and Coronene Molecule



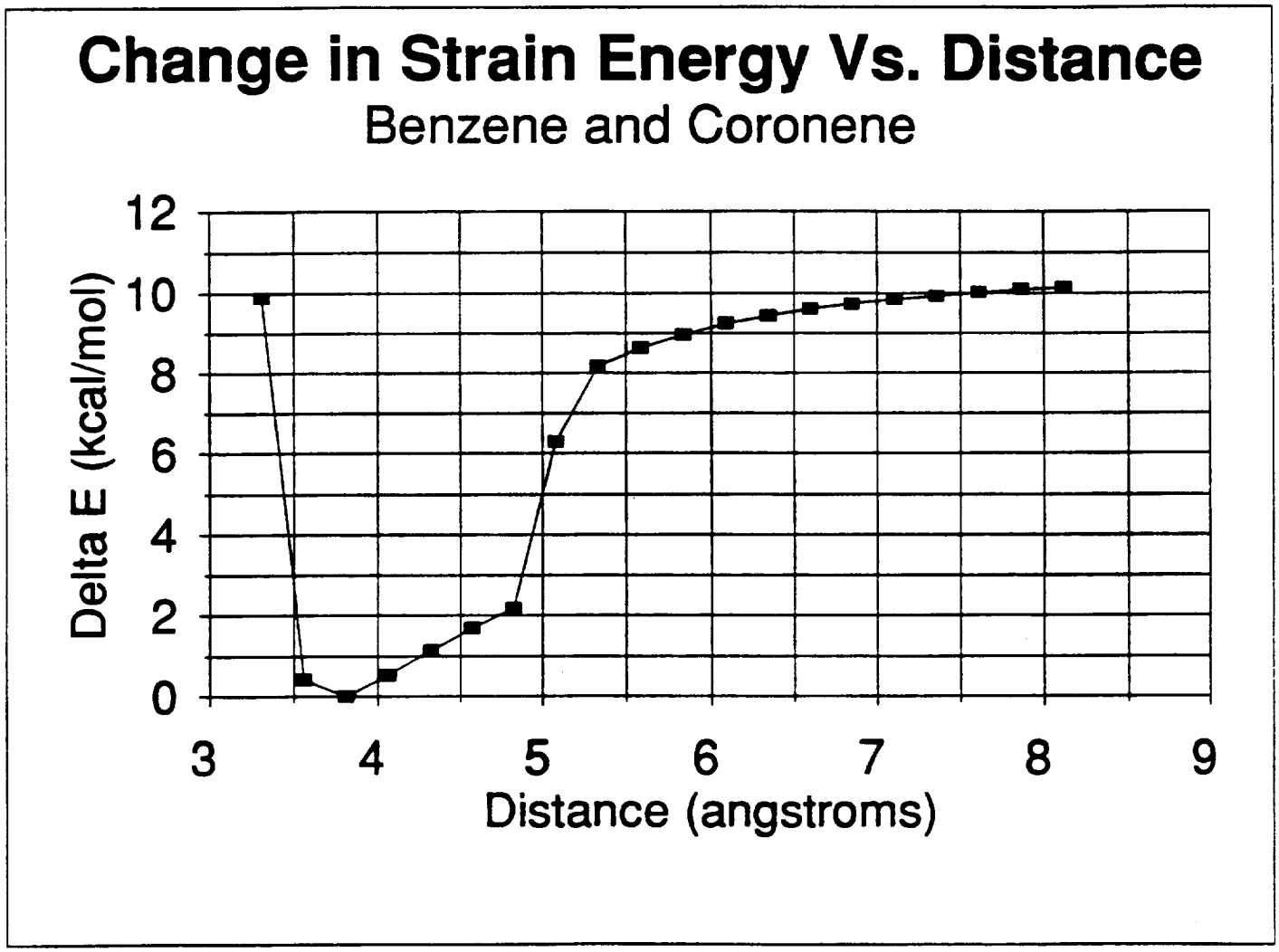
Energy Calculated by Sybyl and Spartan Versus Distance
Formaldehyde and Coronene Molecule



Energy Calculated by Sybyl with Charges Versus Distance
Formaldehyde and Coronene



File
Build Edit
View
Compute
Analyze
Options


Change in Strain Energy Vs. Distance
Benzene and Coronene
Delta E (kcal/mol)
12
10
8
6
4
2
0
3
4
5
6
7
8
9
Distance (angstroms)

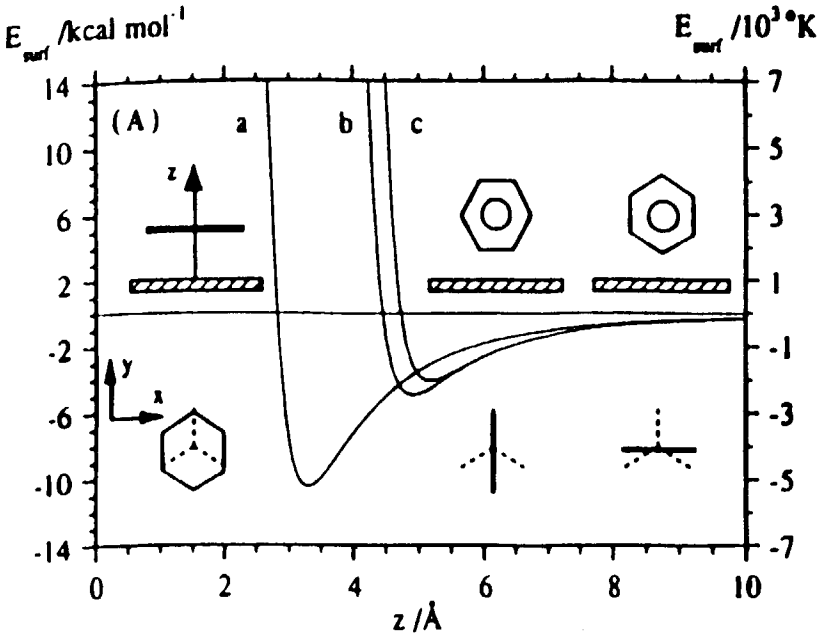
Surface Science 262 (1992) 180–188
North-Holland

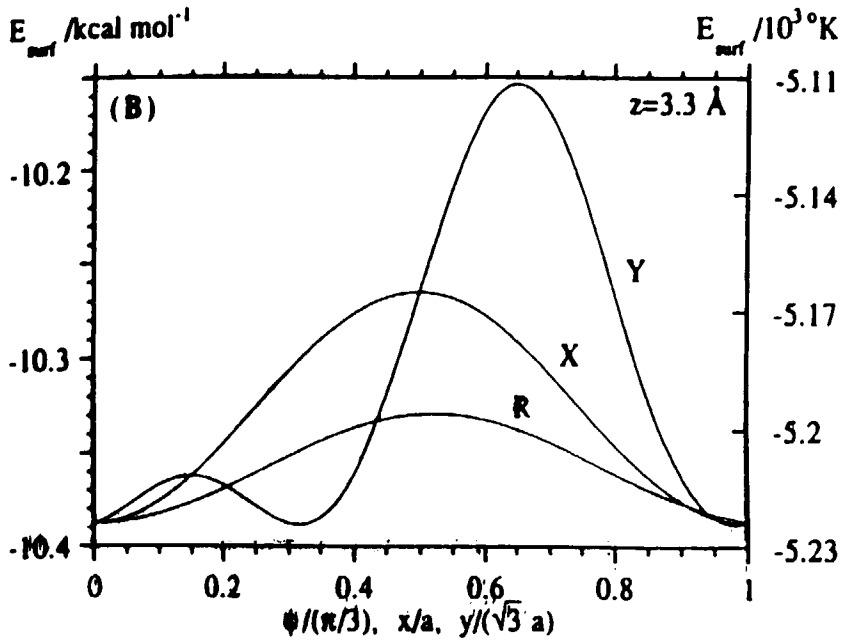
surface science

A molecular dynamics simulation of liquid benzene adsorbed on graphite

Reinhard Hentschke and Britta L. Schürmann
Max-Planck-Institut für Polymerforschung, Postfach 3148, D-6500 Mainz, Germany

Received 17 July 1991; accepted for publication 4 September 1991





EFFECT OF MOLECULAR WEIGHT ON PROPERTIES OF LARC™-SI

E. J. Siochi
Lockheed Martin Engineering and Sciences Company
Hampton, VA 23666

OUTLINE

- Introduction
- Objective
- Materials
- Characterization
  - Molecular Weight Determination
  - Thermal Analysis
  - Melt Viscosity
  - Density
  - Microhardness
  - Fracture Toughness
- Summary

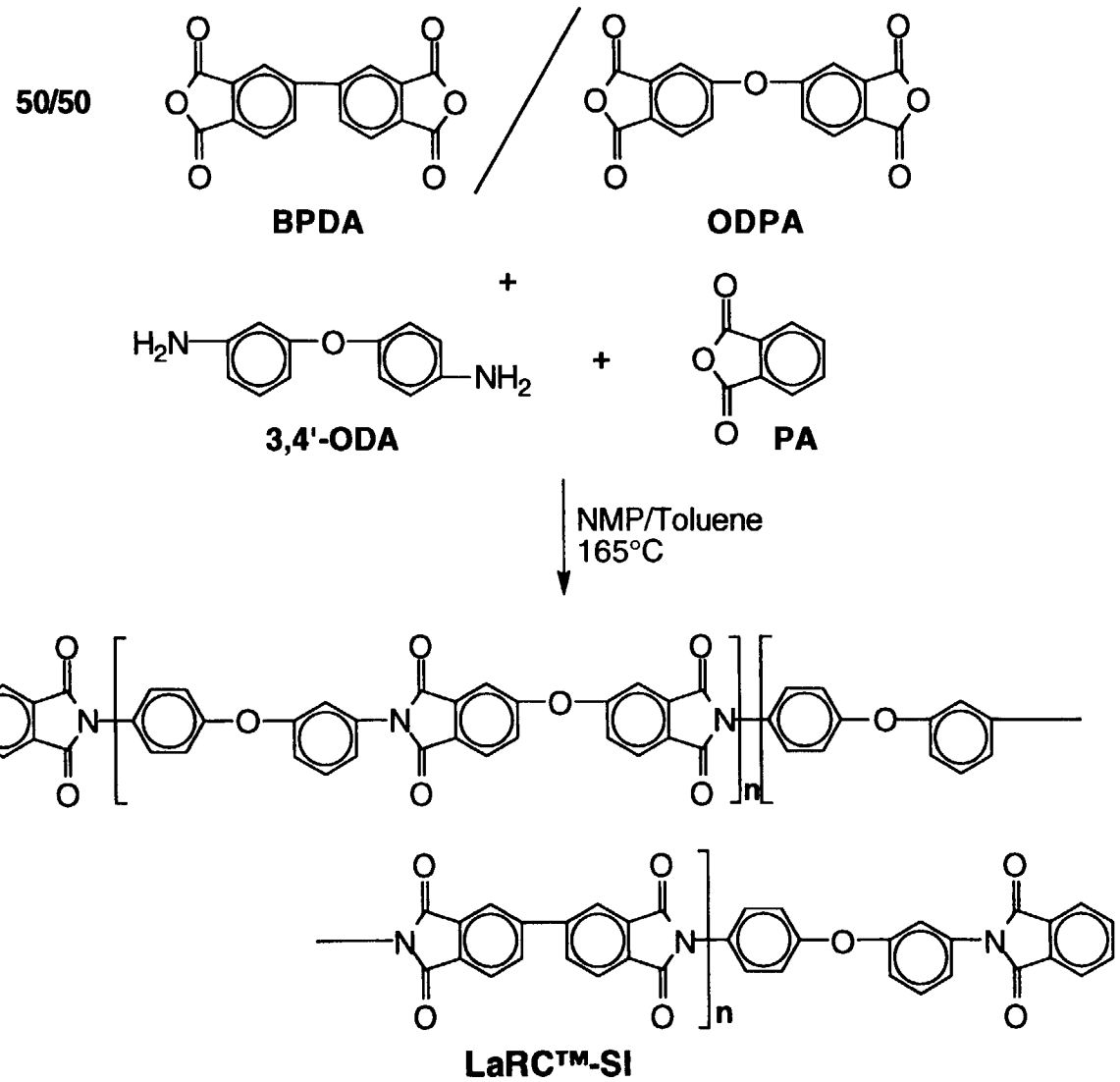
INTRODUCTION

- Polyimides as materials of choice
  - Excellent mechanical properties
  - Excellent thermooxidative stability
  - Good solvent resistance

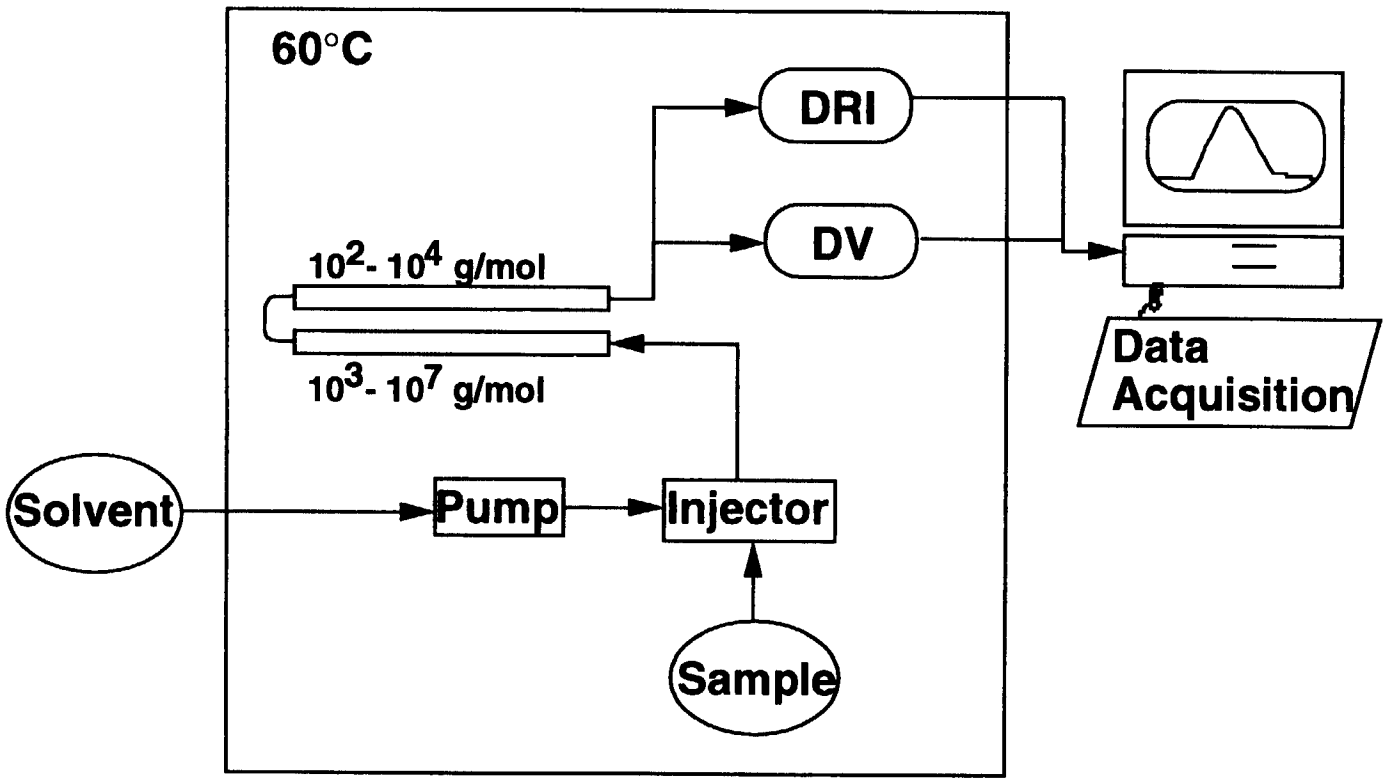
- Tailoring of properties achieved using stoichiometric imbalance during synthesis

- Solubility of LARC™-SI allows systematic investigation of the relationship of molecular weight to properties of interest

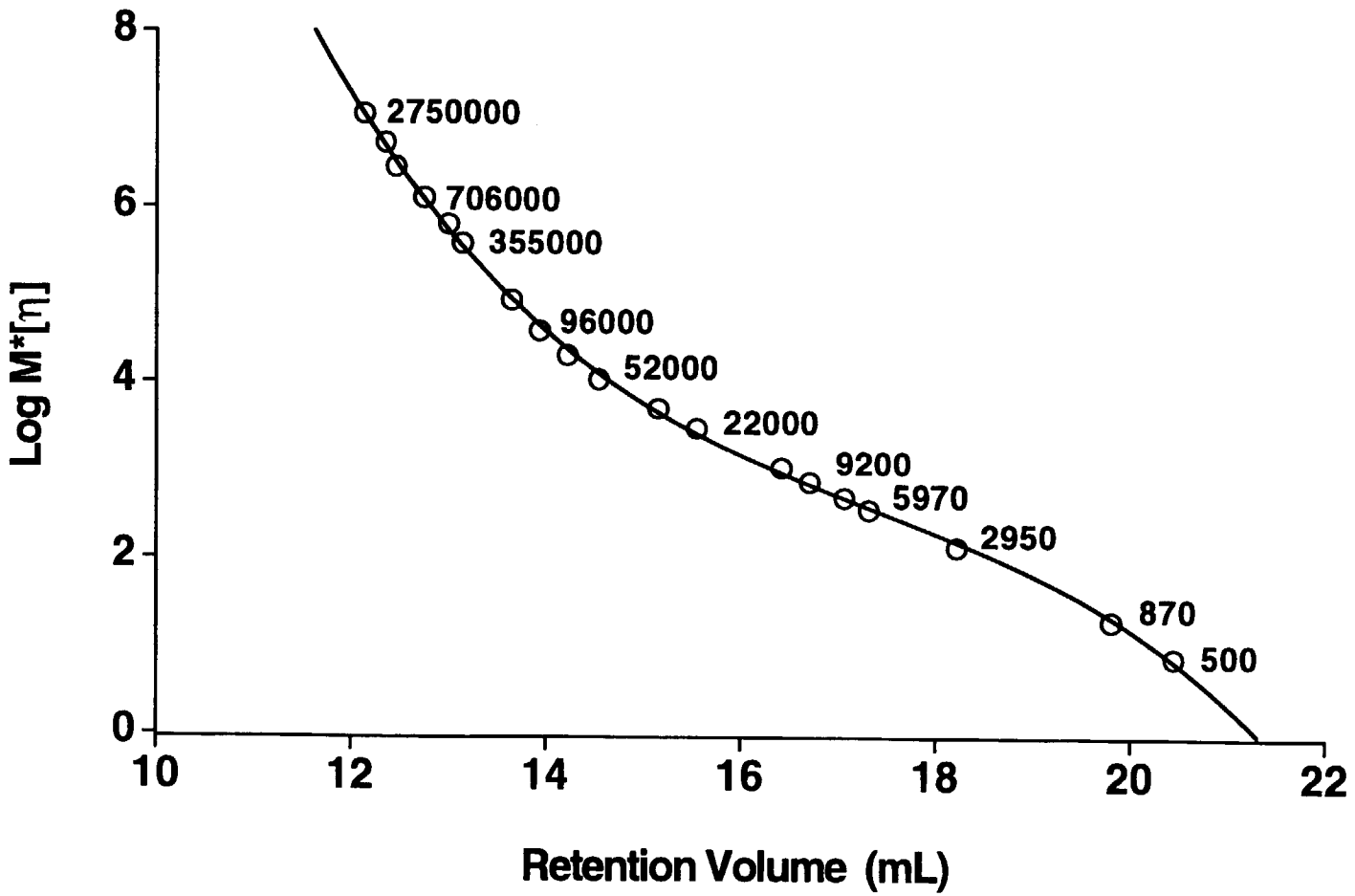
MATERIAL


50/50
BPDA
ODPA
+
H_2N
O
NH_2
3,4'-ODA
+
O
O
O
PA
NMP/Toluene
165°C
N
O
n
LaRC™-SI

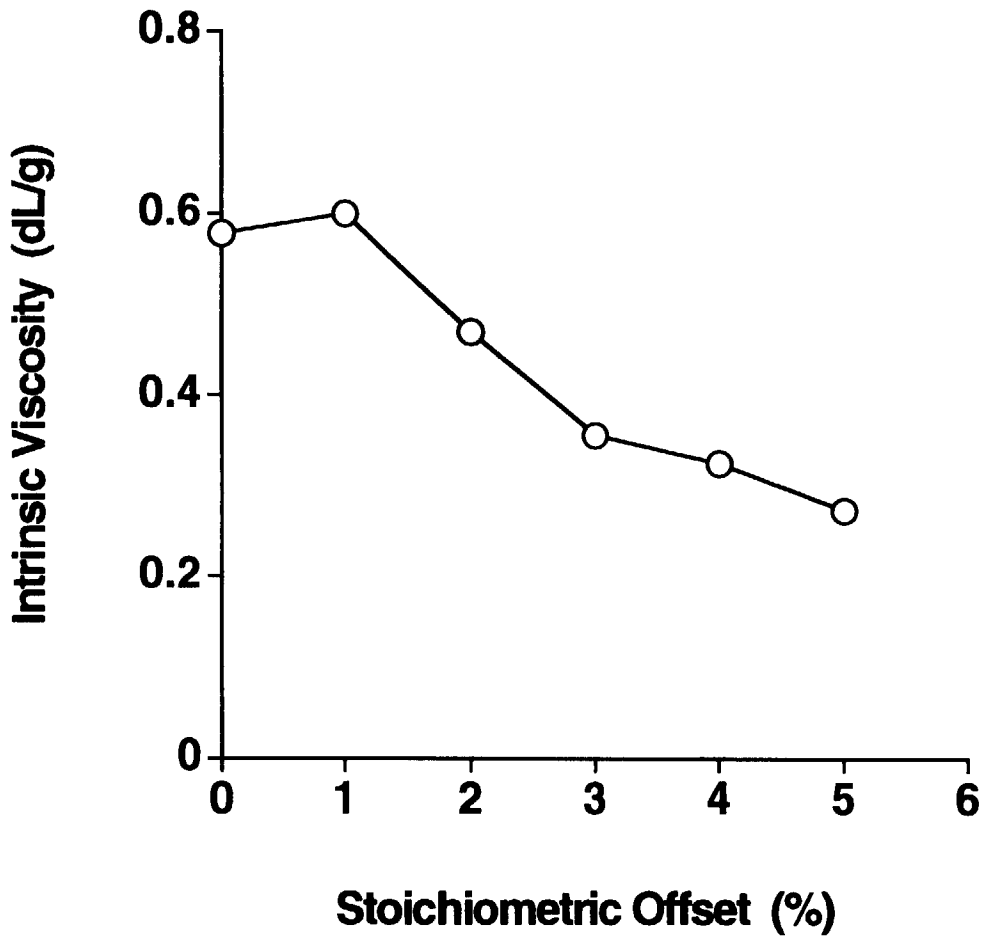
GPC/DV SCHEMATIC



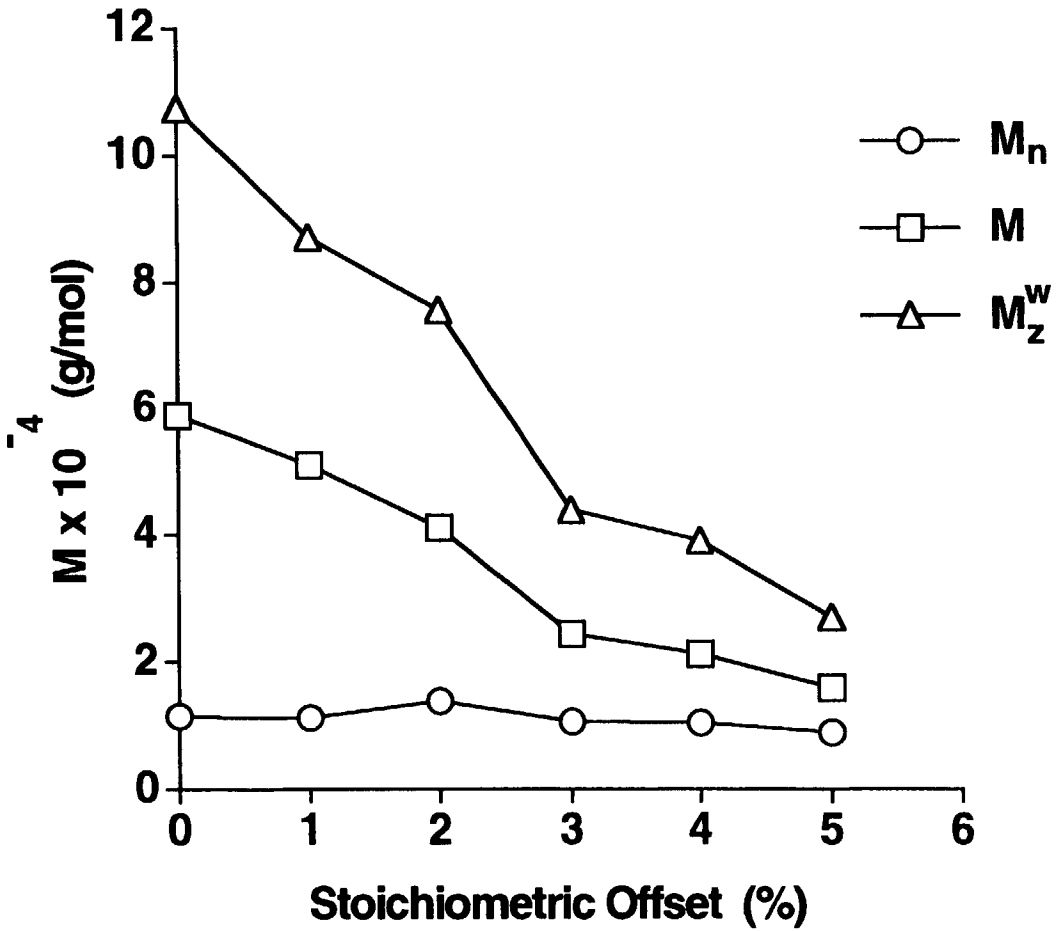
Universal Calibration Curve



Effect of Stoichiometric Offset on Intrinsic Viscosity



Effect of Stoichiometric Offset on Molecular Weight Averages



Molecular Weight Characterization

Sample Offset (%)	M_n (g/mol)	Theoretical M_n (g/mol)	M_w (g/mol)	M_z (g/mol)	M_v (g/mol)	Intrinsic Viscosity (dL/g)
0	11450	∞	58900	107350	43035	0.578
1	11180	44819	51070	87130	37530	0.600
2	13770	22297	41100	75703	31675	0.470
3	10560	14789	24290	43955	19170	0.356
4	10405	11036	21180	39110	17155	0.326
5	8882	8784	15880	26935	13690	0.273

Effect of Molecular Weight on the Properties of a Soluble Polyimide

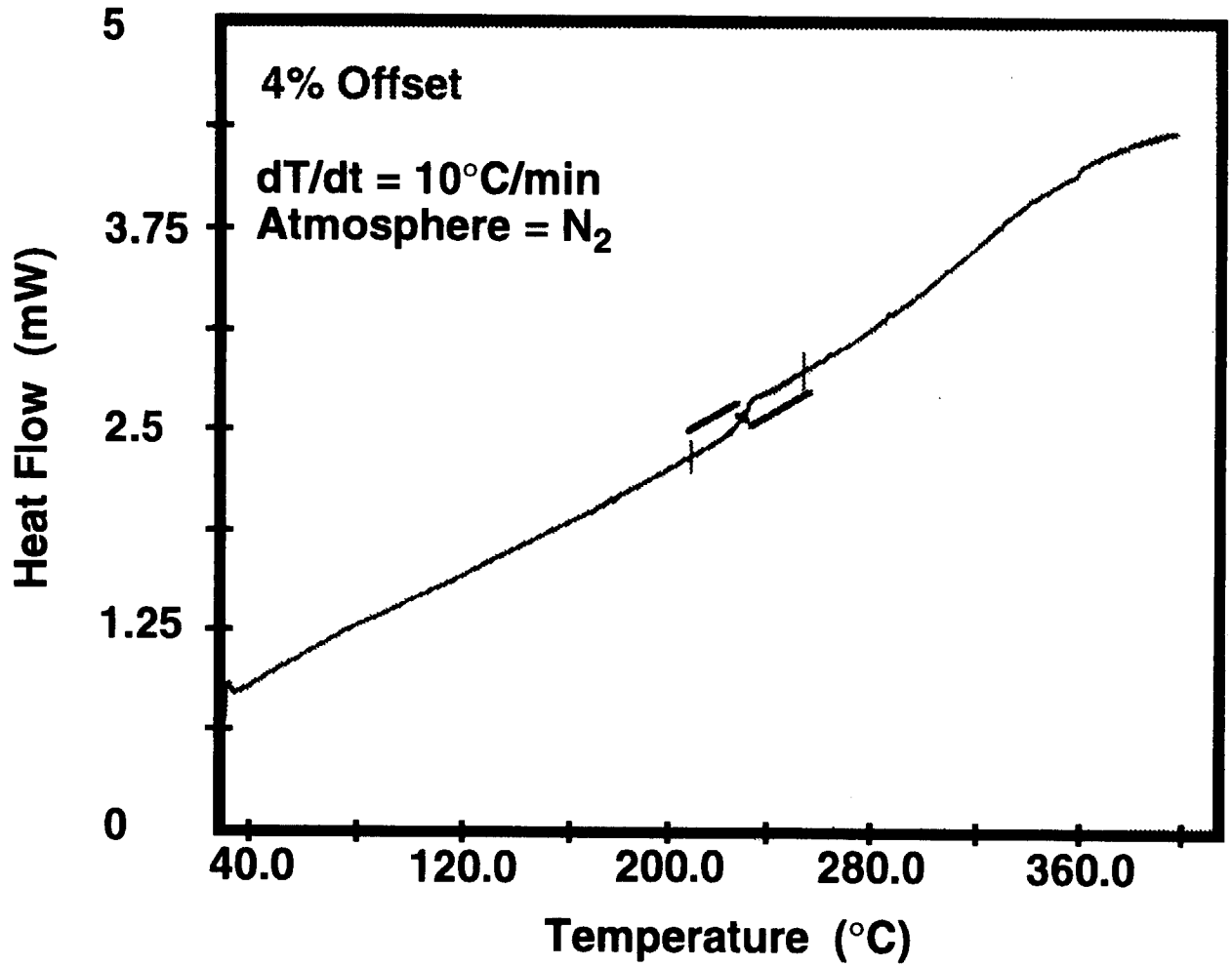
OBJECTIVE

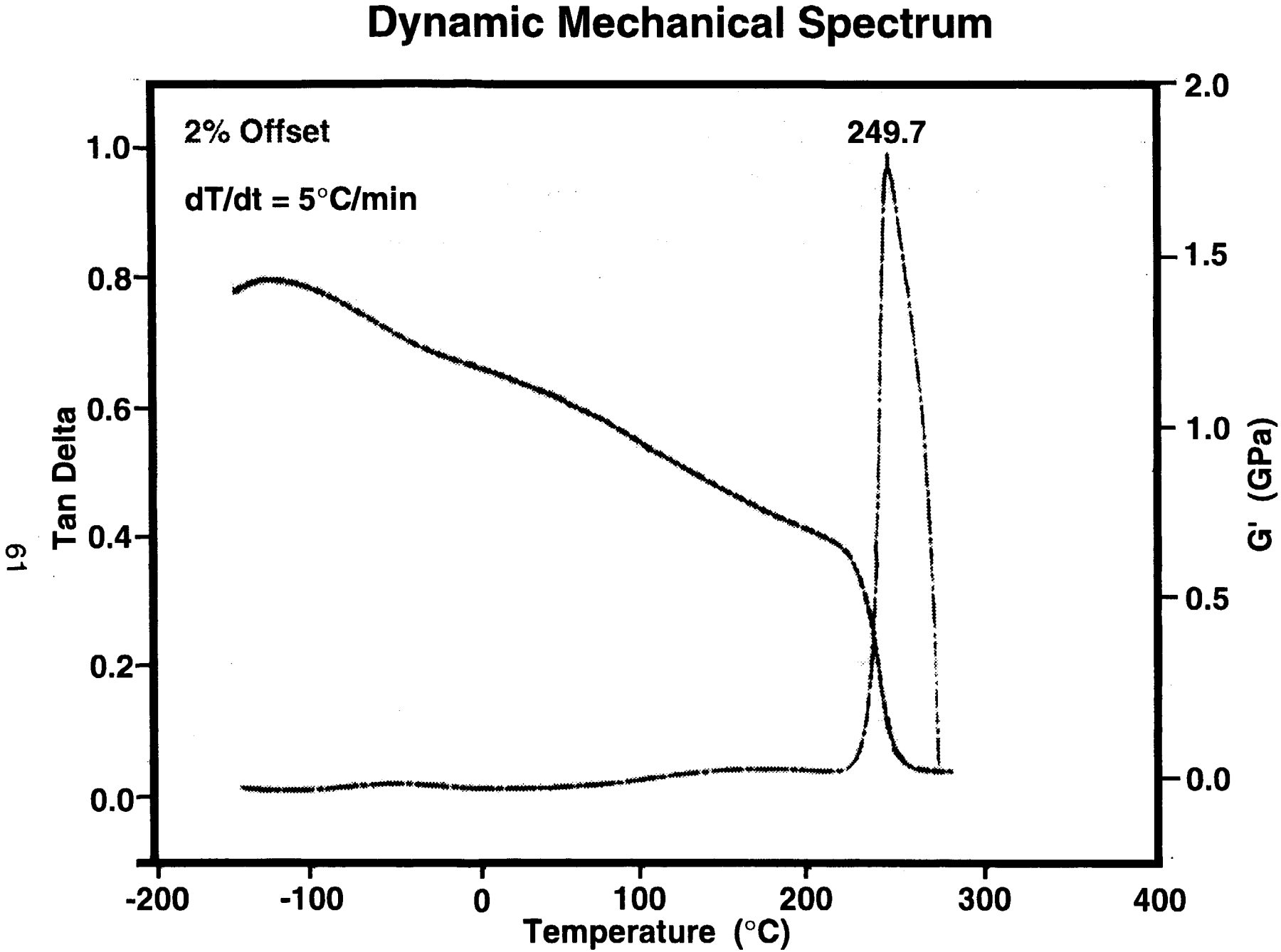
- Quantitative understanding of how molecular weight characteristics influence selected properties of an advanced polymer matrix resin

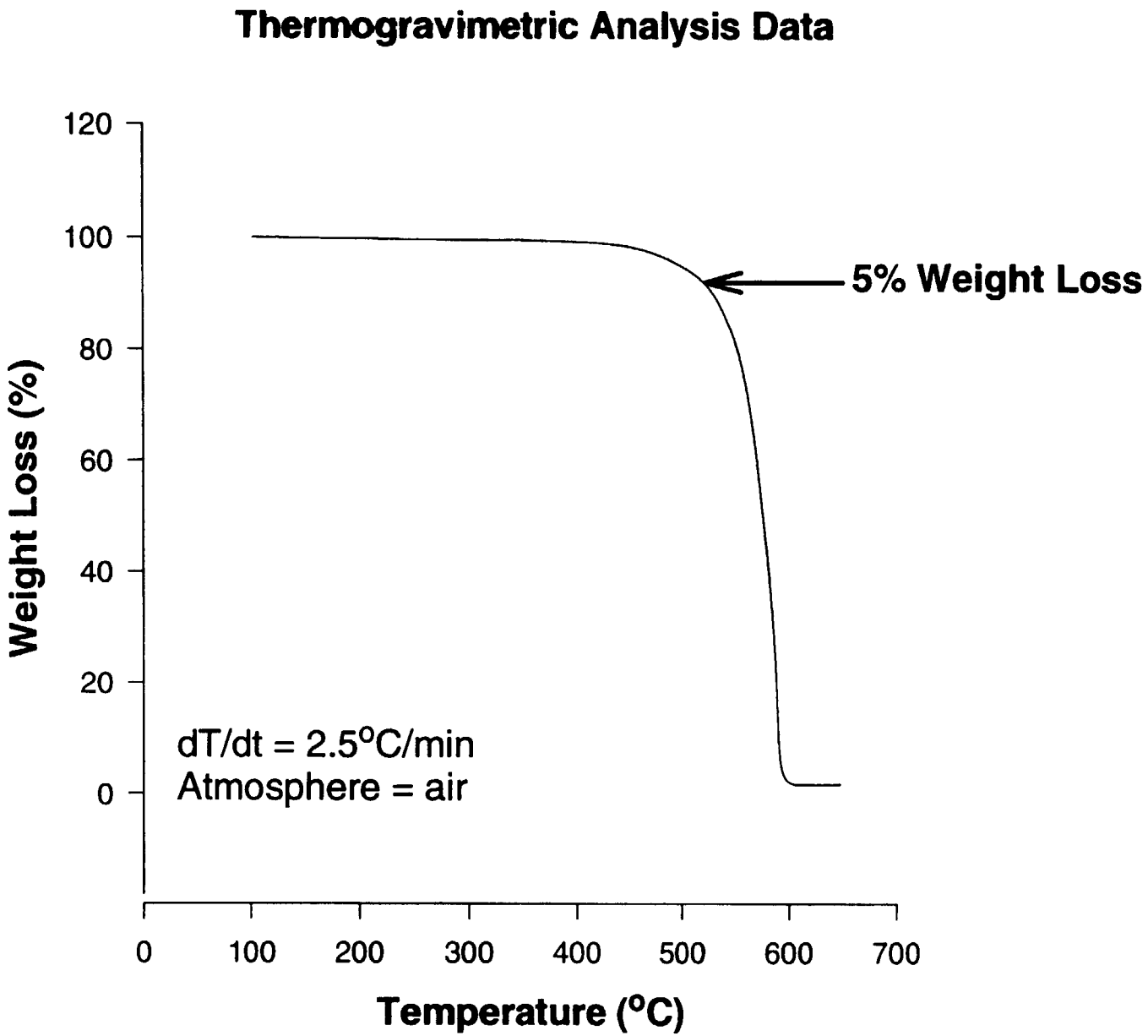
APPROACH

- Synthesize a series of soluble polyimides having controlled molecular weights
- Characterize polymer series with methods of analysis routinely practised by Composites and Polymers Branch
- Find relationships between physical properties of polymers and molecular weights

Differential Scanning Calorimetry



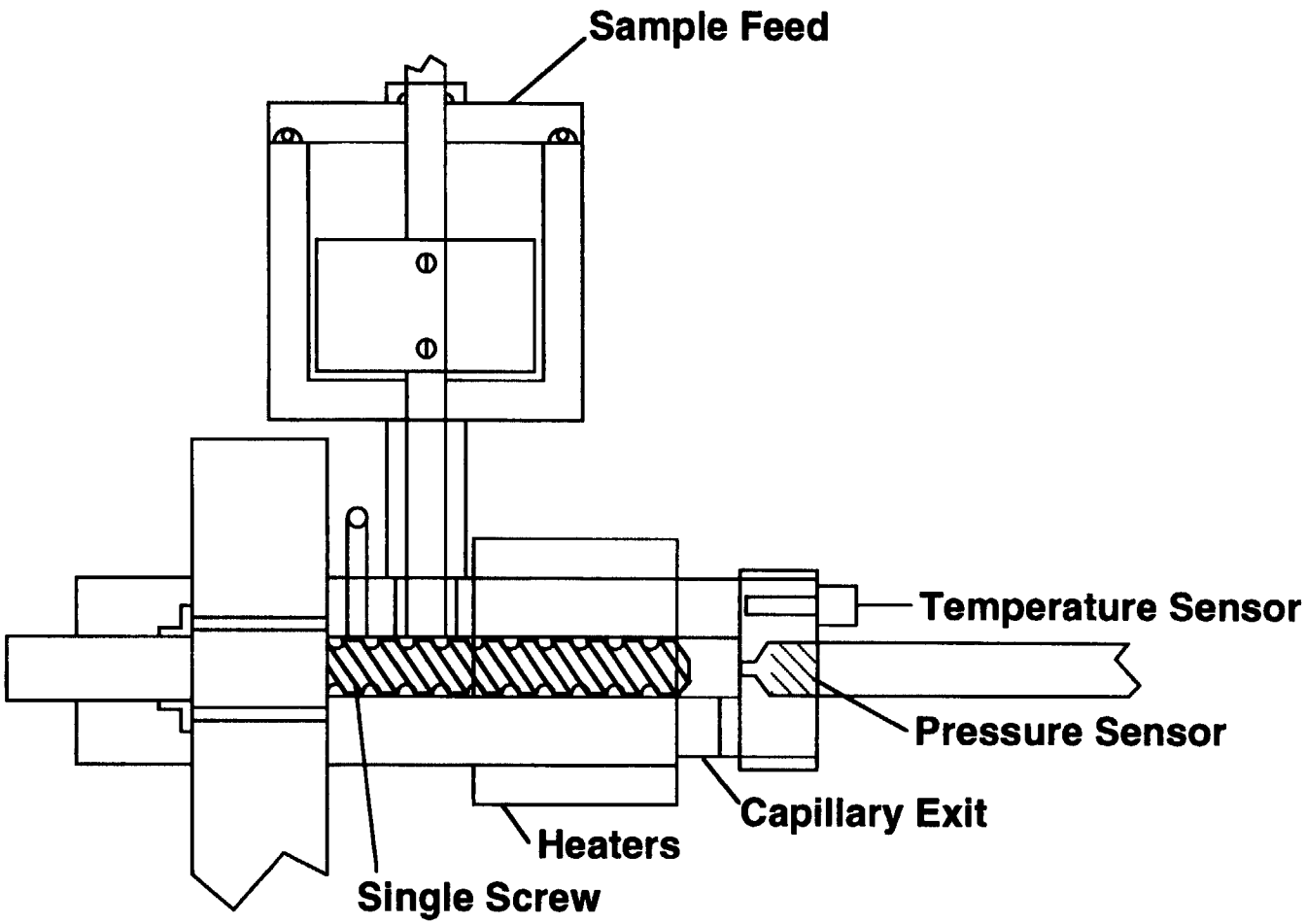

Dynamic Mechanical Spectrum
2% Offset
dT/dt = 5°C/min
249.7
Tan Delta
G' (GPa)
Temperature (°C)
1.0
0.8
0.6
0.4
0.2
0.0
2.0
1.5
1.0
0.5
0.0
-200
-100
0
100
200
300
400


Thermogravimetric Analysis Data
120
100
80
60
40
20
0
Weight Loss (%)
5% Weight Loss
dT/dt = 2.5°C/min
Atmosphere = air
0
100
200
300
400
500
600
700
Temperature (°C)

Thermal Characterization

Sample Offset (%)	Tg from DMA (°C)	Tg from DSC (°C)	5% Weight Loss (°C)	Weight Change at 177°C After 100 Hours (%)
0	253	239	498	-0.2
1	258	248	523	0
2	250	248	467	0
3	249	242	527	0
4	246	230	505	-0.2
5	--	231	520	0

Profile of Vacuum Microextruder



Melt Viscosity Calculation

$$\eta = \tau_w / \dot{\gamma}_w$$

$$\tau_w = RP/2l$$

$$\dot{\gamma}_w = 4Q/\pi R^3$$

η = Melt Viscosity

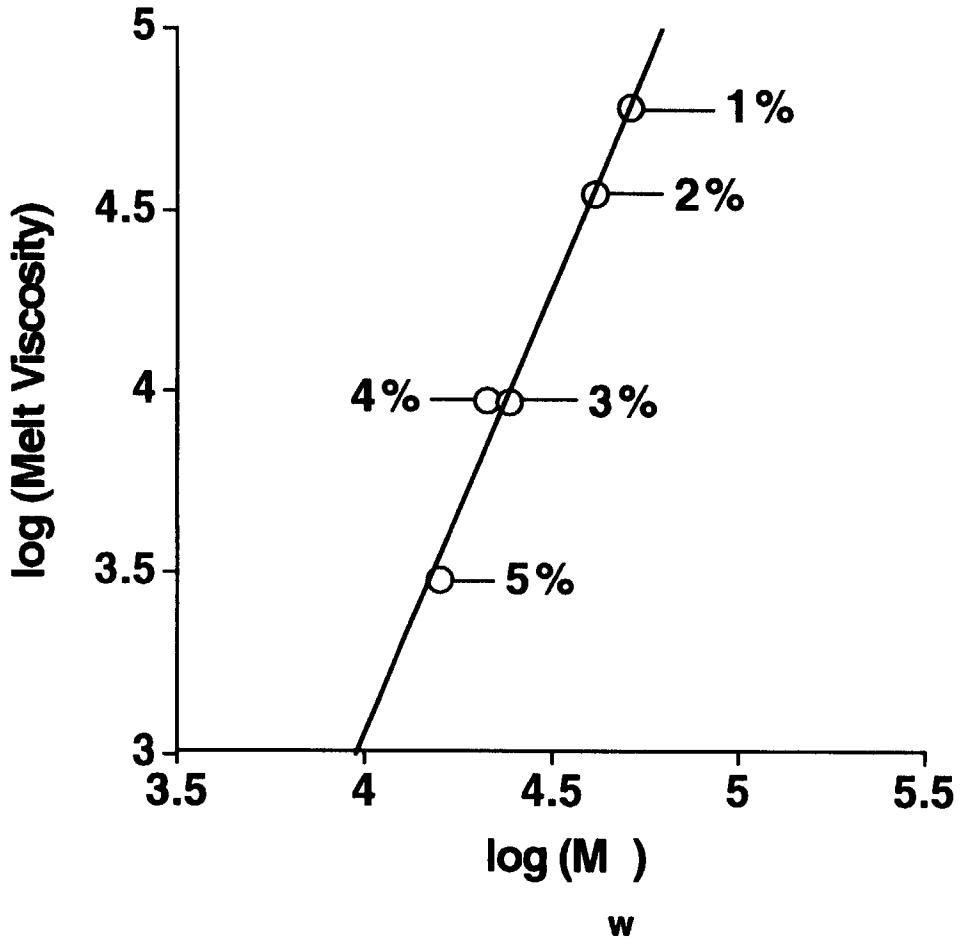
Q = Volume Flow Rate

R = Capillary Radius

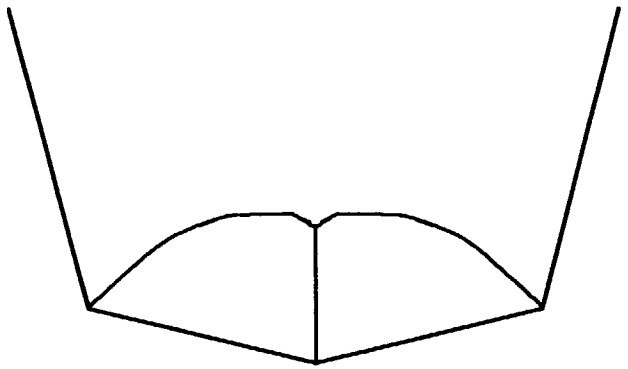
P = Pressure Drop

l = Capillary Length

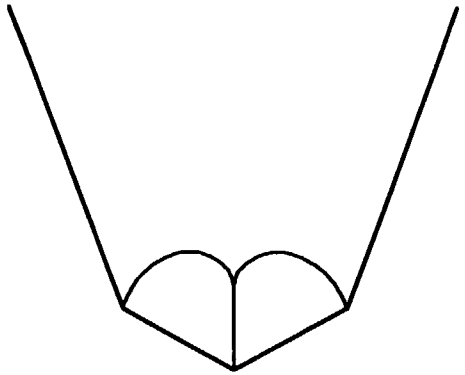
Relationship of Melt Viscosity to Molecular Weight



Microhardness Determination



Front View
(172° 30')

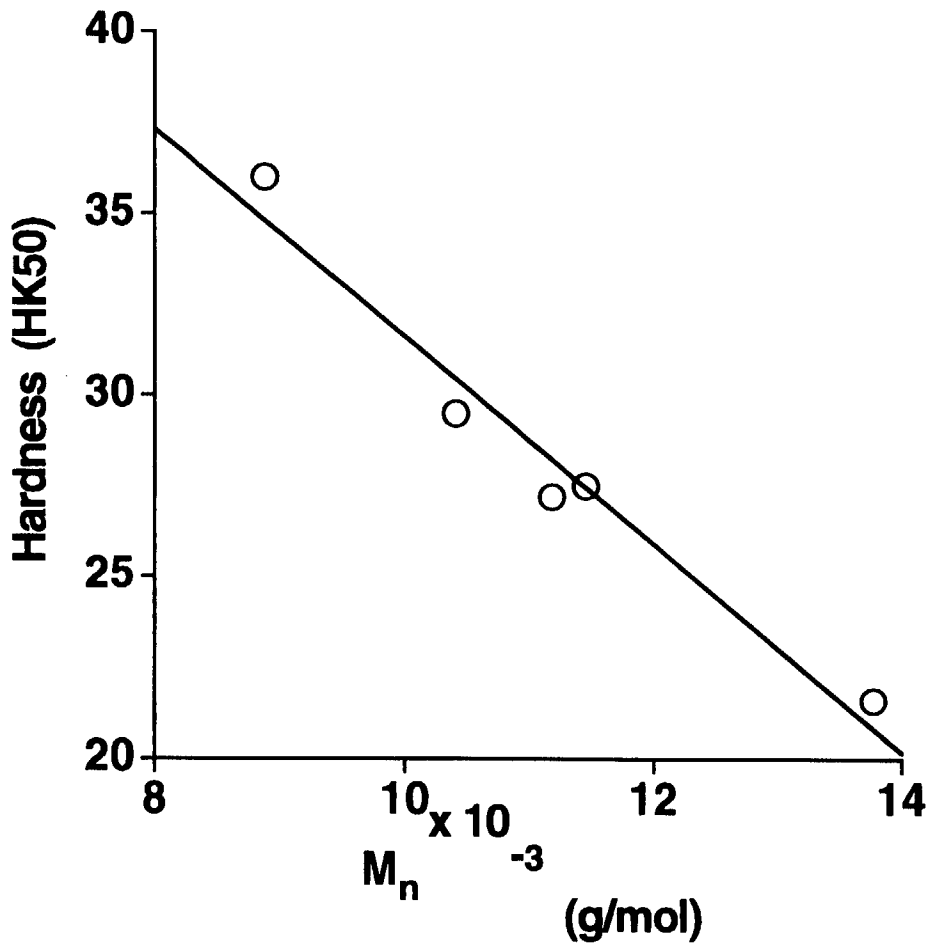


Side View
(130°)

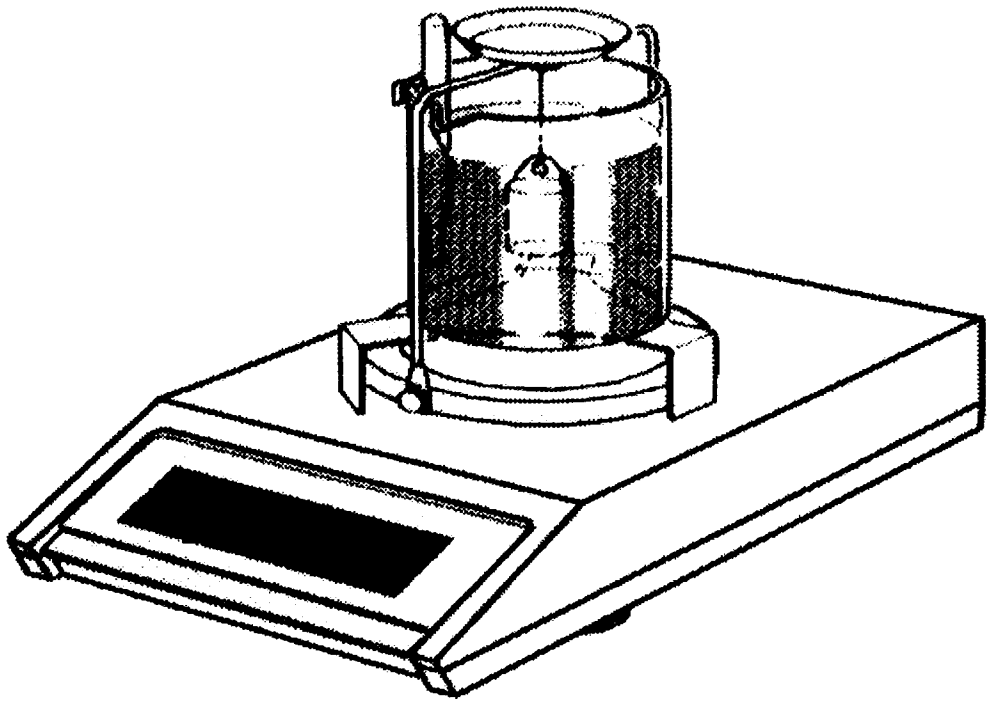
$$KHN = P/AP$$

KHN = Knoop Hardness
P = Load (kg)
AP = Area of the Impression

Relationship of Hardness to Molecular Weight



Density Determination Apparatus



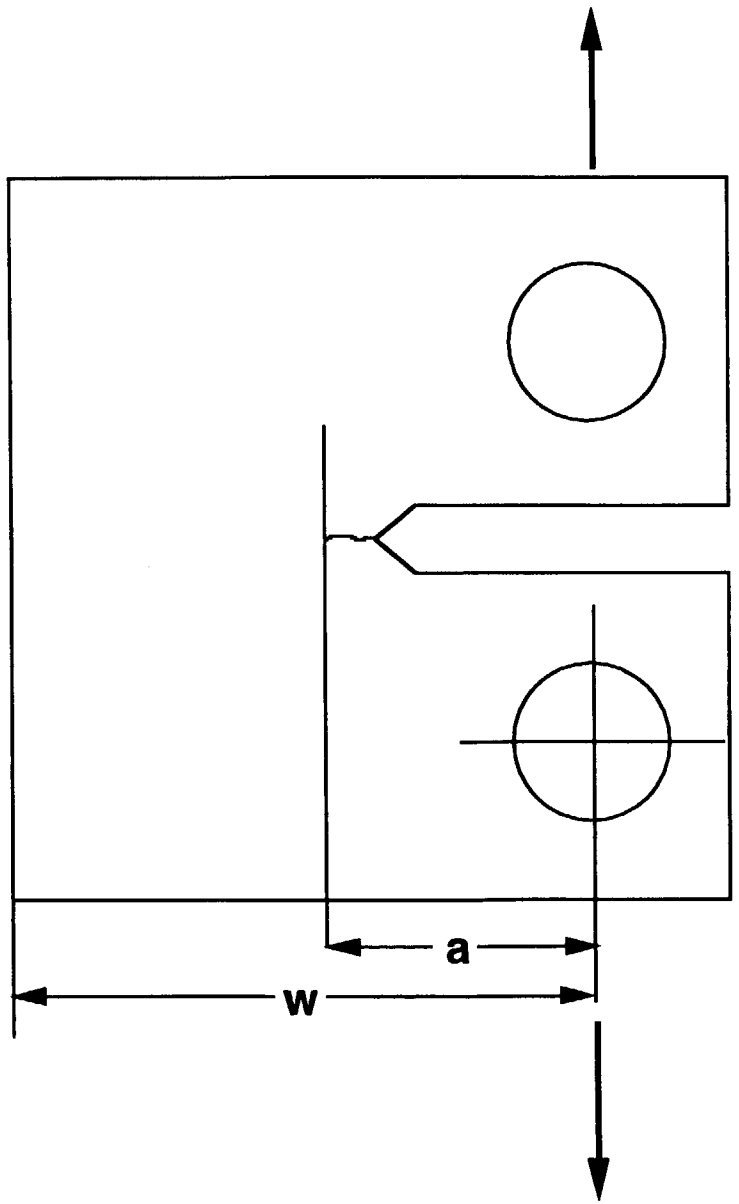
$$\rho_2 = \frac{A}{P} \cdot \rho_o$$

ρ_2 = Density of Solid Body
A = Weight of Solid Body in Air
P = Buoyancy of Solid Body in Test Liquid
ρ_o = Density of Test Liquid at a Given Temperature

Density of LaRC™-SI

Stoichiometric Offset (%)	Density (g/cc)
0	1.365
1	1.360
2	1.361
3	1.359
4	1.359

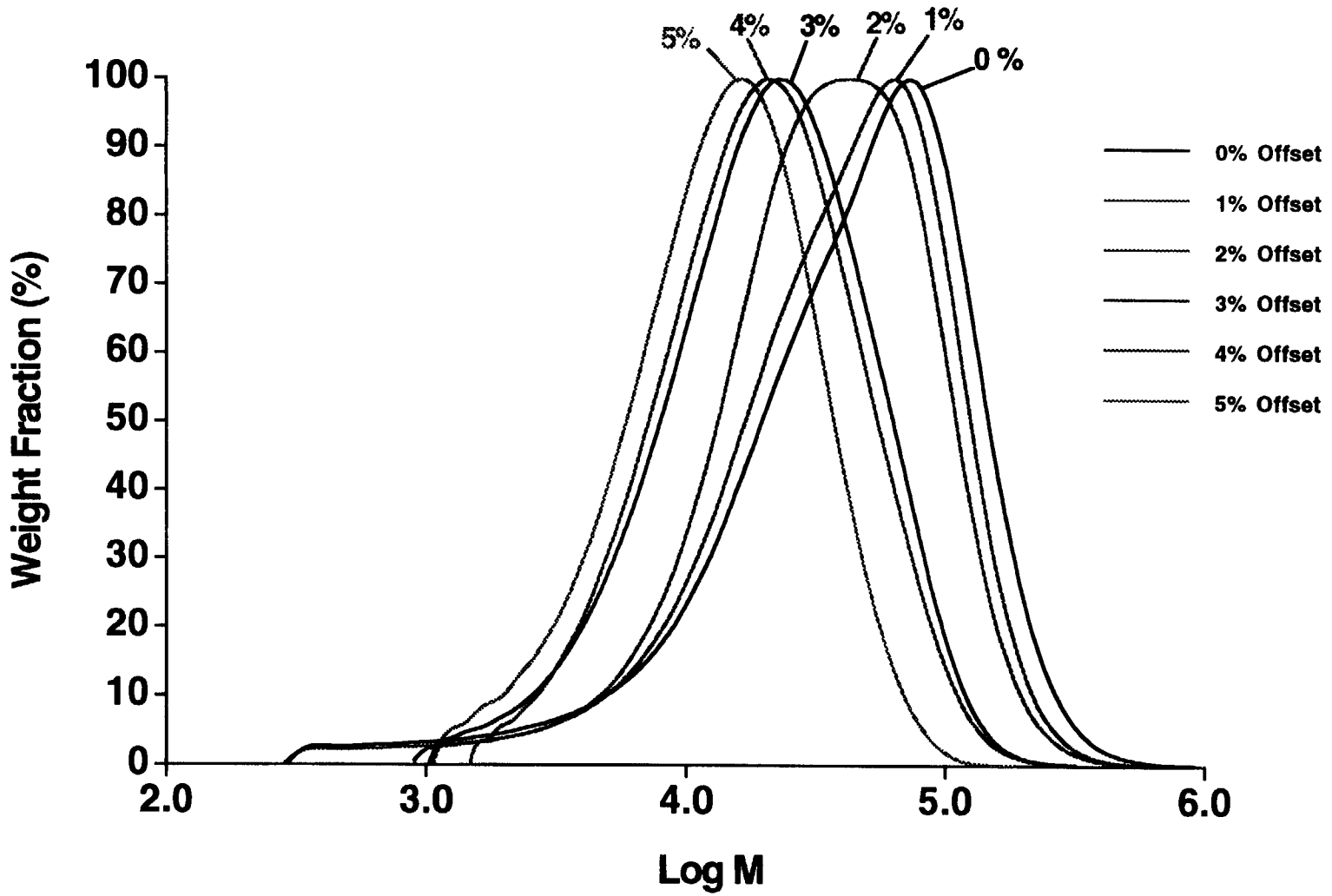
Compact Tension Configuration for Fracture Toughness



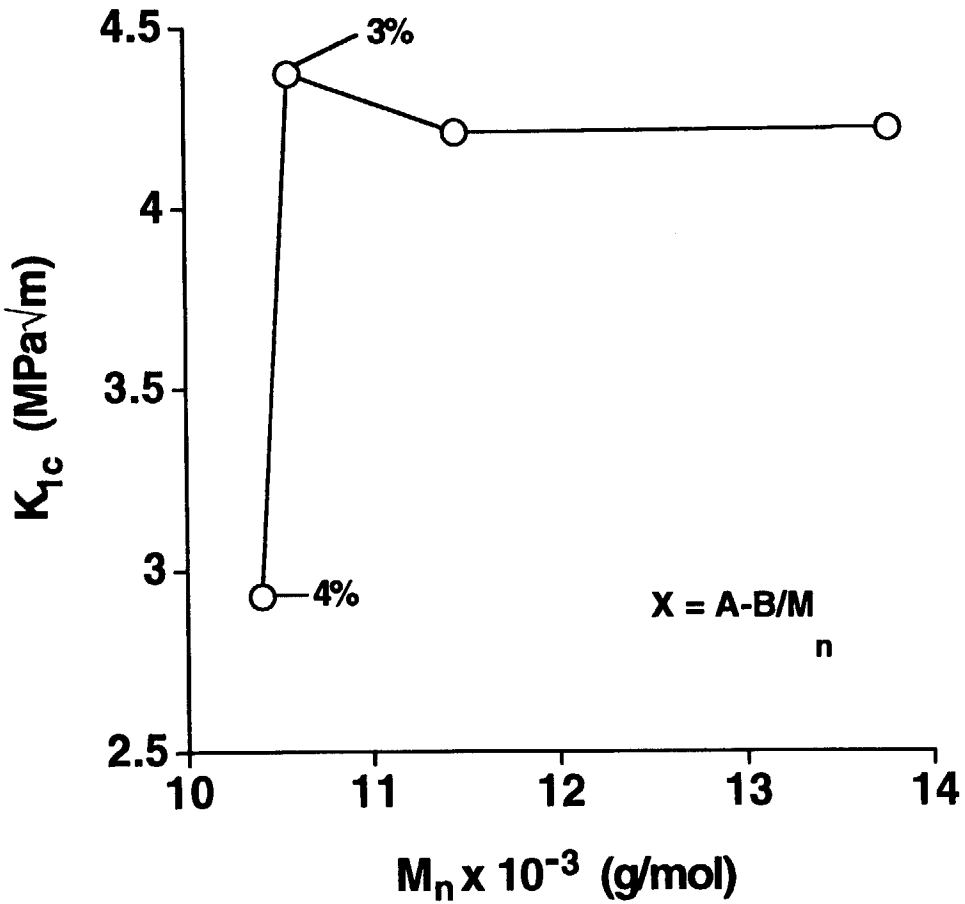
$$K_Q = (P_Q / BW^{1/2}) \cdot f(a/W)$$

K_Q = Fracture Toughness
P_Q = Maximum Load
B = Specimen Thickness
W = Specimen Width
a = Crack Length

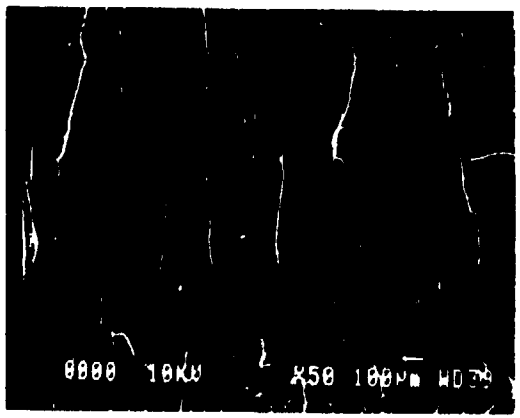
Effect of Stoichiometric Imbalance on Molecular Weight Distribution



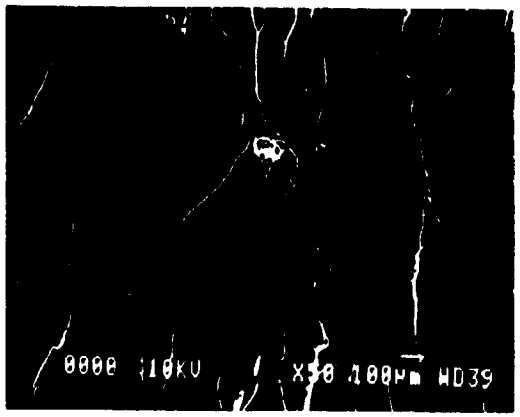
Effect of Molecular Weight on Fracture Toughness



SEM Photomicrographs of LaRC™-SI Fracture Surfaces



0% Offset



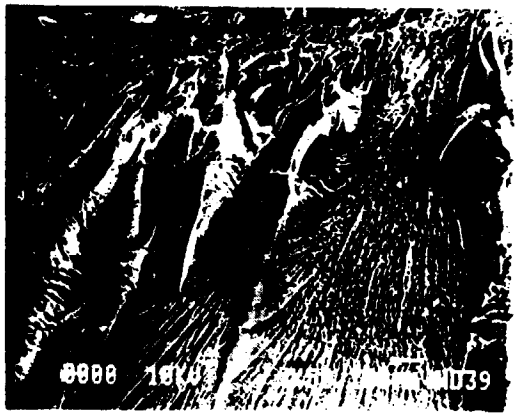
1% Offset



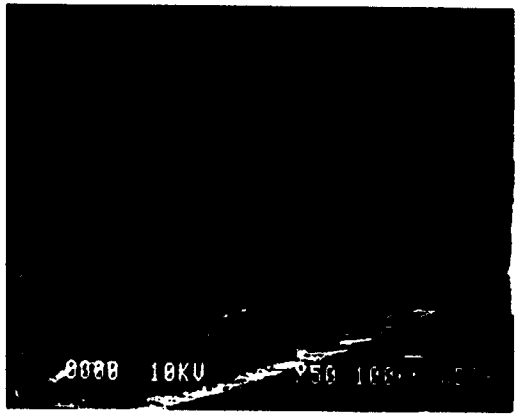
2% Offset



3% Offset



4% Offset



5% Offset

SUMMARY

- Controlled molecular weight soluble polyimides were synthesized.
- Stoichiometric offsets were reflected in the higher moments of the molecular weight distribution.
- Glass transition temperatures ranged from 230-248°C for 0-5% offset in stoichiometry.
- Scatter in TGA data showed no clear dependence of thermooxidative stability on molecular weight.
- Melt viscosity varied logarithmically with M_w.
- Density was not affected by molecular weight.
- Hardness varied linearly with M_n.
- Fracture toughness decreased sharply for materials with greater than 3% offset in stoichiometry.

FUTURE WORK

- Moldings have been made for other members of the NASA LaRC Computational Materials group.
- A series of phenylethynyl terminated LARC™-SI is being synthesized to examine the effect of crosslinking on properties.

Molecular Modeling of Novel Piezoelectric Polyimides

by

J.A. Young and B.L. Farmer
Department of Materials Science and Engineering
University of Virginia
Charlottesville, VA

and

J.A. Hinkley
NASA Langley Research Center
Hampton, VA

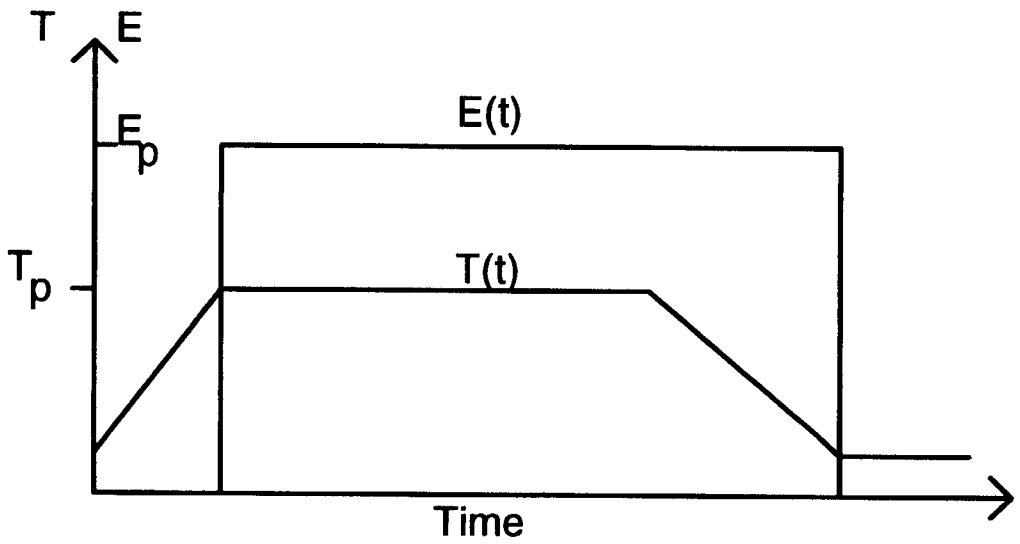
PURPOSE

Computational chemistry techniques are used to model the large piezoelectric responses seen in novel high temperature polyimides. Molecular orbital calculations and molecular dynamics on two dimensional systems are used to investigate the nature of the piezoelectric response by characterizing the underlying molecular physics of the process. This information will then be used to propose mechanisms for enhancing the response by maximizing the polymers ability to assume conformations that enhance the materials polarization and its electrical response to stress.

PIEZOELECTRICITY

Materials which electrically responded to mechanical deformations (or visa versa) are said to be piezoelectric. Piezoelectric materials are formed from polar amorphous polymers by:

1) inducing orientation polarization. Apply an electric field, E_p, at a temperature, T_p, near T_g to induce a remnant polarization, P_r in the material.



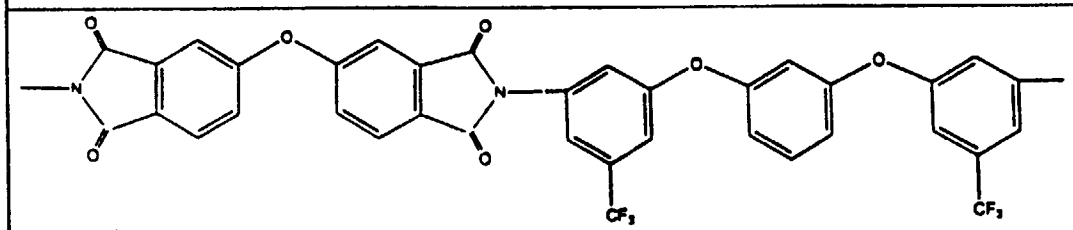
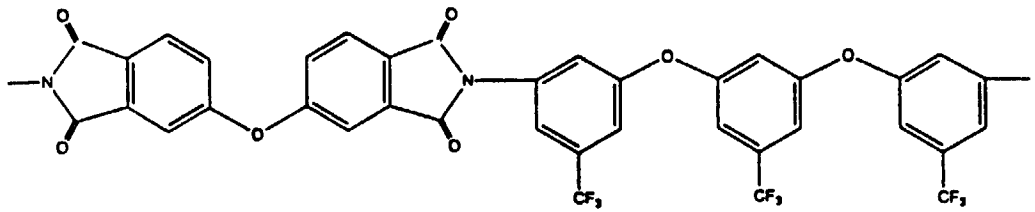
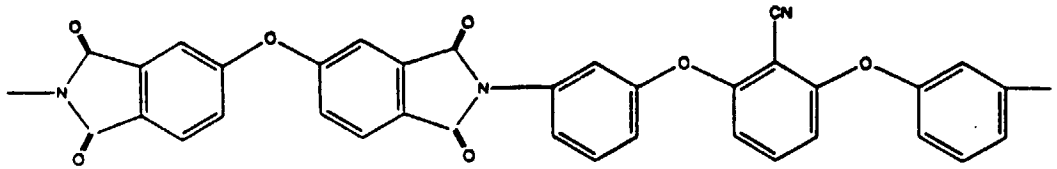
2) characterize the electrical response (electrical current, D or electric field, E) of the material as a function of mechanical deformation, *T*.

$$d=(\delta D/ \delta T)_E \text{ for closed circuit}$$

or

$$g=(\delta E / \delta T)_D \text{ for open circuit}$$

MOLECULES OF INTEREST

Polyimide Structure	Tg (K)	g_{33} (Vm/N) at 353 K *
	449	8.0
	453	8.5
	493	13.5

Note: for PVF_2 g_{33}= 0.2 Vm/N at 353 K.

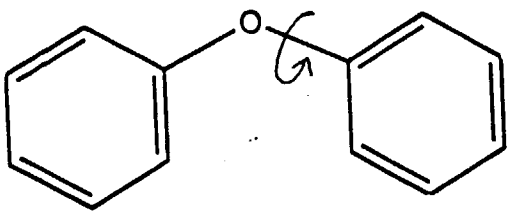
* Joycelyn O. Simpson et al., Novel Piezoelectric Polyimides, Proceedings of the 1995 Fall Meeting of the Materials Research Society (Novemer27-December 1, 1995) Boston, Massachusetts.

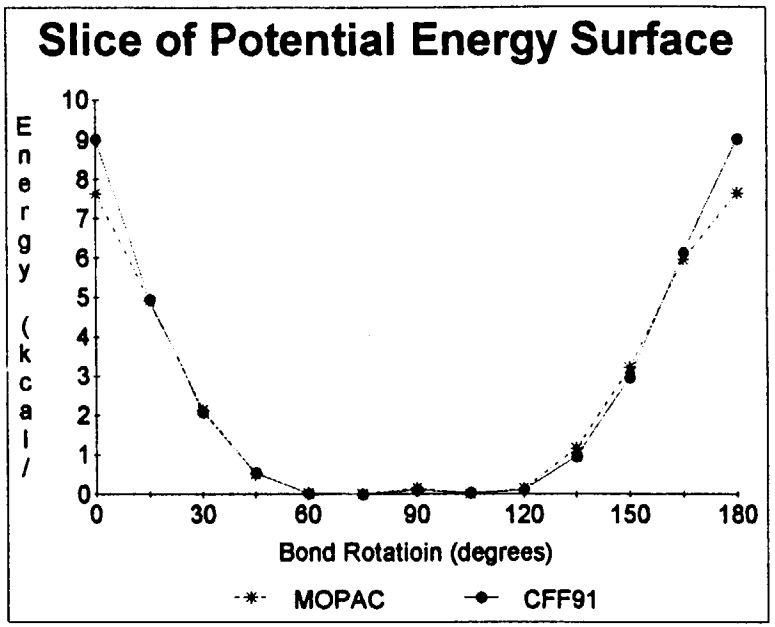
PARAMETERIZATION

Prior to being able to carry out force field based calculations (molecular mechanics or molecular dynamics) the proper force field parameters must be obtained.

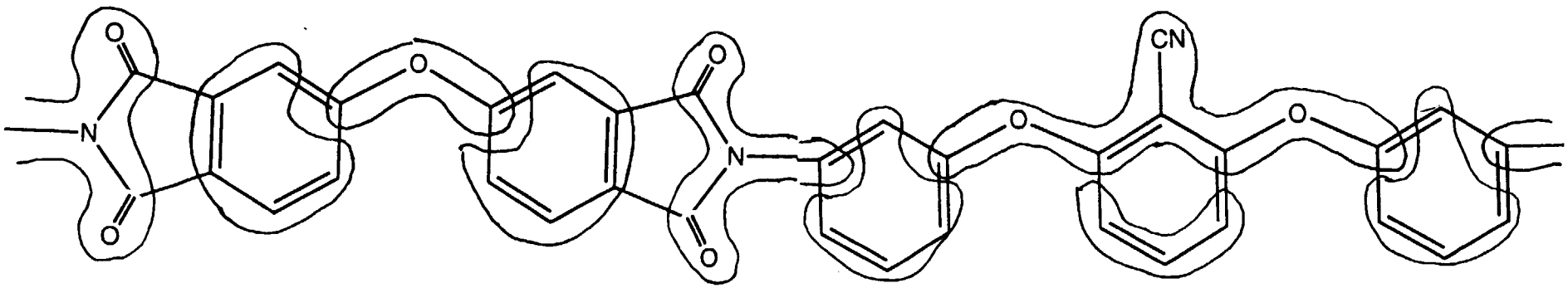
⌘ Compare the potential energy surfaces of components of the polyimide backbone calculated via quantum mechanical methods and molecular mechanics with various force fields.

❖ Modification of BIOSYM's CFF91 force field reproduced the MOPAC / Ab Initio surfaces.





⌘MOPAC with the AM1 parameterization was used to generate partial atomic charges for the polyimides. Charge neutral groups were then formed while maintaining the original dipole moment.



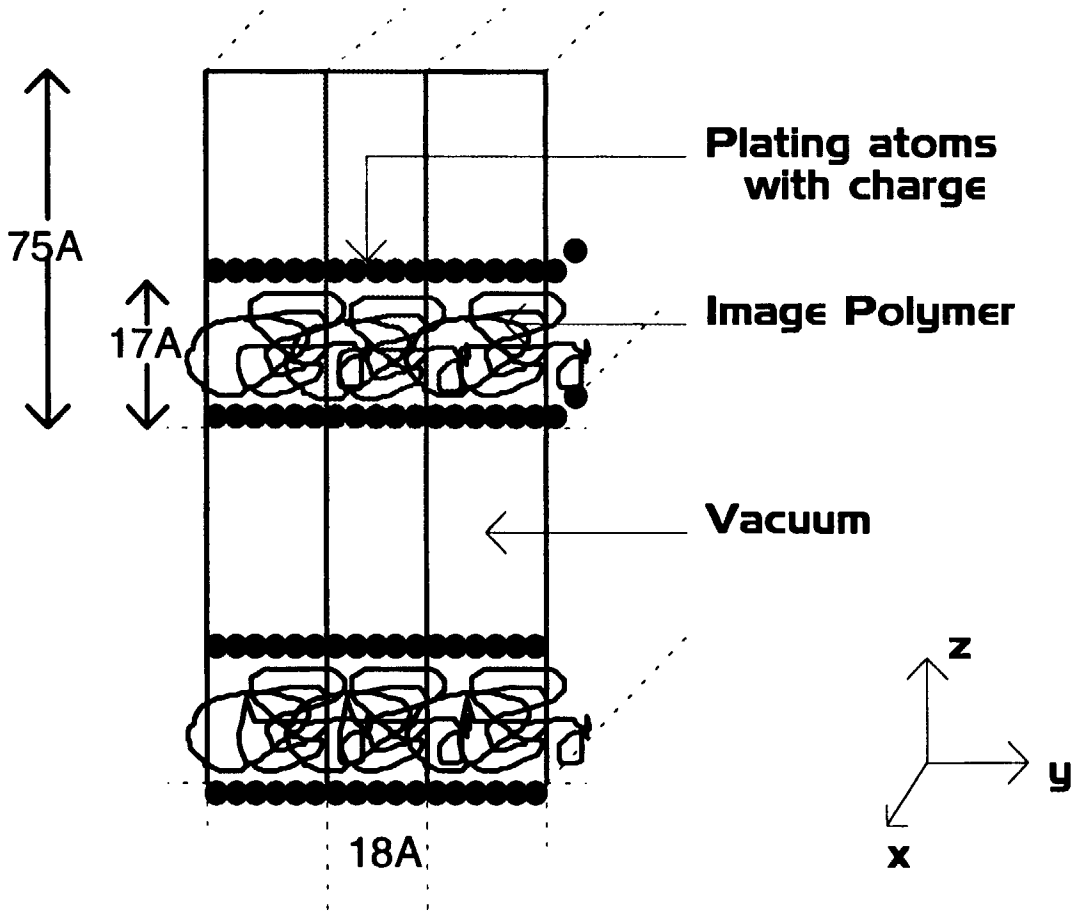
GENERATE AMORPHOUS CELL

Construction of a two dimensionally periodic amorphous box was done via the Amorphous Cell module in BIOSYM.

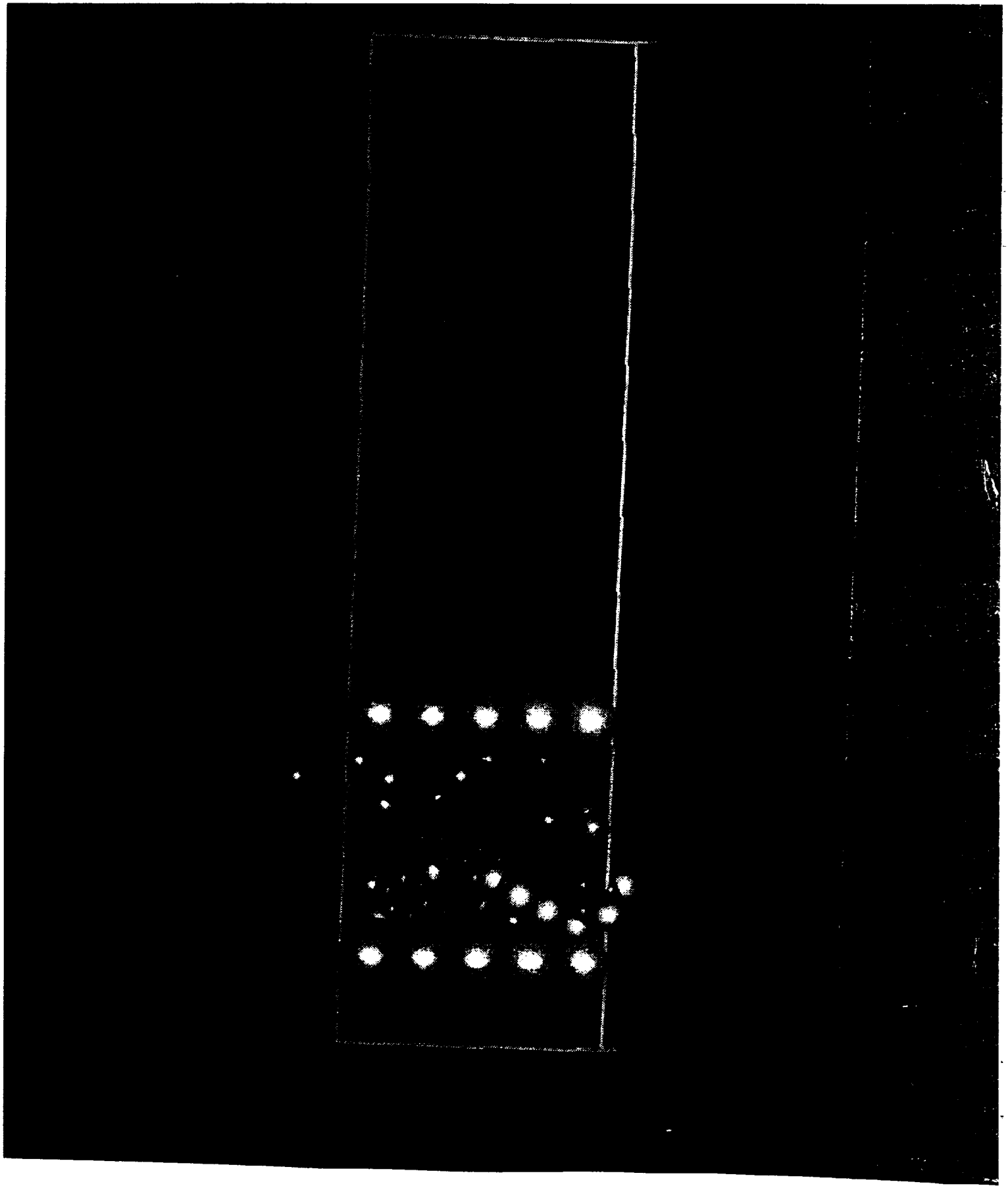
⌘ Build a low density (0.2 g/cm^3) five-mer polyimide cell.

⌘ Run high pressure (5000 bar) molecular dynamics until system reaches experimental density (1.34 g/cm^3).

⌘Merge plates of tightly packed 'dummy atoms' to x-y faces of polymer cell. Placing charges on these plates will simulate the electric poling field.



View of parent box (red) within the systems periodic boundaries.



The parent cell containing a five-mer polyimide and plating atoms.

⌘Molecular dynamics was done to obtain a starting configuration.

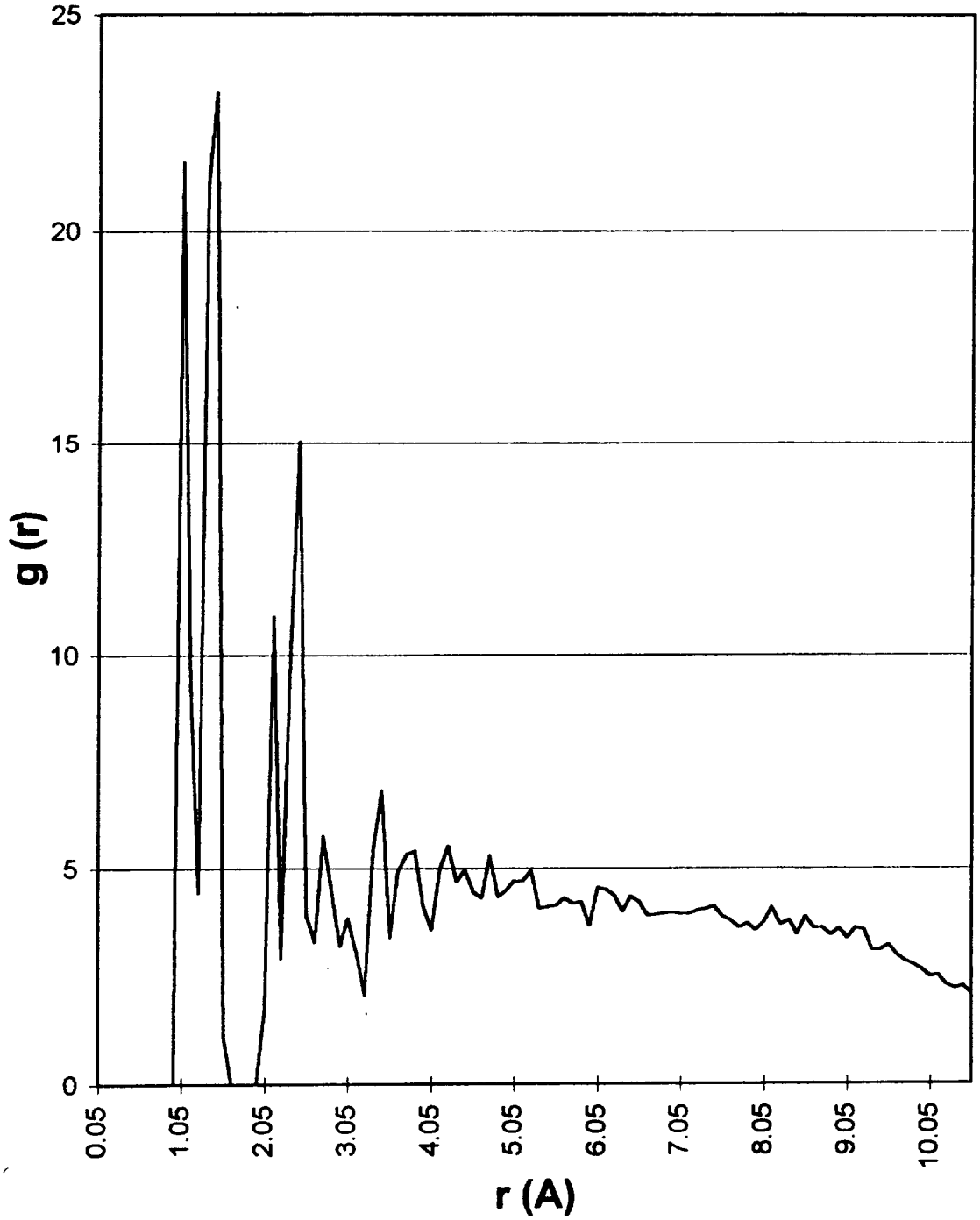
- ❖ The plates of dummy atoms were fixed in space.
- ❖Group based non-bonded cutoffs of 9.5 A for the Lennard Jones contribution and 17.5A (the distance between the plates) for the Coulombic terms were used.

⌘The total pair distribution function is the probability of finding any two atoms at a distance r apart relative to the expected probability for a homogeneous system with random atoms.

$$g(r)=(N_r*V) / (N*4*\pi*r^2*dr)$$

- ❖The peaks are associated with specific covalent bonds and interatomic distances along the rings. The absence of peaks at long distances, r>5A, indicates the lack of long range order in the system.

Pair Distribution Function



POLE MATERIAL

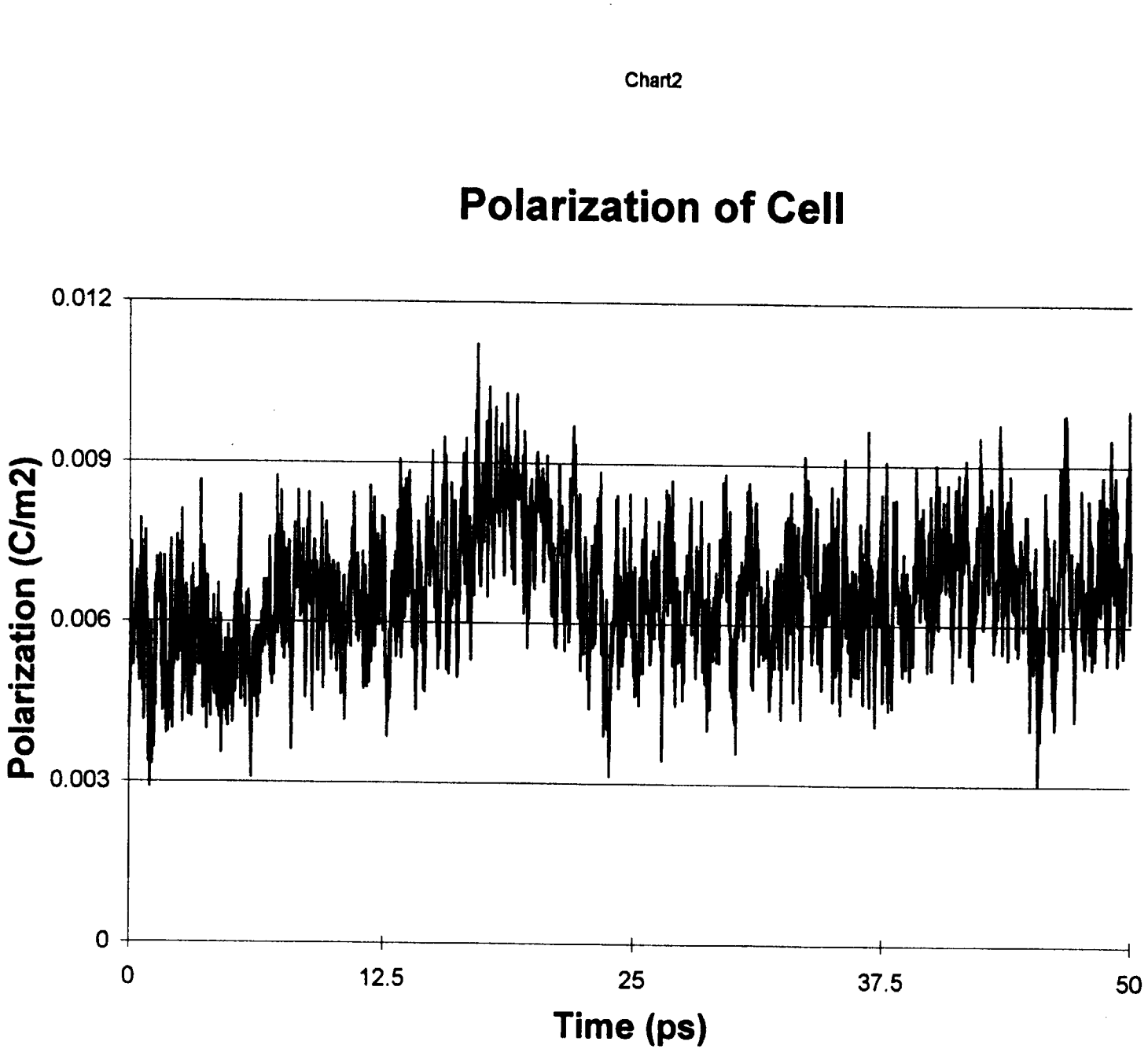
Molecular dynamics was used to simulate the poling of the material.

Following Experimental Variables

- A poling field of 150 MV/m (+/- 0.013 e^-/plating atom) was placed on the system at T_p=500K.

- 50ps for dynamics were run at 500K.

- System was cooled to 300 K in 10 K steps each lasting 10 ps. Once at 300 K the system was simulated for 50 ps.



A small polarization of 0.006 C/m2 was obtained when using experimental parameters.

Collapse Time Scale

⌘ Dipole relaxation times are of the order of micro-seconds. Molecular dynamics calculations cover only the pico-second / nano-second range.

⌘ Collapse the time scale of the polarization process into the pico-second range.

❖Translate time and temperature.

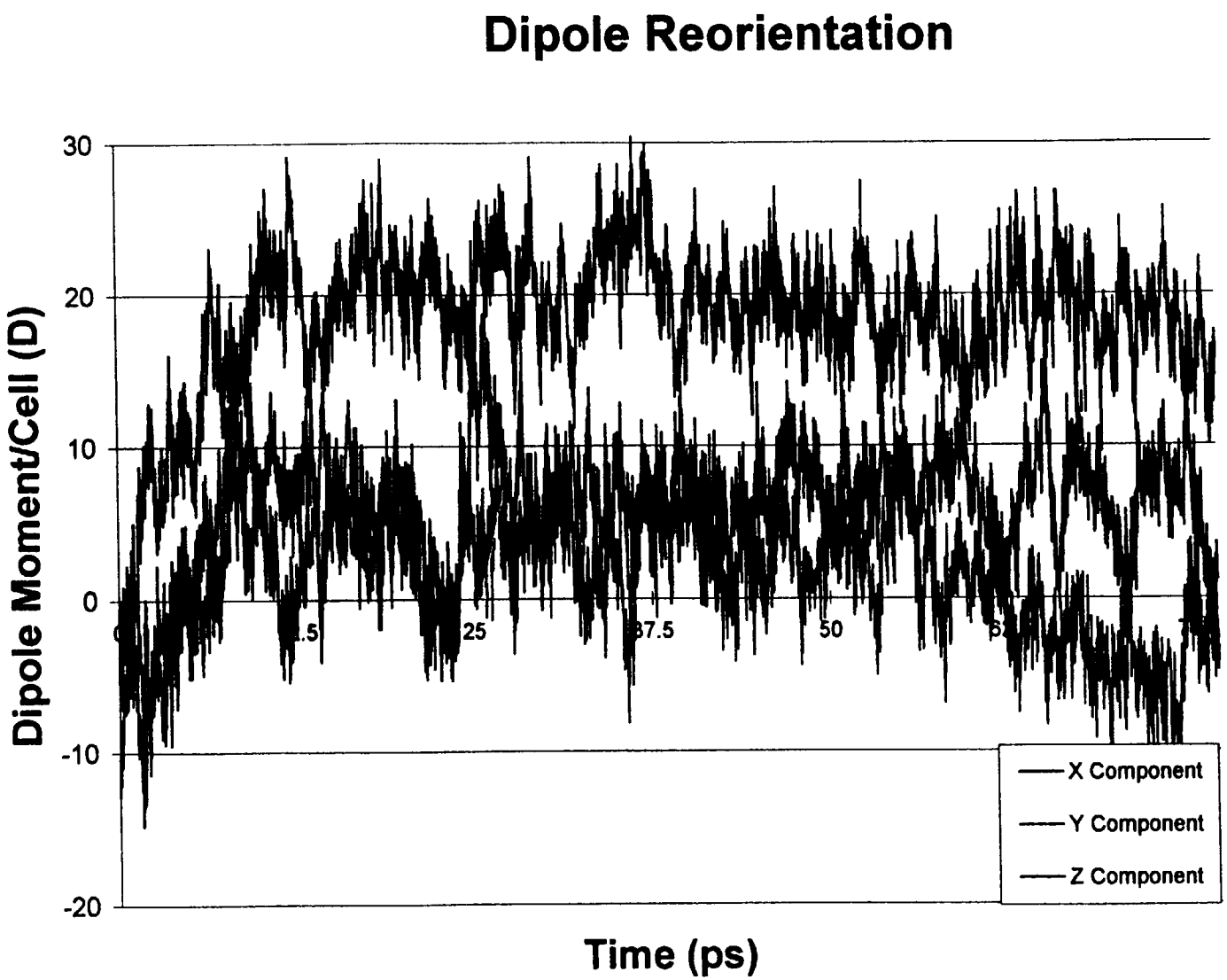
$$\tau = [3\varepsilon_s/(2\varepsilon_s+\varepsilon_\alpha)]*[h/kT]*[\exp(\Delta F/kT)]$$

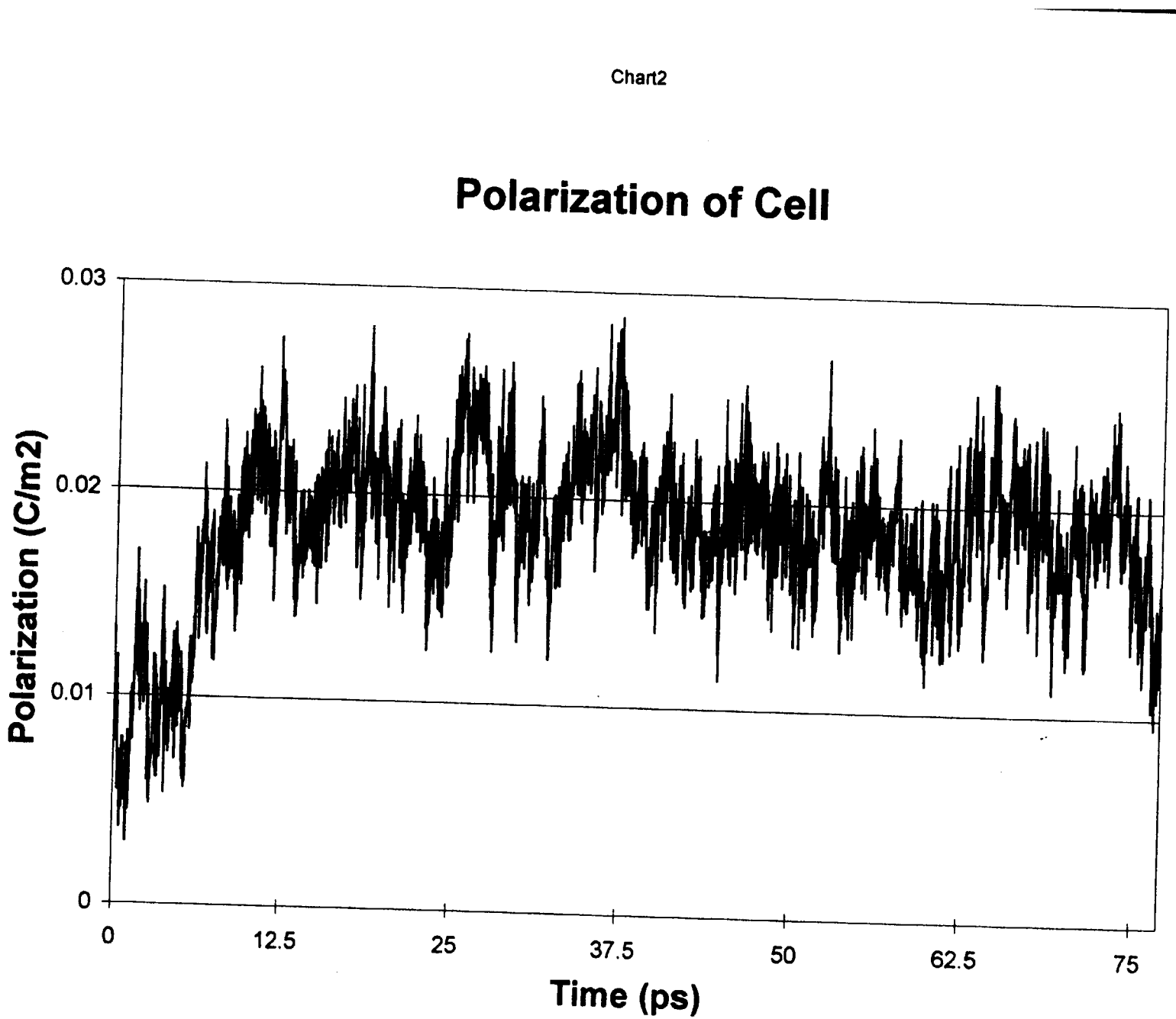
❖ Maintain the population densities of the dipoles.

$$\mathbf{mE} / kT$$

- Collapsed parameters for dynamics simulation.
  - T_p = 2100 K
  - E_p = 700 MV/m (i.e. +/- 0.052 e^-/plating atom)

The calculated polarization of 0.02 C/m^2 is obtained when using the parameters obtained after collapsing the time scale.


Dipole Reorientation
30
20
10
0
-10
-20
Dipole Moment/Cell (D)
25
50
Time (ps)
X Component
Y Component
Z Component



A polarization of 0.02C/m2 was obtained when using the collapsed time scale parameters

CONCLUSIONS

♋ Force field parameters were corrected then validated to give agreement with quantum mechanical results.

♋ The bulk polyimide was modeled by creating a two dimensionally periodic amorphous cell.

♋ Computer simulation techniques have been developed to model the poling of amorphous polyimides.

- ♓ High temperatures and high poling fields were used to account for the long relaxation times.
- ♓ Polarizations of 0.02 C/m^2 were calculated for the polyimide.

FUTURE WORK

- Construct and simulate several initial configurations to achieve better statistics.

- Calculate piezoelectric response by monitoring dipole orientation during constant stress dynamics.

- Analyze molecular motions which occur as a result of the poling and deformation processes.

- Propose novel polyimide structures and rank their piezoelectric responses, calculation of absolute values is not the focus of this research.

ACKNOWLEDGMENTS

We would like to thank the following:

NASA Langley the sponsor of this project:
The Graduate Student Researchers Program

Joycelyn O. Simpson of NASA Langley Research Center, Hampton, VA for providing the experimental input.

Fiona Case of BIOSYM Technologies,San Diego, CA for providing software support.

Monte Carlo Simulation of a Polyimide Melt

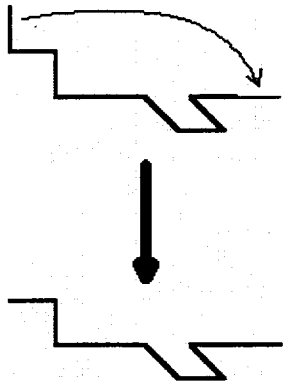
Monte Carlo

- Bridge the gap between sub-microscopic and macroscopic
  - Retain knowledge and detail of sub-microscopic system
  - Determine macroscopic quantities
- Larger system sizes
- Faster simulations (larger time frame available)

Types of Monte Carlo

- Slithering Snake
- Kink-Jump
- Bond Fluctuation

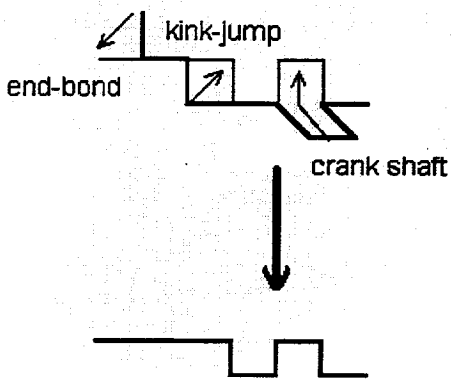
Slithering Snake Monte Carlo



- One move type
- Unrealistic on local scale

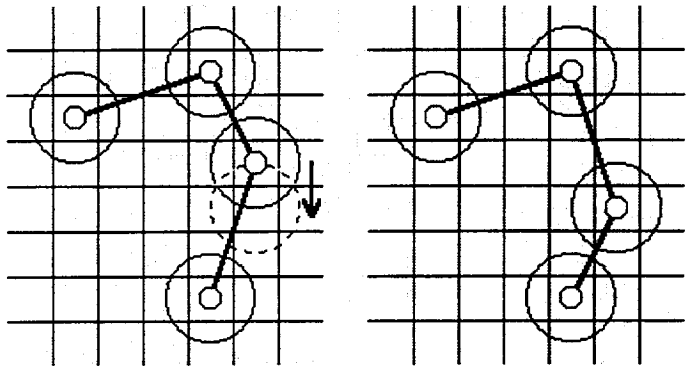
T. Wall and F. Mandel, *J. Chem. Phys.* **63**, 4592 (1975)

Kink Jump Monte Carlo



H. Verdier and W. H. Stockmayer, *J. Chem. Phys.* **36**, 227 (1962).

Bond Fluctuation Monte Carlo



1. H. P. Deutsch and K. Binder, *J. Chem. Phys.* **94**, 2294 (1991).
2. W. Paul, K. Binder, J. Batoulis, B. Pittel and K. H. Sommer, *Makromol. Chem., Macromol. Symp.* **65**, 1 (1993).
3. M. Schulz and J. U. Sommer, *J. Chem. Phys.* **96**, 7102 (1992).
4. J. U. Sommer, M. Schulz and H. L. Trautenberg, *J. Chem. Phys.* **98**, 7515 (1993).

Bond Fluctuation vs Kink-Jump

BFMC	KJMC

ADVANTAGES

BFMC	KJMC
☐ Computationally more efficient	☐ Longer move length
☐ One move type	☐ Faster equilibration in less dense systems
☐ Acceptance probability higher	
☐ Faster equilibration in dense systems	

DISADVANTAGES

BFMC	KJMC
☐ Short move length	☐ Three types of motion
☐ More steps to reach equilibrium	☐ Lower acceptance probabilities
☐ Slower equilibration time in less dense systems	☐ Computationally less efficient
	☐ Slower equilibration time in dense systems

Bond Fluctuation Monte Carlo: The details

Allowed motion:

P(1,0,0)

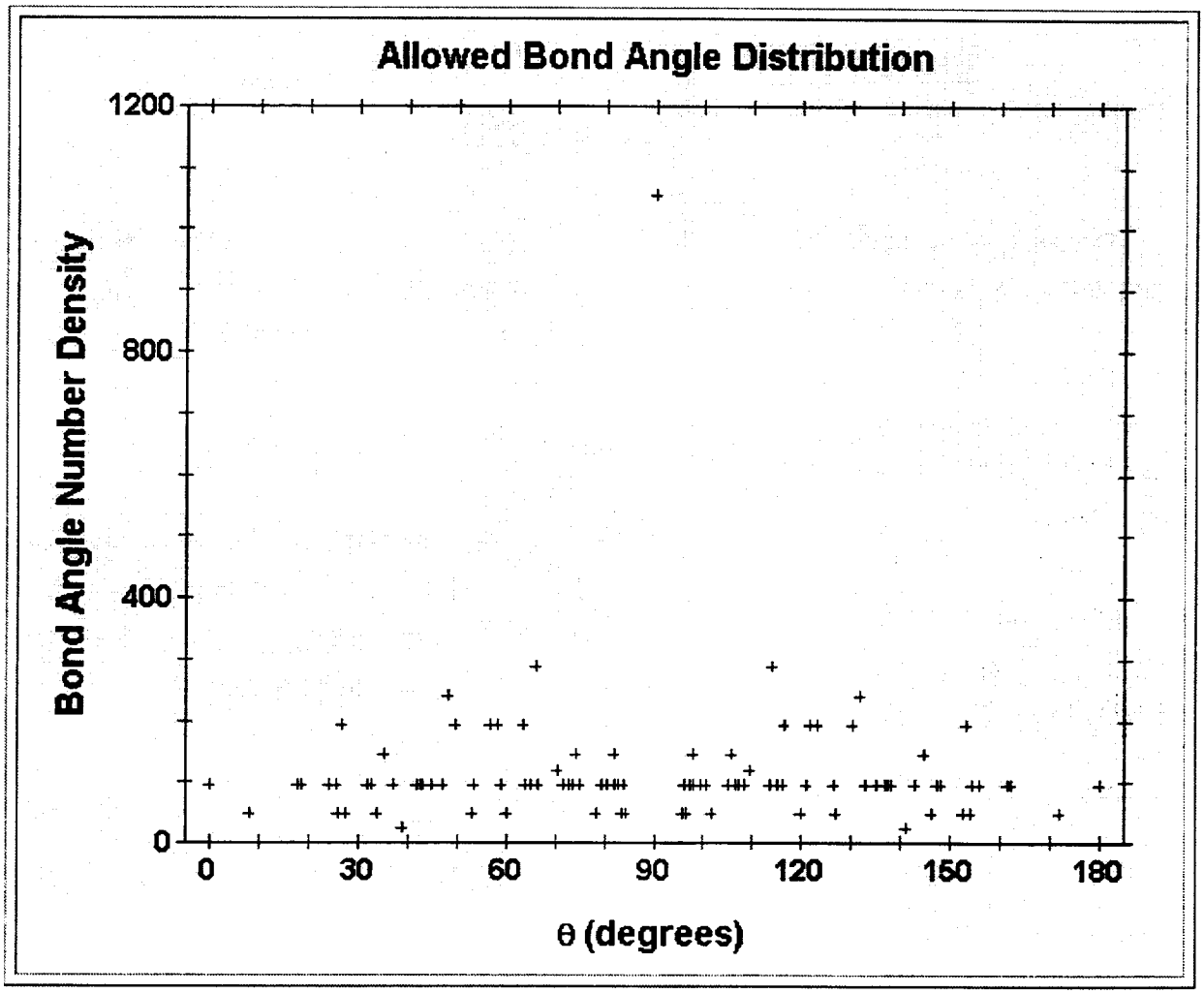
Allowed bond vectors:
Union of:

p(2,0,0), **p**(2,1,0),
p(2,1,1), **p**(2,2,1),
p(3,0,0), **p**(3,1,0)

This yields 108 Bonds with 5 different bond lengths

$b = 4^{1/2}$ (2), $5^{1/2}$, $6^{1/2}$, $9^{1/2}$ (3), $10^{1/2}$

Two successive bonds may have up to 87 different angles over the interval [0-180] degrees.


Allowed Bond Angle Distribution
Bond Angle Number Density
1200
800
400
0
0
30
60
90
120
150
180
θ (degrees)

Summary of Restrictions

Excluded Volume:

The surrounding 26 grid locations must be vacant.

Bond Vector:

Set of allowed bond vectors prevents intrachain crossing.

Allows only 5 bond lengths.

Allows only 87 bond angles.

What About Energetics?

Metropolis Transition Probability: $w = \min[1, e^{(-E/kT)}]$

Energy Restrictions

- **Psuedo Bond Length**

  No Restrictions

- **Bond Angles**

  Restricted by bond bend stiffness (calculated via biosym)

- **"Long Range Torsions"**

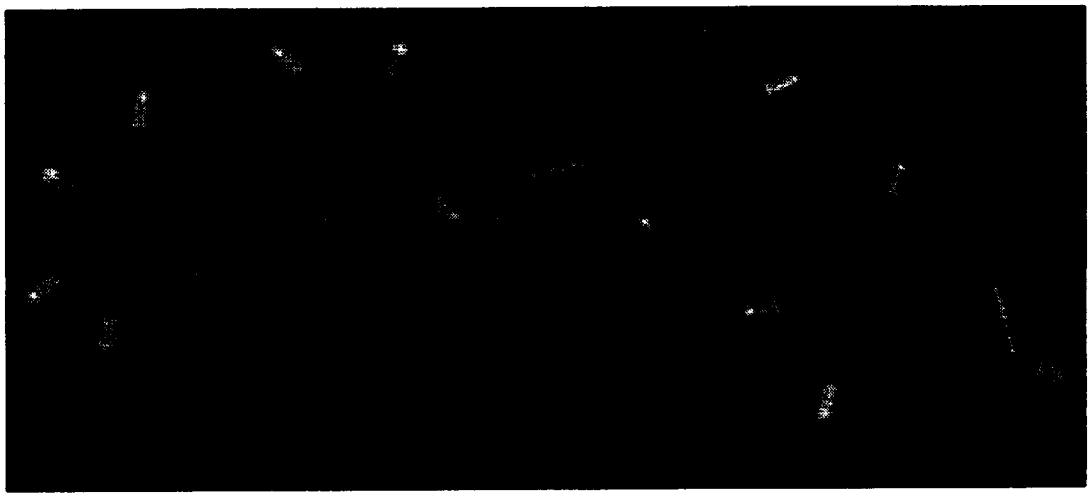
  Calculate Energies for torsions and restrict accordingly

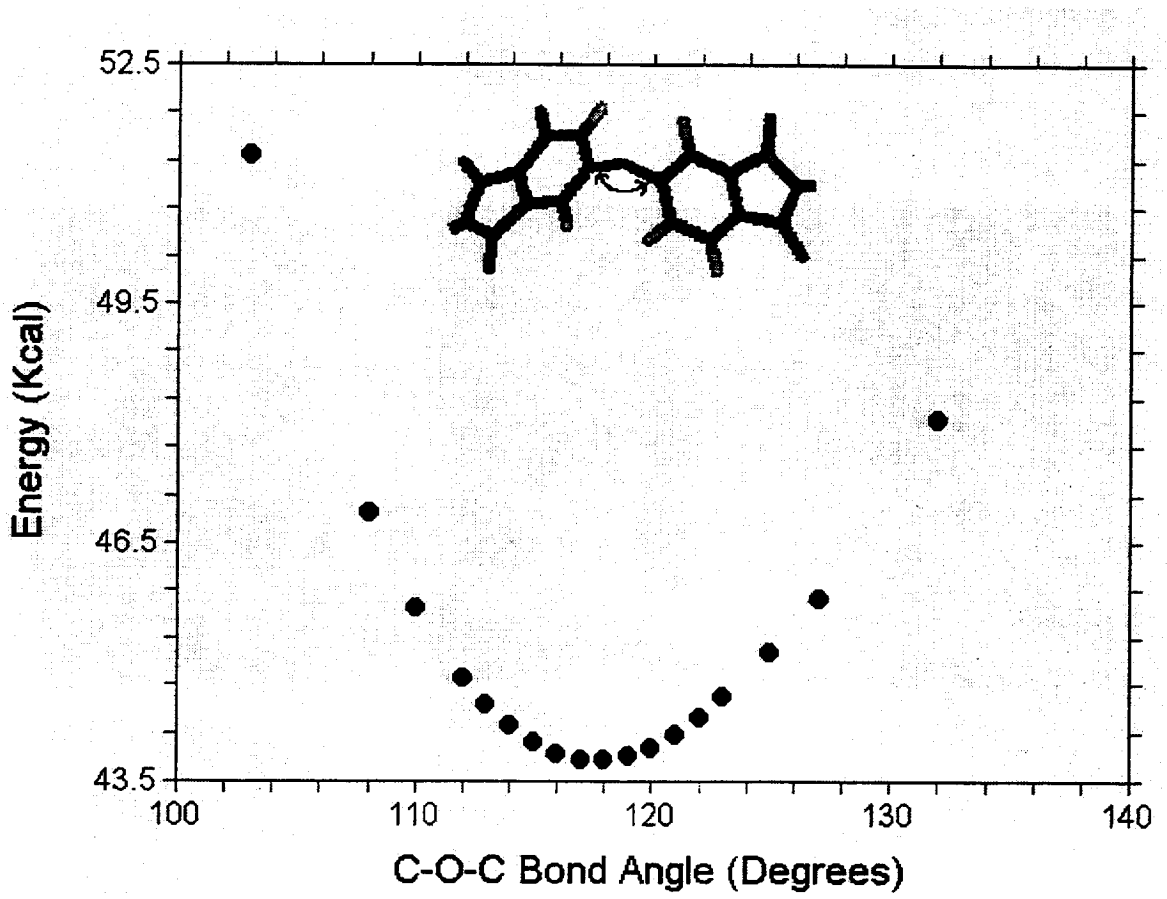
- **Inter-chain interactions:**

  Not accounted for as of yet

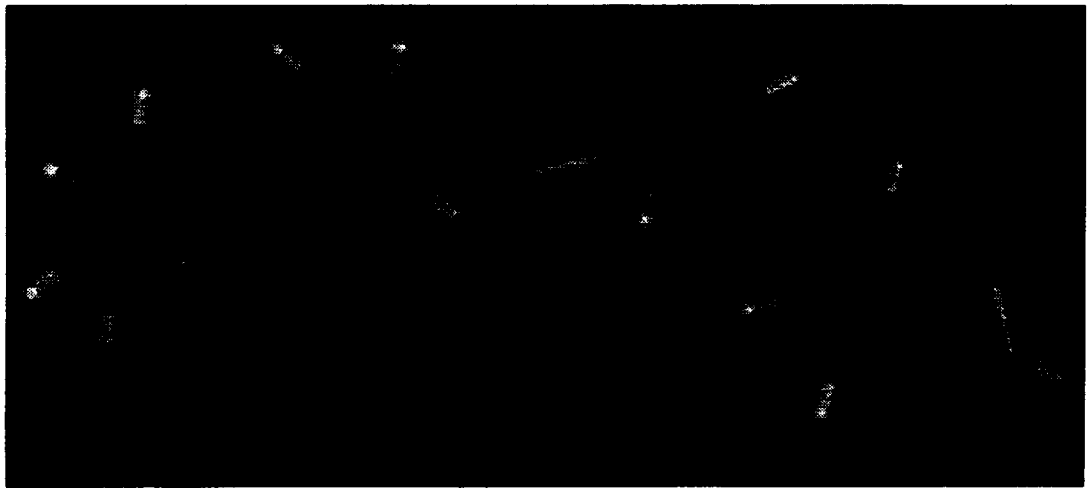
Go to Page Seven

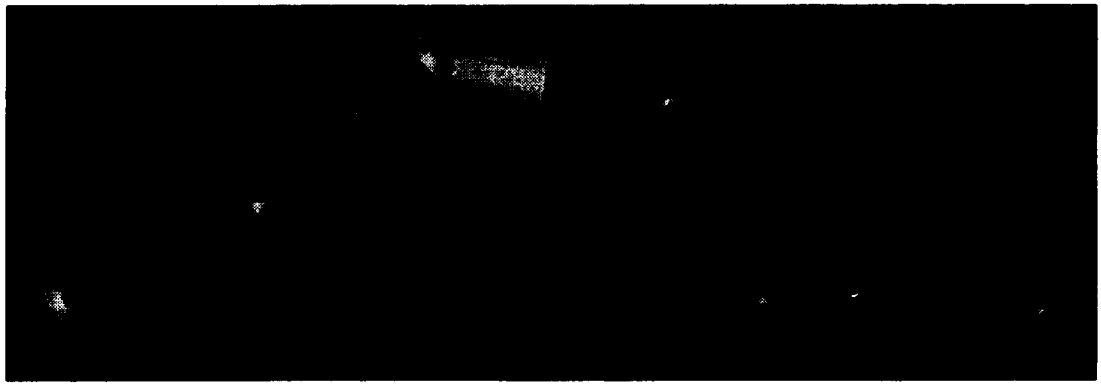
LARC-IA

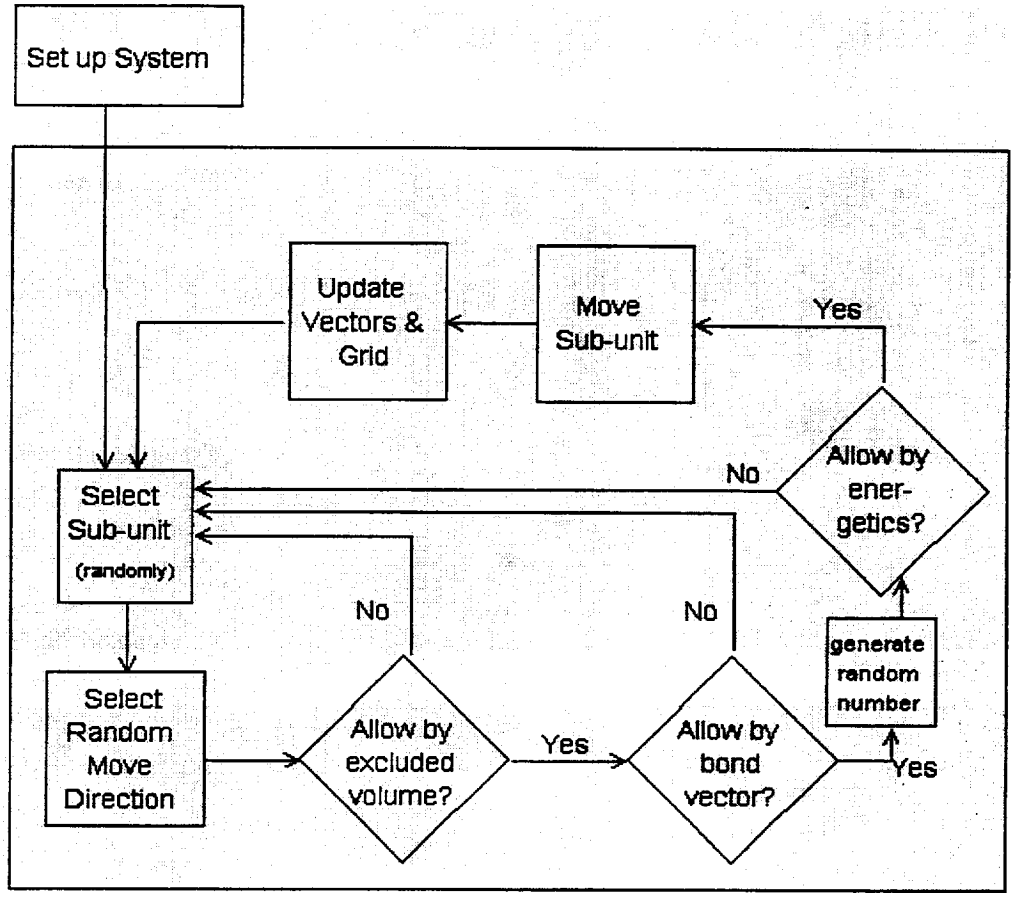



52.5
49.5
46.5
43.5
Energy (Kcal)
100
110
120
130
140
C-O-C Bond Angle (Degrees)

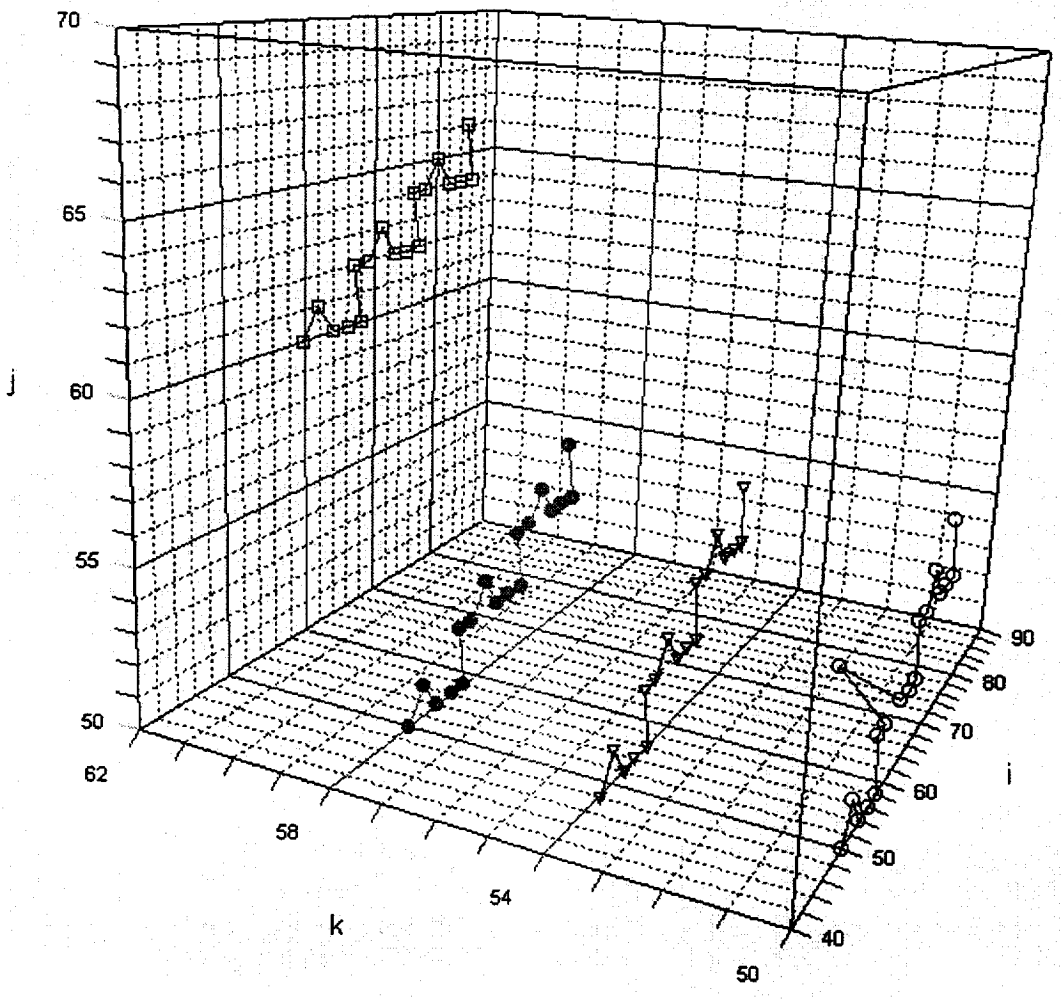
Bond Fluctuation representation of LARC-IA



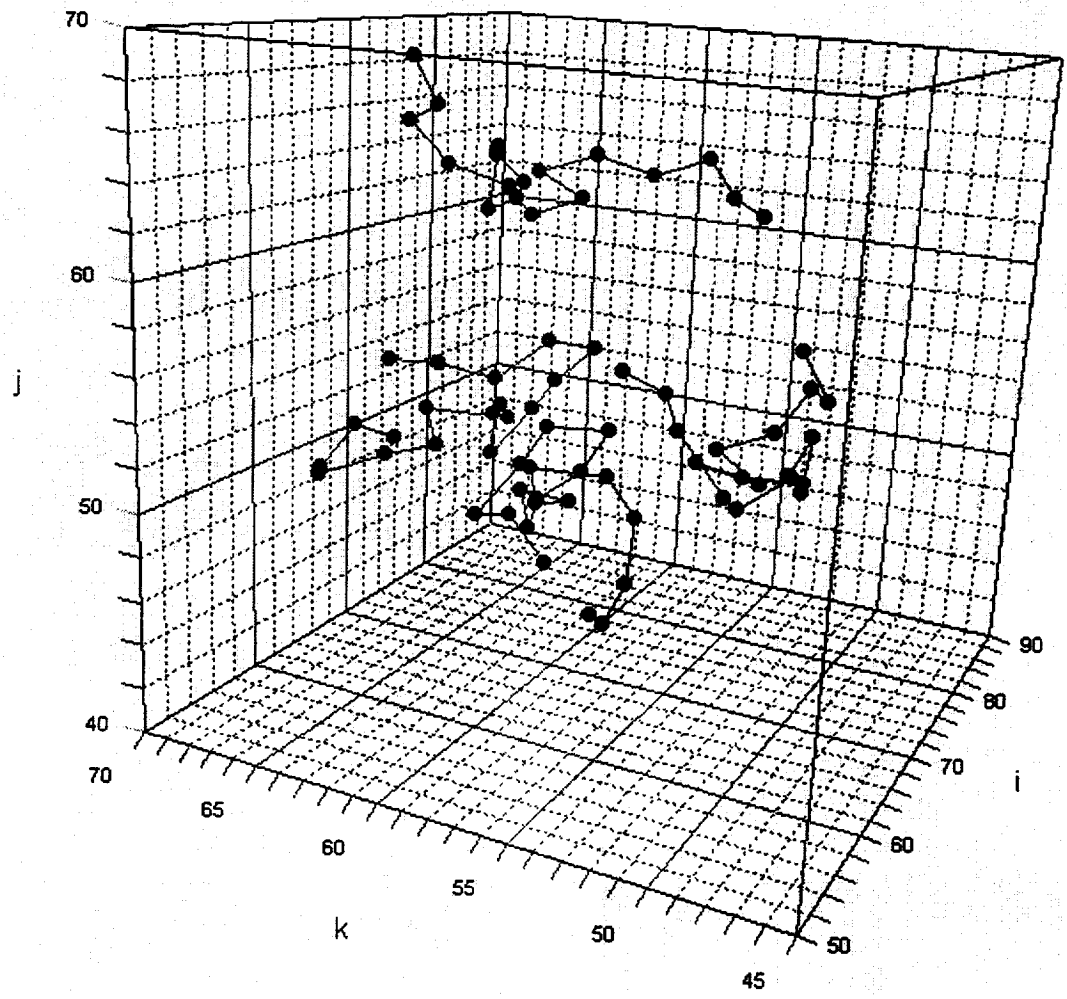



Set up System
Update Vectors & Grid
Move Sub-unit
Yes
Allow by ener-getics?
No
Select Sub-unit (randomly)
No
No
generate random number
Select Random Move Direction
Allow by excluded volume?
Yes
Allow by bond vector?
Yes

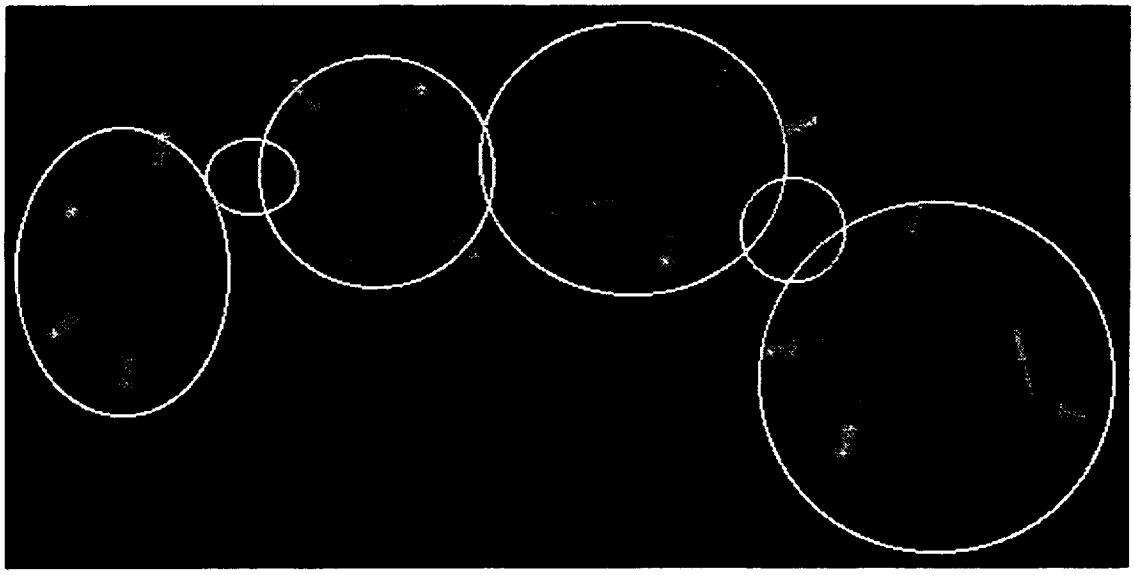
Four Larc-IA Chains
3 monomers each
18 subunits each



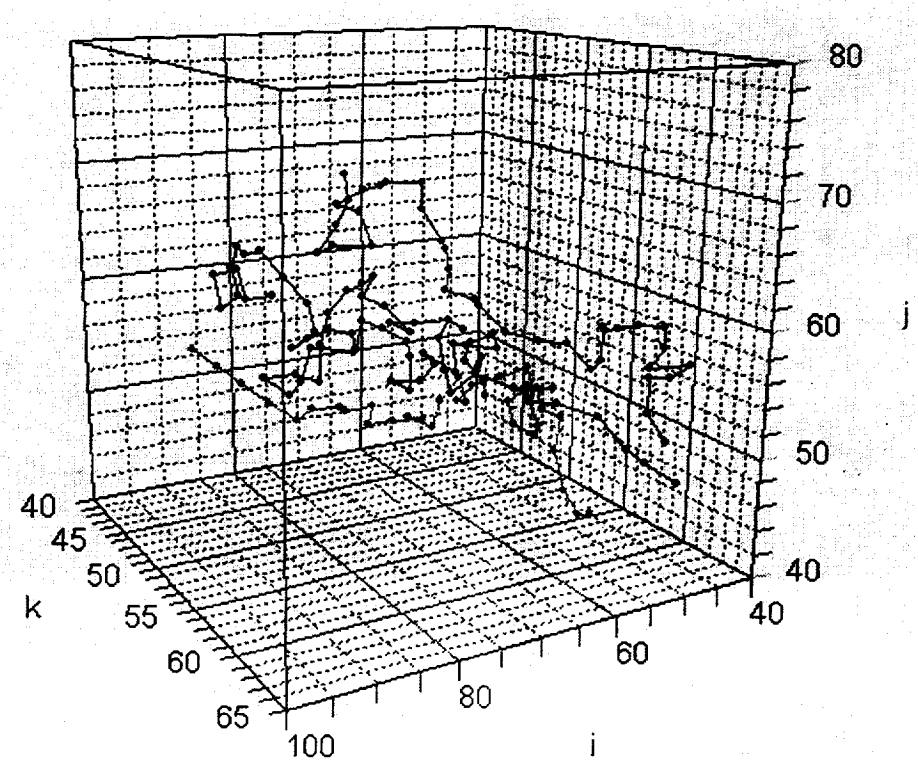
Four Larc-IA Chains
3 monomers each
18 subunits each



Six sub-units of one monomer of LARC-IA



4 Chains of Larc-IA
(6 monomers,6 subunits)
after 50,000 MC steps



Cross Linking

- Allow only end cross linking.
- Chain Ends will be allowed to cross link with other chain ends.
- All restrictions must still be met.
- Cross link kinetics as function of MC step (and also Time?).

Computational Materials Workshop, January 4-5, 1996

Equation of State Measurements: Thermal Pressure Coefficient of an Imide-Ketone Model Compound

Robert Orwoll and Rachel Ward
Department of Chemistry
College of William and Mary
Williamsburg, VA 23187

$$\frac{\Delta E_{vap}}{V_{liq}} = \textit{Cohesive Energy Density}$$

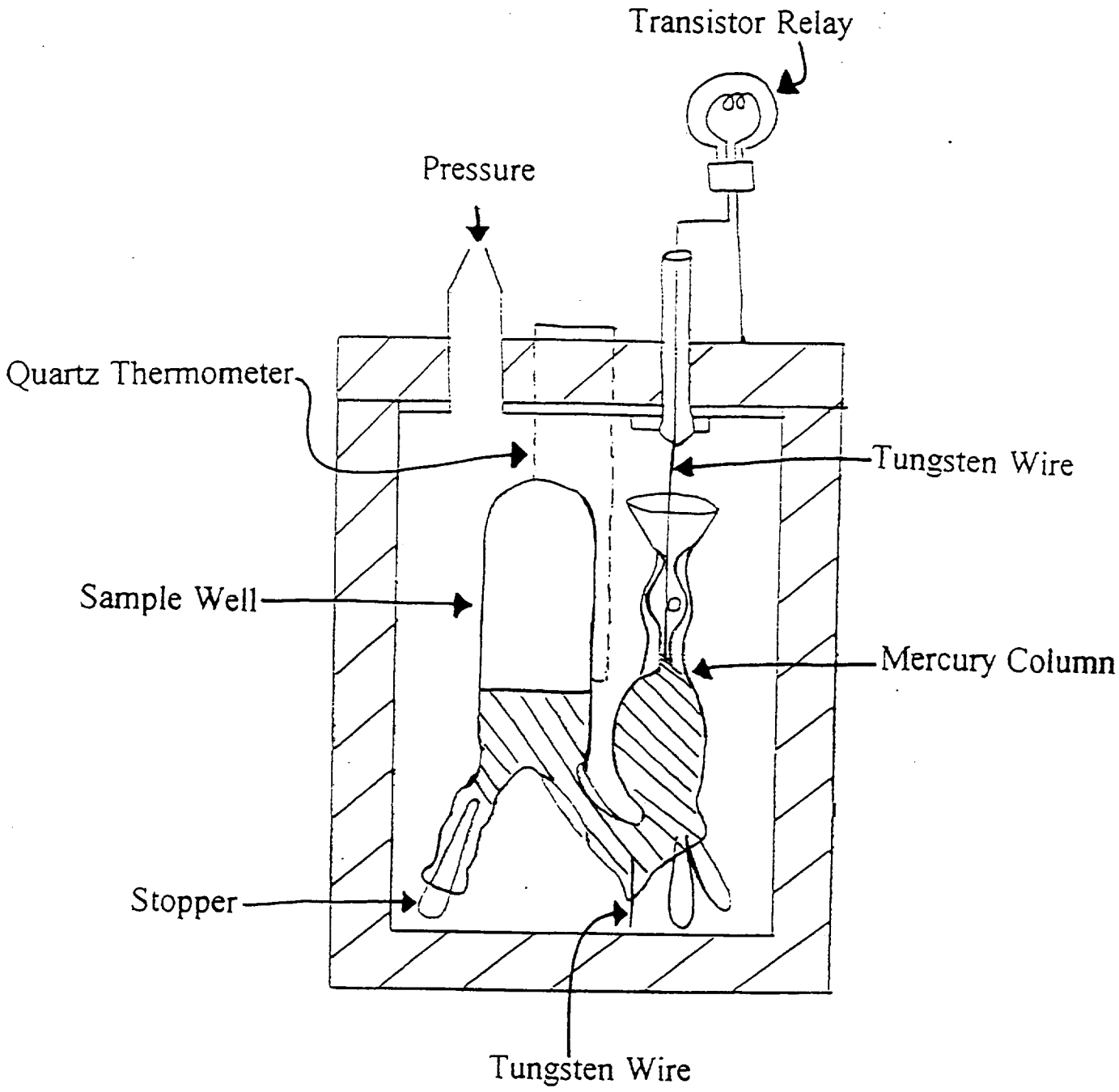
$$p = T\left(\frac{\partial p}{\partial T}\right)_V - \left(\frac{\partial E}{\partial V}\right)_T$$

$$\textit{Internal Pressure} = \left(\frac{\partial E}{\partial V}\right)_T = T\left(\frac{\partial p}{\partial T}\right)_V - p$$

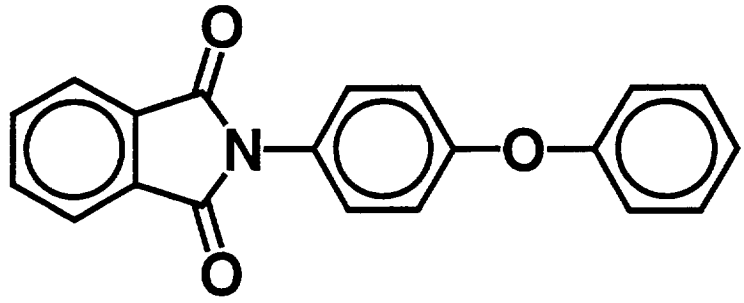
$$\left(\frac{\partial p}{\partial T}\right)_V = \frac{\frac{1}{V}\left(\frac{\partial V}{\partial T}\right)_p}{-\frac{1}{V}\left(\frac{\partial V}{\partial p}\right)_T}$$

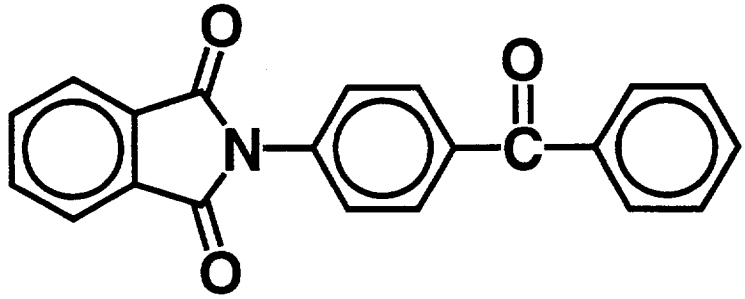
$$\textit{Thermal Pressure Coefficient} = \gamma_V = \frac{\alpha_p}{\kappa_T}$$

THERMODYNAMIC RELATIONSHIPS CONNECTING THE DESIRED $(\partial E/\partial V)_T$ AND THE MEASURED THERMAL PRESSURE COEFFICIENT $(\partial p/\partial T)_V$

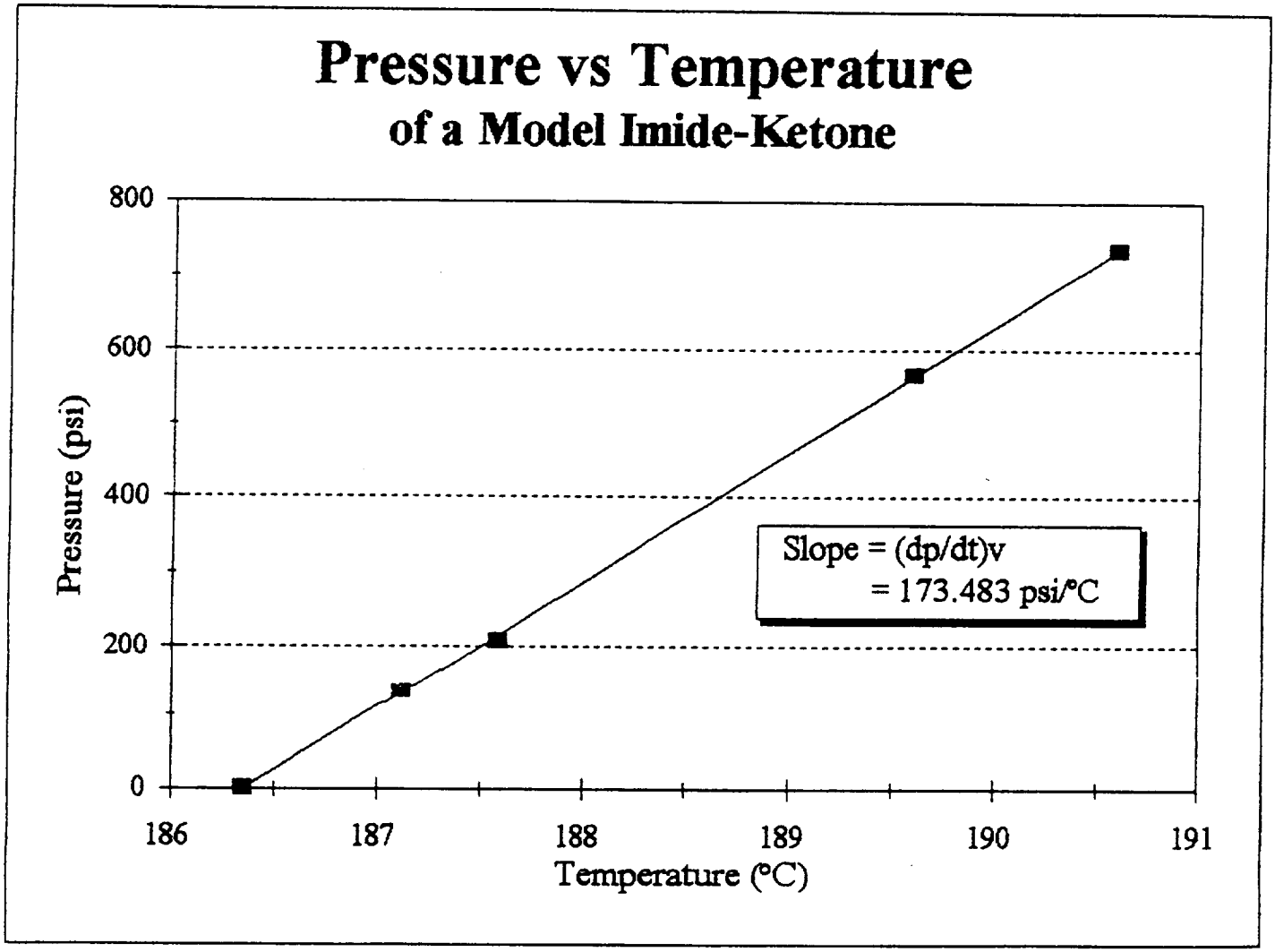


"CONSTANT" VOLUME CELL FOR MEASURING THE THERMAL PRESSURE COEFFICIENT





MOLECULAR STRUCTURES FOR THE MODEL ETHER-IMIDE (TOP) AND KETONE-IMIDE (BOTTOM)



RESULTS FOR THE KETONE-IMIDE (BEFORE CORRECTION FOR THE EXPANSION AND COMPRESSION OF THE MERCURY AND GLASS)

Comparison with Other Amorphous Compounds

	$(\partial E/\partial V)_T$, J/cm^3	Temp, °C
n-octane	265	25
benzene	379	25
cyclohexanone	413	25
poly(dimethyl siloxane)	145	180
polyethylene	275	180
polyethylene oxide	433	100
imide ketone	440	186

p-V-T Results to Date

Model Cmpd	CTE = $(1/V)(\partial V/\partial T)_p$, K^{-1}	$(\partial E/\partial V)_T$, J/cm^3
imide ketone	6.59×10^{-4} ($\pm 3 \times 10^{-6}$)	440±10
imide ether	6.83×10^{-4} ($\pm 3 \times 10^{-6}$)	next measurement

Mechanical Properties from Acoustical Measurements on LaRC-SI

Tom Yost and John Cantrell

Outline

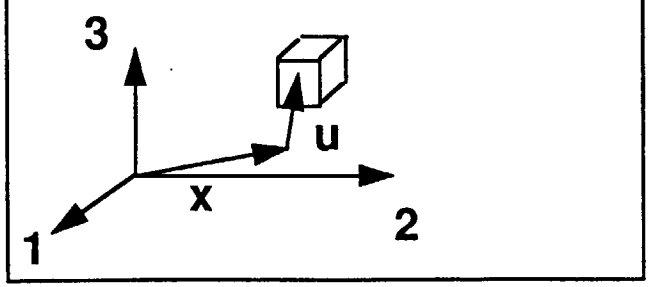
1. Relationship between acoustical measurements and mechanical properties. The application of F=ma to the material, the results from which elastic constants and engineering moduli can be determined.
2. Thermodynamic definitions for major concepts in above.
3. Schematic view of ultrasonic measurement system.
4. Measurements to determine the effects of molecular weight on engineering moduli, and discussion.
5. Future Plans

1. Relationship between Acoustical Measurements and Moduli

Relationship between Acoustical Measurements and Mechanical Properties

- We begin with the force acting on a small segment of isotropic material. We apply F=ma to the segment.
- This leads to the equation

$$\frac{\partial \sigma_{s1}}{\partial x_1} + \frac{\partial \sigma_{s2}}{\partial x_2} + \frac{\partial \sigma_{s3}}{\partial x_3} = F_s$$



$$\frac{\partial \sigma_{sk}}{\partial x_k} = \rho \ddot{u}_s$$

where

u is the particle displacement,

ρ is the density

x_k is the particle location (at rest)

σ_{sk} is the stress acting on the segment

Hooke's Law

- For the general case Hooke's Law can be expressed as

$$\sigma_{sk} = c_{sklm} \varepsilon_{lm}$$

where the c_{sklm} are the second-order elastic constants

- The strain is expressed as

$$\varepsilon_{lm} = \frac{1}{2}\left(\frac{\partial u_l}{\partial x_m} + \frac{\partial u_m}{\partial x_l} + \frac{\partial u_p}{\partial x_m}\frac{\partial u_p}{\partial x_l} \right)$$

The Wave Equation

- Combining Eq. 1 with Hooke's Law we obtain

$$\rho \ddot{u}_s = c_{sklm} \frac{\partial^2}{\partial x_k \partial x_l} u_m$$

- Consider a plane harmonic travelling wave of the form

$$u_s = A_s e^{i(k_j x_j - \omega t)}$$

where A_s are the amplitudes of the displacement components

k_j are the components of the wave vector (magnitude of wave vector= $2\pi/\lambda$)

ω is the angular frequency of the wave (= $2\pi f$, f is frequency)

i is the square root of -1

Wave Speed and Elastic Constants

- We substitute the expression for the wave into the equation of motion and obtain

$$\rho \omega^2 u_s = c_{sklm} k_k k_l u_m$$

which gives

$$(\rho \omega^2 \delta_{sm} - c_{sklm} k_k k_l) u_m = 0$$

and finally to the relationship between the elastic constants and the wave velocity

$$| c_{sklm} n_k n_l - \rho c^2 \delta_{sm} | = 0$$

Elastic Constants and Engineering Moduli

- Once the elastic constants are determined the engineering moduli (Young's Modulus,E, Poisson's contraction, μ, and bulk modulus, K, can be determined. For an isotropic material with Lame' constants, λ and G, we have

$$E = \frac{G(3\lambda + 2G)}{\lambda + G}$$

$$\mu = \frac{\lambda}{2(\lambda + G)}$$

$$K = \lambda + \frac{2}{3}G$$

where

$$\lambda = c_{1122} = c_{1133} = c_{2233}$$

$$G = \frac{1}{2}(c_{1111} - c_{1122})$$

$$= c_{2323} = c_{3131} = c_{1212}$$

2. Thermodynamic Basis

Thermodynamic Definitions of Elastic Constants

- The elastic constants can also be defined in terms of thermodynamic variables

$$c^{S}_{sklm} = \rho \left. \frac{\partial^2 U}{\partial \varepsilon_{sk} \partial \varepsilon_{lm}} \right|_{\substack{\text{(adiabatic conditions)} \\ \text{0 stress}}}$$

where U is the internal energy

- These are the elastic constants used in this study

Thermodynamic Definitions of Stresses and Strains

We start with the second law of thermodynamics and write the differential work in terms of stress and strain. This gives

$$dU = \sigma_{ik} d\varepsilon_{ik} + TdS$$

The Helmholtz free energy is given as

$$F = U - TS$$

$$dF = \sigma_{ik} d\varepsilon_{ik} - SdT$$

The Gibbs free energy is given as

$$\Phi = F - \sigma_{ik} \varepsilon_{ik}$$

$$d\Phi = -SdT - \varepsilon_{ik} d\sigma_{ik}$$

Hence

$$\sigma_{ik} = \left(\frac{\partial U}{\partial \varepsilon_{ik}} \right)_S = \left(\frac{\partial F}{\partial \varepsilon_{ik}} \right)_T \quad \& \quad \varepsilon_{ik} = -\left(\frac{\partial \Phi}{\partial \sigma_{ik}} \right)_T$$

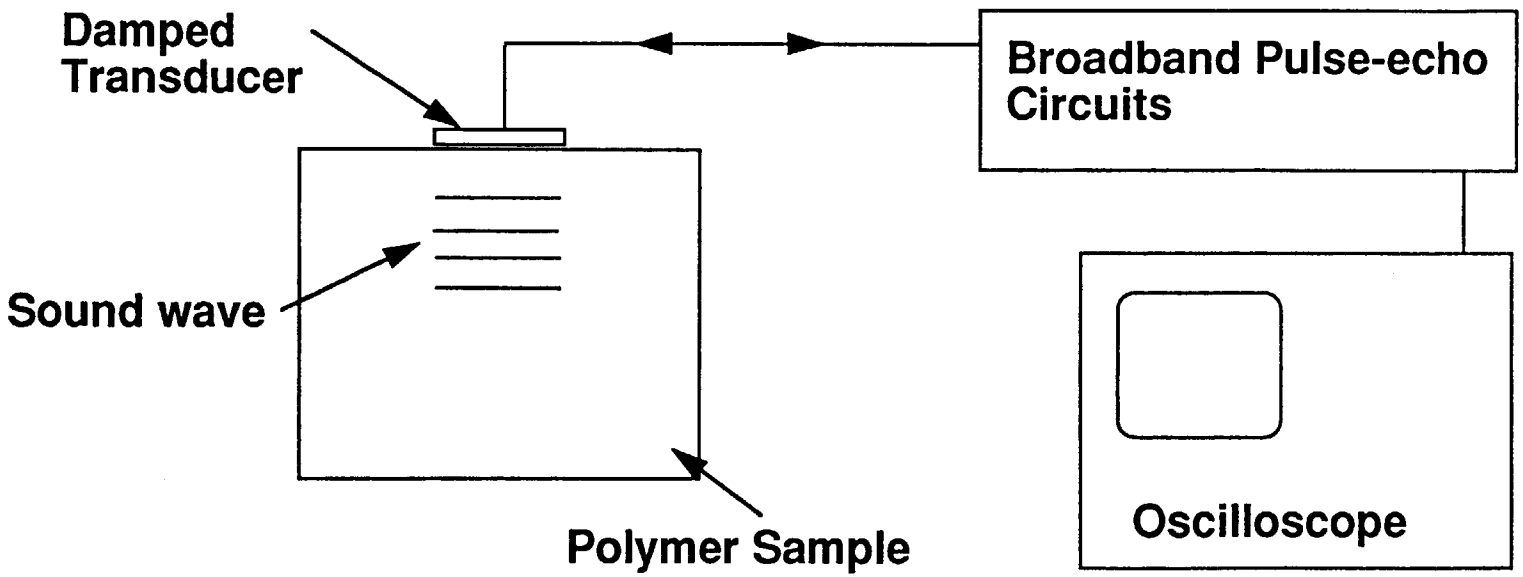
Thermodynamic Definition of Elastic Constants

$$c^{S}_{ijkl} = \rho_0 \left(\frac{\partial^2 U}{\partial \eta_{ij} \eta_{kl}} \right)$$

The elastic constants used in this study are isentropic elastic constants

3. Overview of Ultrasonic Measurements

Viscoelastic Materials and Ultrasonic Measurements (Linear Moduli)



Before measurement the sample thickness is determined. The oscilloscope measures the transit time. From these two measurements the sound velocity can be determined.

This ultrasonic technique measures the unrelaxed second-order moduli of the LaRC-SI sample

4. Sample Set Preparation and Measurements

Five sample sets were prepared from each of the molecular weight offset stocks. Each set consisted of one sample from each molecular weight offset. Every sample was lapped and polished so that the surfaces were flat (to one band of green light) and parallel to better than 20 Arc sec. The following measurements include:

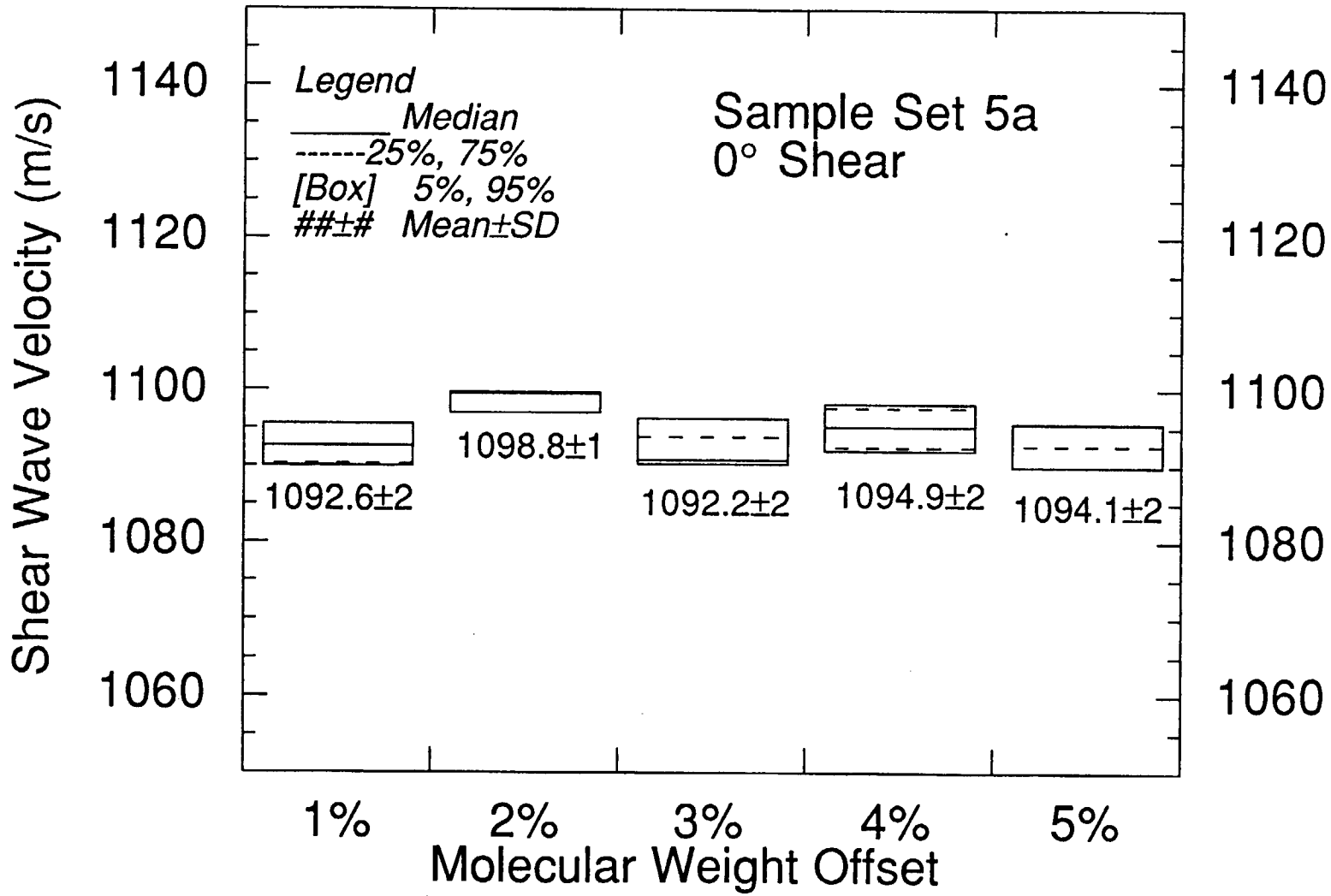
- Density measurements on 5 sample Sets
- Ultrasonic Wave Velocities (Set 5a and Averages)
- Moduli of LaRC-SI at room temperature (Set 5a and Averages)

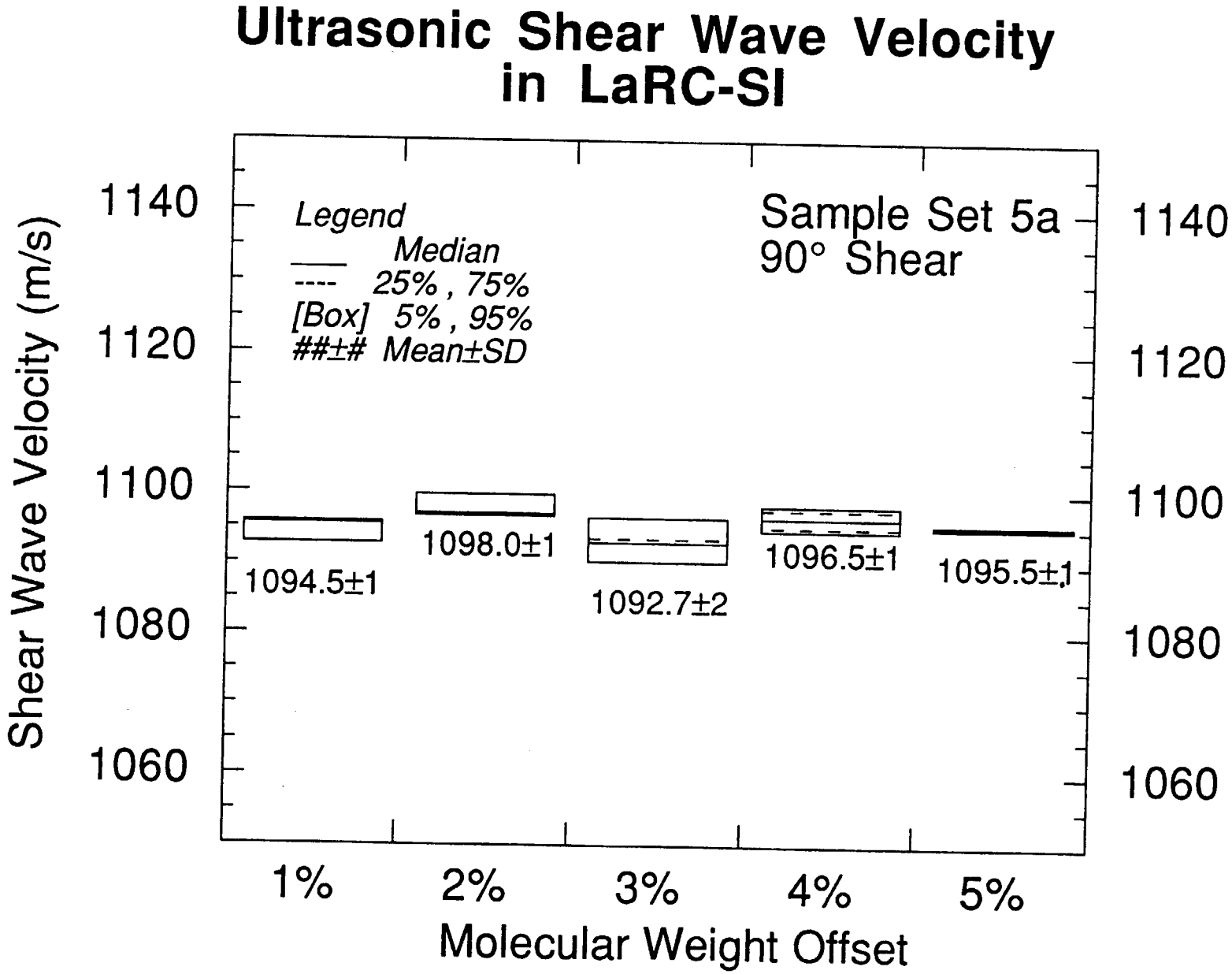
4. Summary of Measurements

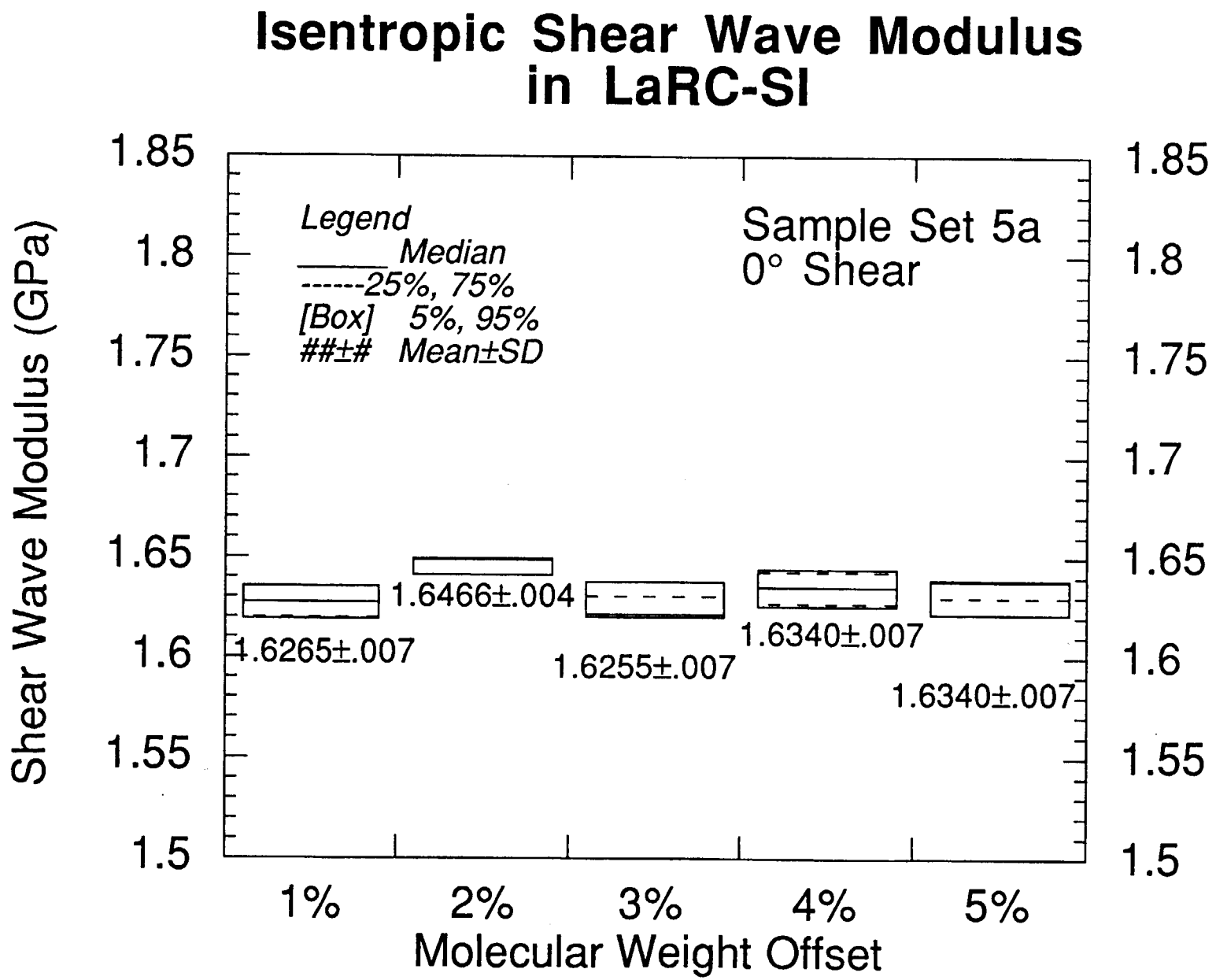
Measurements on a Typical Sample Set

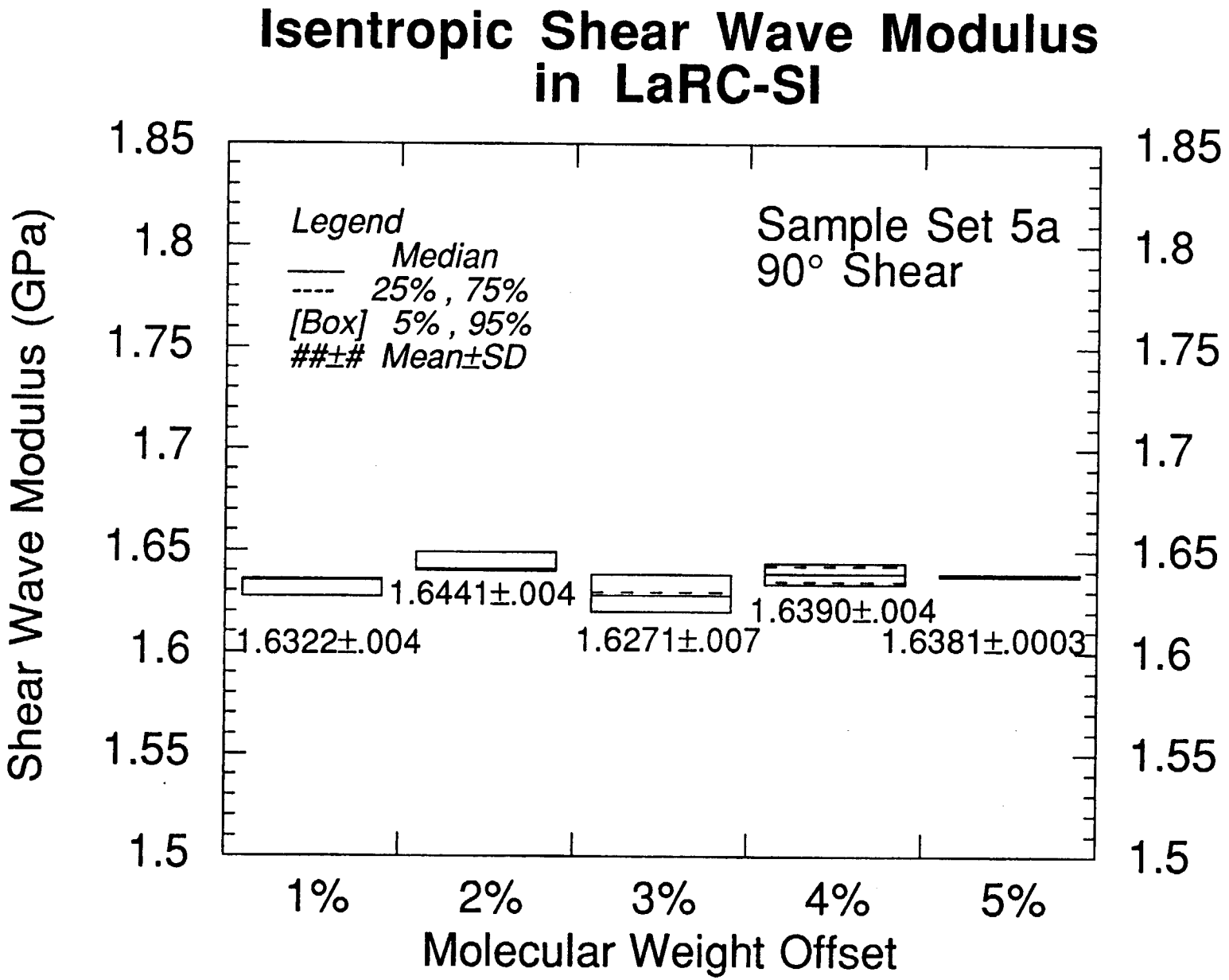
Graphs show compressional and shear velocities as well as moduli calculated from them. Enclosed is a chart of measured densities.

Ultrasonic Shear Wave Velocity in LaRC-SI

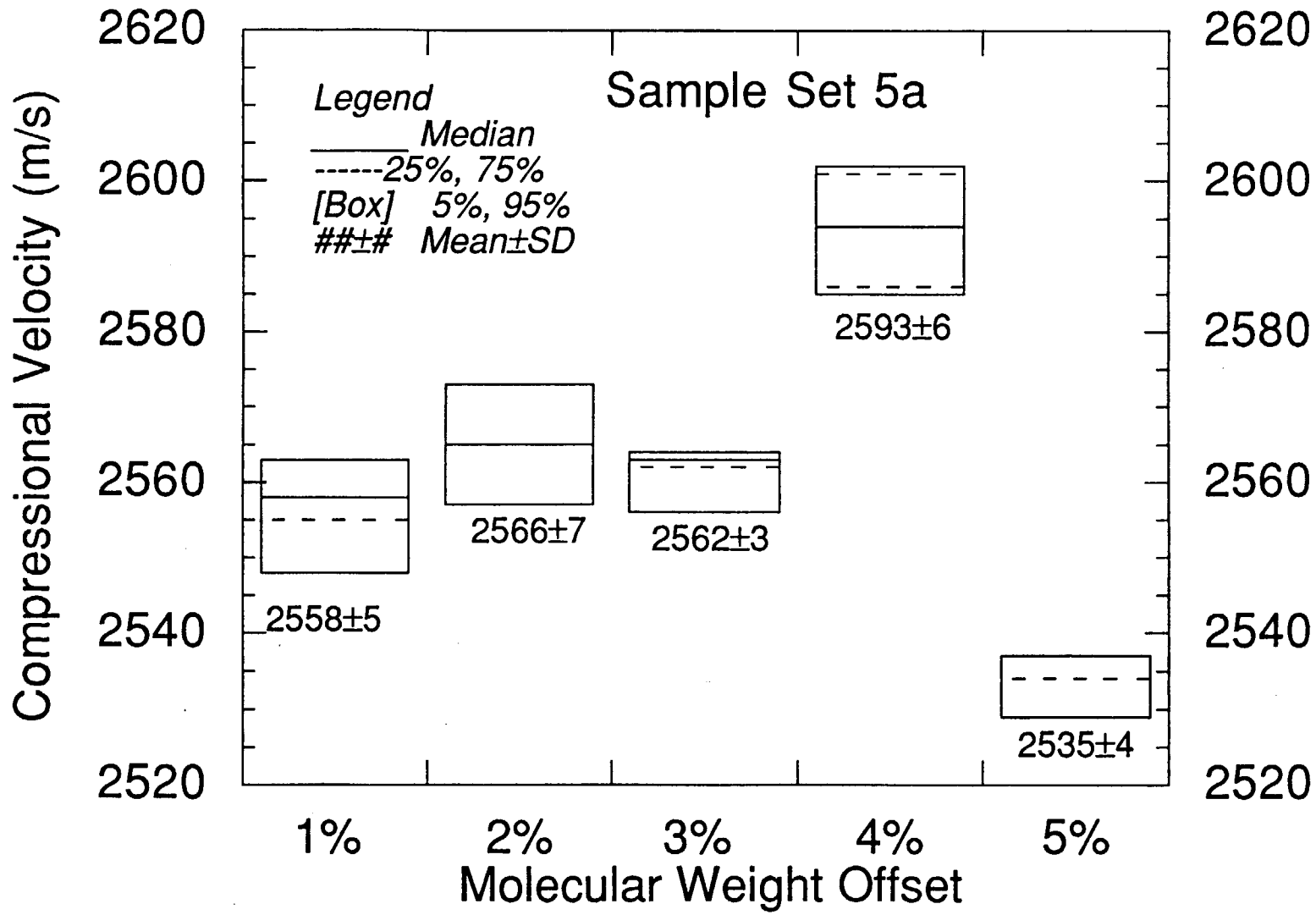


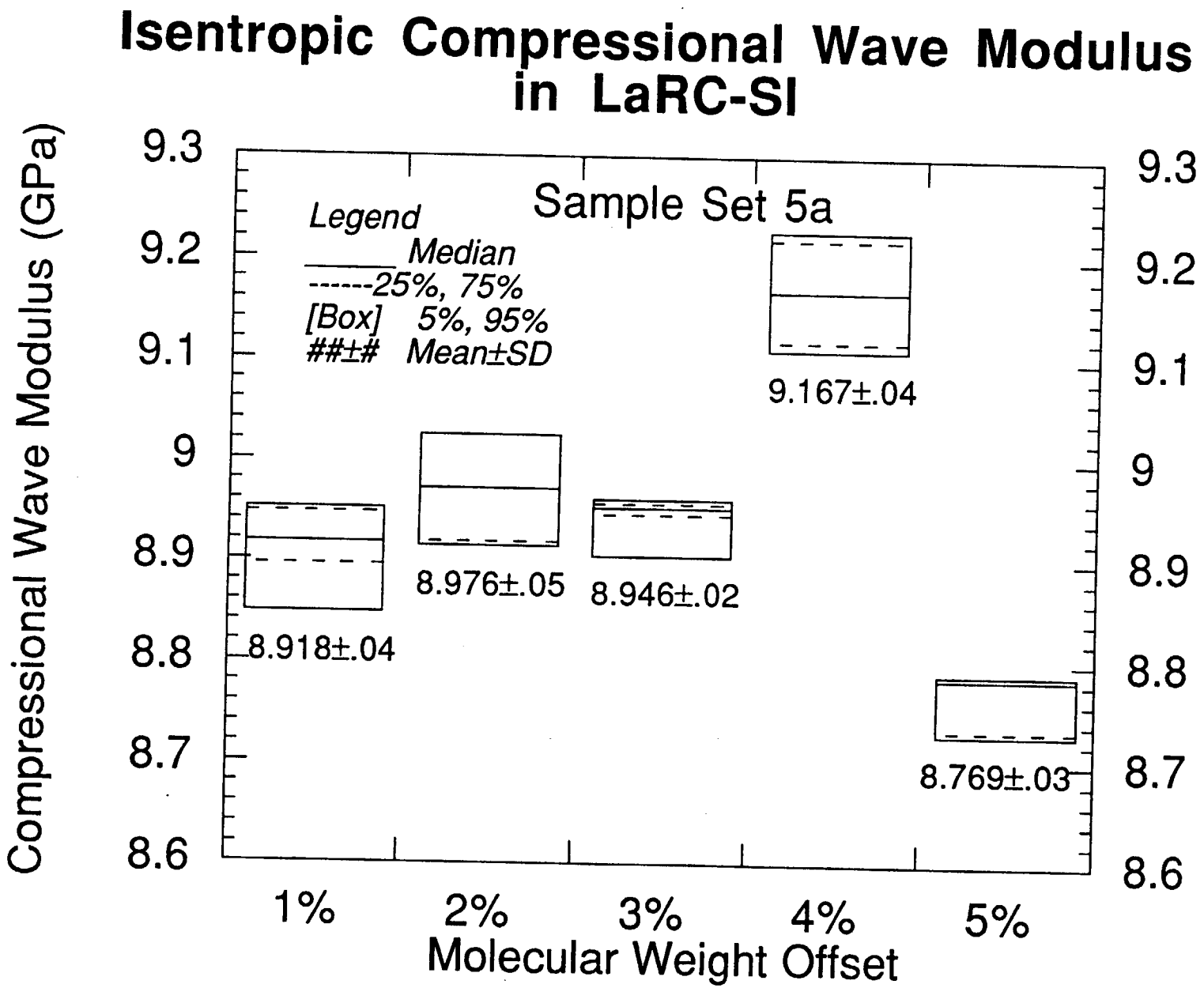

Ultrasonic Shear Wave Velocity
in LaRC-SI
Legend
Median
25%, 75%
[Box] 5%, 95%
##±# Mean±SD
Sample Set 5a
90° Shear
Shear Wave Velocity (m/s)
1140
1120
1100
1080
1060
1094.5±1
1098.0±1
1092.7±2
1096.5±1
1095.5±1
1%
2%
3%
4%
5%
Molecular Weight Offset


Isentropic Shear Wave Modulus
in LaRC-SI
Shear Wave Modulus (GPa)
1.85
1.8
1.75
1.7
1.65
1.6
1.55
1.5
Legend
Median
------25%, 75%
[Box] 5%, 95%
##±# Mean±SD
Sample Set 5a
0° Shear
1.6265±.007
1.6466±.004
1.6255±.007
1.6340±.007
1.6340±.007
1%
2%
3%
4%
5%
Molecular Weight Offset


Isentropic Shear Wave Modulus
in LaRC-SI
Shear Wave Modulus (GPa)
1.85
1.8
1.75
1.7
1.65
1.6
1.55
1.5
Legend
Median
25%, 75%
[Box] 5%, 95%
##±# Mean±SD
Sample Set 5a
90° Shear
1.6322±.004
1.6441±.004
1.6271±.007
1.6390±.004
1.6381±.0003
1%
2%
3%
4%
5%
Molecular Weight Offset

Ultrasonic Wave Compressional Velocity
LaRC-SI




Isentropic Compressional Wave Modulus in LaRC-SI
Compressional Wave Modulus (GPa)
9.3
9.2
9.1
9
8.9
8.8
8.7
8.6
Sample Set 5a
Legend
Median
25%, 75%
[Box] 5%, 95%
##±# Mean±SD
8.918±.04
8.976±.05
8.946±.02
9.167±.04
8.769±.03
1%
2%
3%
4%
5%
Molecular Weight Offset

Measured Density of Molded Samples Using Archimede's Principle

Molecular Weight % Offset	Density (x 10^3 Kg/m^3)
1	1.3624±0.0003
2	1.3635±0.0003
3	1.3628±0.0002
4	1.3612±0.004
5	1.3648±0.0002

Elastic Properties

- Unrelaxed moduli, linear
- Elastic constants, Young's modulus, shear modulus, Poisson's ratio, bulk modulus

Wave Velocities as a Function of Molecular Weight Offset

Molecular Weight Offset	Shear Velocity(m/s) 0°	Shear Velocity(m/s) 90°	Compressional Velocity (m/s)
1%	1.0927±.001	1.0935±.001	2.5589±.005
2%	1.0984±.001	1.0986±.001	2.5659±.003
3%	1.0928±.0007	1.0940±.001	2.5623±.0007
4%	1.0943±.002	1.0949±.002	2.5657±.002
5%	1.0942±.002	1.0948±.002	2.5660±.003

Moduli from Wave Velocities

Molecular Weight Offset	Shear Modulus (GPa) 0°	Shear Modulus (GPa) 90°	Compressional Modulus (GPa)
1%	1.6266±.004	1.6290±.004	8.921±.03
2%	1.6451±.003	1.6456±.003	8.977±.02
3%	1.6277±.002	1.6311±.004	8.948±.005
4%	1.6301±.007	1.6319±.006	8.957±.03
5%	1.6341±.006	1.6358±.006	8.978±.03

Moduli Derived from Ultrasonics Results: Engineering Moduli (Isentropic)

Molecular Weight Offset	Shear Modulus (GPa)	Young's Modulus (GPa)	Poisson's Ratio
1%	1.6278±.004	4.5199±.046	0.3860±.007
2%	1.6453±.003	4.5667±.026	0.3878±.003
3%	1.6294±.004	4.5265±.013	0.3887±.001
4%	1.6320±.007	4.5324±.062	0.3886±.004
5%	1.6350±.006	4.5409±.041	0.3887±.004

Moduli Derived from Ultrasonics Isentropic Bulk Modulus

Molecular Weight Offset	Isentropic Bulk Modulus (GPa)
1%	6.7504±.04
2%	6.7836±.03
3%	6.7751±.02
4%	6.781±.05
5%	6.798±.05

Conclusions

- Molding of LaRC Samples affected the densities of the samples
- Samples have inclusions and show evidence of residual stresses under polarized light. We think that this is responsible for some of the data scatter.
- The 0° and 90° shear measurements show that the assumption of isotropy is a valid one in this case, even with the residual effects left from the moulding process.
- It is possible to calculate the significant engineering moduli from ultrasonic measurements.

Future Planned Activities

- Measurement of the nonlinear moduli
- Measurement of coefficients of linear expansion
- Measurements of effects on moduli (linear and nonlinear) of raising LaRC to glass transition temperature and beyond to

PREDICTING BULK POLYMER PROPERTIES FROM MOLECULAR STRUCTURE

Elizabeth Collantes, Tamara Gahimer, and William Welsh
University of Missouri

Michael Grayson
McDonnell Douglas Aerospace-St. Louis

GOALS & OBJECTIVES

- DEVELOP AND APPLY METHODS IN COMPUTATIONAL CHEMISTRY FOR FAST, RELIABLE, PREDICTION OF POLYMER PROPERTIES
- RELATE BULK MACROSCOPIC POLYMER PROPERTIES TO MICROSCOPIC MOLECULAR STRUCTURE AND PROPERTIES
- DEVELOP STRUCTURE-PROPERTY RELATIONSHIPS

COMPUTATIONAL APPROACHES

- QUANTITATIVE STRUCTURE-PROPERTY RELATIONSHIPS (QSPR)
  - → Group-Additivity Techniques (van Krevelen, Dow)
  - → Connectivity Indices (Bicerano's Synthia)
- MULTIVARIATE REGRESSION
  - → Partial Least Squares (PLS)
- ARTIFICIAL NEURAL NETWORKS (ANNs)
- ATOMISTIC MOLECULAR MODELING
  - → Cerius^2 Mechanical Properties Module

DESCRIPTION OF METHODS

QSPR Approaches

QSPR Approaches

The van Krevelen Method

D. W. van Krevelen, Properties of Polymers: Their Estimation and Correlation with Chemical Structure (Elsevier, 1976)

- assumes that the physiochemical properties of a polymer can be obtained by adding contributions from the constituent chemical groups
- this approach is commonly known as Group Additivity (GA)
- based on empirical and semi-empirical fitting to expt'l data
- relies on large database containing group contributions, typically one for each property of interest (e.g., T_g, α_T,)
- property values apply to bulk amorphous and semi-crystalline homopoloymers, statistical polymers, and for polymer solutions

Advantages

→ fast
→ easy to use
→ applicable to many properties
→ usually reliable

Disadvantages

→ depends on chemical-fragment library
→ theoretically less rigorous than atomistic methods
→ do not account for special interactions (e.g., solvent)
→ do not provide insight into mechanism

Table 9–12. QSPR Groups (Page 1 of 3)

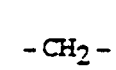
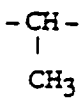
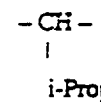
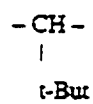
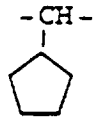
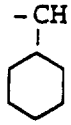
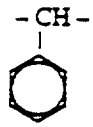
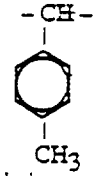
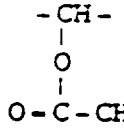
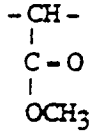
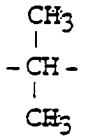
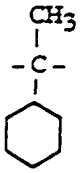
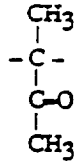
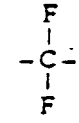
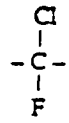
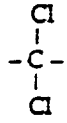
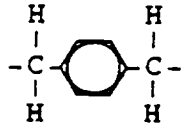
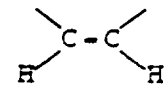
			
1. methylene	2. methylmethylene	3. isopropylmethylene	4. t-butylmethylene
			
5. cyclopentylmethylene	6. cyclohexylmethylene	7. phenylmethylene	8. p-methphenmethylene
			
9. hydroxymethylene	10.methethermethylene	11.acetylmethylene	12.methacrylmethylene
			
13.cyanomethylene	14.fluoromethylene	15.chloromethylene	16.dimethylmethylene
			
17.phenmethylmethylene	18.methmethacmethylene	19.difluoromethylene	20.chlorfluormethylene
			
21.dichloromethylene	22.paraxylylene	23.transcyclohexyl	24.cisethene

Table 9–12. QSPR Groups (Page 2 of 3)

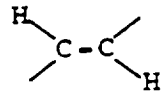
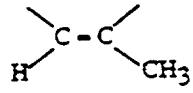
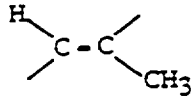
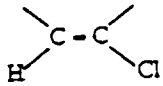
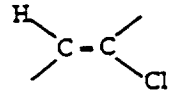
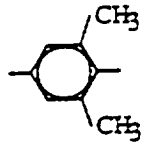
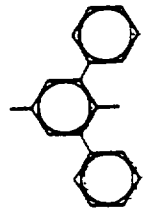
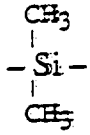
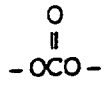
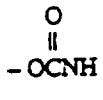
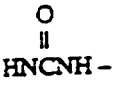
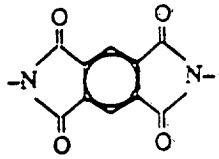
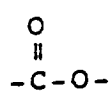
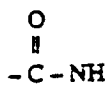
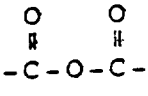
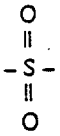
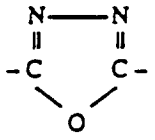
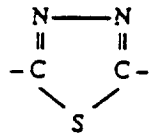
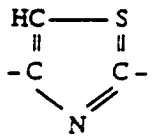
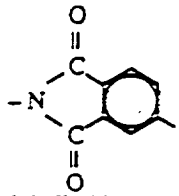
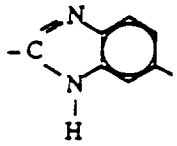
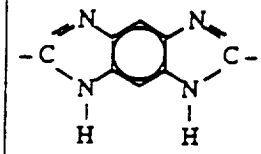
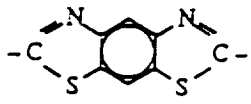
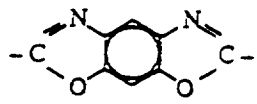
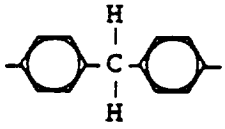
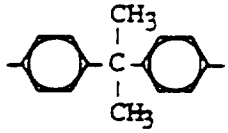
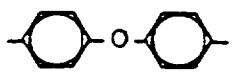
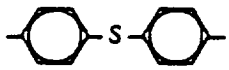
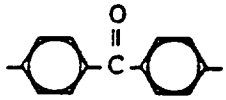
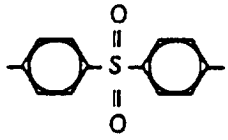
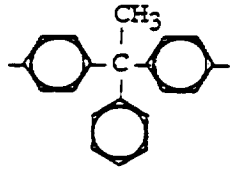
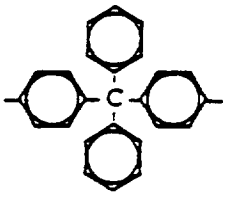
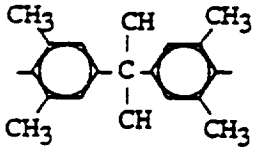
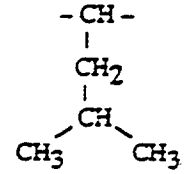
 25.transethene	 26.cismethylethene	 27.transmethylethene	 28.cischloroethene
 29.transchloroethene	 30.ethyne	31.carbonyl	 32.orthophenylene
 33.metaphenylene	 34.paraphenylene	 35.26dimethpphenylene	 36.26diphenpphonylene
 37.26naphthalene	 38.oxide	39.sulfide	 40.dimethysilene
 41.carbonate	 42.urethane	 43.urea	 44.benzoditimide
 45.ester	 46.amide	 47.anhydride	 48.sulfonyl

Table 9–12. QSPR Groups (Page 3 of 3)

 49. oxadiazole	 50. thiodiazole	 51. 25thiazole	 52. phthalimide
 53. benzoimidazole	 54. benzodiimidazole	 55. benzodithiazole	 56. benzodioxazole
 57. parabiphenylene	 58. pbisphenylmethylene	 59. pbisphenylA	 60. pbisphenylether
 61. pbisphenylS	 62. pbisphenylcarbonyl	 63. pbisphenylsulphone	 64. pbisphenyl-methphenmeth
 65. pbisphendiphenmeth	 66. ptetmethbisphenolA	 67. 27naphthalene	 68. ibutylmethylene

van Krevelen Methodology

The polymer properties that can be calculated with the van Krevelen methodology are:

Thermophysical Properties

- glass transition temperature
- crystalline melt transition temperature
- attainable degree of crystallinity
- maximum linear growth rate of sperulitic crystallites
- density of glassy, rubbery and crystalline phases
- volume coefficients of thermal expansion
- volume change on melting
- molar heat capacity at constant pressure
- molar heat capacity at constant volume
- molar entropy of fusion
- molar latent heat of fusion
- cohesive energy
- solubility parameter
- surface tension

Mechanical Properties

- bulk modulus
- Poisson's ratio
- longitudinal velocity of sound
- shear modulus of an amorphous or semicrystalline polymer
- tensile modulus of an amorphous or semicrystalline polymer

Ultimate Mechanical Properties

- tensile yield strength
- compressive strength
- flexural strength
- indentation hardness

Transport Properties

Permeation of a Gas

- specific permachor
- permeability of a gas

Viscoelastic Properties of a Polymer Melt

- activation energy of viscous flow
- Newtonian viscosity
- characteristic deformation time
- non-Newtonian viscosity

Dilute Solution Properties in a theta Solvent

- Mark–Houwink prefactor
- intrinsic viscosity
- radius of gyration
- critical molecular mass for entanglement

Dilute Solution Properties in a Good Solvent

- Mark–Houwink prefactor and exponent
- excluded volume expansion factor
- intrinsic viscosity
- radius of gyration

Concentrated Solution Property in a Good Solvent

- Newtonian viscosity

Electrical, Optical, and Magnetic Properties

- dielectric constant
- resistivity
- refractive index
- magnetic susceptibility

Properties Relating to Thermal Stability

- free enthalpy of formation
- temperature at half thermal decomposition
- char residue
- oxygen index

The van Krevelen methodology relies on the calculation of various molar properties of the average repeat unit. These molar properties are denoted here by enclosure in braces {}. The molar properties are then used in the calculation of the macroscopic properties of the polymer. The molar properties that are calculated are listed below:

- mass $\{M\}$
- number of QSPR groups $\{N\}$
- number of backbone atoms $\{Z\}$
- van der Waals volume $\{V_W\}$
- glass transition temperature $\{Y_g\}$
- melt transition temperature $\{Y_m\}$
- volume at 298 K in the amorphous phase $\{V_a\}$
- heat capacity of the solid $\{C_{p,s}\}$
- heat capacity of the liquid $\{C_{p,l}\}$
- entropy of melting $\{\Delta S_m\}$
- cohesive energy $\{E_{coh}\}$
- interaction $\{F\}$
- parachor $\{P_s\}$
- permachor $\{\Pi\}$
- elastic wave velocity $\{U\}$
- intrinsic viscosity $\{J\}$
- viscosity–temperature gradient $\{H_h\}$
- polarization $\{P_{LL}\}$
- optical refraction $\{R_{GD}\}$
- magnetic susceptibility $\{\chi\}$
- enthalpy of formation $\{\Delta G_a\}$
- entropy of formation $\{\Delta G_b\}$
- half thermal decomposition temperature $\{Y_{d,1/2}\}$
- char forming tendency $\{C_{ft}\}$

QSPR Approaches

The Dow Method

J. Seitz, J. Appl. Polym. Sci., 49, 1331 (1993)

- adopts group-additivity (GA) concept, but uses only six group contributions of the repeat unit to predict polymer properties: (1) molecular weight; (2) length; (3) vdW volume; (4) cohesive energy; (5) rotational df of the backbone; and (6) T_g
- focuses on mechanical properties
- limited to amorphous (not semi-crystalline) polymers

Advantages

→ same advantages as van Krevelen: fast, reliable
→ less dependent on large database of group contributions
→ better fitted to high-performance engineering polymers
→ conceptually more rigorous than van Krevelen

Disadvantages

→ same disadvantages as van Krevelen
→ restricted to amorphous polymers
→ depends on library of group contributions, although smaller

Properties Calculable

Dow Methodology

With the Dow methodology implemented within the QSPR module it is possible to predict 17 different properties of amorphous thermoplastic polymers. These are:

- Molar volume per repeat unit
- Density
- Thermal expansion coefficient
- Cohesive energy
- Solubility parameter
- Surface tension
- Dielectric constant
- Average molecular cross-sectional area
- Glass transition temperature
- Poisson's ratio
- Tensile modulus
- Tensile yield strength
- Brittle strength
- Crazing strength
- Entanglement molecular weight
- Distance between entanglements
- Plateau modulus

In addition, if $T_g > 300$ K, many of these properties may be calculated as a function of temperature.

The group parameters required to predict these properties are:

- Molecular weight
- Length per repeat unit
- van der Waals volume
- Cohesive energy
- Molar glass transition temperature
- Number of backbone rotatable units

QSPR Approaches

Bicerano's *Synthia* Method

J. Bicerano, Prediction of Polymer Properties (Marcel Dekker, 1993)

- circumvents reliance on group contributions by relating polymer properties to topological information about polymers using connectivity indices derived from graph theory
- useful for any polymer comprised of the following elements: C, H, N, O, Si, S, F, Cl, Br
- applicable to bulk amorphous homopolymers and statistical copolymers

Advantages

→ independent of large group-contribution library
→ thermodynamic, mechanical, and transport properties

Disadvantages

→ restricted to nine atom-types
→ restricted to amorphous polymers
→ does no account for special interactions

Table 11–1. Properties Calculable By the Synthia Module

Thermophysical Properties	Electrical, Optical and Magnetic Properties
Glass transition temperature	Refractive index
Temperature of half decomposition	Molar refraction
Coefficient of volumetric thermal expansion	Dielectric constant
Molar volume	Volume resistivity
Density	Diamagnetic susceptibility
Molar heat capacity at constant pressure	
Cohesive energy	Chain Stiffness and Entanglement Properties
Solubility parameter	
Surface tension	Steric hindrance parameter
Thermal conductivity	Characteristic ratio
	Molar stiffness function
Mechanical Properties	Entanglement molecular weight
Bulk modulus	Critical molecular weight
Shear modulus	Entanglement length
Young's modulus	
Poisson's ratio	Transport Properties
Shear yield stress	Activation energy for viscous flow
Brittle fracture stress	Permeability of gases

DESCRIPTION OF METHODS

Multivariate PLS Approach

Multivariate PLS Approach

Attempts to eliminate any dependence on group contributions or connectivity indices

- relate bulk polymer properties to specific molecular descriptors associated with the repeat unit
- focused on two polymer properties: T_g and Tensile Modulus
- selected seven easily-obtainable molecular descriptors: (1) molecular weight; (2) length; (3) number of atoms; (4) number of non-H atoms; (5) vdW volume; (6) rotational df, and (7) number of backbone atoms
- develops linear regression equation to map bulk polymer property onto calculable descriptors thereby allowing prediction of polymer property solely from knowledge of descriptors

$$property\ value = a_1 (PC_1) + a_2 (PC_2) + a_3 (PC_3) + \ldots$$

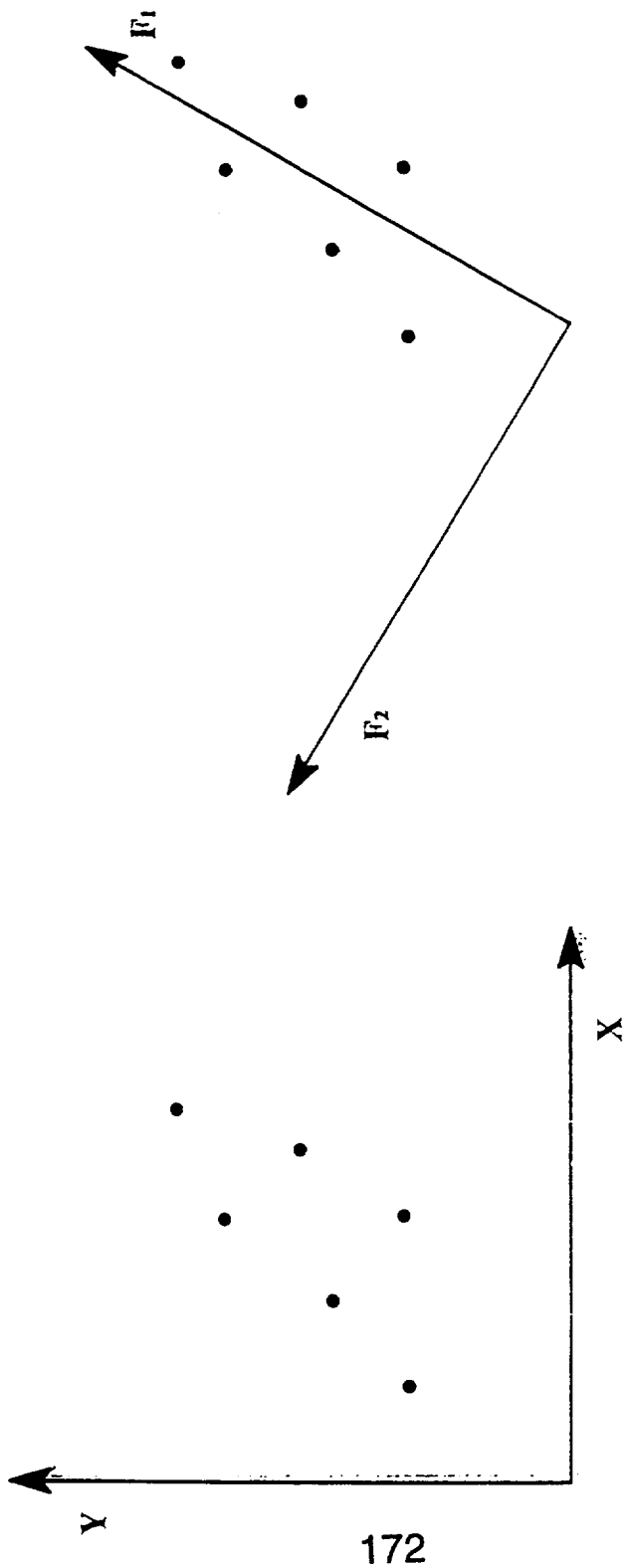
- applicable to any series of polymers for which experimental data is available

Advantages

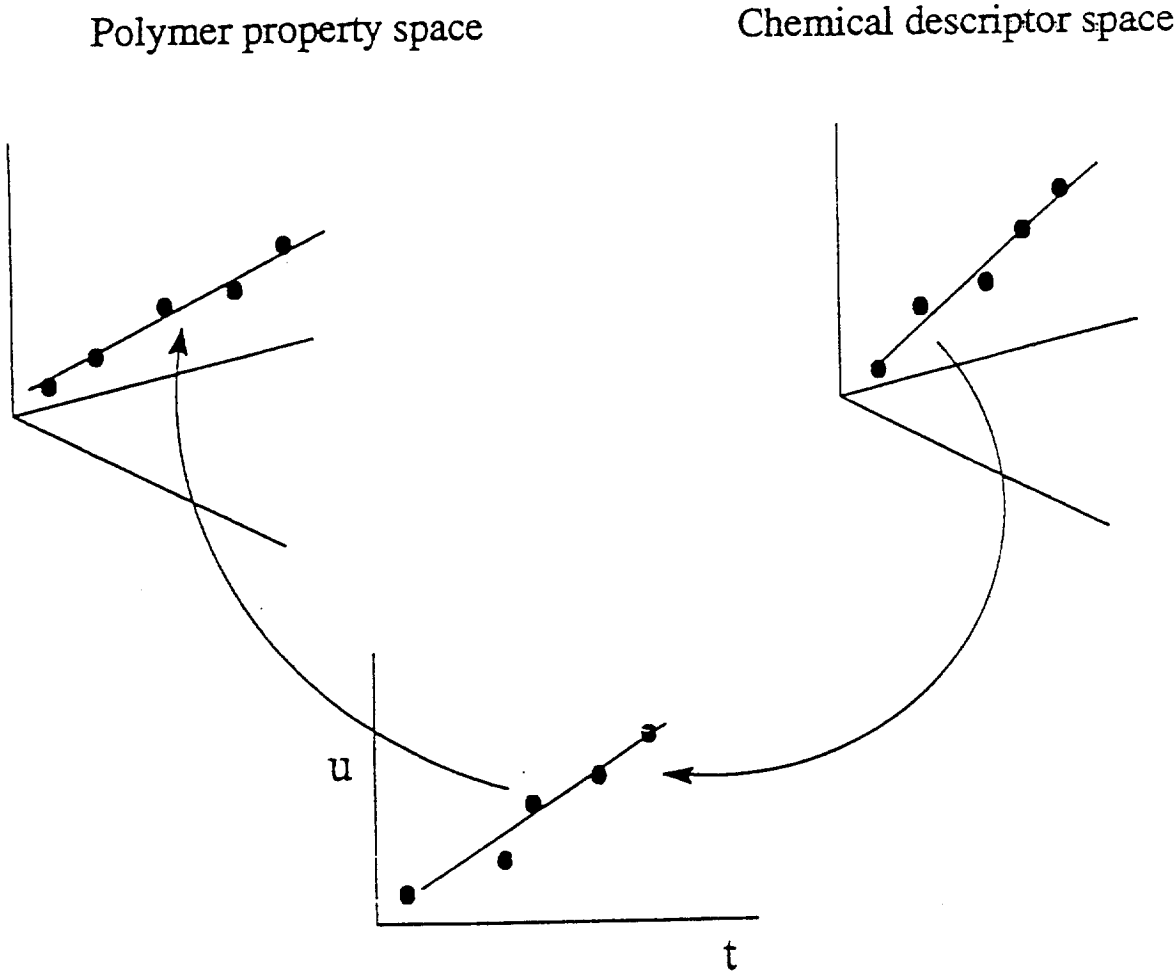
→ totally independent of any database library
→ generally applicable to any property and any polymer
→ from Loadings, evaluates contribution by each descriptor to property of interest

Disadvantages

→ assumes linear relationship between property and descriptors
→ need expt'l data on related polymers to develop regression equation


F1
F2
X
Y

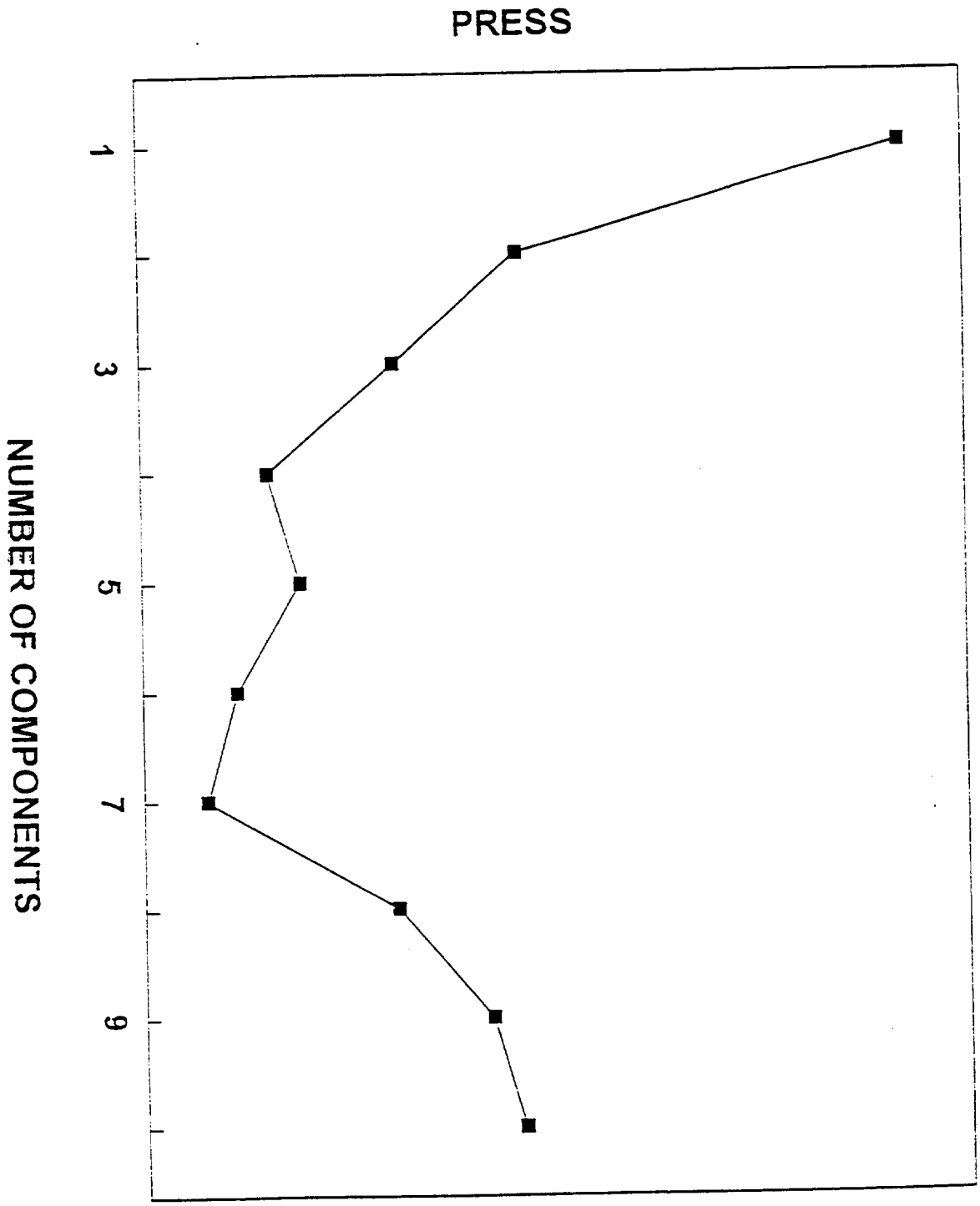
PLS: GRAPHICAL REPRESENTATION



Inner relation

Determining the number of significant components

- cross-validation


PRESS
NUMBER OF COMPONENTS
1
3
5
7
9

DESCRIPTION OF METHODS

Artificial Neural Networks

Artificial Neural Networks (ANN)

paradigm based on architecture of biological network of neurons in human brain

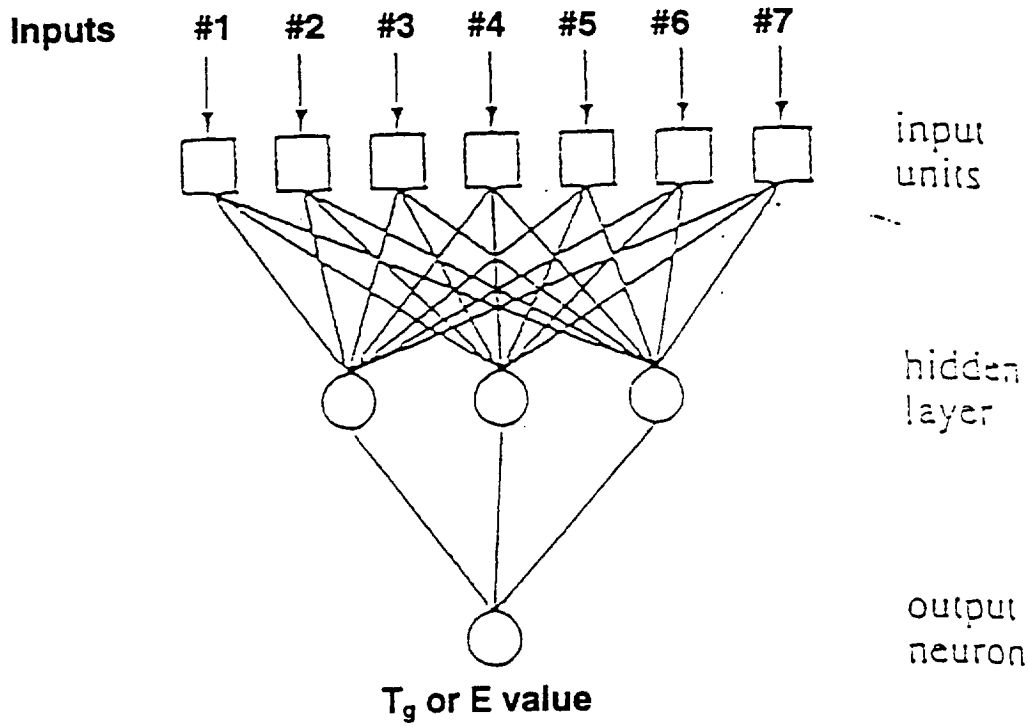
- **ANNs learn by repetition (like a child) to generate a desired response (output) based on knowledge of specific stimuli (inputs)**
- **learns to map bulk polymer property (output) onto calculable molecular descriptors (inputs), thereby allowing prediction of polymer properties solely from knowledge of these descriptors**
- **applicable to any series of polymers for which experimental data is available**
- **focused on same two polymer properties as outputs: T_g and Tensile Modulus**
- **selected identical seven molecular descriptors as inputs: (1) molecular weight; (2) length; (3) number of atoms; (4) number of non-H atoms; (5) vdW volume; (6) rotational df, and (7) number of backbone atoms**

Advantages

→ **totally independent of any fragment database**
→ **generally applicable to any property and to any polymer**
→ **inherently nonlinear and tolerant of noisy data**

Disadvantages

→ **requires expt'l data on related polymers to train the network prior to making predictions**



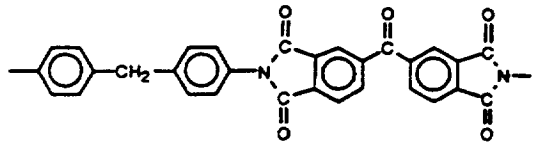
List of Inputs (*per repeat unit*)

#1 molecular weight
#2 end-to-end length
#3 number of atoms
#4 number of non-H atoms
#5 vdW volume
#6 rotational degrees of freedom
#7 number of backbone atoms

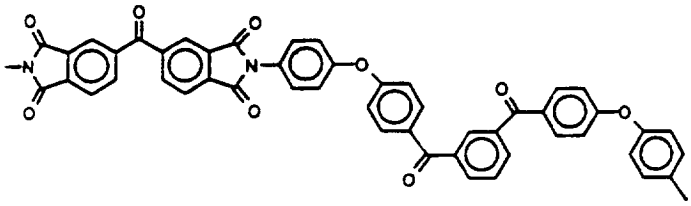
SUMMARY OF RESULTS

Figure 1. Repeat units of polymers included in this QSPR study

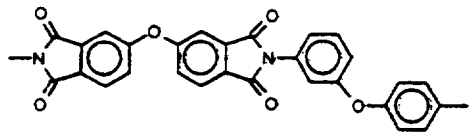
PMR-15



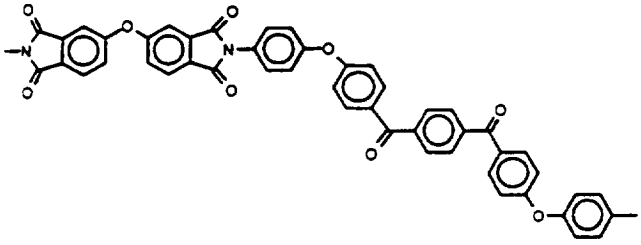
LARC-CPI



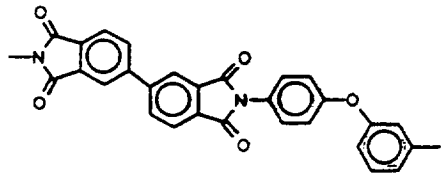
PETI-2



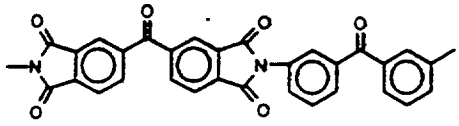
LARC-CPI-2



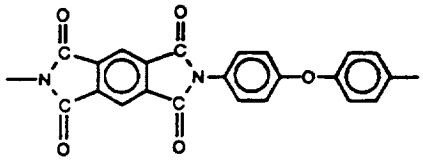
PETI-4



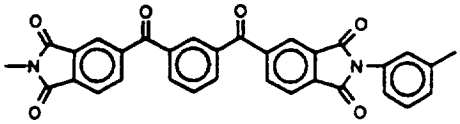
LARC-TPI



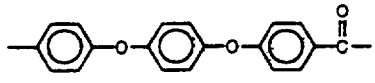
Kapton



LARC-I-TPI



PEEK



LARC-SI

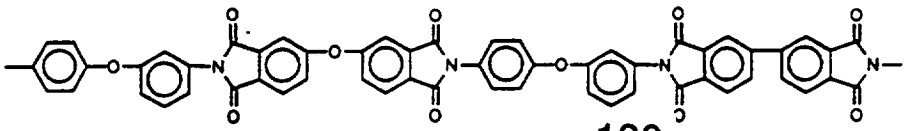


Table I
Abbreviated List of Calculated Properties of Polyimides and PEEK

PROPERTY[a]	UNIT	LARC-CPI	LARC-CPI2	LARC-TPI	LARC-ITPI	LARC-SI	PMR-15	PETI-2	PETI-4	KAPTON	PEEK
THERMOPHYSICAL PROPERTIES											
Glass Transition Temperature, T_g	K	486	488	532	534	520	518	516	522	628	411
Melt Transition Temperature[b], T_m	K	707	726	744	746	755	733	755	754	850	627
Coef. of Thermal Expansion[c], α	ppm/K	206	204	192	187	183	186	190	177	147	227
Density, ρ, at 298 K	g/cm^3	1.36	1.36	1.43	1.43	1.43	1.40	1.44	1.43	1.38	1.25
Solubility Parameter, δ	MPa$^{1/2}$	25.6	25.3	27.2	27.2	26.5	26.6	26.5	26.6	25.3	22.8
Cohesive Energy, E_{coh}	kJ/mole	378.5	364.5	258.6	258.6	457.8	246.2	230.6	227.2	177.2	119.9
Attainable Degree of Crystallinity[b], X_c	vol frac	0.43	0.46	0.37	0.37	0.42	0.39	0.43	0.42	0.32	0.49
Free Enthalpy of Formation[b], ΔG_f	kJ/mole	-1046	-1046	-686.0	-686.0	-1224	-600.0	-686.0	-538.0	-565.0	-360.0
MECHANICAL PROPERTIES at 298 K											
Tensile Modulus, E	GPa	3.63	3.41	4.24	4.13	4.46	4.03	4.02	3.90	3.93	2.42
Tensile Yield Strength, σ_y	MPa	90.8	85.3	105.9	103.2	111.5	100.8	100.4	97.4	98.3	60.4
Poisson's Ratio, μ		0.406	0.410	0.408	0.411	0.397	0.407	0.406	0.410	0.407	0.414
Ultimate Compressive Strength[b], σ_{comp}	MPa	235.7	237.9	283.1	284.8	270.2	268.4	266.5	272.3	394.0	168.9
Brittle Strength, σ_b	MPa	124.4	134.3	128.7	135.1	104.7	126.8	124.2	134.4	128.1	142

[a] *Based on DOW QSPR method, unless otherwise noted.*
[b] *Based on van Krevelen QSPR method.*
[c] *Based on Synthia method.*

Table II. Expanded List of Calculated Properties of Polyimides and PEEK

PROPERTY[a]	UNIT	LARC-CPI	LARC-CPI2	LARC-TPI	LARC-ITPI	LARC-SI	PMR-15	PETI-2	PETI-4	KAPTON	PEEK
THERMOPHYSICAL PROPERTIES											
Glass Transition Temperature, T_g	*K*	486	488	532	534	520	518	516	522	628	411
Melt Transition Temperature[b], T_m	*K*	707	726	744	746	755	733	755	754	850	627
Coef. of Thermal Expansion[c], α	*ppm/K*	206	204	192	187	183	186	190	177	147	227
Molar Volume at 298 K	*cm³/mo*	579.2	569.2	348.4	348.3	651.0	347	329.4	321.7	277.5	
Density, ρ, at 298 K	*g/cm³*	1.36	1.36	1.43	1.43	1.43	1.40	1.44	1.43	1.38	1.25
Solubility Parameter, δ	*MPa$^{1/2}$*	25.6	25.3	27.2	27.2	26.5	26.6	26.5	26.6	25.3	22.8
Cohesive Energy, E_{coh}	*kJ/mol*	378.5	364.5	258.6	258.6	457.8	246.2	230.6	227.2	177.2	
Molar Heat Capacity[b]: at constant P,	*J/mol-K*	766.0	760.5	473.7	473.7	905.6	476.1	461.2	444.4	365.0	
at constant V,	*J/mol-K*	674.9	661.9	419.6	419.6	781.7	410.4	399.1	382.7	330.2	
Surface Tension, γ	*dyn/c*	56.48	55.72	61.49	61.50	59.31	59.66	59.13	59.49	55.62	
Thermal Conductivity[c] : at 298 K	*J/Kms*	0.20	0.20	0.20	0.20	0.21	0.20	0.21	0.21	0.21	0.20
at Tg		0.23	0.23	0.23	0.23	0.24	0.23	0.24	0.24	0.25	0.22
Attainable Degree of Crystallinity[b], X_c	*vol frac*	0.43	0.46	0.37	0.37	0.42	0.39	0.43	0.42	0.32	0.49
Av. Molecular Cross Sectional Area	*A²*	20.21	18.71	19.63	18.70	24.11	19.90	20.30	18.78	19.89	
PROPERTY RELATING TO THERM. STABILITY											
Free Enthalpy of Formation[b], ΔG_f	*kJ/mol*	-1046	-1046	-686.0	-686.0	-1224	-600.0	-686.0	-538.0	-565.0	-369.0

Table II (continued)

PROPERTY[a]	UNIT	LARC-CPI	LARC-CPI2	LARC-TPI	LARC-ITPI	LARC-SI	PMR-15	PETI-2	PETI-4	KAPTON	PEEK
MECHANICAL PROPERTIES at 298 K											
Tensile Modulus, E	*GPa*	3.63	3.41	4.24	4.13	4.46	4.03	4.02	3.90	3.93	2.42
Tensile Yield Strength, σ_y	*MPa*	90.8	85.3	105.9	103.2	111.5	100.8	100.4	97.4	98.3	60.4
Bulk Modulus[c]	*GPa*	6.055	5.875	6.855	6.94	6.355	6.483	6.172	6.382	7.115	4.899
Shear Modulus[c]	*GPa*	1.329	1.258	1.492	1.387	1.463	1.392	1.368	1.343	1.369	1.039
Poisson's Ratio, μ		0.406	0.410	0.408	0.411	0.397	0.407	0.406	0.410	0.407	0.414
Ultimate Compressive Strength[b],	*MPa*	235.7	237.9	283.1	284.8	270.2	268.4	266.5	272.3	394.0	168.9
Brittle Strength, σ_b	*MPa*	124.4	134.3	128.7	135.1	104.7	126.8	124.2	134.4	128.1	142
Crazing Strength, σ_c	*MPa*	93.2	92.4	132.0	133.0	110.5	118.7	116.1	120.1	160.0	44.5
Ultimate Flexural Strength[b], σ_{fl}	*MPa*	123.7	123.3	128.3	128.5	125.9	125.4	125.7	126.0	136.7	116.8
Shear Yield Stress[c]	*MPa*	104.0	98.64	116.8	109.2	114.2	109.2	107.0	105.4	108.1	81.54
Hardness[b], H_p	*MPa*	15.2	15.2	15.9	15.9	15.5	15.5	15.5	15.6	17.0	14.3
Plateau Modulus, G_N^0	*MPa*	1.75	2.01	2.31	2.52	1.53	2.17	2.05	2.58	2.89	1.63
ELECTRICAL, OPTICAL AND MAGNETIC[c]											
Refractive Index, n		1.643	1.644	1.657	1.657	1.664	1.66	1.661	1.667	1.663	1.619
Molar Refraction (Lorentz and		215.7	213.1	133.3	133.3	251.4	133.2	128.1	125.8	103.07	82.08
Dielectric Constant, ε		3.42	3.36	3.65	3.65	3.46	3.49	3.48	3.44	3.60	3.04
Volume Resistivity ($x10^{-16}$)	*ohm-cm*	1.45	1.89	0.49	0.49	1.20	1.03	1.12	1.29	0.641	8.29
Diamagnetic Susceptibility ($x10^{6}$)	*cm^3/mo*	423.8	422.5	254.6	254.6	497.9	258.6	251.9	245.9	196.0	169.2

Table II (continued)

PROPERTY[a]	UNIT	LARC-CPI	LARC-CPI2	LARC-TPI	LARC-ITPI	LARC-SI	PMR-15	PETI-2	PETI-4	KAPTON	PEEK
MECHANICAL PROPERTIES AT INCEPTION OF RUBBERY PLATEAU [c]											
Temperature	*K*	512	517	549	564	576	566	555	594	717	463
Molar Volume	*cm³/mo*	626.41	618.41	382.06	382.52	715.92	381.10	365.57	357.41	296.56	244.33
Density	*g/cm³*	1.256	1.253	1.305	1.303	1.303	1.271	1.298	1.283	1.289	1.180
Bulk Modulus	*MPa*	2766	2604	3121	3074	3000	2917	2598	2721	2344	2301
Shear Modulus	*MPa*	1.59	1.72	2.06	2.70	1.81	2.17	1.86	2.59	3.96	1.31
Tensile Modulus	*MPa*	4.78	5.15	6.17	8.11	5.42	6.51	5.58	7.76	11.89	3.92
Poisson's Ratio		0.50	0.50	0.50	0.50	0.50	0.50	0.50	0.50	0.499	0.500
TRANSPORT PROPERTIES [c]											
Activation Energy for Viscous Flow	*kJ/mol*	69.55	68.87	70.96	70.96	69.80	69.91	68.81	70.83	69.70	67.14
Permeability at 298 K : O_2	*Dow*	23.2	34.1	10.9	10.9	33.5	24.3	39.0	39.3	32.4	71.6
N_2	*Units*	5.1	7.8	2.3	2.3	7.6	5.4	8.9	9.0	7.3	17.2
CO_2		89.6	136.2	39.4	39.4	133.4	94.1	157.2	158.7	128.9	305.0

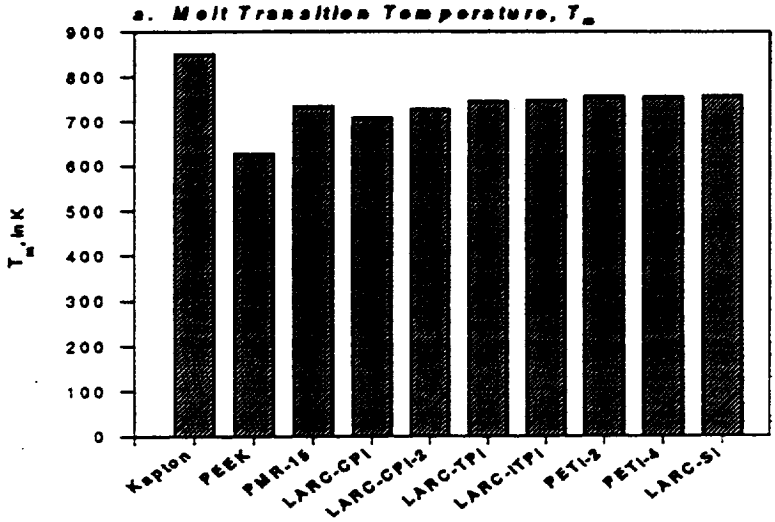
[a] *Based on DOW QSPR method, unless otherwise noted.*
[b] *Based on van Krevelen QSPR method.*
[c] *Based on Synthia method.*

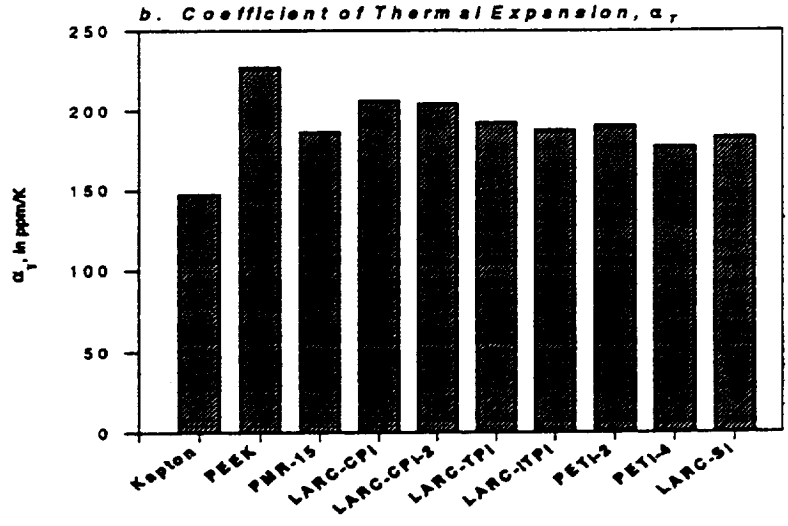
Table III. List of Experimental Properties of Polyimides and PEEK

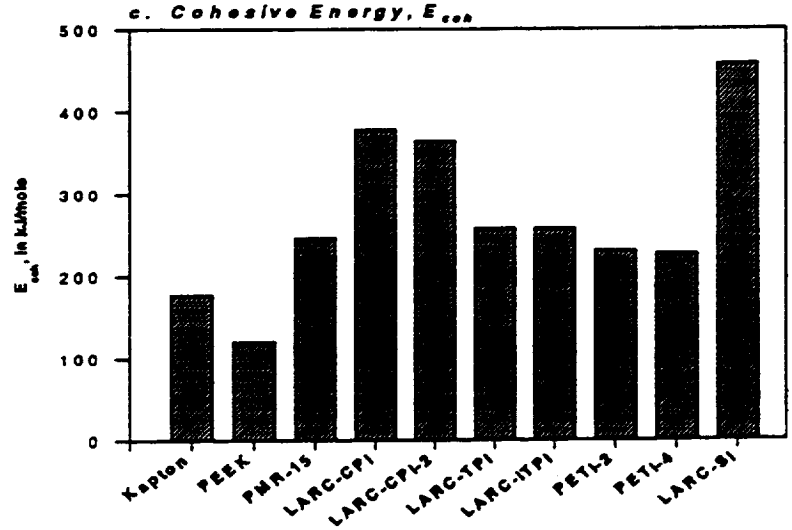
PROPERTY	UNIT	LARC-CPI	LARC-CPI2	LARC-TPI	LARC-ITPI	LARC SI	PMR-15	PETI-2	PETI-4	KAPTON	PEEK
Glass Transition Temperature,	*K*	495[2,6]	490[4]	513[2]	532[6,11]		600[2]			658[1]	418[1]
		493[10]		523[6]	533[10]		611[2]				416[2]
				533[11]			613[9]				417[2]
Melt Transition Temperature, T_m	*K*	623[2,6]		548 -						770[1]	597[1]
				578[2]							616[2,12]
											613[7]
Coef. of Thermal Expansion, α	*in/in/°F*						28(10^{-6})[8]				22(10^{-6})[7]
Density, ρ	*g/cm³*			1.55[2]			1.58[2]			1.42[1]	1.20[6]
				1.37[9]			1.32[8,9]				1.26[7]
											1.3[12]
Tensile Modulus, E	*GPa*	4.27[10]		3.5[9]	3.7[10,11]		3.2[8]			2.10[2]	3.7[1]
	(ksi)			3.7[11]			3.9[9]			2.96[3]	3.8[12]
				(465)[2]						(430)[11]	(550)[2]
Tensile Yield Strength, σ	*MPa*			103.4[2]	96.6[2]						
Dielectric Constant, ε		3.10[2,6]		3.30[6]	3.29[6]					3.5[1]	3.3[7]
										3.2[2,6]	

References

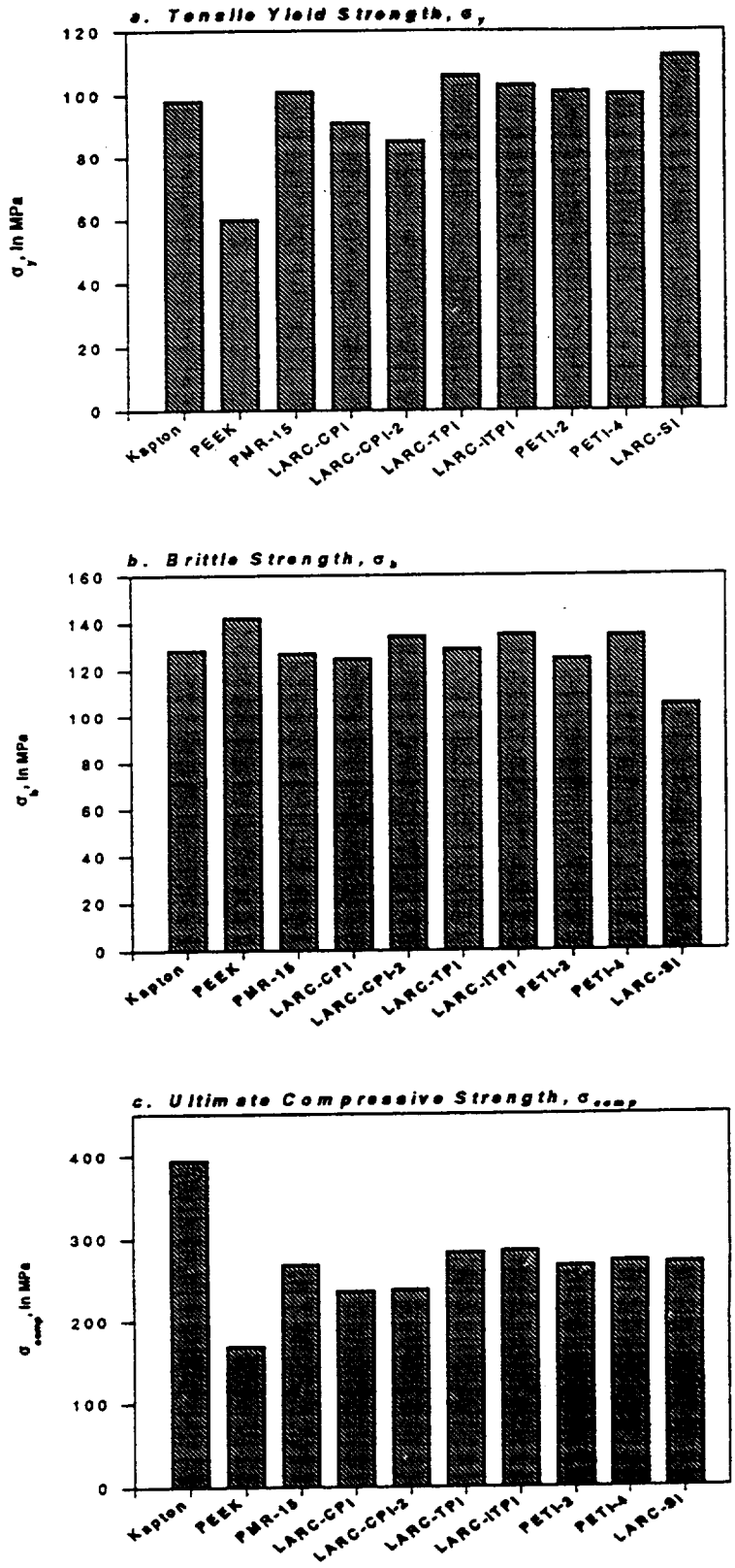
1. van Krevelen, D.W. *Properties of Polymers: Their Correlation with Chemicall Structure; Their Numerical Estimation and Prediction from Additive Group Contributions*; Elsevier: Amsterdam, 1990.
2. *Proceedings of the Interdisciplinary Symposium on Recent Advances in Polyimides and other High Performance Polymers*, San Diego, CA, January 22-25, 1990.
3. Hergenrother, P.M. *Angew. Chem. Int. Ed. Eng.* **1990**, *29*, 1262-1268.
4. Wilkes, G.L. *Polymer* **1994**, *35*, 5672-5677.
5. Fetters, L.J.; Lohse, D.; Richter, D.; Witten, T.; Zirkel, A. *Macromolecules* **1994**, 27, 4439-4647.
6. Croall, C.I.; St. Clair, T.L. Technical Memorandum NASA TM-104202, NASA Langley Research Center, January 1992.
7. Data Sheet for STABAR K200.
8. Data Sheet for Fiberite®966C.
9. Scola, D.A.; Vontell, J.H. *Polymer Composites* **1988**, *9*, 443-452.
10. Hergenrother, P.M.; Rogalski, M.E. *Composites for High Speed Commercial Transports*. pp. 354-366.
11. Pratt, J.R.; St. Clair, T.L. *SAMPE Journal* **1990**, *26*, 29-34.
12. Pratte, J.F.; Krueger, W.H.; Chang, I.Y. *34th International SAMPE Symposium and Exhibition*, Reno, NV, May 8-11, 1989.



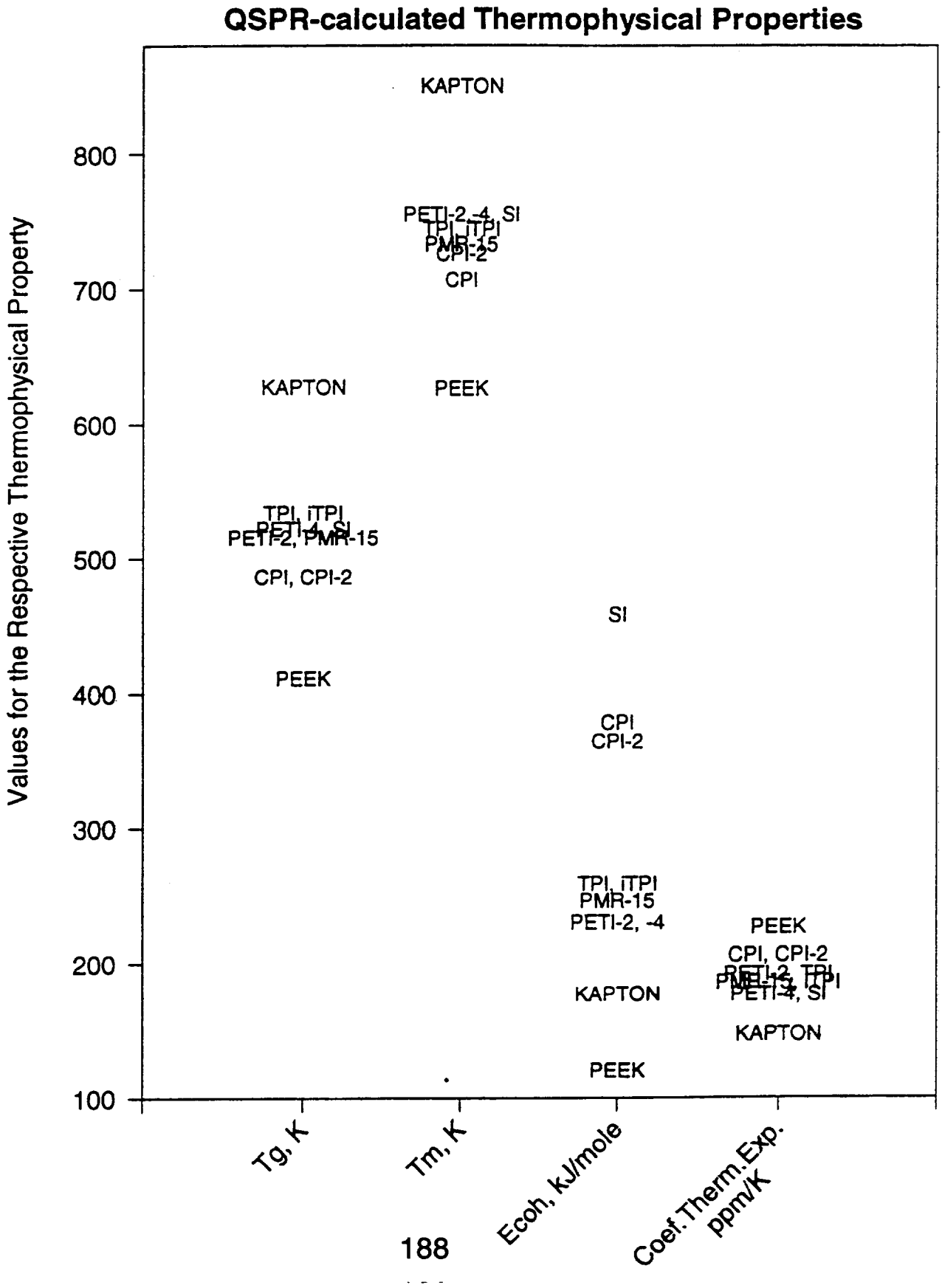


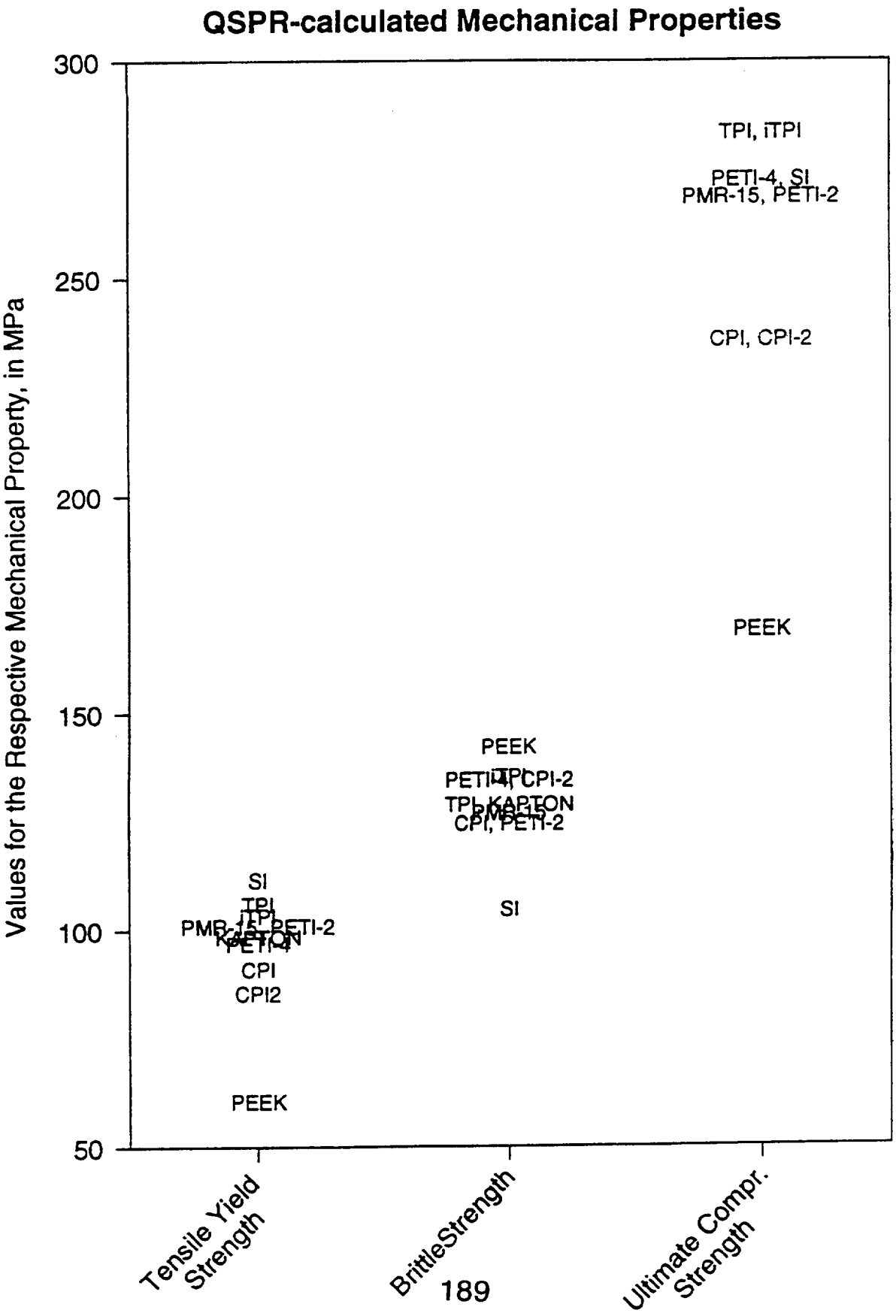


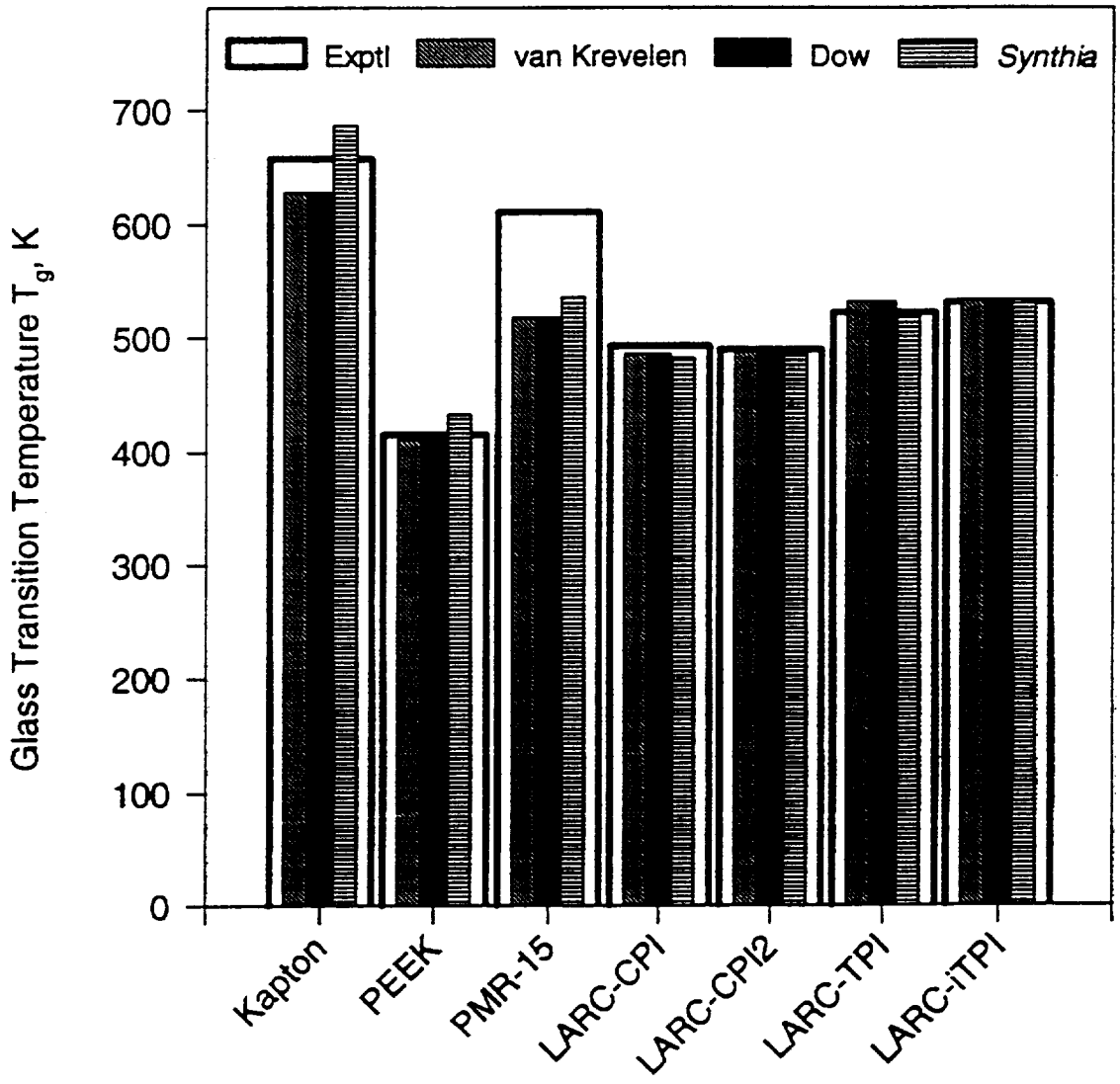
QSPR-calculated Thermophysical Properties for Various Polyimides



QSPR-calculated Mechanical Properties for Various Polyimides


QSPR-calculated Thermophysical Properties
Values for the Respective Thermophysical Property
800
700
600
500
400
300
200
100
KAPTON
PETI-2, -4, SI
TPI, iTPI
PMR-15
CPI-2
CPI
KAPTON
PEEK
TPI, iTPI
PETI-4, SI
PETI-2, PMR-15
CPI, CPI-2
SI
PEEK
CPI
CPI-2
TPI, iTPI
PMR-15
PETI-2, -4
PEEK
CPI, CPI-2
KAPTON
PETI-4, SI
KAPTON
PEEK
Tg, K
Tm, K
Ecoh, kJ/mole
Coef.Therm.Exp.
ppm/K


QSPR-calculated Mechanical Properties
Values for the Respective Mechanical Property, in MPa
300
250
200
150
100
50
TPI, iTPI
PETI-4, SI
PMR-15, PETI-2
CPI, CPI-2
PEEK
PEEK
PETI-4, CPI-2
TPI, KAPTON
CPI, PETI-2
SI
SI
TPI
PMR-15, PETI-2
KAPTON
PETI-4
CPI
CPI2
PEEK
Tensile Yield Strength
BrittleStrength
Ultimate Compr. Strength


Exptl
van Krevelen
Dow
Synthia
Glass Transition Temperature T_g, K
700
600
500
400
300
200
100
0
Kapton
PEEK
PMR-15
LARC-CPI
LARC-CPI2
LARC-TPI
LARC-iTPI

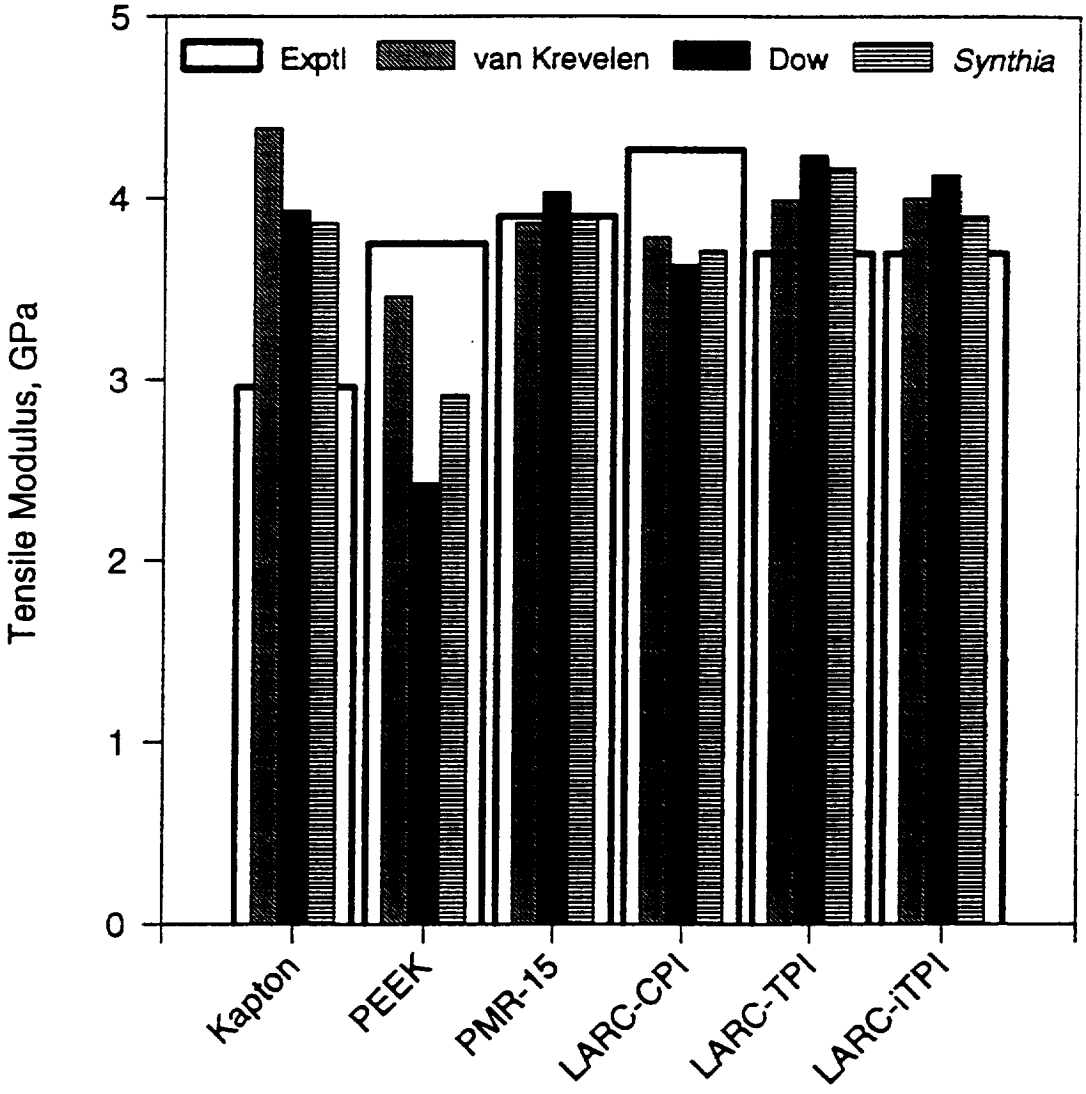
EXPERIMENTAL POLYMER PROPERTIES

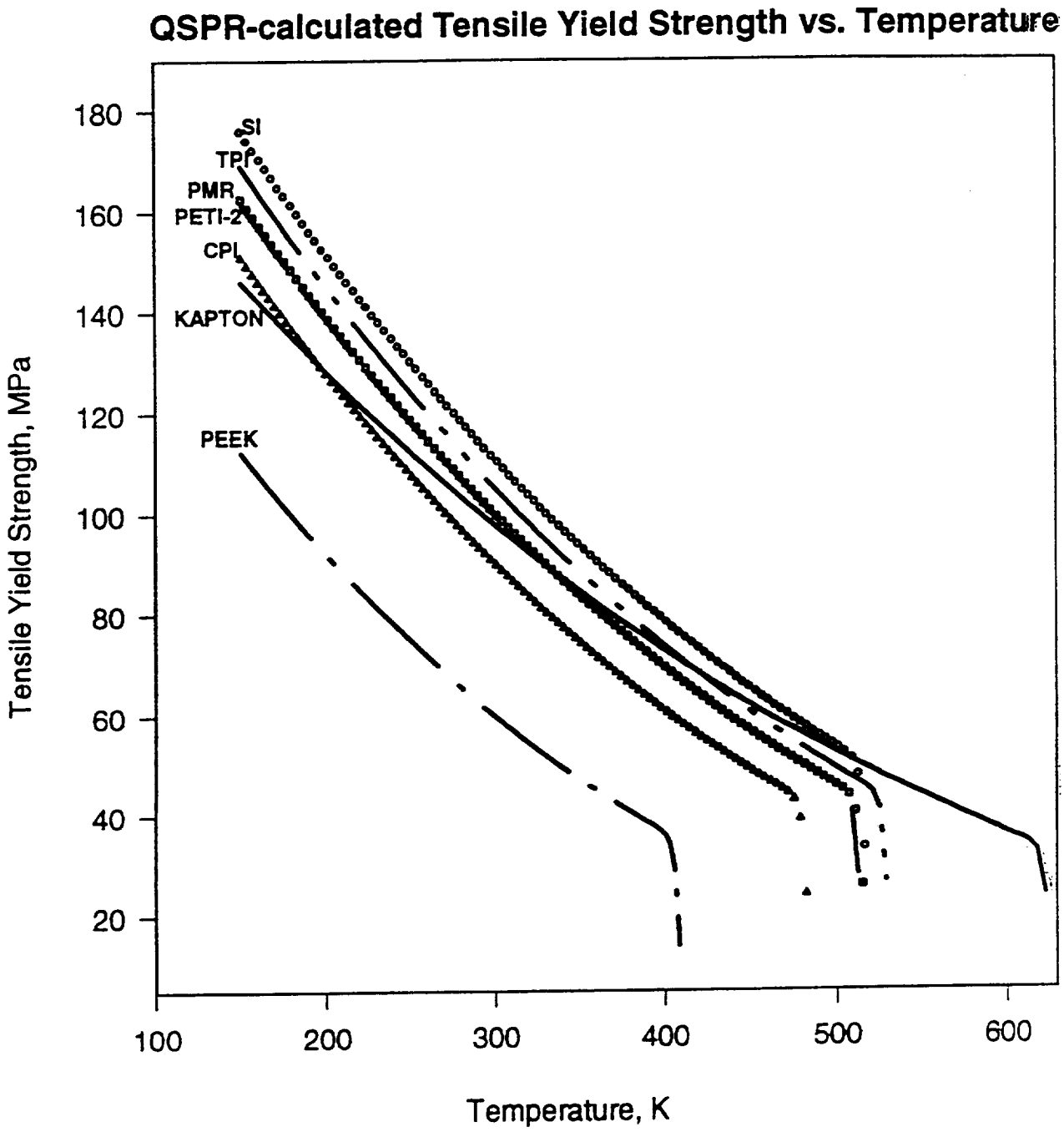


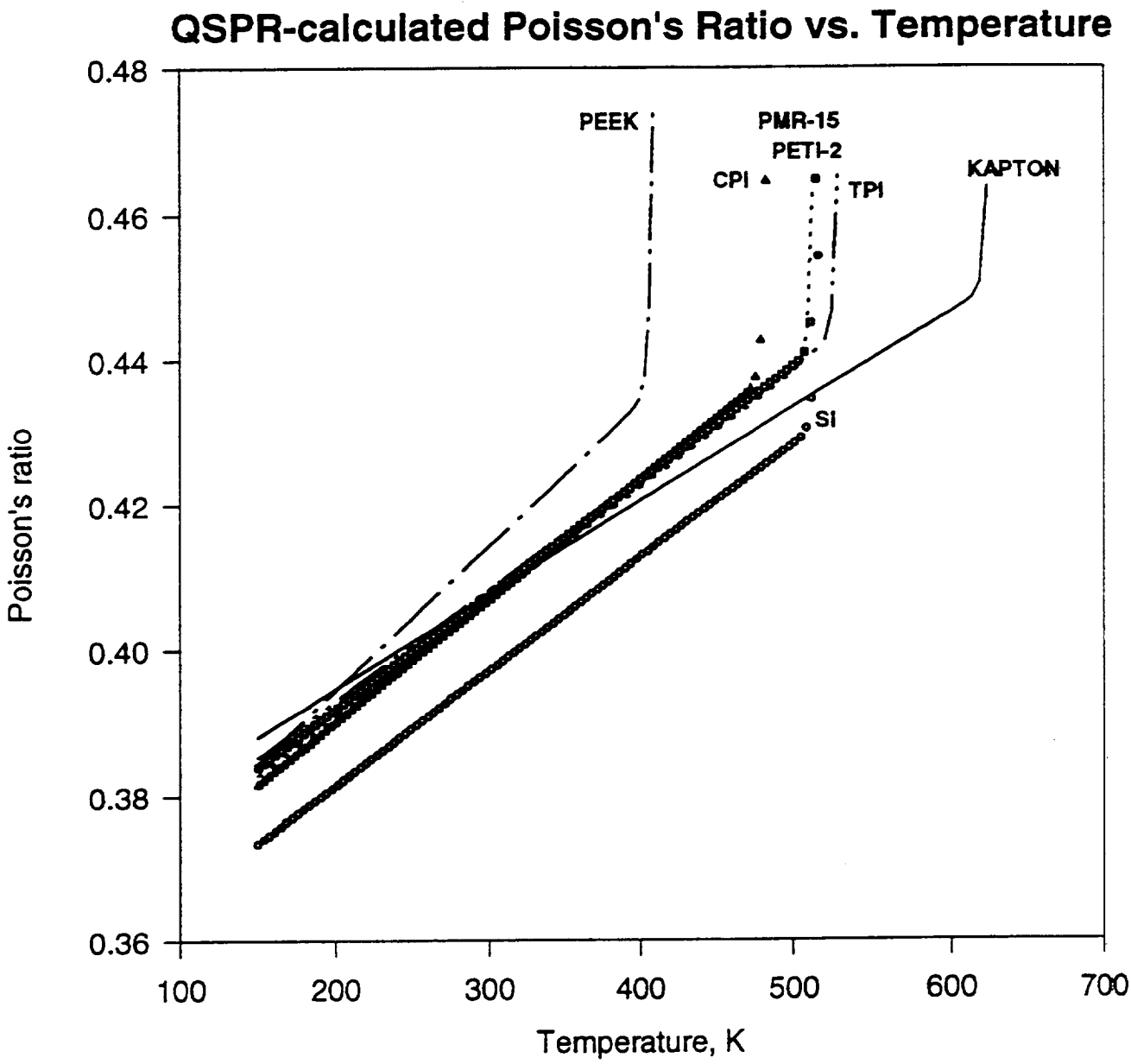
NEURAL NETS **QSPR METHODS** **REGRESSION METHODS** **ATOMISTIC METHODS**

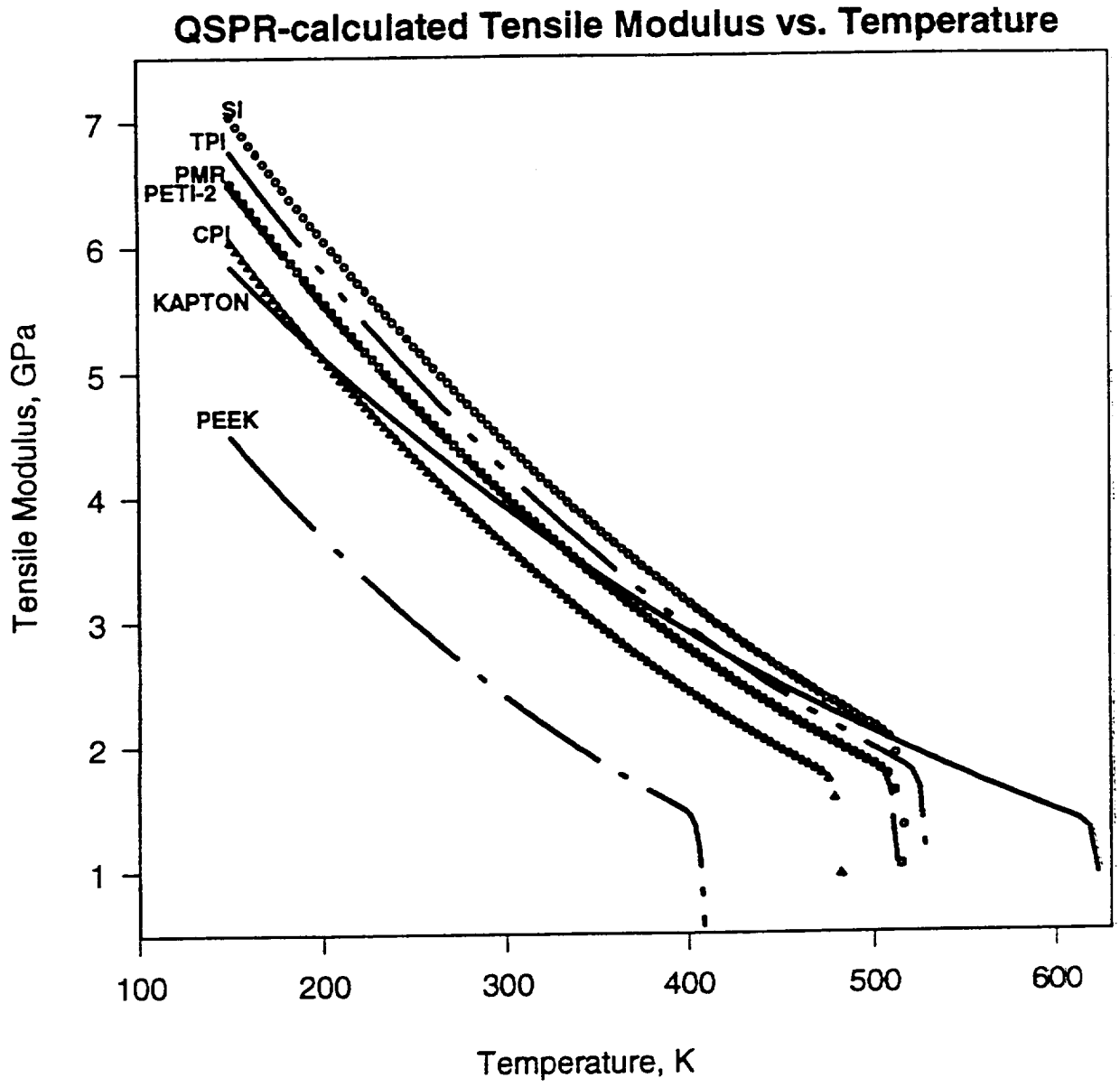


ESTABLISH STRUCTURE-PROPERTY RELATIONSHIPS
RELATE MICROSCOPIC TO MACROSCOPIC PROPERTIES
PREDICT BULK PROPERTIES FROM MOLECULAR DESCRIPTORS
CORRELATE WITH EXPERIMENTAL RESULTS


Expt
van Krevelen
Dow
Synthia
Tensile Modulus, GPa
0
1
2
3
4
5
Kapton
PEEK
PMR-15
LARC-CPI
LARC-TPI
LARC-iTPI


QSPR-calculated Tensile Yield Strength vs. Temperature
Tensile Yield Strength, MPa
Temperature, K
SI
TPI
PMR
PETI-2
CPI
KAPTON
PEEK
180
160
140
120
100
80
60
40
20
100
200
300
400
500
600


QSPR-calculated Poisson's Ratio vs. Temperature
Poisson's ratio
0.48
0.46
0.44
0.42
0.40
0.38
0.36
100
200
300
400
500
600
700
Temperature, K
PEEK
PMR-15
PETI-2
CPI
TPI
KAPTON
SI


QSPR-calculated Tensile Modulus vs. Temperature
SI
TPI
PMR
PETI-2
CPI
KAPTON
PEEK
Tensile Modulus, GPa
7
6
5
4
3
2
1
100
200
300
400
500
600
Temperature, K

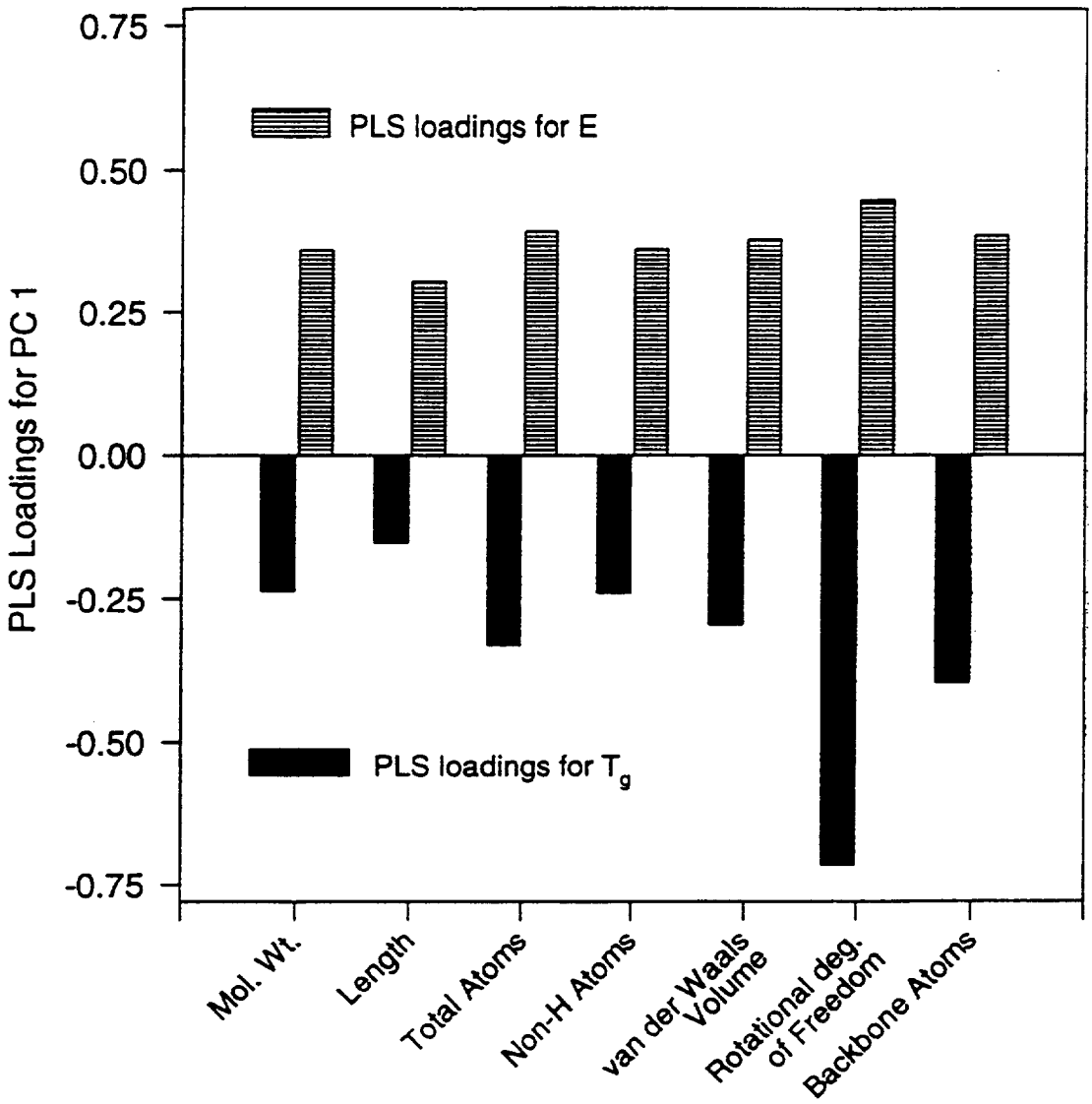
ANN and PLS Calculated T_g vs. Experimental Values

	Expt'l	Calculated/Predicted T_g, K			
	T_g, K	ANN	Residual	PLS	Residual
CPI	493	506	-13	473	20
TPI	523	546	-23	520	3
Kapton	658	634	24	664	-6
PMR-15	611	587	24	583	28
CPI-2	490	513	-23	513	-23
iTPI	532	556	-24	550	-18
PEEK	416	440	-24	420	-4
PETI-2		562		540	
PETI-4		620		617	
SI		519		633	

ANN and PLS Calculated Tensile Modulus (E)

vs. Experimental Values

	Expt'l	Calculated/Predicted E, GPa			
	E, GPa	ANN	Residual	PLS	Residual
CPI	4.27	4.15	0.12	4.39	-0.12
TPI	3.7	3.83	-0.13	3.62	0.08
Kapton	2.96	3.09	-0.13	3.32	-0.36
PMR-15	3.9	3.77	0.13	3.65	0.25
CPI-2	3.7	3.7	0	3.53	0.17
iTPI	3.75	3.62	0.13	3.77	0.02
PEEK		3.77		3.68	
PETI-2		3.4		3.49	
PETI-4		3.97		4.26	
SI		4.13		4.38	


0.75
0.50
0.25
0.00
-0.25
-0.50
-0.75
PLS Loadings for PC 1
PLS loadings for E
PLS loadings for T_g
Mol. Wt.
Length
Total Atoms
Non-H Atoms
van der Waals Volume
Rotational deg. of Freedom
Backbone Atoms

CURRENT WORK

- Atomistic Cerius^2 calculations of polymer properties: tensile modulus, bulk modulus, speed of sound, Poisson's ratio, density
- EGAMS of neat LaRC-SI resin (with Mike Grayson): experimental and theoretical investigation of thermal degradation
- Dynamic mechanical analysis (DMA) of LaRC-SI resin (with Mike Grayson): measure T_g, characterize sub-T_g transitions
- Extend multivariate regression and neural network analysis relating bulk polymer properties to molecular descriptors

SUMMARY AND CONCLUSIONS

QSPR

- ALL THREE QSPR METHODS AGREE WITH EACH OTHER REASONABLY WELL IN PREDICTING MECHANICAL AND THERMOPHYSICAL POLYMER PROPERTIES

- VALUES OF T_g AND E PREDICTED BY ALL THREE QSPR METHODS AGREE REASONABLY WELL (WITHIN 15%) WITH THE CORRESPONDING EXPT'L VALUES

- COMPARING THE POLYIMIDES, KAPTON RANKS HIGH IN T_g AND T_m BUT LOW IN α_T; T_g IS SLIGHTLY HIGHER FOR PARA OVER META CATENATION (488K FOR CPI2 VS. 486K FOR CPI)

- HIGH T_g AND E ARE INVERSELY RELATED TO α_T: KAPTON VS. PEEK

- LARC-SI EXHIBITS HIGH VALUES OF TENSILE MODULUS AND TENSILE YIELD STRENGTH (AND LOW VALUES OF POISSON'S RATIO) ACROSS THE T = 100-600 K TEMPERATURE RANGE

PLS REGRESSION AND NEURAL NETS (ANN)

- FOR T_g, THE RESIDUAL STANDARD DEVIATION (RSD) WAS 18K FOR PLS, 20K FOR ANN, AND 37K FOR QSPR

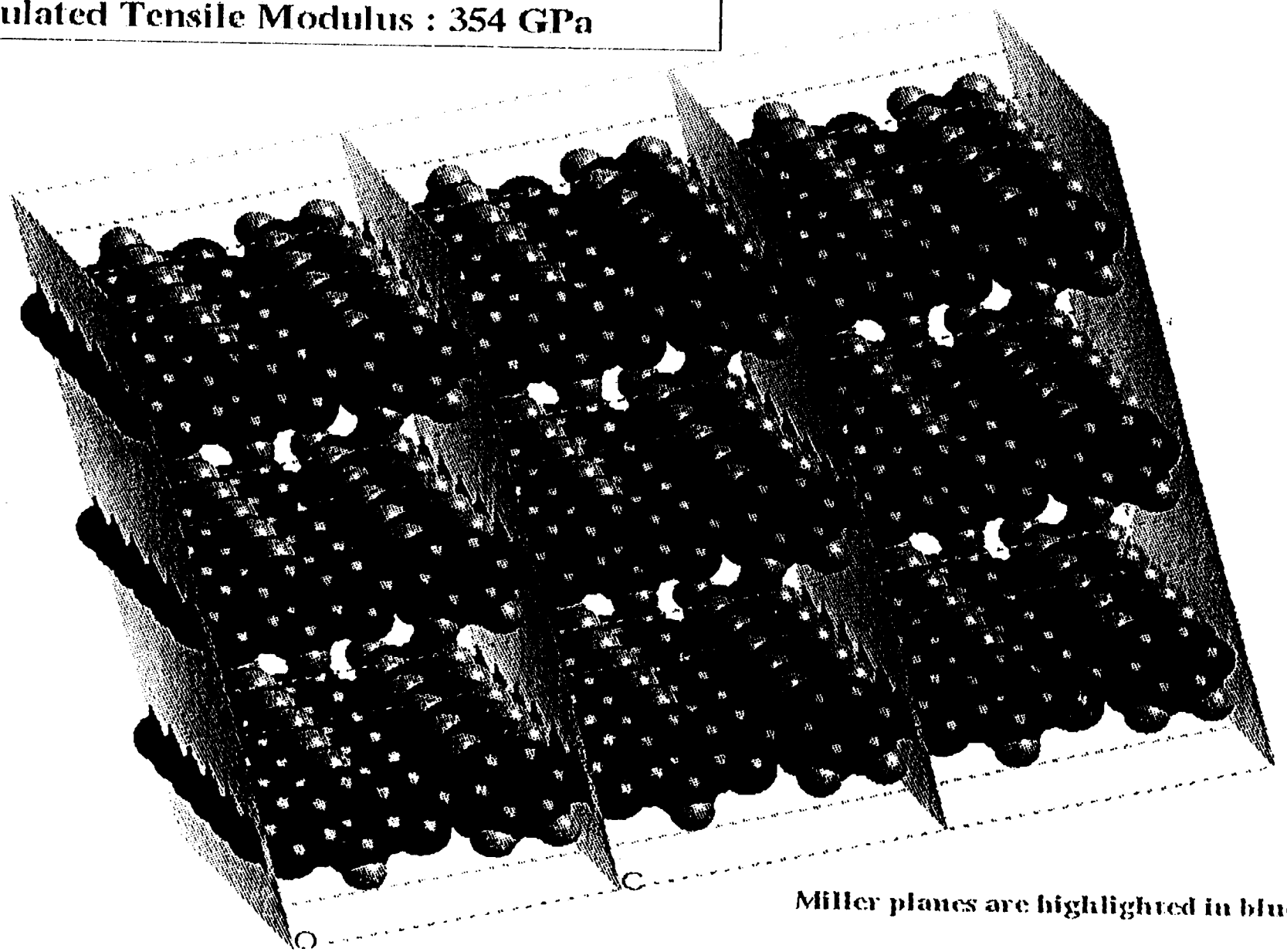
- FOR E, THE RSD WAS 0.20 GPA FOR PLS, 0.12 GPA FOR ANN, AND 0.91 GPA FOR QSPR-DOW

- THE MOLECULAR DESCRIPTOR WITH THE HIGHEST PLS LOADING WAS THE ROTATIONAL DEGREES OF FREEDOM FOR BOTH T_g AND E

RESULTS OF ATOMISTIC CERIUS^2 CALCULATIONS

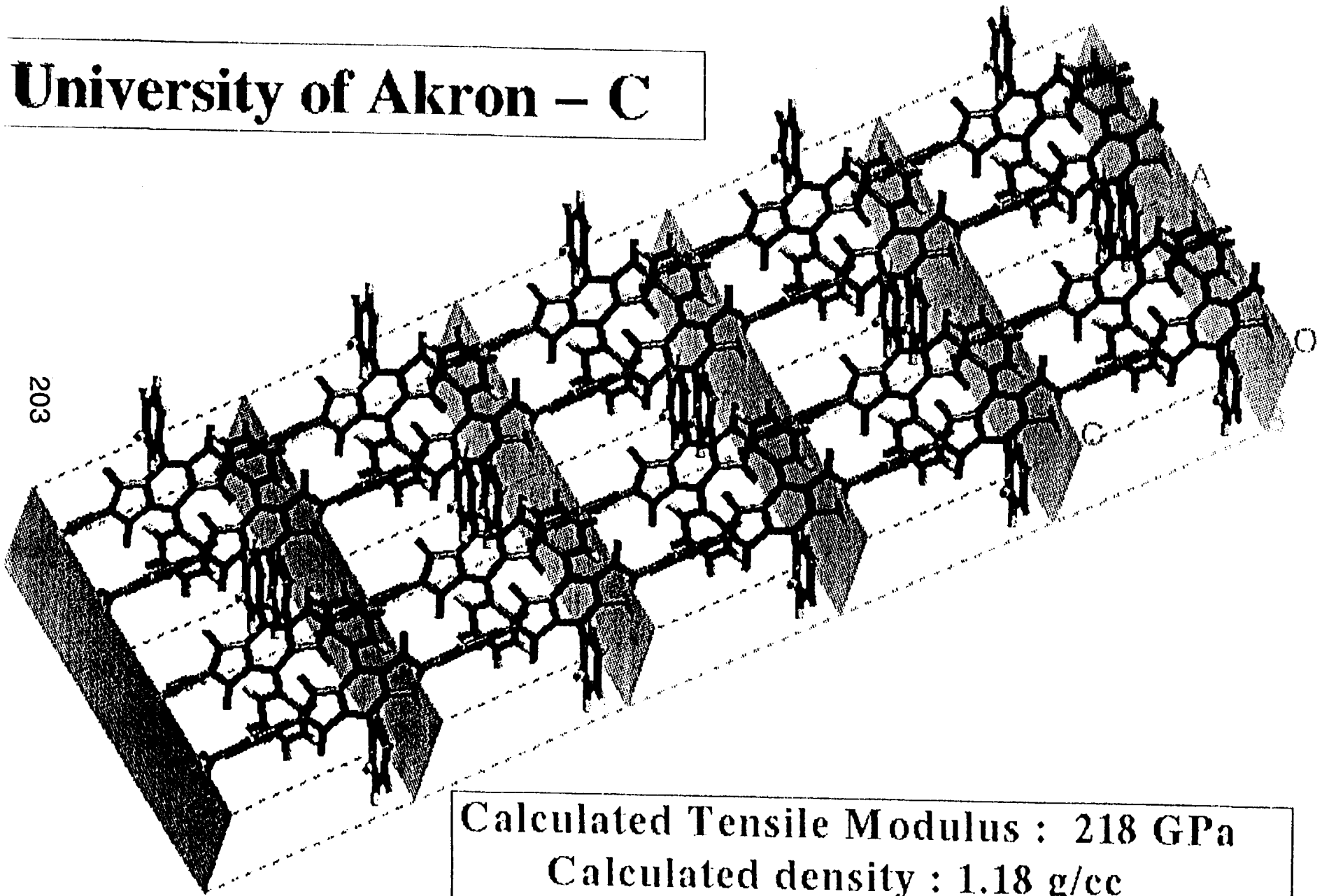
cis – PBO

Calculated Tensile Modulus : 354 GPa



Miller planes are highlighted in blue

University of Akron – C

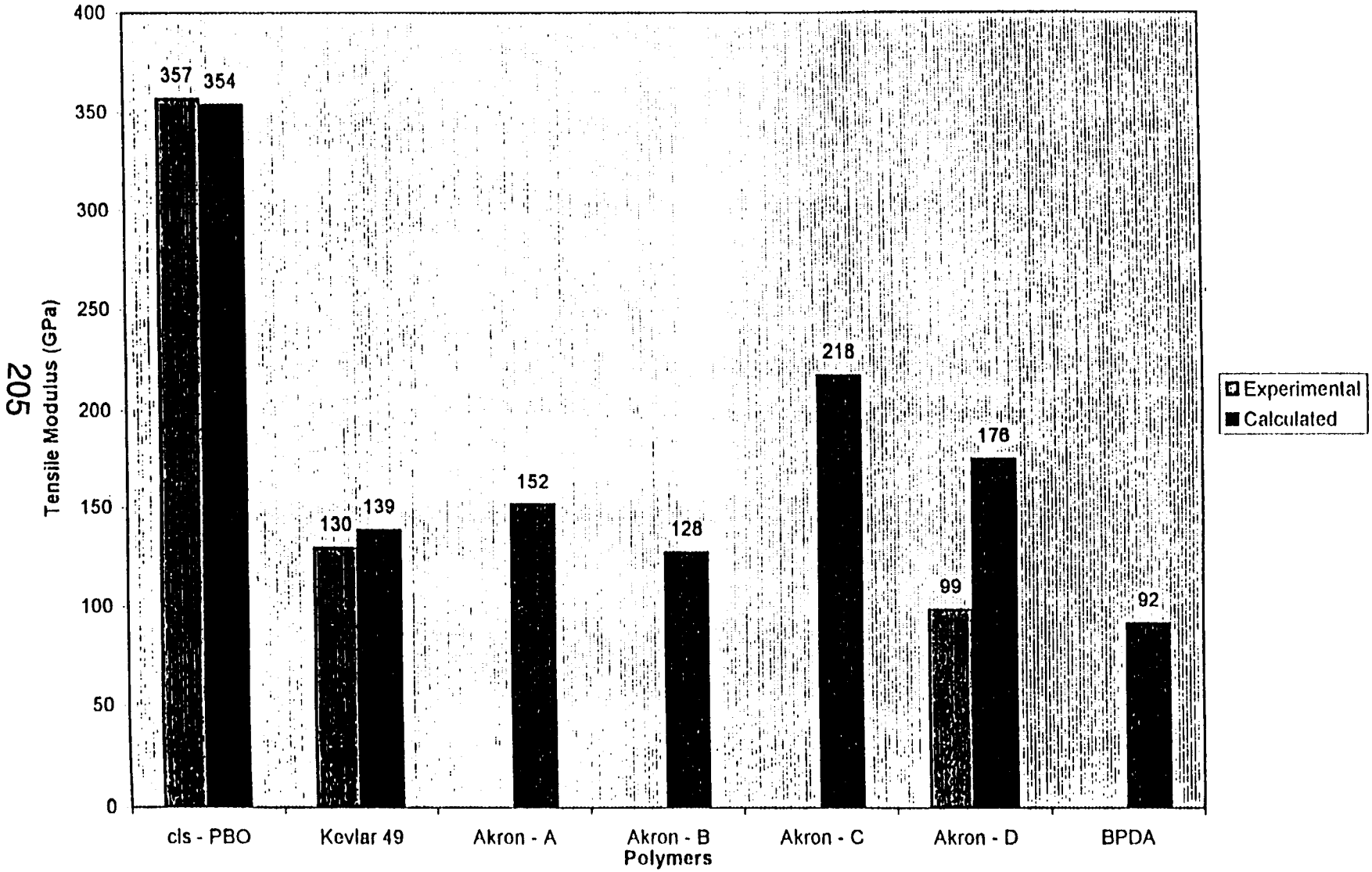


Calculated Tensile Modulus : 218 GPa
Calculated density : 1.18 g/cc

Table C: University of Akron - C Cerius^2 Data

Structure	Energy kcal/mol	density g/cc	Tensile Modulus (GPa) Z axis
a	145.0534	1.1860	221.3720
b	***144.7304***	***1.1840***	***217.1443***
c	144.9722	1.1830	222.4243
d	***144.6897***	***1.1840***	***219.5773***
e	***144.6852***	***1.1830***	***215.7280***
f	***144.6677***	***1.1840***	***219.6206***
g	145.0247	1.1860	219.7376
h	145.0469	1.1860	200.7676
i	***144.7431***	***1.1840***	***217.9189***
j	145.0385	1.1860	233.4200
Average			218.195

Chart 1: Predicted Tensile Modulus for Control and Experimental Polymers



Multiaxial and Time DependentResponse of Rigid Polymers

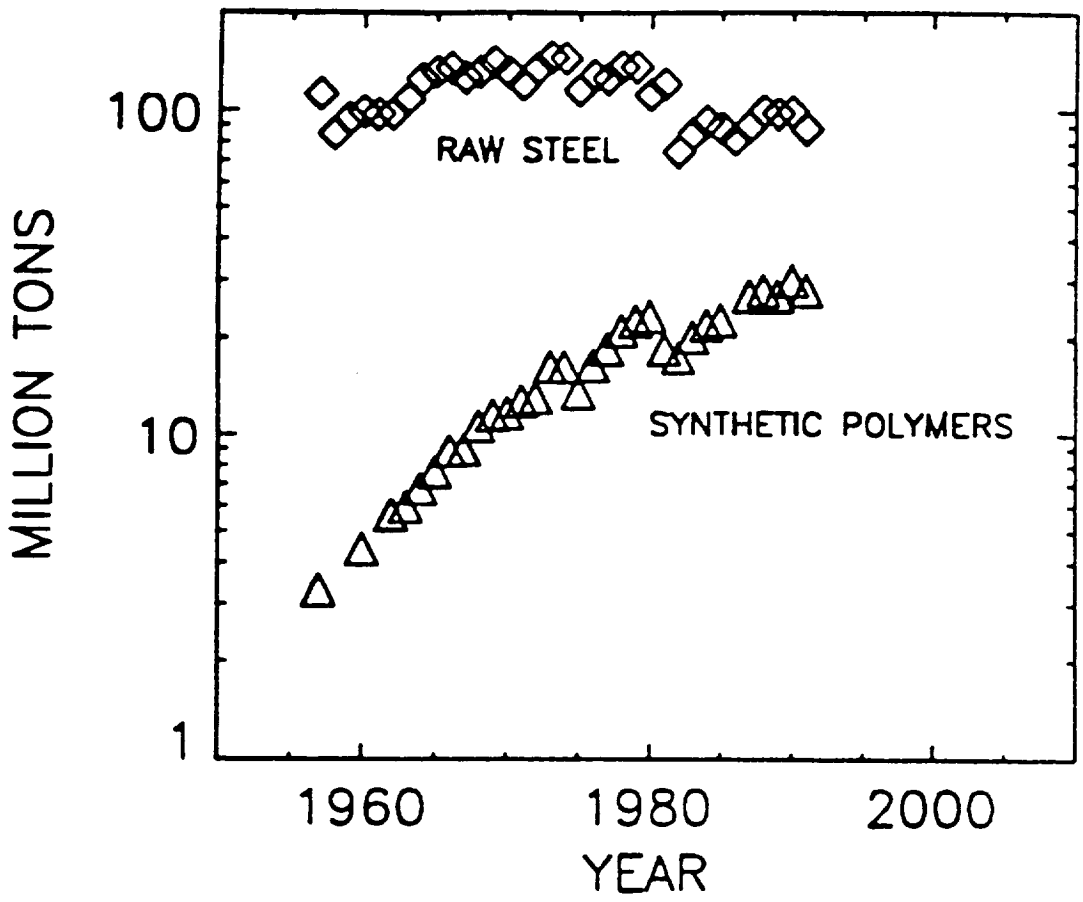
W.G. Knauss

California Institute of Technology
Pasadena, California

Supported in part by the Materials Branch at NASA, Langley

The following are the captions for the figures.

1. Title
2. Productions of steel and polymer during last 35 years
3. Long range objectives
4. Constitutive Interest
5. Range of Issues
6. Yield-like behavior
7. Experimental Approaches to Physical Characterization
8. A free volume based constitutive model
9. Comparison of material responses between the free volume model prediction and experimental observation for uniaxial loading and unloading
10. Comparison of material responses between the free volume model prediction and experimental observations for relaxation at different small strain levels
11. Simulation of yield-like behavior from the free volume model
12. Free volume model for large uniaxial strains (polymide)
13. Creep compliance at different stress levels measured by Govaert
14. Master creep compliance curve shifted by Govaert. The master curve is not smooth
15. Comparison of the master creep compliance curve shifted by Govaert and that shifted by H. Lu and W.G. Knauss
16. Zoom of a portion of the master curve "shifted" by Govaert. (The curves do not really fit a shift.)
17. The shift factors measured by Govaert
18. The shift factors measured by H. Lu and W.G. Knauss
19. Displacement measurement resolution of the digital image correlation
20. Shear relaxation modulus measured at 0.2% of shear strain
21. Shear relaxation master curve
22. Young's relaxation modulus measured at 0.2% of axial strain
23. Young's relaxation master curve
24. Shift factors for the Young's and shear modulus master curves
25. Superposed tension or compression increases the shear creep rate under pure torsion well below glass transition (results at 22°C)
26. Superposed tension or compression increases the shear creep rate under pure torsion well below glass transition (results at 50°C)
27. Shear stress also controls the shear creep rate - shear creep compliances at different stress levels
28. Superposed tension or compression increases the shear creep rate under pure torsion well below glass transition (results at 80°C)
29. Under the same torque, a superposed tension increases the torsional creep rate while a superposed compression decreases it in the vicinity of the glass transition (results at 100°C)
30. Under the same torque, a superposed tension increases the torsional creep rate while a superposed compression decreases it in the vicinity of the glass transition (results at 110°C)
31. Under the same shear stress, a superposed tension has a much higher creep rate than a superposed compression, indicating free volume plays a major role in the glassy state
32. Some thoughts on an "activation" rate model incorporating the coupling of volumetric deformation and shear deformation



Annual Tonnage of Steel and Polymer produced during the last 35 years

Long range objectives:

Establish general polymer constitutive behavior and

Analytically model this behavior

Constitutive behavior must incorporate

- **Linear and nonlinear viscoelasticity at small and moderate strains (yield-like response)**
- **Nonlinear viscoelasticity at very large strains**
- **under arbitrary load histories, including ageing and "recovery"**
- **Environmental factors:**
  - **Temperature dependence, including the range around the glass transition**
  - **Solvent influence, including water**

Constitutive Interest

Physical properties descriptions involve the whole spectrum of size scales and approaches to analytical formulation

1) **Model material behavior for engineering analyses:**
   Application oriented and global view

2) **Structure - property relationships:**
   Molecular science orientation and microscopic view

Physics-based Observation and Issues

Yield-like behavior is physically different from yielding in metals. In thermoplastic solids it is not necessarily associated with crazing

"Yield-like behavior" occurs at small strains ($\varepsilon_{uniaxial}<5\%$)

"Yield-deformations" are usually recoverable under thermal control

Yield-like behavior does not involve large scale molecular re-orientation and organization unless it is associated with very localized shear bands

Molecular orientation occurs in uniaxial deformation at extension ratios exceeding 100%

Very small changes in volume (>0.1%) have a disproportionate effect on the time-temperature rade-off

To what degree is yield-like behavior the result of local material instability augmented or controlled by small volume changes?

To what degree is yield-like response controlled or influenced by organized molecular rearrangement

Range of Issues

1) Time and rate dependence

2) Nonlinear response

3) Thermorheology

4) Glass transition behavior

5) Physical ageing

Experimental Approaches to Physical Characterization

Different stress state histories

There is a lot of data on pressure superposed on uniaxial tension in the literature

There is no data on biaxial stress states shear-plus-tension or shear-plus-compression

There is virtually no data on time-dependent bulk behavior

Constitutive Model (Emri and Knauss, 1981)

Free volume

$$f = f_o + A\alpha(t) * dT + \delta\epsilon_{kk}$$

Time-shift factor, ϕ

$$\log \phi = \frac{b}{2.303}\left(\frac{1}{f} - \frac{1}{f_o}\right)$$

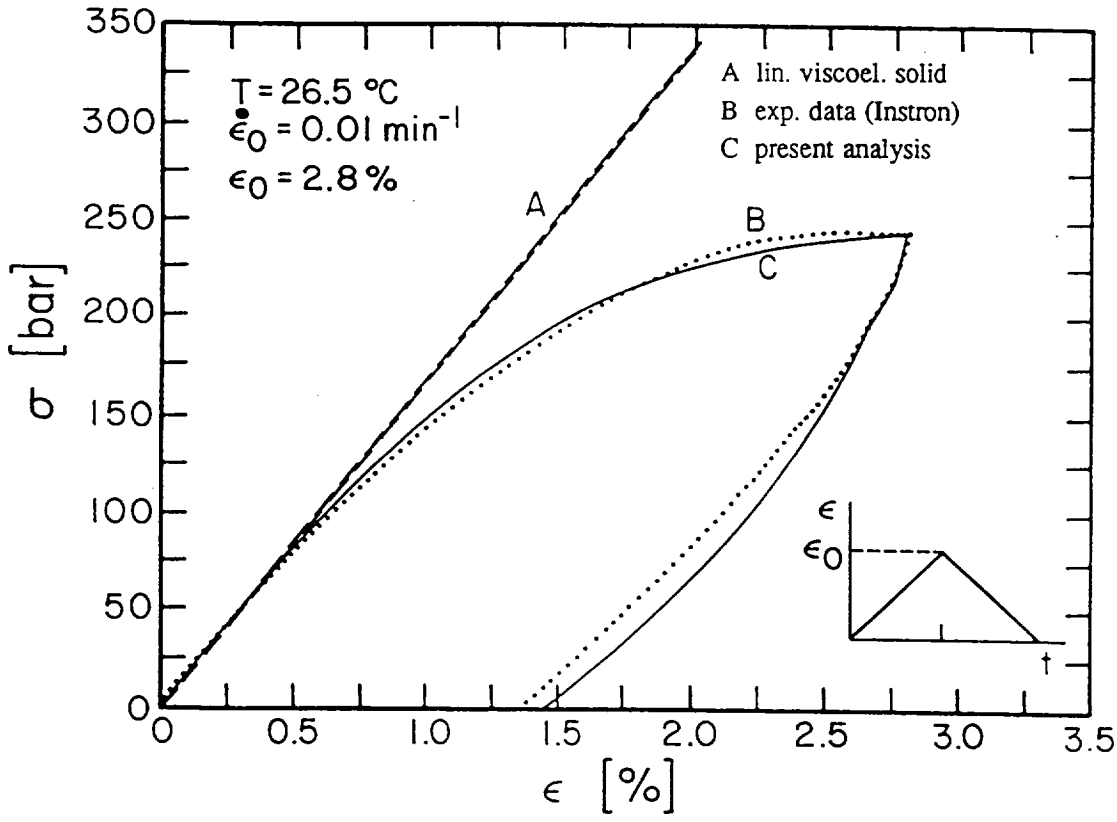
Internal (reduced) time

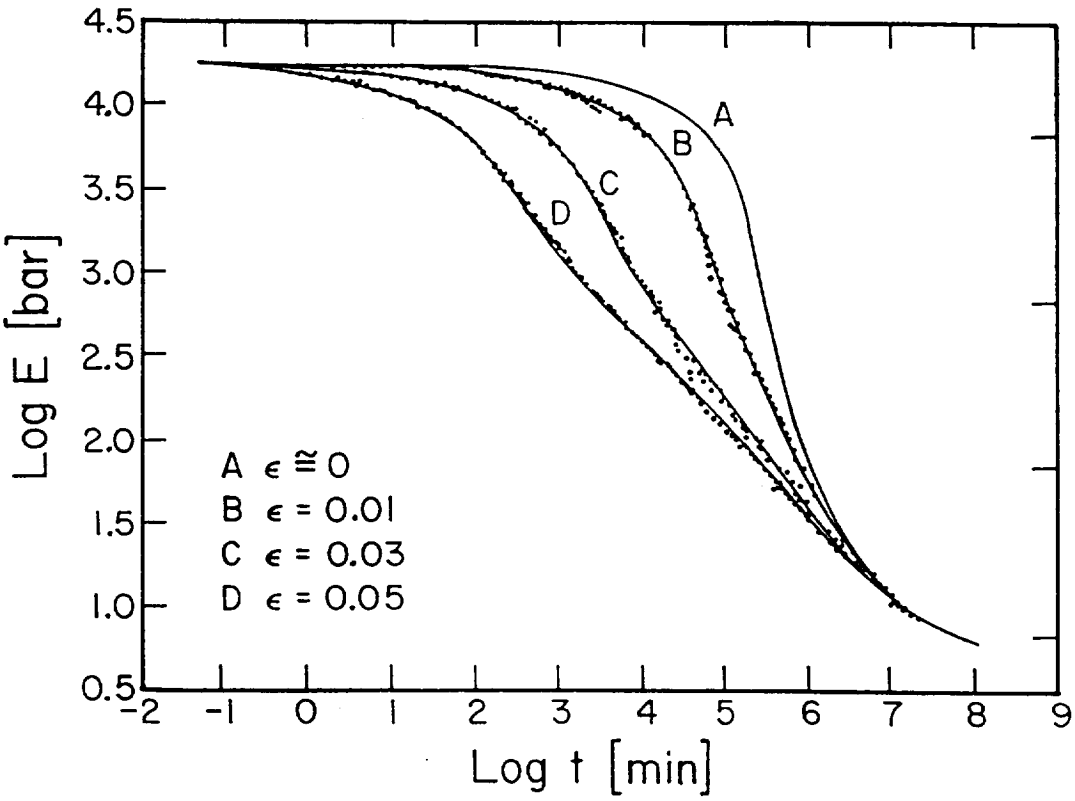
$$d\xi(t) = \frac{dt}{\phi(t)} \qquad \text{or} \qquad \xi(t) = \int_0^t \frac{du}{\phi[T(u), \theta(u)]}$$

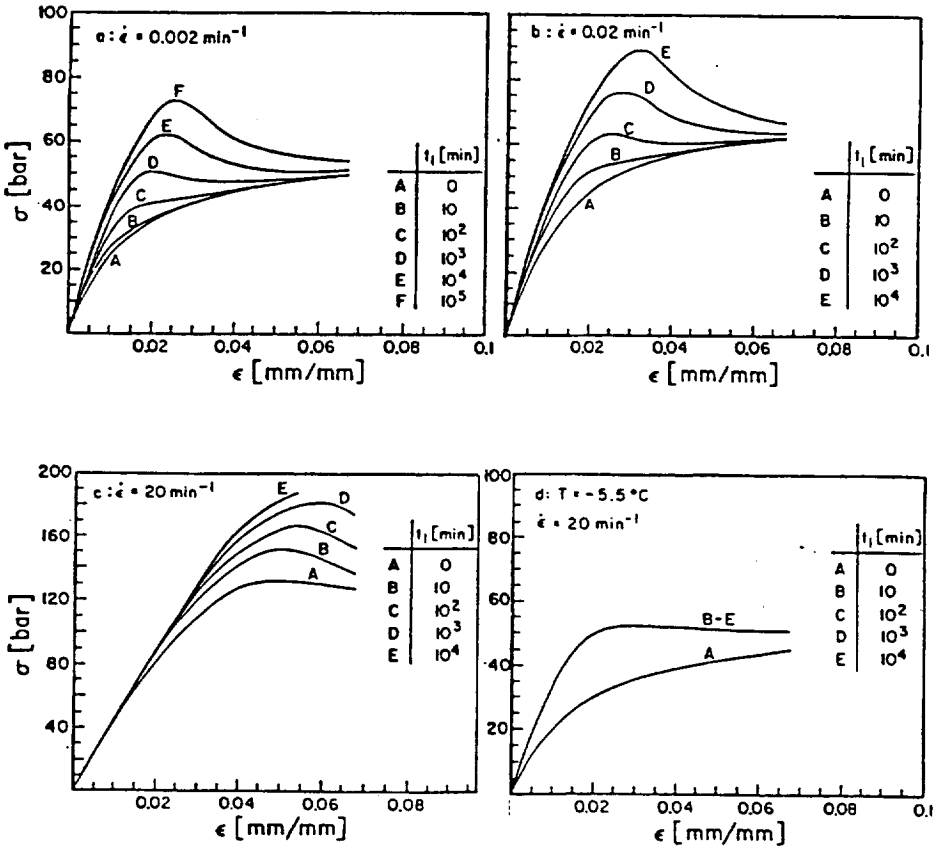
Thermorheologically simple material

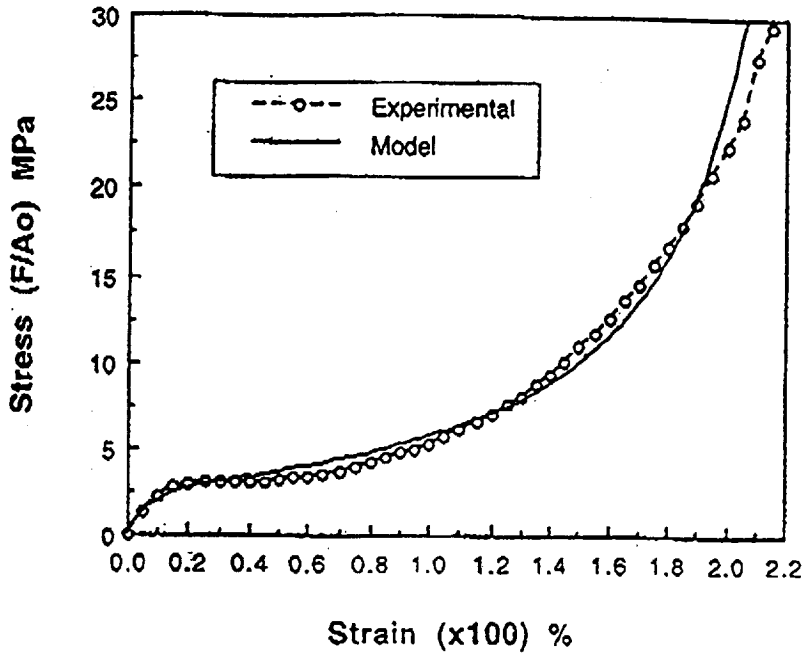
$$S_{ij} = 2\int_{-\infty}^{t} \mu(\xi - \xi')\frac{\partial e_{ij}(t')}{\partial t'}\, dt'$$

$$\sigma_{kk} = 3\int_{-\infty}^{t} K(\xi - \xi')\frac{\partial \epsilon_{kk}(t')}{\partial t'}\, dt'$$


T = 26.5 °C
$\dot{\epsilon}_0$ = 0.01 min^{-1}
ϵ_0 = 2.8 %
A lin. viscoel. solid
B exp. data (Instron)
C present analysis
A
B
C
σ [bar]
ϵ [%]
ϵ
ϵ_0
t
0
50
100
150
200
250
300
350
0.5
1.0
1.5
2.0
2.5
3.0
3.5


Log E [bar]
Log t [min]
A
B
C
D
A ε ≅ 0
B ε = 0.01
C ε = 0.03
D ε = 0.05
4.5
4.0
3.5
3.0
2.5
2.0
1.5
1.0
0.5
-2
-1
0
1
2
3
4
5
6
7
8
9


a : $\dot{\epsilon}$ = 0.002 min^{-1}
b : $\dot{\epsilon}$ = 0.02 min^{-1}
c : $\dot{\epsilon}$ = 20 min^{-1}
d: T = -5.5 °C
$\dot{\epsilon}$ = 20 min^{-1}
σ [bar]
ε [mm/mm]
t_1 [min]
A 0
B 10
C 10^2
D 10^3
E 10^4
F 10^5
B-E



M. R. Monaghan
P. Mallon, Univ. of Limerick
Polyimide film
380° C
C/Head 65 mm/min

Figure 4.6 Three Term Model Tensile Response

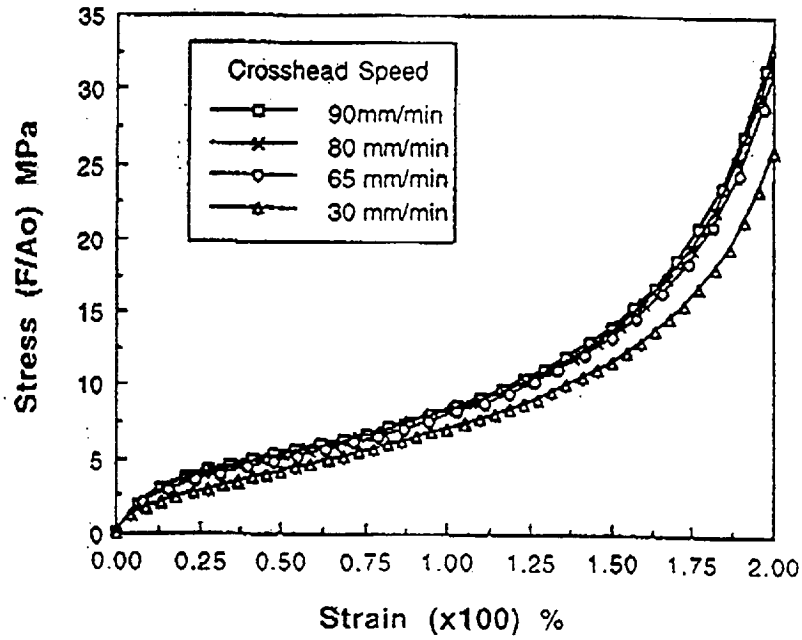
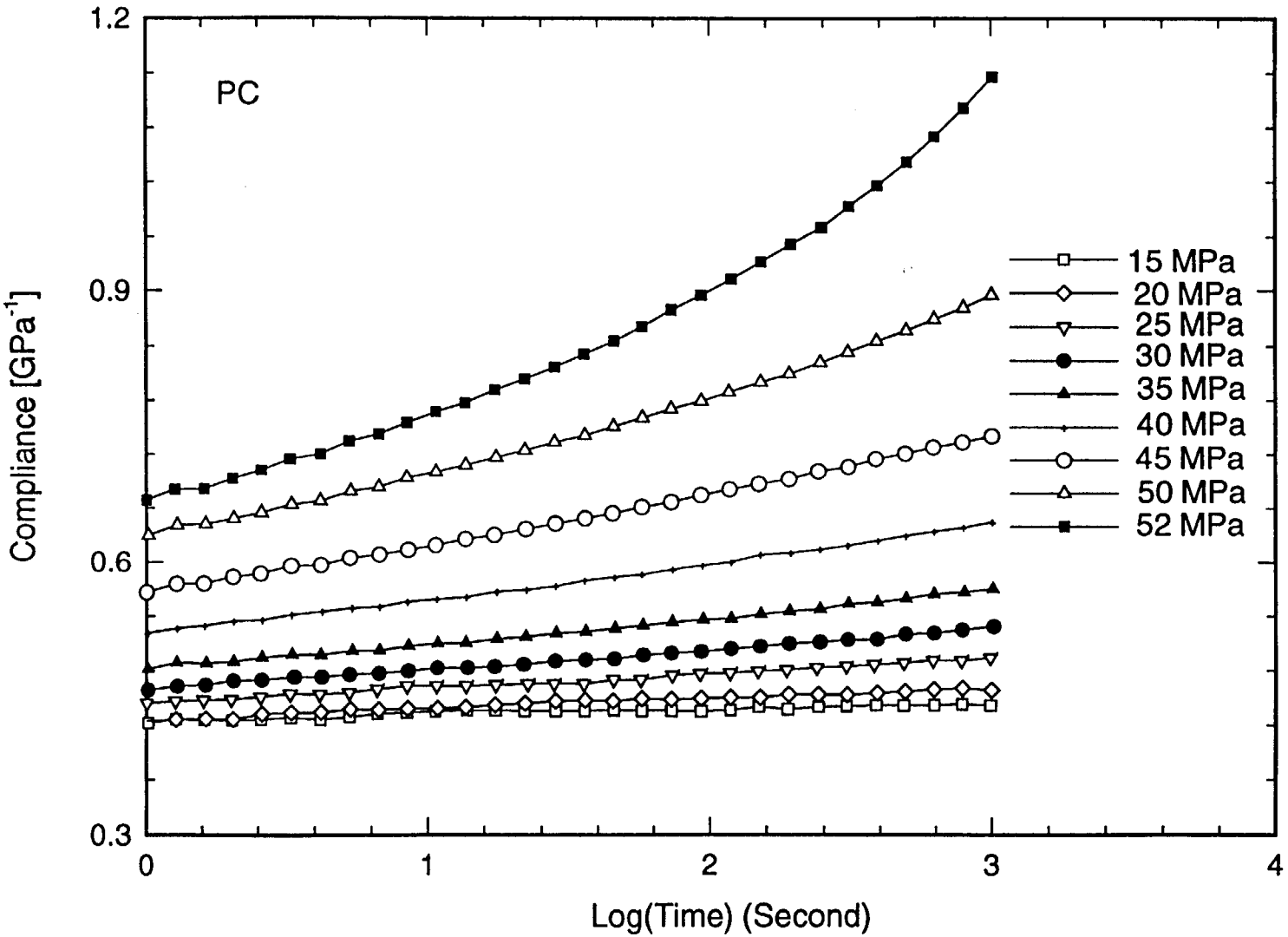
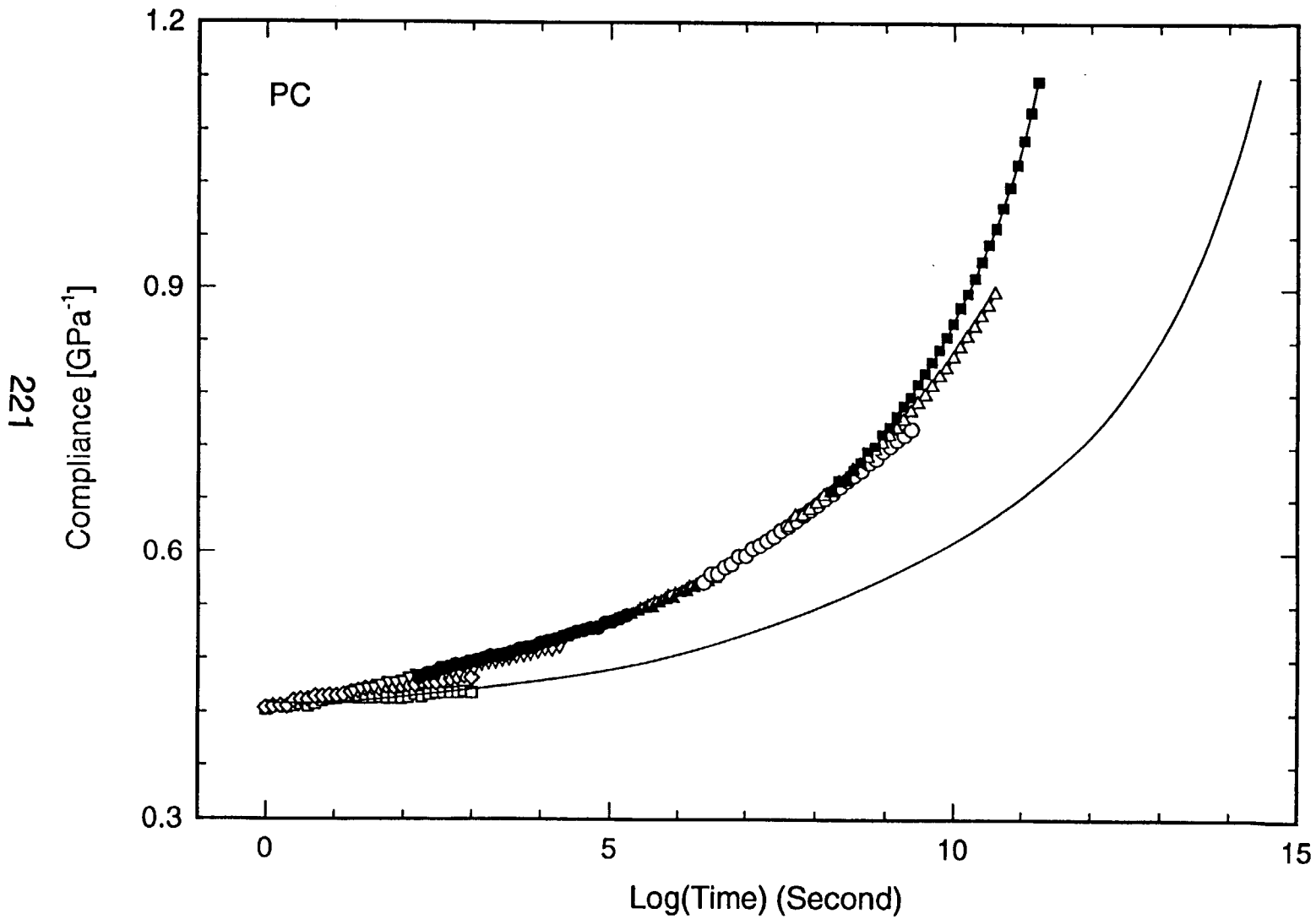
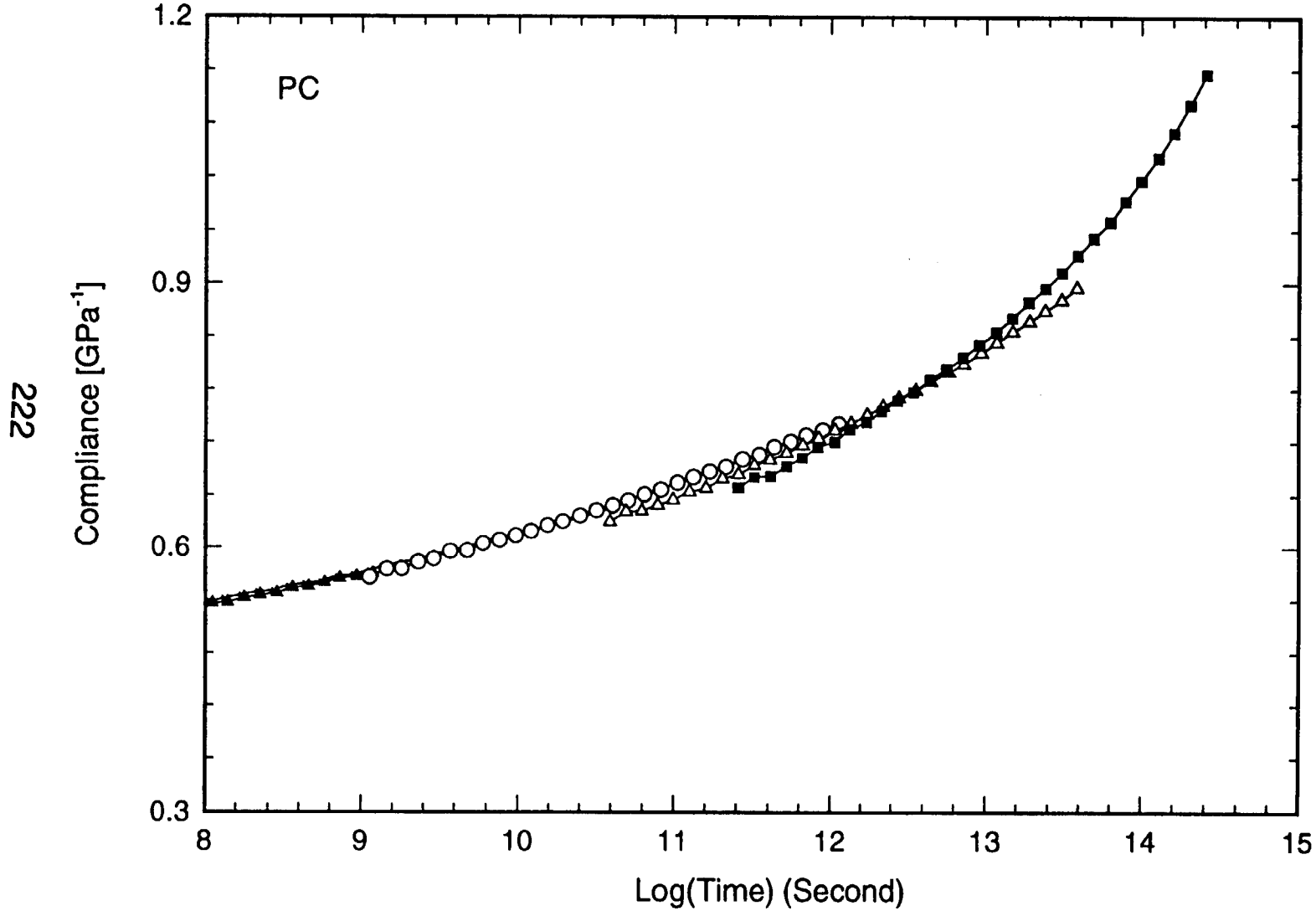


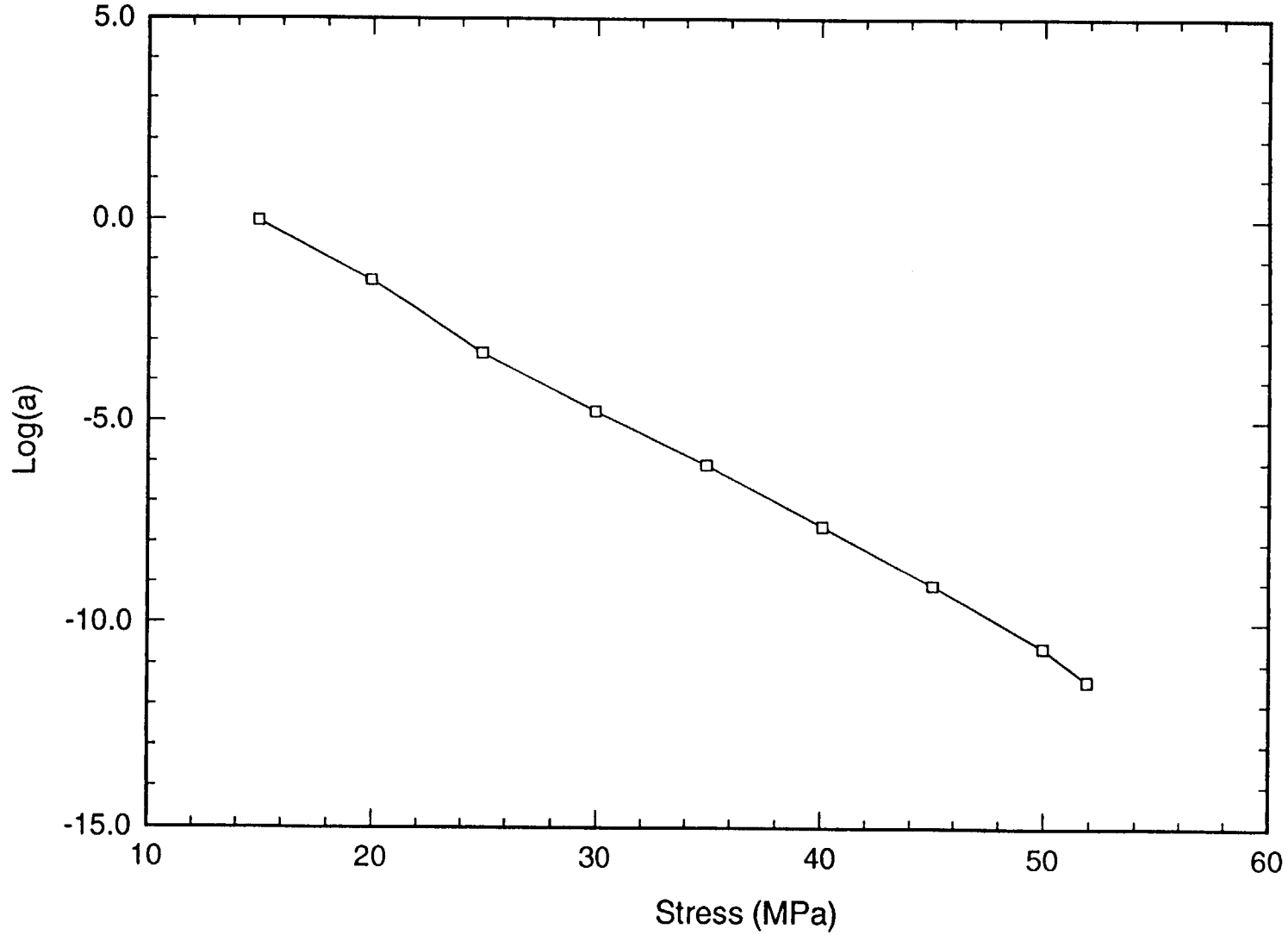
Figure 4.7 Model Results for Variation in Straining Rates on Specimen of 65mm Gauge Length.

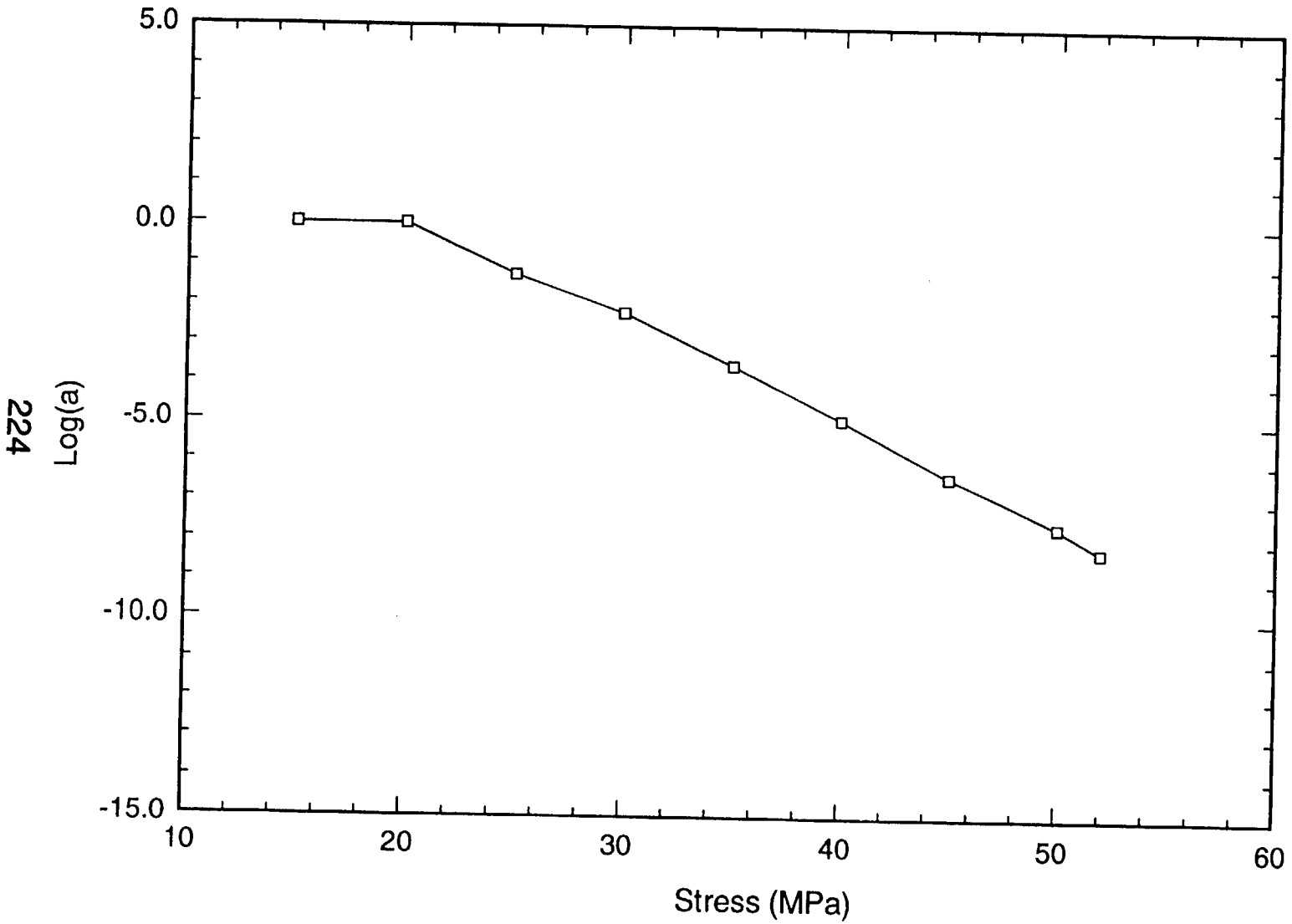

PC
Compliance [GPa^{-1}]
Log(Time) (Second)
1.2
0.9
0.6
0.3
0
1
2
3
4
15 MPa
20 MPa
25 MPa
30 MPa
35 MPa
40 MPa
45 MPa
50 MPa
52 MPa

PC
Compliance [GPa-1]
Log(Time) (Second)
1.2
0.9
0.6
0.3
0
5
10
15


PC
1.2
0.9
0.6
0.3
0
5
10
15
Compliance [GPa^{-1}]
Log(Time) (Second)


PC
222
Compliance [GPa-1]
1.2
0.9
0.6
0.3
8
9
10
11
12
13
14
15
Log(Time) (Second)


5.0
0.0
-5.0
-10.0
-15.0
Log(a)
10
20
30
40
50
60
Stress (MPa)


5.0
0.0
-5.0
-10.0
-15.0
Log(a)
10
20
30
40
50
60
Stress (MPa)

Displacement Resolution of the Method

A typical field of view is 25 mm (1 inch)

Pixel size: 50 microns/pixel side

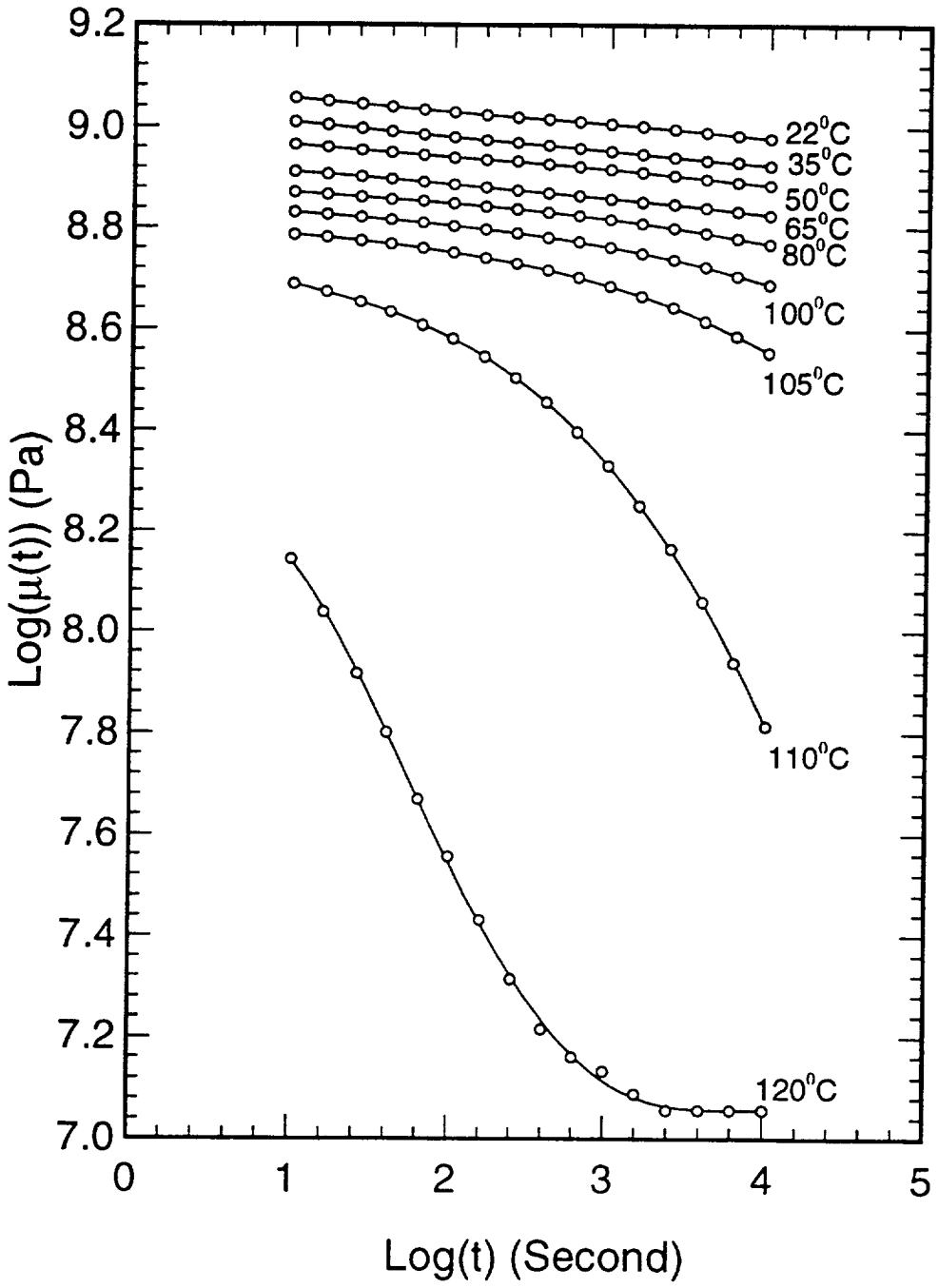
The resolution limit for displacements is 3 microns

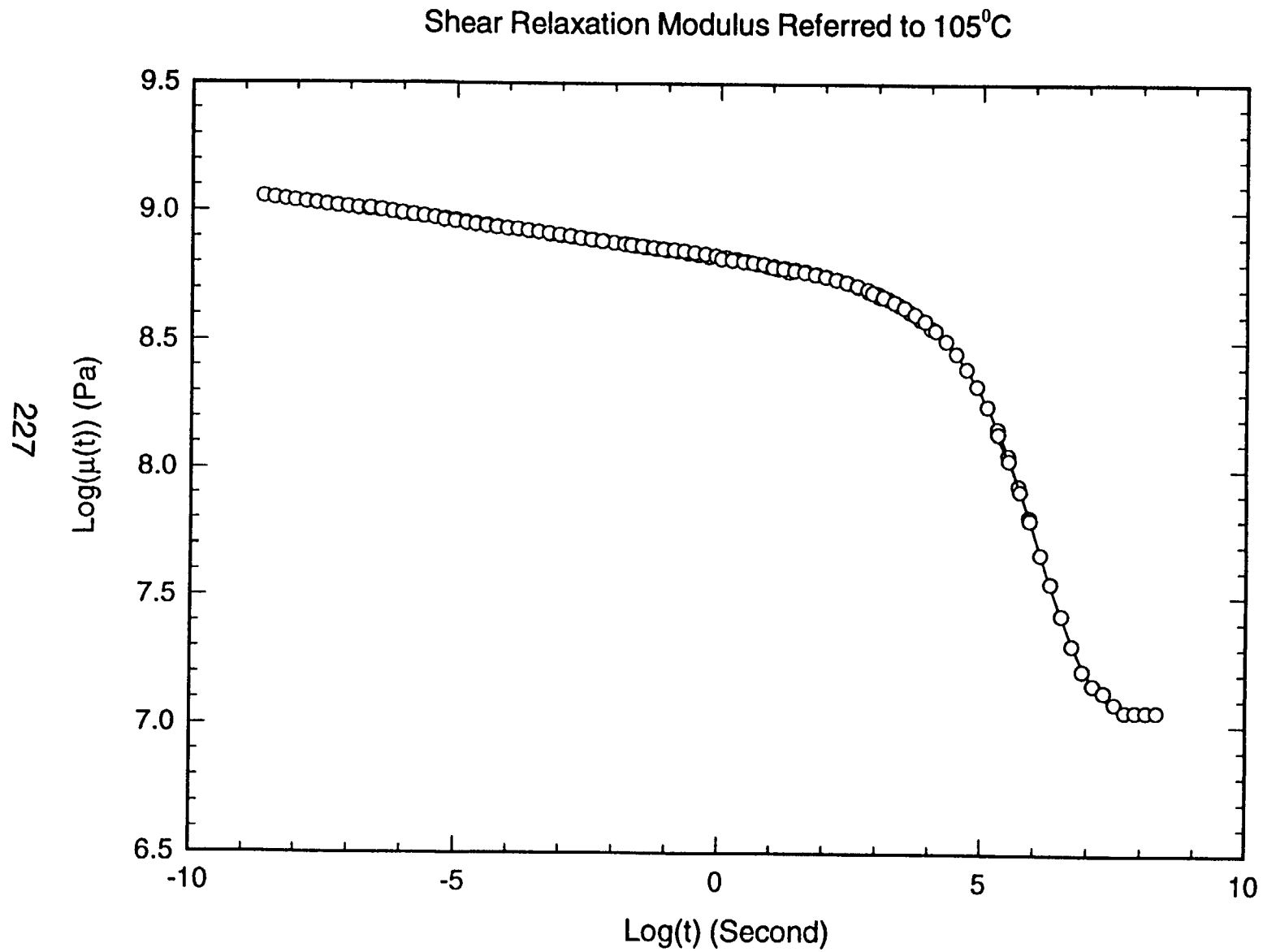
This translates into resolution of

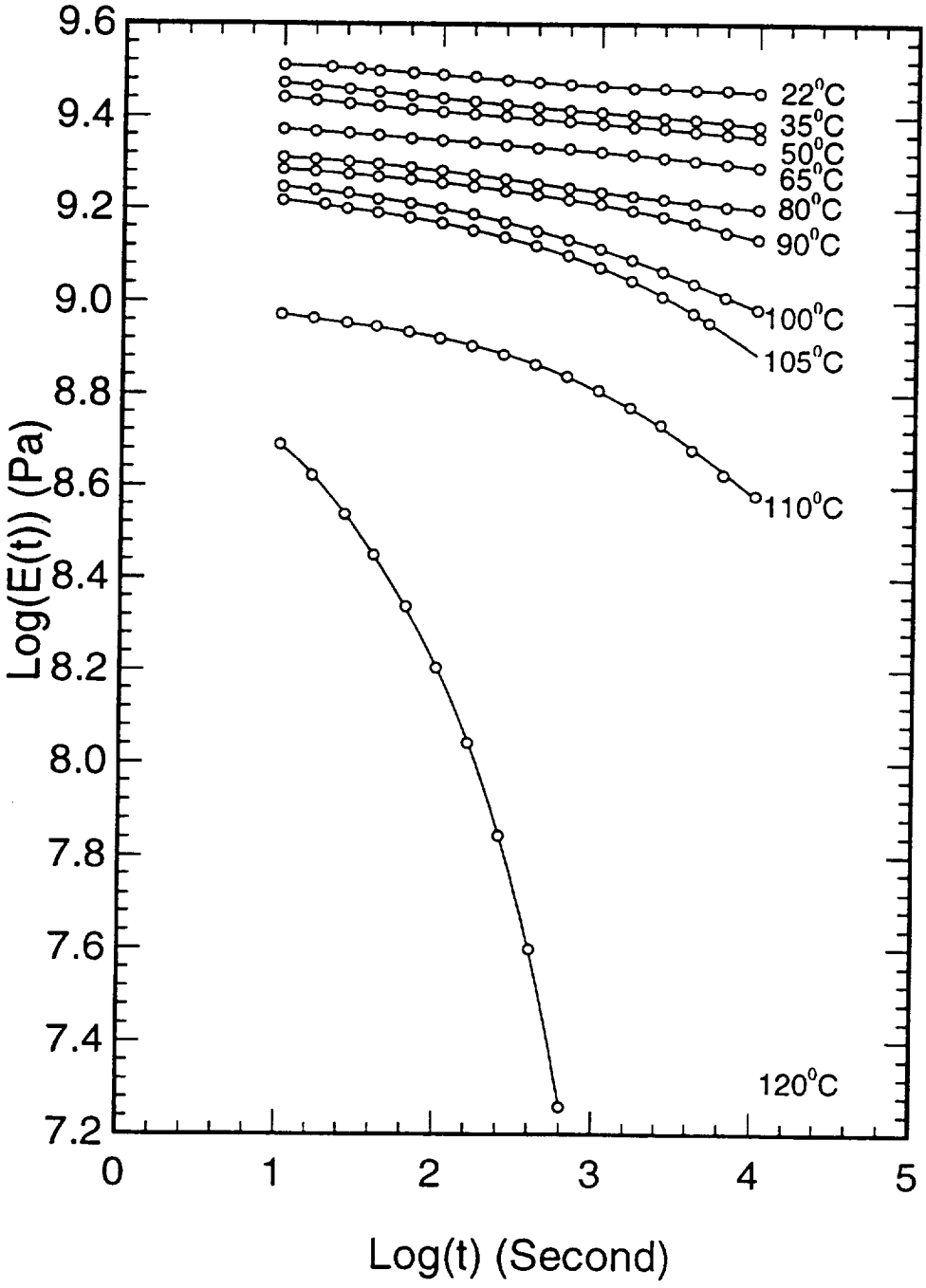
normal strains of 0.05%

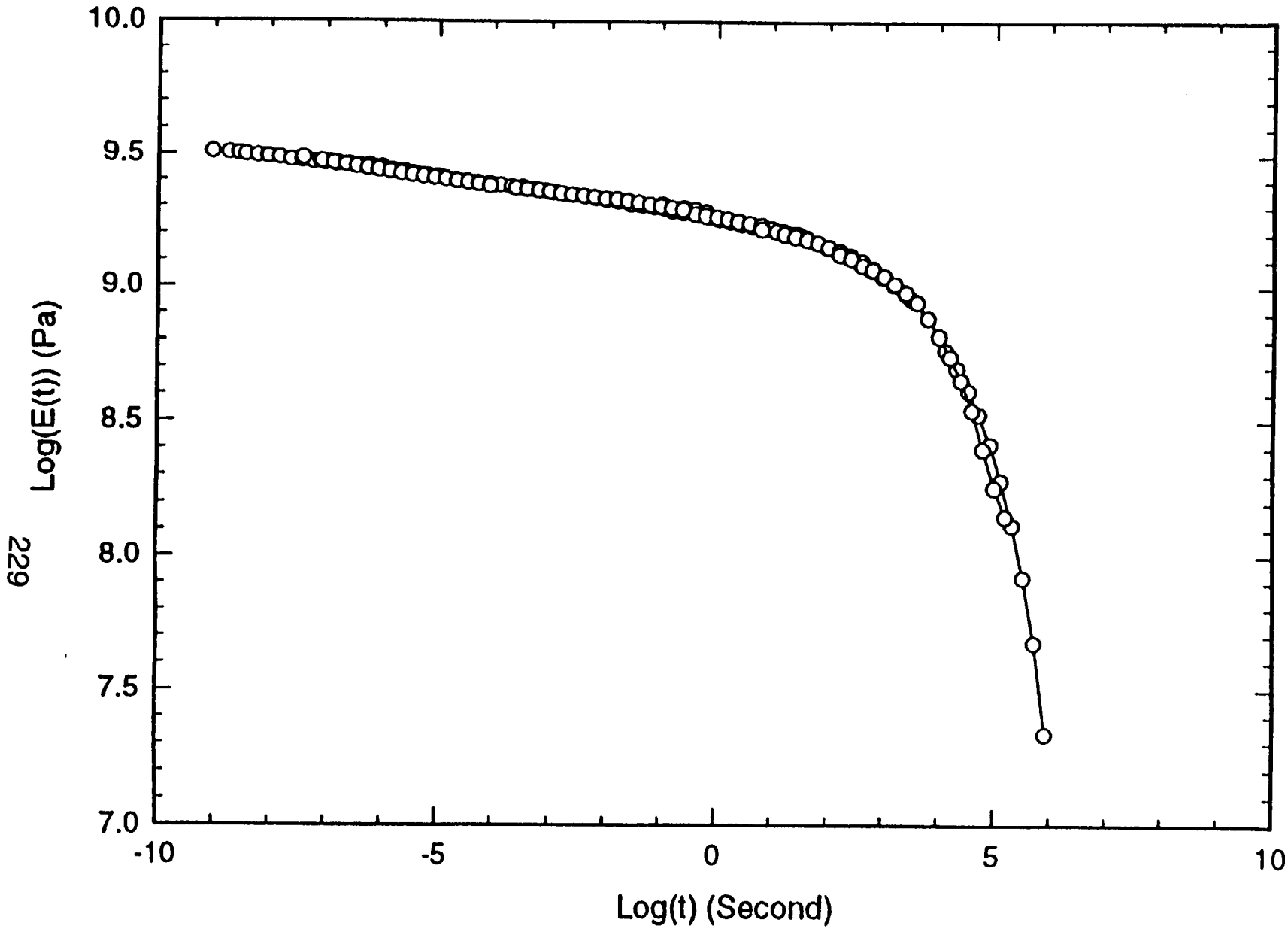
shear strains of 0.05%

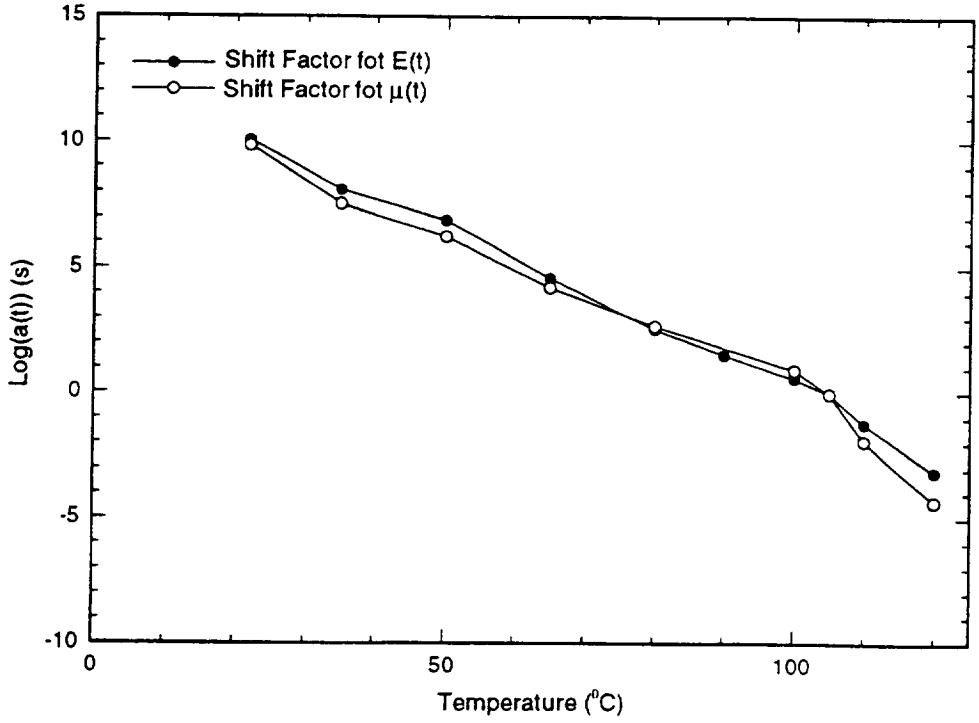
circumferential strains of 0.08%

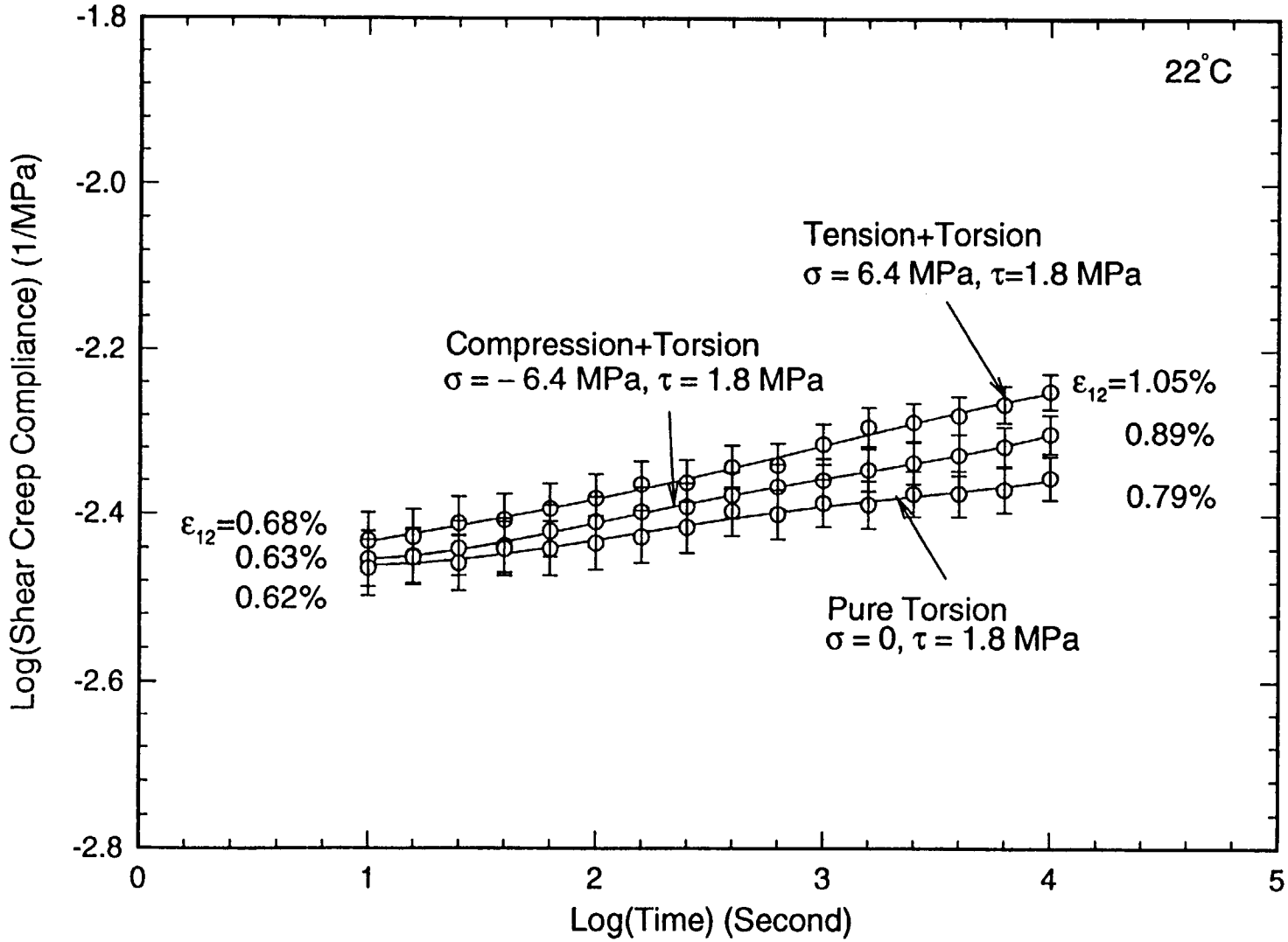

9.2
9.0
8.8
8.6
8.4
8.2
8.0
7.8
7.6
7.4
7.2
7.0
Log(μ(t)) (Pa)
0
1
2
3
4
5
Log(t) (Second)
22°C
35°C
50°C
65°C
80°C
100°C
105°C
110°C
120°C

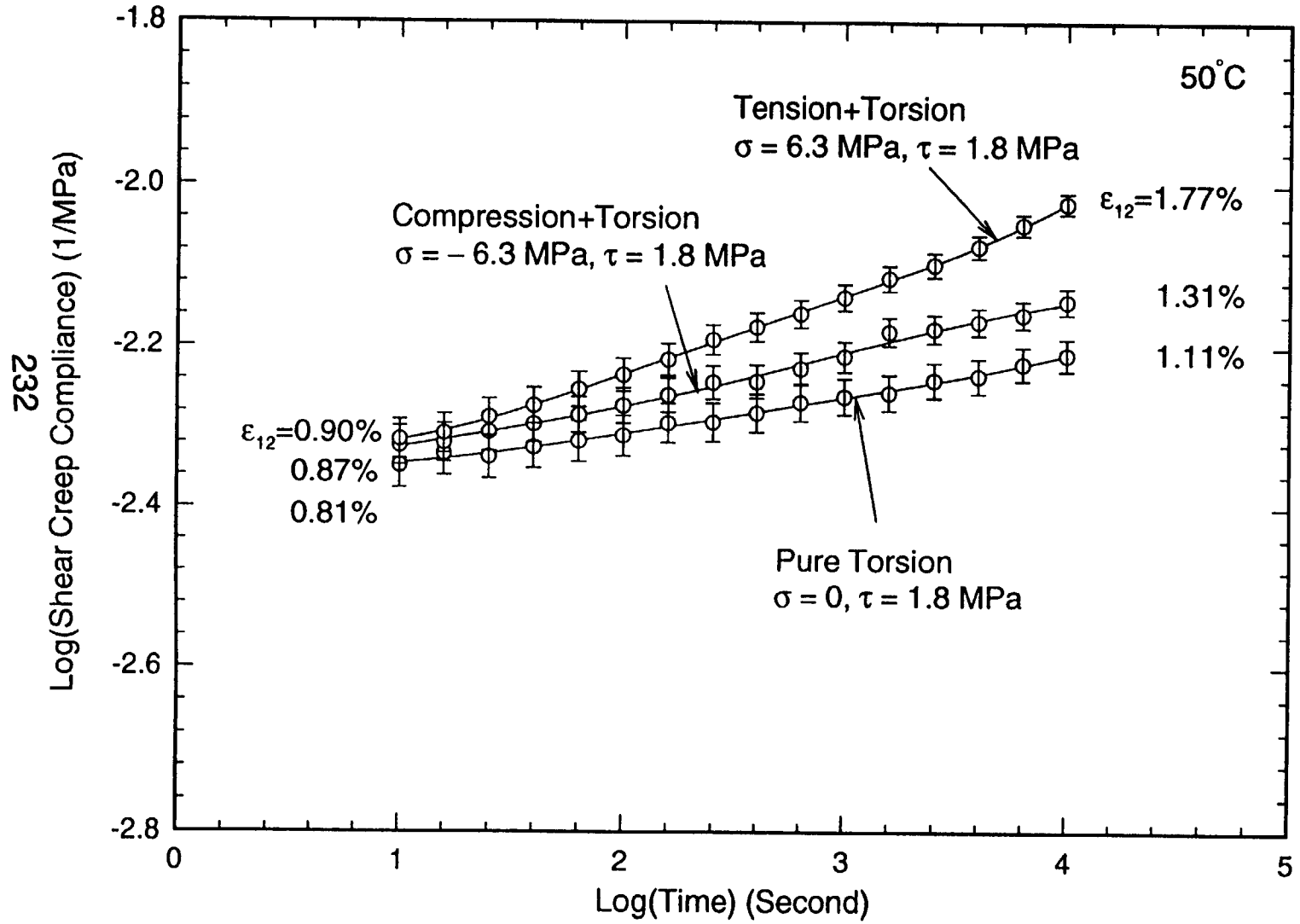

Shear Relaxation Modulus Referred to 105^{0}C
Log(μ(t)) (Pa)
9.5
9.0
8.5
8.0
7.5
7.0
6.5
-10
-5
0
5
10
Log(t) (Second)

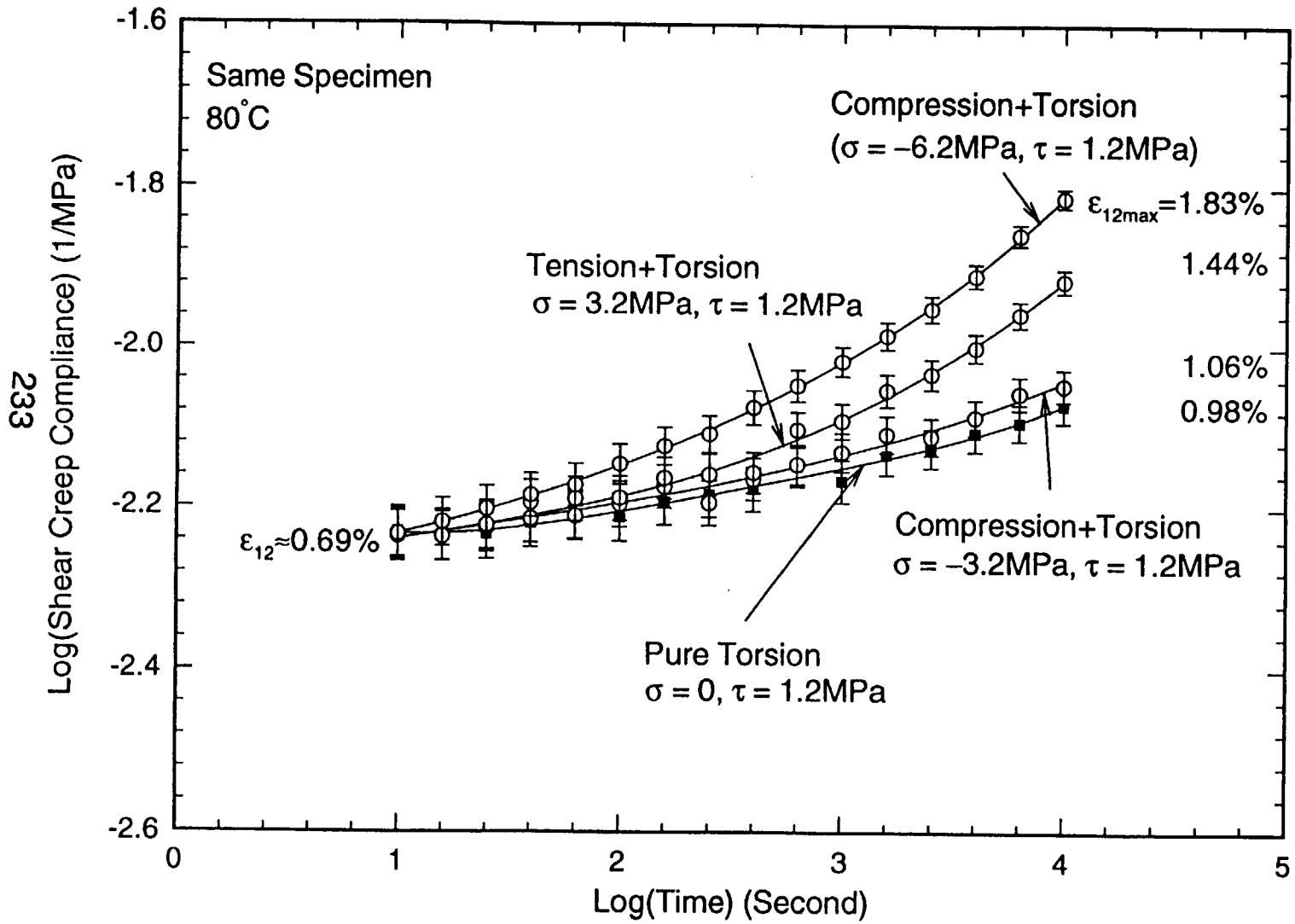

9.6
9.4
9.2
9.0
8.8
8.6
8.4
8.2
8.0
7.8
7.6
7.4
7.2
Log(E(t)) (Pa)
0
1
2
3
4
5
Log(t) (Second)
22°C
35°C
50°C
65°C
80°C
90°C
100°C
105°C
110°C
120°C

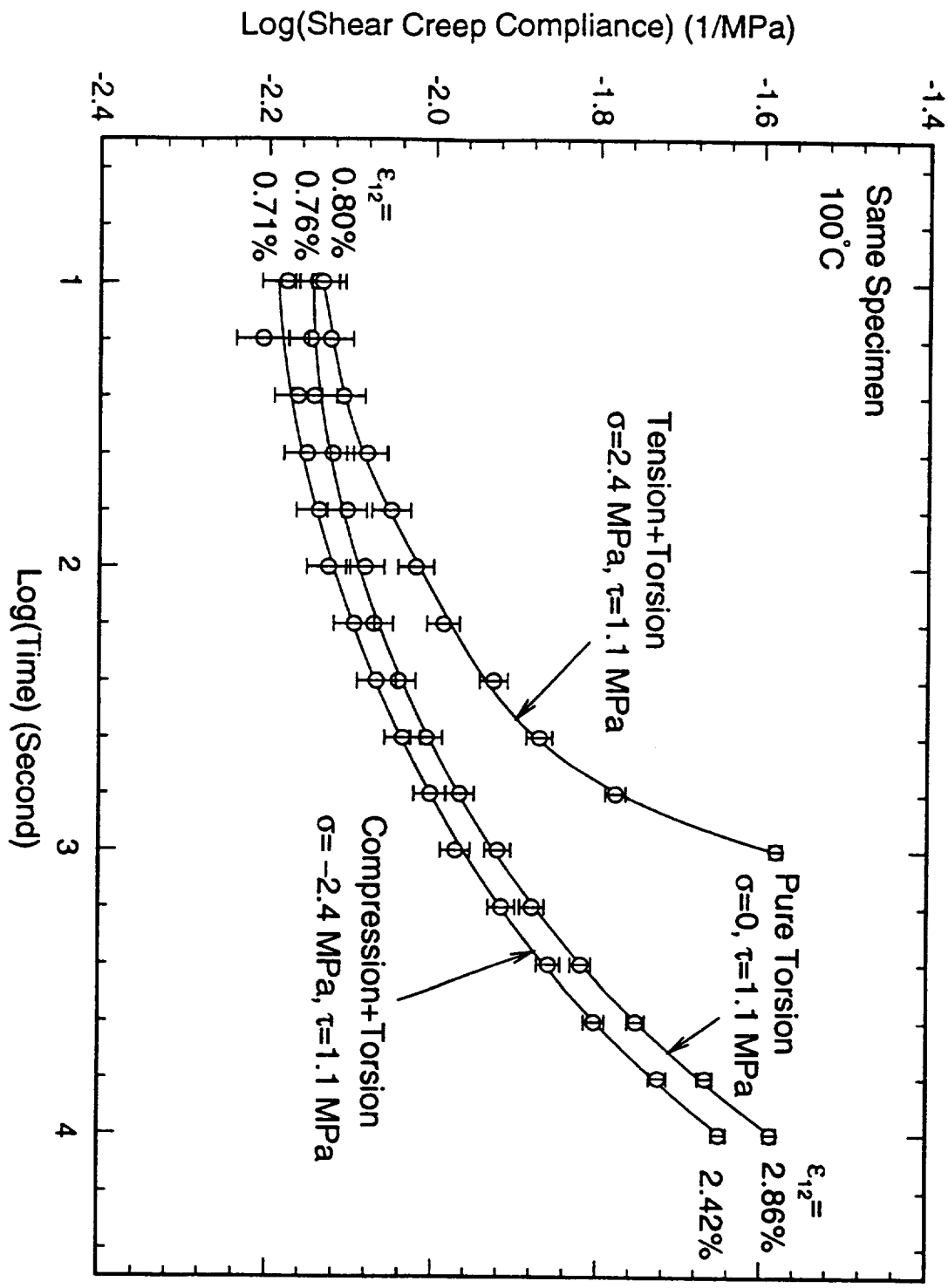

10.0
9.5
9.0
8.5
8.0
7.5
7.0
Log(E(t)) (Pa)
-10
-5
0
5
10
Log(t) (Second)

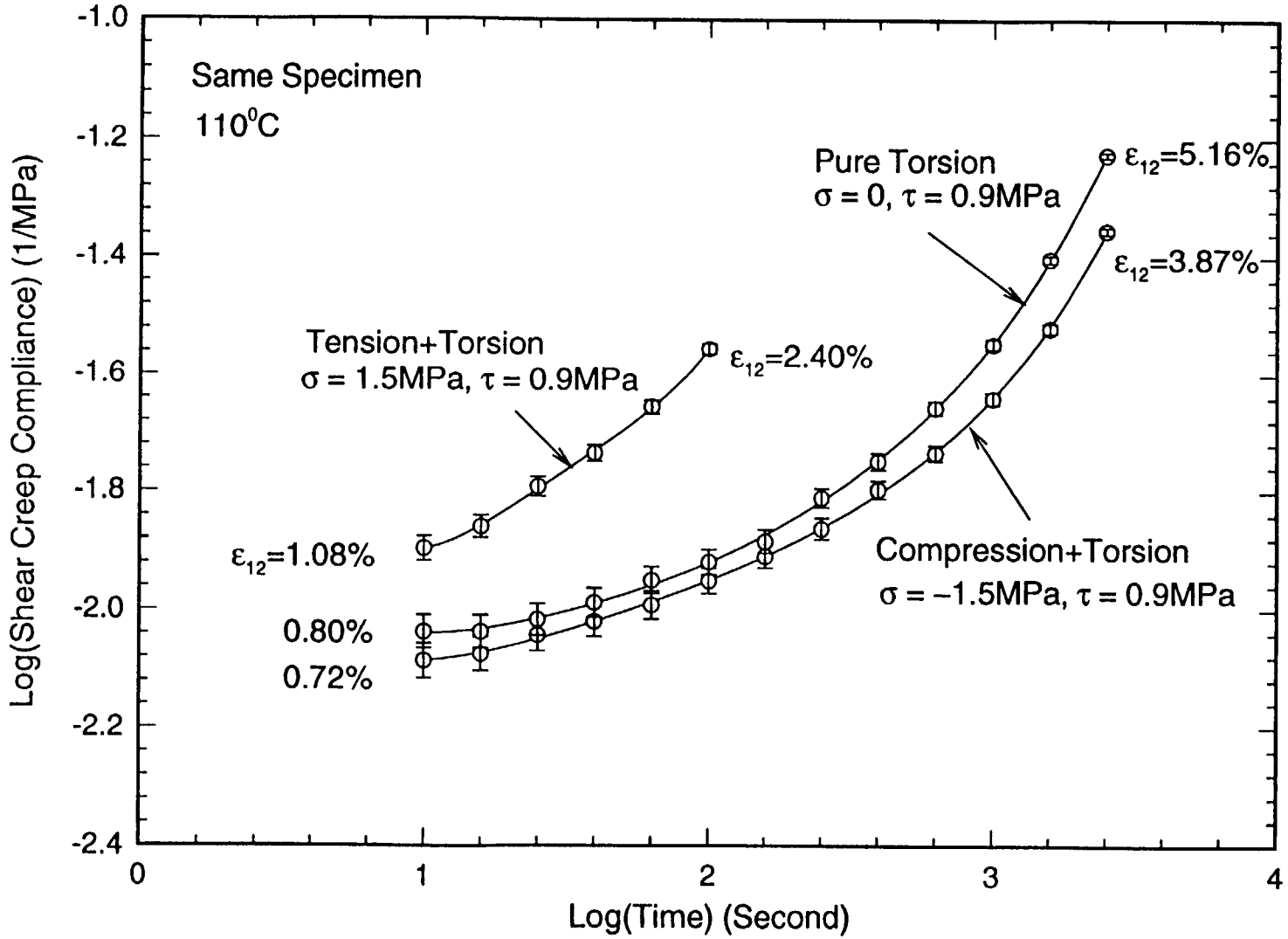

Shift Factor fot E(t)
Shift Factor fot μ(t)
Log(a(t)) (s)
15
10
5
0
-5
-10
0
50
100
Temperature (°C)

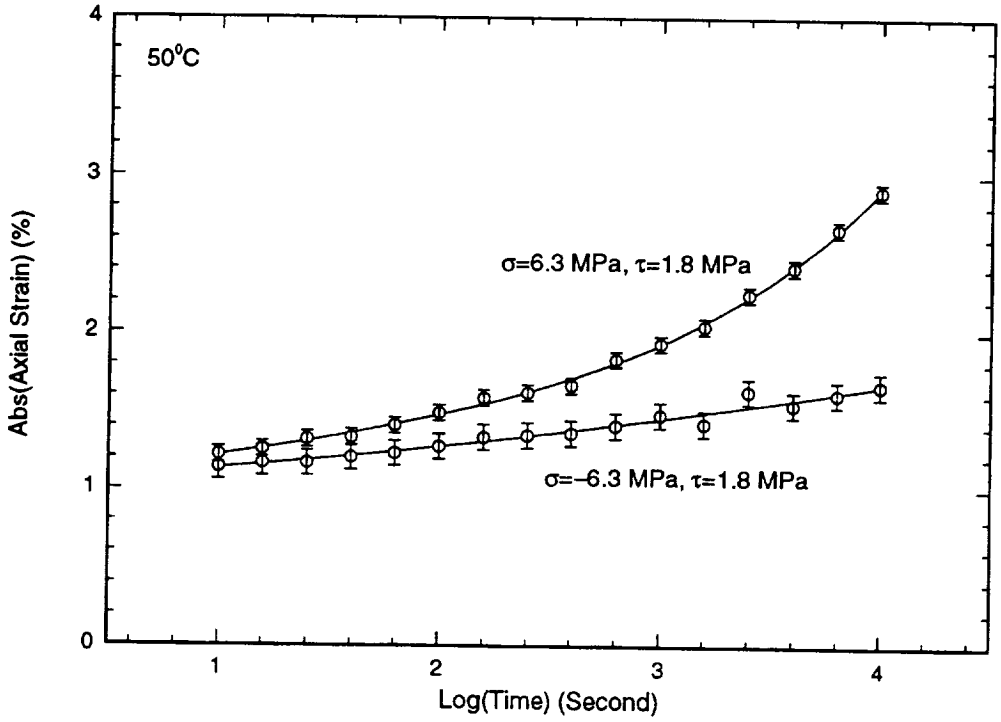

22°C
Tension+Torsion
σ = 6.4 MPa, τ=1.8 MPa
Compression+Torsion
σ = – 6.4 MPa, τ = 1.8 MPa
ε12=1.05%
0.89%
0.79%
ε12=0.68%
0.63%
0.62%
Pure Torsion
σ = 0, τ = 1.8 MPa
Log(Shear Creep Compliance) (1/MPa)
Log(Time) (Second)
-1.8
-2.0
-2.2
-2.4
-2.6
-2.8
0
1
2
3
4
5


50°C
Tension+Torsion
σ = 6.3 MPa, τ = 1.8 MPa
ε12=1.77%
Compression+Torsion
σ = – 6.3 MPa, τ = 1.8 MPa
1.31%
1.11%
ε12=0.90%
0.87%
0.81%
Pure Torsion
σ = 0, τ = 1.8 MPa
Log(Shear Creep Compliance) (1/MPa)
Log(Time) (Second)
-1.8
-2.0
-2.2
-2.4
-2.6
-2.8
0
1
2
3
4
5


Same Specimen
80°C
Compression+Torsion
(σ = −6.2MPa, τ = 1.2MPa)
ε12max=1.83%
1.44%
1.06%
0.98%
Tension+Torsion
σ = 3.2MPa, τ = 1.2MPa
ε12≈0.69%
Compression+Torsion
σ = −3.2MPa, τ = 1.2MPa
Pure Torsion
σ = 0, τ = 1.2MPa
Log(Shear Creep Compliance) (1/MPa)
233
Log(Time) (Second)
-1.6
-1.8
-2.0
-2.2
-2.4
-2.6
0
1
2
3
4
5


Log(Shear Creep Compliance) (1/MPa)
-1.4
-1.6
-1.8
-2.0
-2.2
-2.4
Same Specimen
100°C
Tension+Torsion
σ=2.4 MPa, τ=1.1 MPa
Pure Torsion
σ=0, τ=1.1 MPa
Compression+Torsion
σ= -2.4 MPa, τ=1.1 MPa
ε12=
0.80%
0.76%
0.71%
ε12=
2.86%
2.42%
1
2
3
4
Log(Time) (Second)


Same Specimen
110°C
Pure Torsion
σ = 0, τ = 0.9MPa
ε12=5.16%
ε12=3.87%
Tension+Torsion
σ = 1.5MPa, τ = 0.9MPa
ε12=2.40%
ε12=1.08%
0.80%
0.72%
Compression+Torsion
σ = −1.5MPa, τ = 0.9MPa
Log(Shear Creep Compliance) (1/MPa)
Log(Time) (Second)
-1.0
-1.2
-1.4
-1.6
-1.8
-2.0
-2.2
-2.4
0
1
2
3
4


50°C
σ=6.3 MPa, τ=1.8 MPa
σ=–6.3 MPa, τ=1.8 MPa
Abs(Axial Strain) (%)
Log(Time) (Second)
0
1
2
3
4
1
2
3
4

Coupling Between

Volumetric and Shear Response

as Based on an "Activation" Rate Model

$$\dot{\gamma}_n^{\pm}(\tau,\sigma_{ii}) = \pm A_n \exp\{-\frac{1}{RT}[\Delta E_n^* - |v_n^*\tau| - \sigma_{ii}\Omega_n]\}$$

Pool size

$$\dot{\gamma}_n^{\pm}(\tau,\sigma) = \pm A_n \exp\{-\frac{\Delta E_n^* - \sigma_{ii}\Omega_n}{RT}\} \cdot \exp\{\frac{|v_n^*(\tau)\cdot\tau|}{RT}\}$$

$$\dot{\gamma}_n = \dot{\gamma}_n^+ + \dot{\gamma}_n^- \doteq 2A_n \exp\{-\frac{\Delta E_n^* - \sigma_{ii}\Omega_n}{RT}\} \cdot \sinh\{\frac{|v_n^*(\tau)\cdot\tau|}{RT}\}$$

volumetric contribution **shear contribution**

$$\dot{\gamma} = \Sigma\dot{\gamma}_n \doteq \sum_n 2A_n \exp\{-\frac{\Delta E_n^* - \sigma_{ii}\Omega_n}{RT}\} \cdot \sinh\{\frac{|v_n^*(\tau)\cdot\tau|}{RT}\}$$

Static and Viscoelastic Testing/Modeling of LaRC SI

Tom Gates

January 4, 1996

Objectives:

- Measure effects of :
  1) Molecular Weight
  2) Cross-link Density

on the static and viscoelastic properties of LaRC SI

- Develop analytical models to account for these effects
  Elastic constants
  Elastic/plastic constants
  Fracture/strength
  Viscoelastic constants, physical aging

Static Properties: RT to (T_g - 15°C)

Elastic

Youngs Modulus (E), *CTE*

Poissons ratio (ν)

Shear Modulus $\left(G = \dfrac{E}{2(1+\nu)}\right)$

Plastic

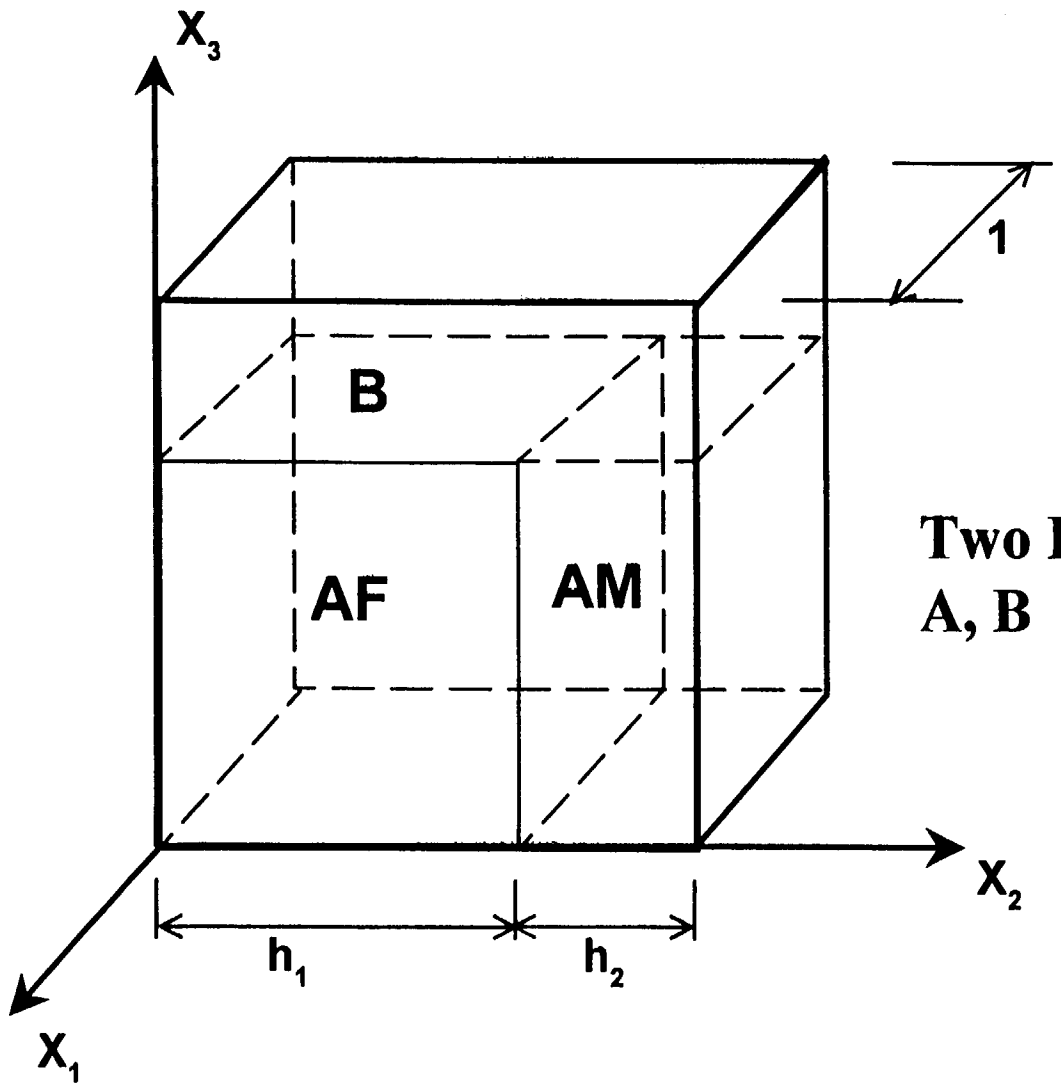
$$d\varepsilon_{ij}^{p} = d\lambda \frac{\partial J}{\partial \sigma_{ij}}$$

$$J = \frac{1}{3}\left[r_{11}(\sigma_{11})^2 + (\sigma_{22})^2 + 2r_{12}\sigma_{11}\sigma_{22} + 2r_{66}(\sigma_{12})^2\right]$$

Effective Stress $\quad \bar{\sigma} = \sqrt{3J}$

Effective Plastic Strain $\quad \bar{\varepsilon}^{p} = \beta(\bar{\sigma})^{\alpha}$

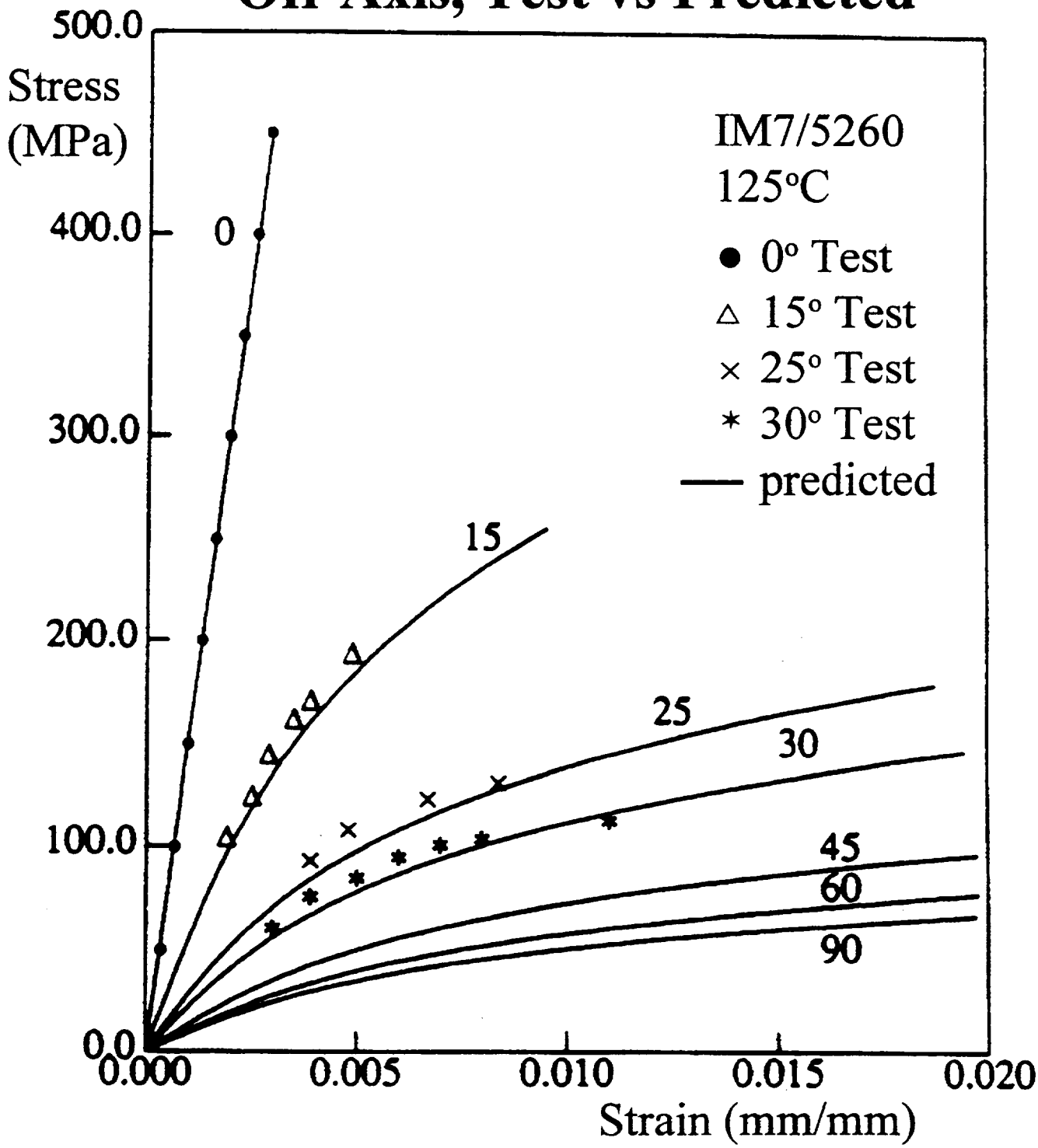
Geometry of Unit Cell



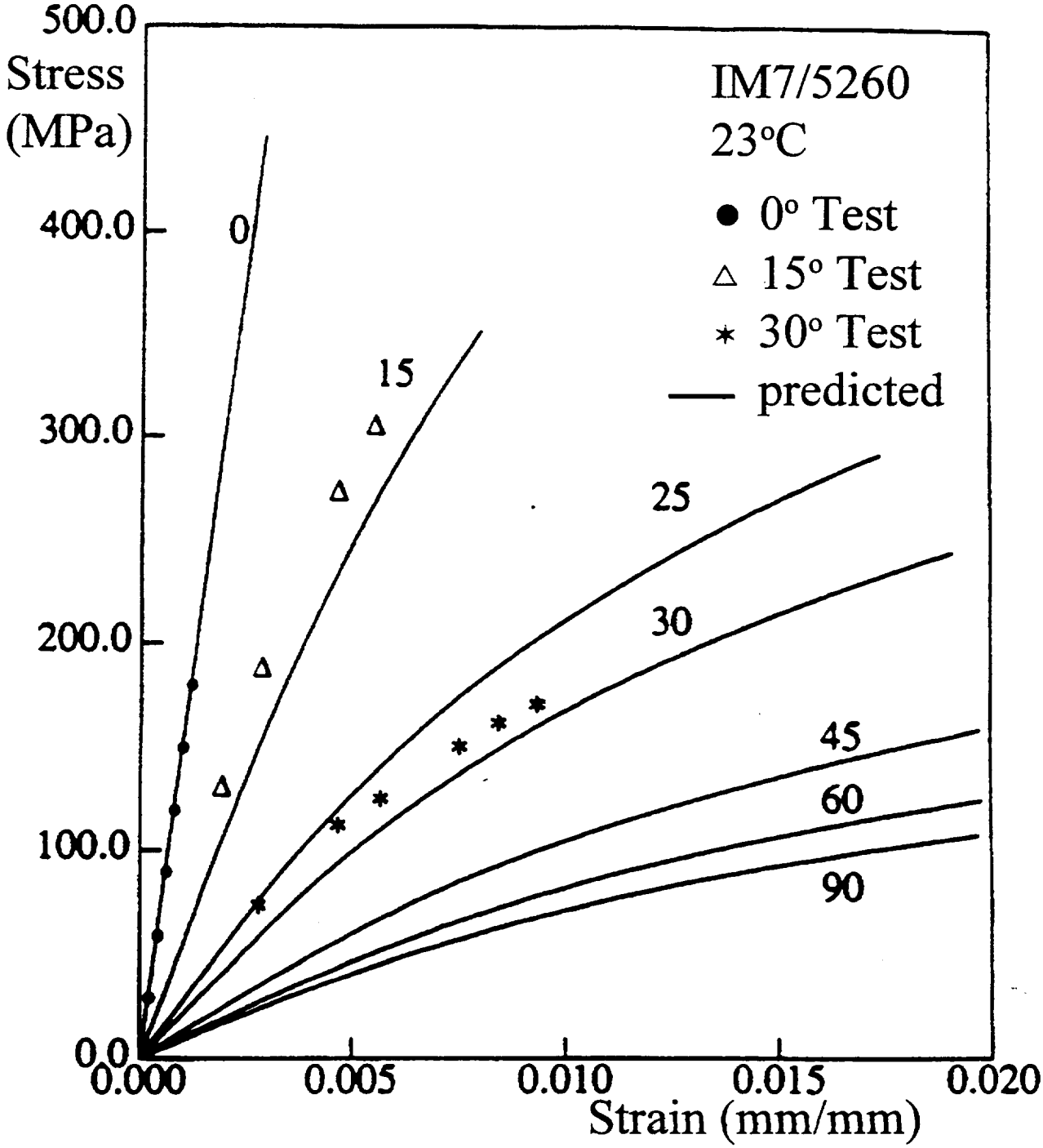
F=Fiber
M=Matrix

Two Regions:
A, B

Micro-Model
Off-Axis, Test vs Predicted



Micro-Model
Off-Axis, Test vs Predicted



Fracture/Strength RT to (T_g-15°C)

- Edge Notched tensile tests
- Fracture surface morphology

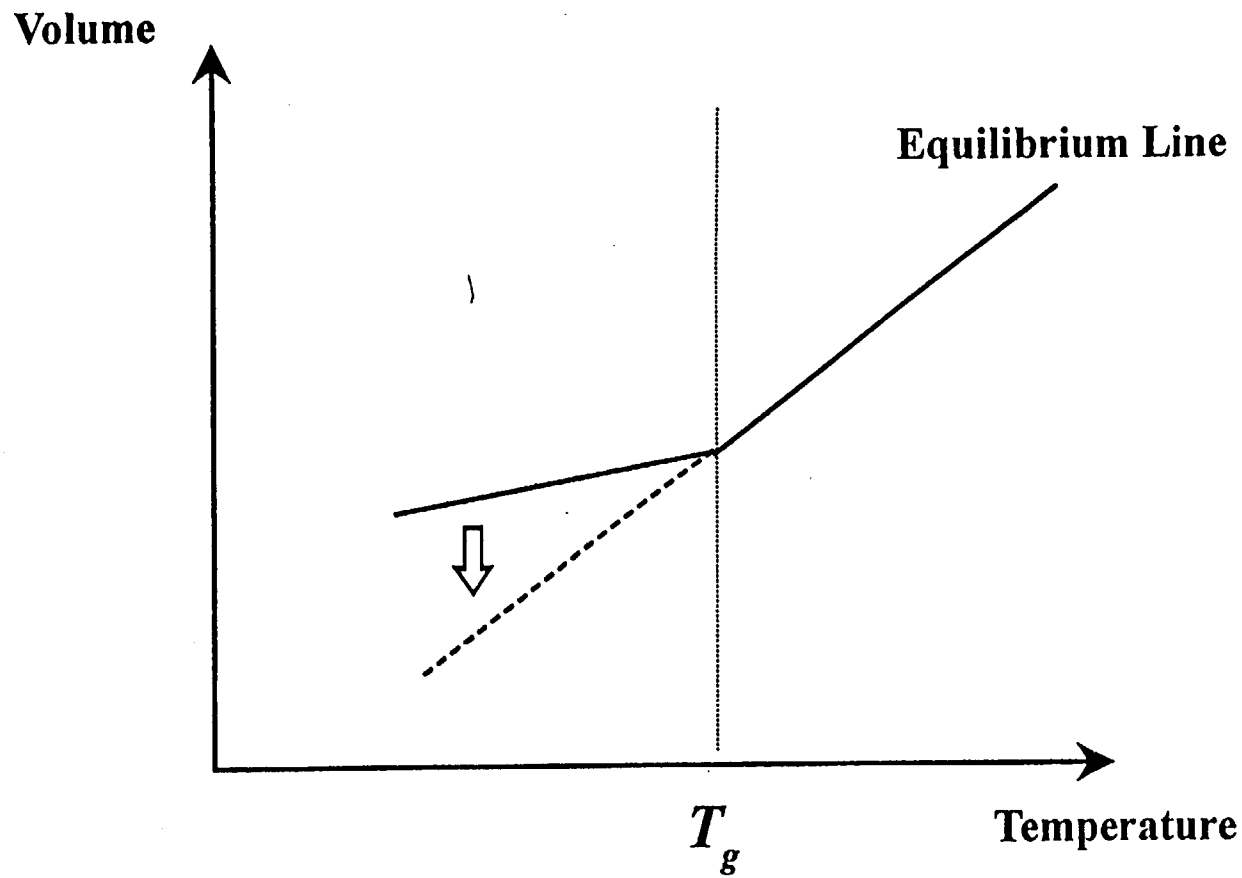
Viscoelasticity, Physical Aging (T_g-15°,20°,25°C)

$$\varepsilon(t) = \int_{-\infty}^{t} S(t-\tau)\frac{d\sigma(\tau)}{d\tau}d\tau$$

Compliance $S_{ij}(t) = S_o e^{(\lambda/\ \tau)^{\beta}}$

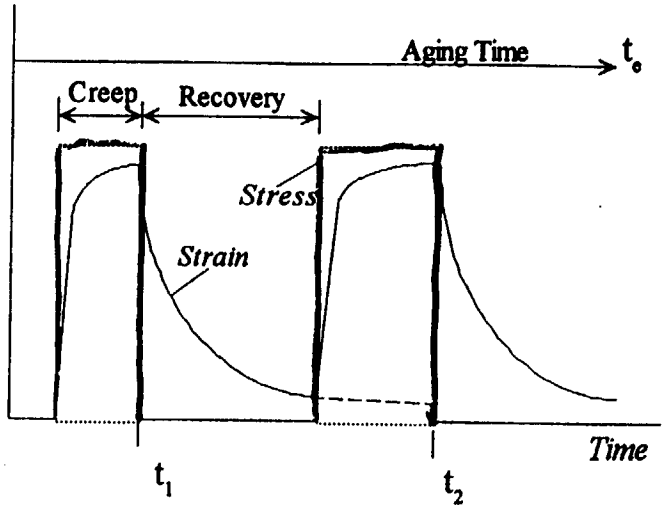
Effective Time $d\lambda = a_{t_e}(t)dt$

Free Volume Evolution During Aging



TheEffects of Physical Aging on Creep Compliance

- **Sequenced creep/recovery**

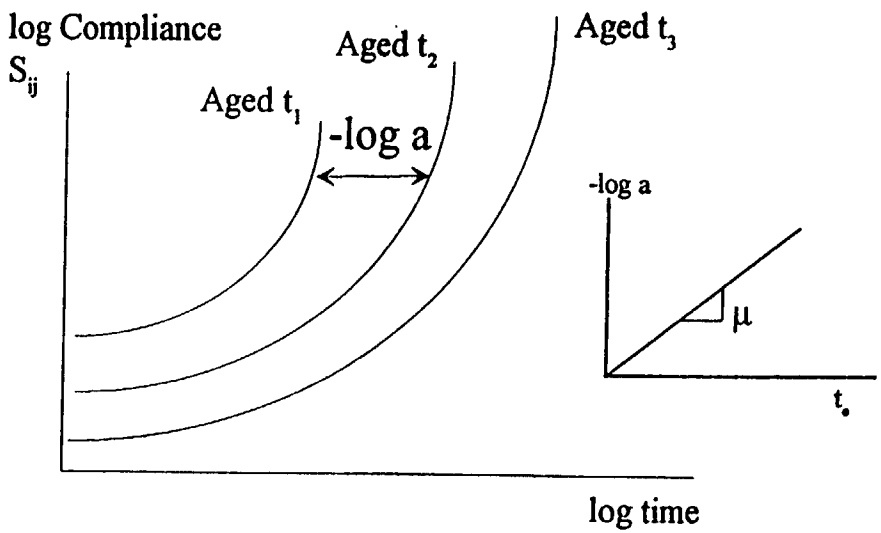


For each sequence $\dfrac{creep\ time}{aging\ time} = \dfrac{1}{10}$

- **Measure compliance shifts and shift rates due to aging**

$$\text{aging shift factor} \equiv -\log a$$

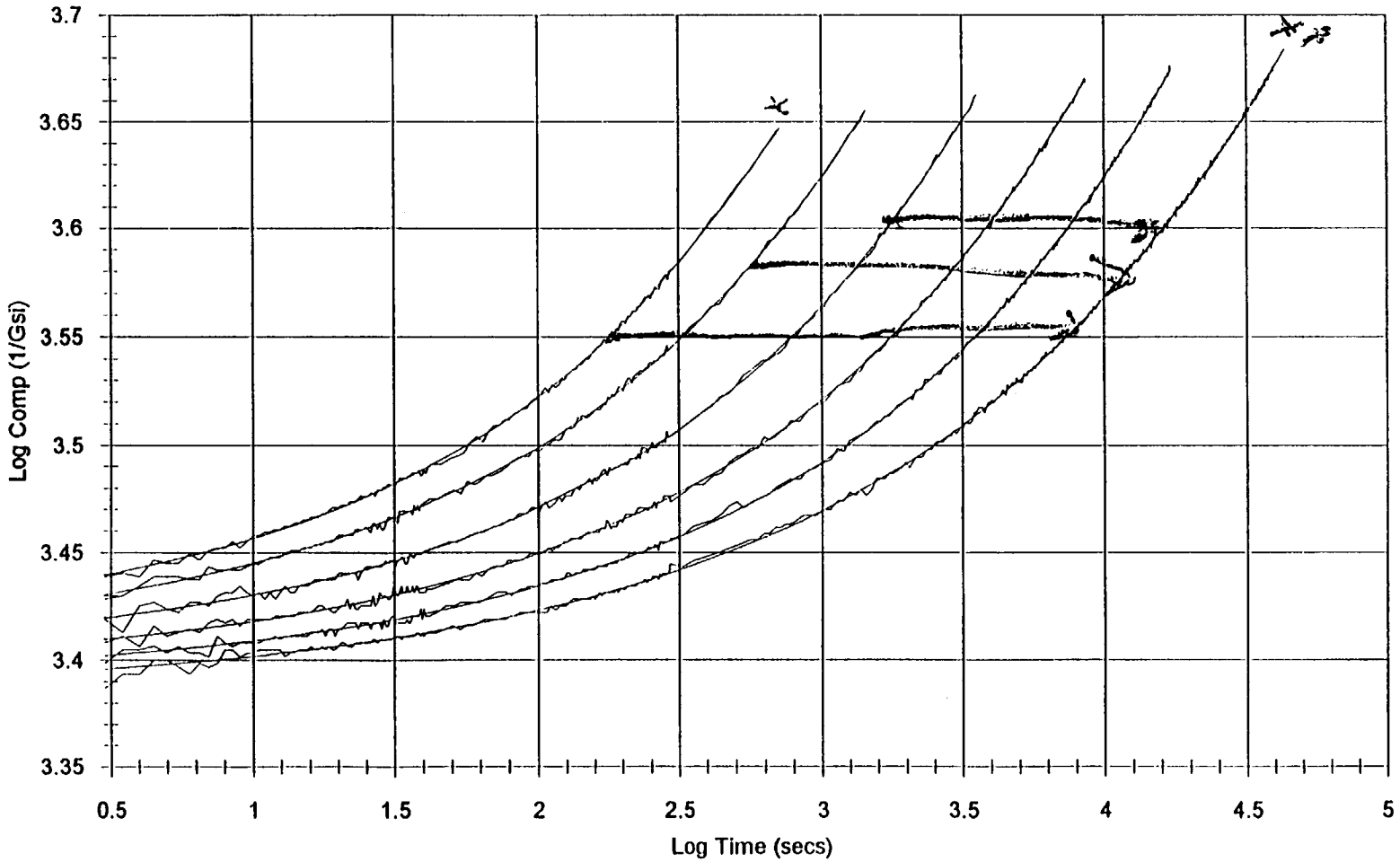
$$\text{aging shift rate} \equiv \mu = \frac{d\log(a_{te})}{d\log(t_e)}$$



K3B-Resin Creep 8-14

Log Compliance vs Log Time

Resin Specimen 72-3 Test Temperature 215C Stress 387.6 Psi



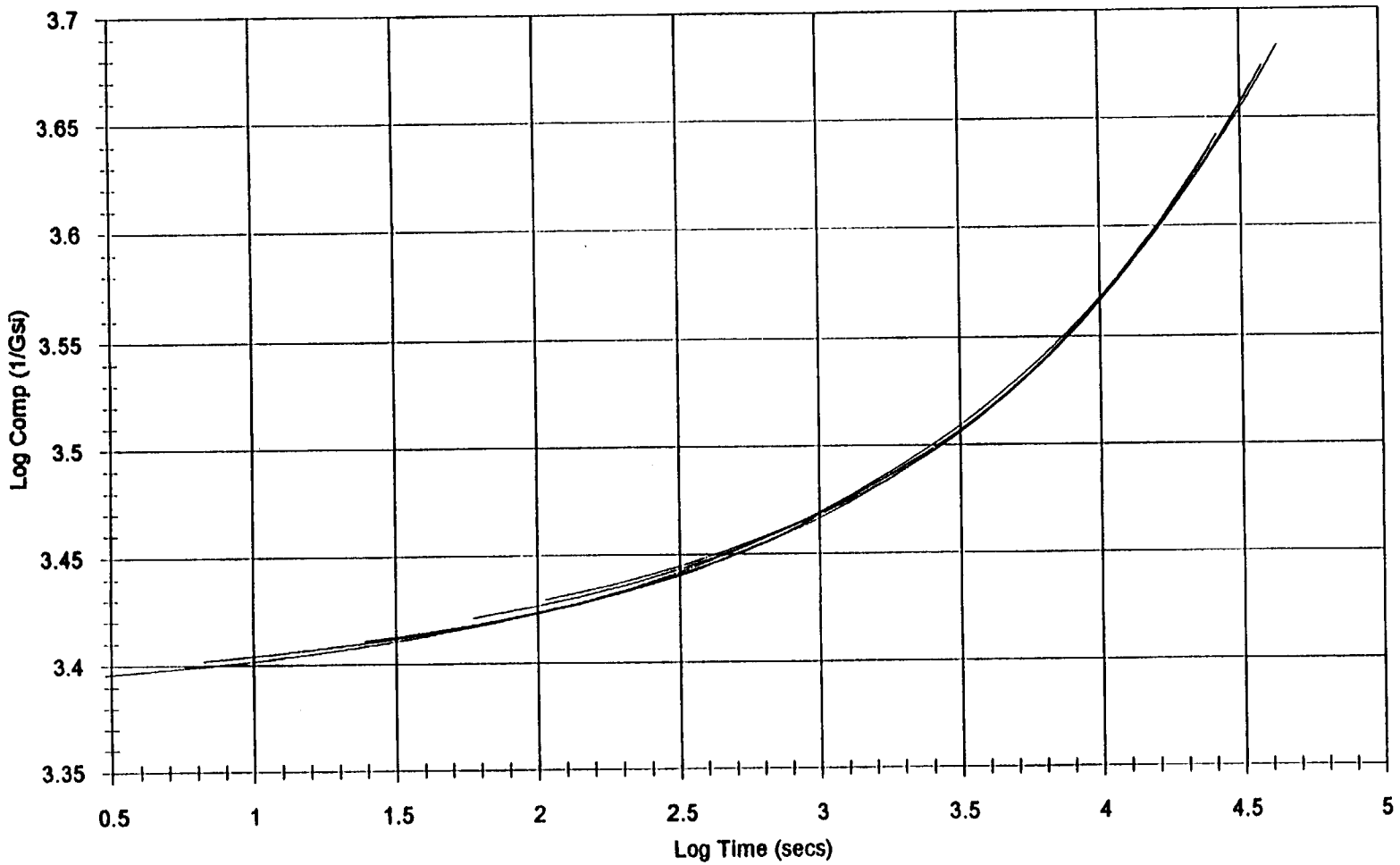
* $t_c = 2\,hr$

** $t_c = 96\,hr.$

K3B Resin Creep 8-14

Log Compliance vs Log Time

Resin Specimen 72-3 Test Temperature 215C Stress 387.6 Psi



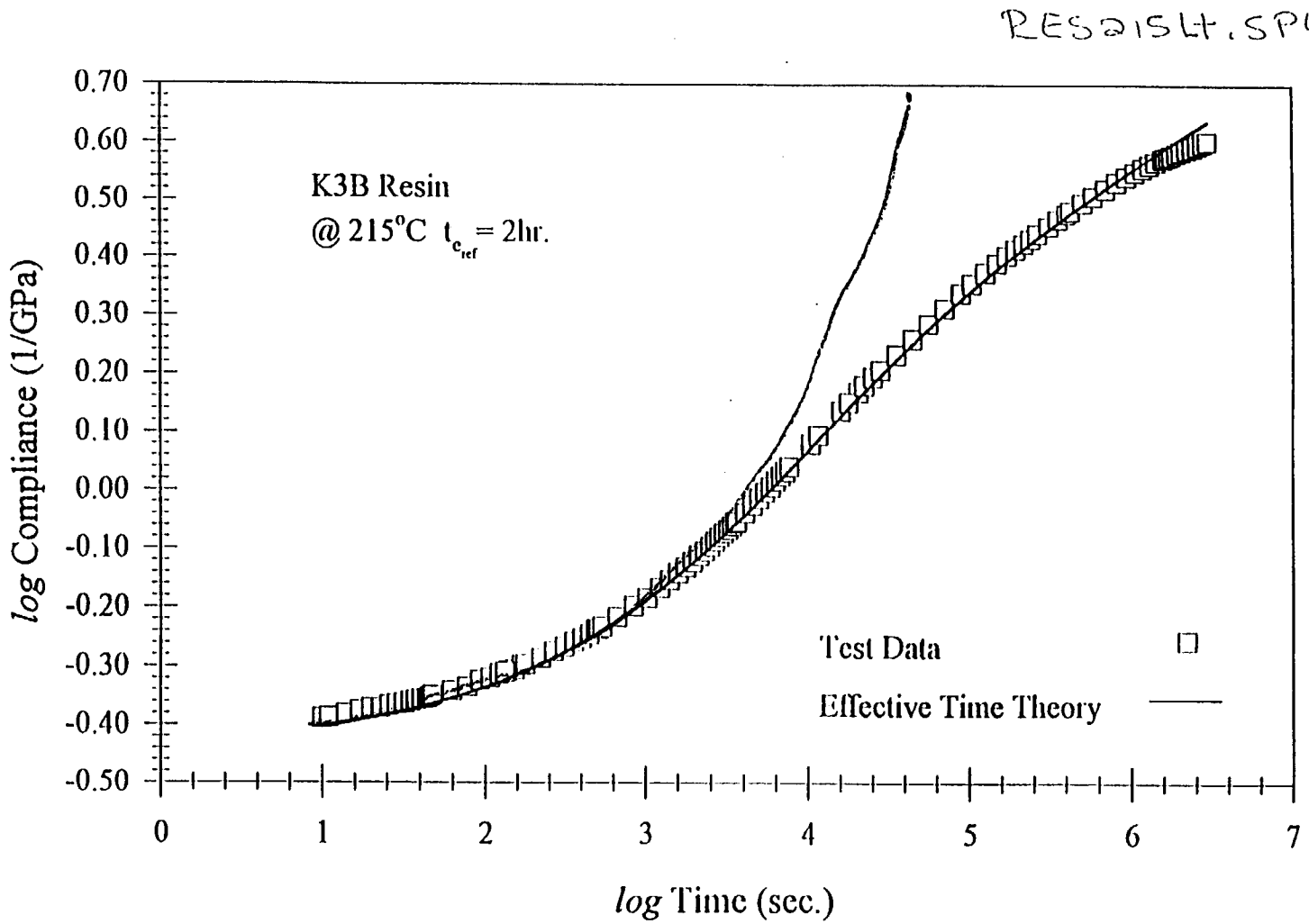


Figure XX: Long term 215°C resin data versus effective time theory prediction.

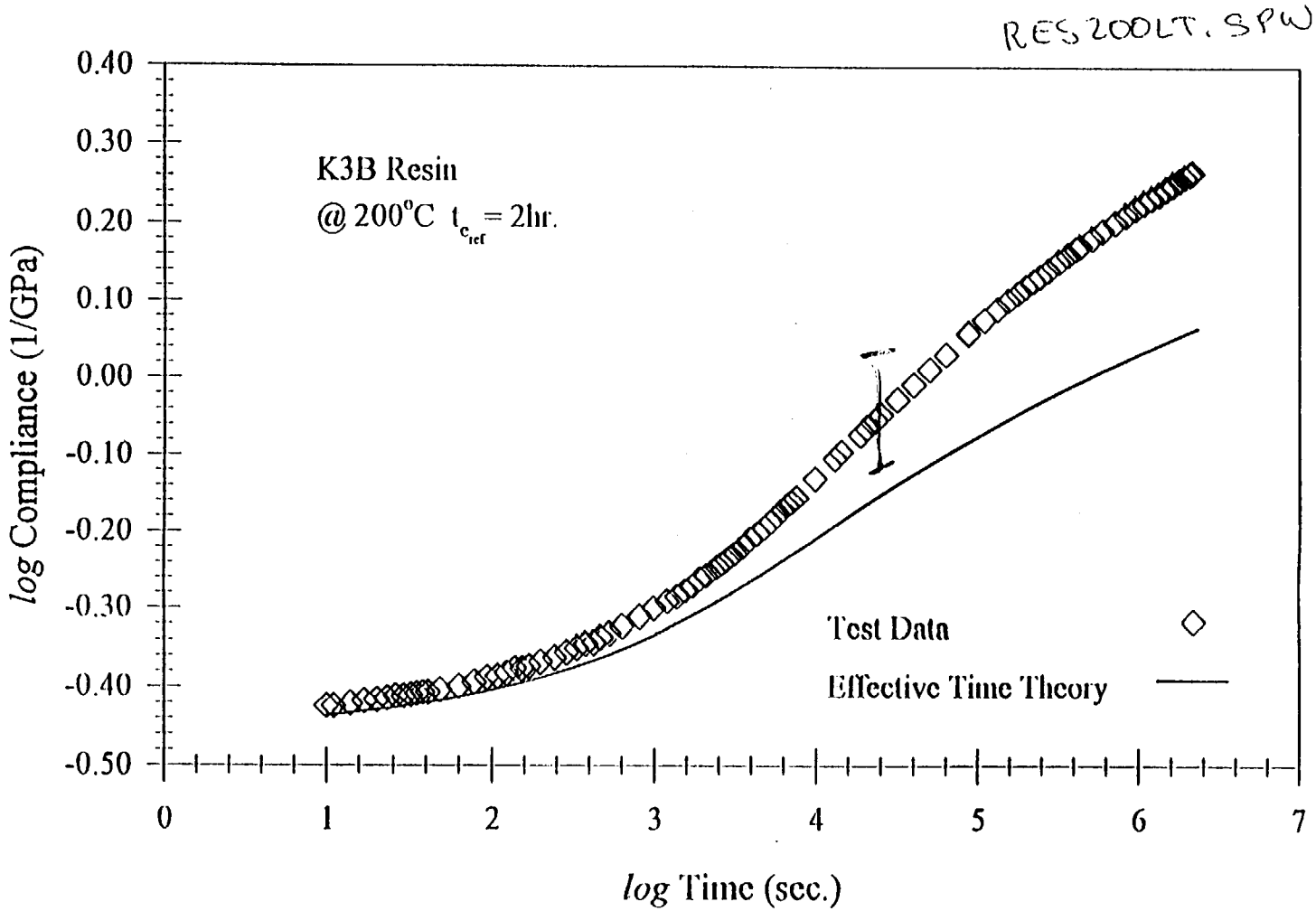


Figure XX: Long term 200°C resin data versus effective time theory prediction.

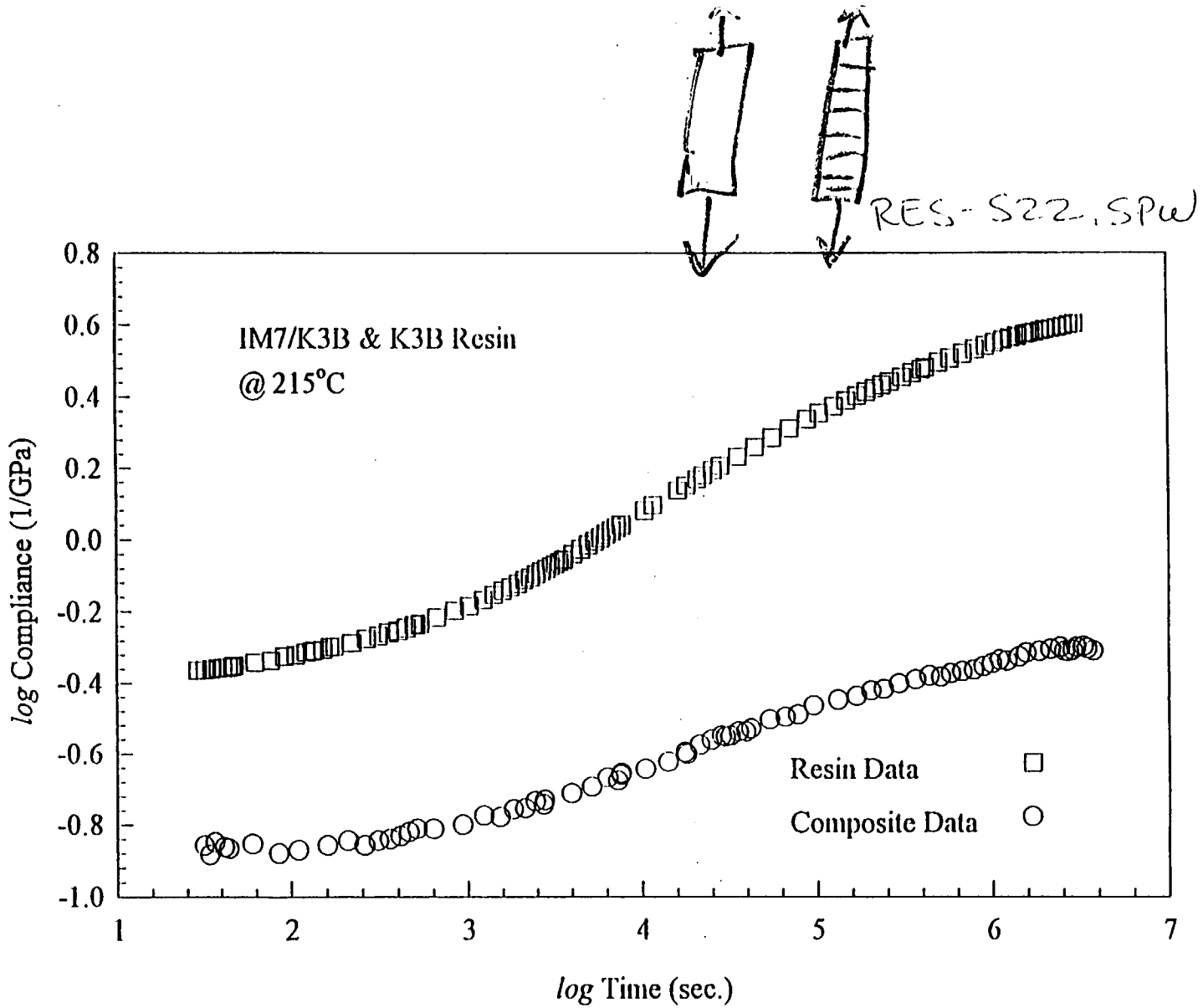


Figure: Comparison between resin and composite long term data at 215°C.

Computational Matl's. Related Issues

- Constituent Stiffness Properties $\not\Rightarrow$ Composite Properties
- Recovered Stiffness Properties $\not\Rightarrow$ Constituent Properties
- Can evaluate relative property differences between matl's.

- Unexplored material properties may correlate
  eg. Strength, CTE, Interface, ?
- Alternative constitutive relations may be required
  Need to expand beyond use of properties from macro level materials testing

REPORT DOCUMENTATION PAGE

Form Approved
OMB No. 0704-0188

Public reporting burden for this collection of information is estimated to average 1 hour per response, including the time for reviewing instructions, searching existing data sources, gathering and maintaining the data needed, and completing and reviewing the collection of information. Send comments regarding this burden estimate or any other aspect of this collection of information, including suggestions for reducing this burden, to Washington Headquarters Services, Directorate for Information Operations and Reports, 1215 Jefferson Davis Highway, Suite 1204, Arlington, VA 22202-4302, and to the Office of Management and Budget, Paperwork Reduction Project (0704-0188), Washington, DC 20503.

1. AGENCY USE ONLY (*Leave blank*)	2. REPORT DATE	3. REPORT TYPE AND DATES COVERED
	November 1996	Conference Publication

4. TITLE AND SUBTITLE
Computational Materials Research

5. FUNDING NUMBERS
WV 505-63-50-18

6. AUTHOR(S)
Jeffrey A. Hinkley and Thomas S. Gates, Editors

7. PERFORMING ORGANIZATION NAME(S) AND ADDRESS(ES)
NASA Langley Research Center
Hampton, VA 23681-0001

8. PERFORMING ORGANIZATION REPORT NUMBER

9. SPONSORING / MONITORING AGENCY NAME(S) AND ADDRESS(ES)
National Aeronautics and Space Administration
Washington, DC 20546-0001

10. SPONSORING / MONITORING AGENCY REPORT NUMBER
NASA CP-10190

11. SUPPLEMENTARY NOTES
Proceedings of Workshop held January 4-5, 1996, at The College of William and Mary

12a. DISTRIBUTION / AVAILABILITY STATEMENT
Unclassified - Unlimited
Subject Category 27

12b. DISTRIBUTION CODE

13. ABSTRACT (*Maximum 200 words*)

Computational Materials aims to model and predict thermodynamic, mechanical, and transport properties of polymer matrix composites. This workshop, the second coordinated by NASA Langley, reports progress in measurements and modeling at a number of length scales: atomic, molecular, nano, and continuum. Assembled here are presentations on quantum calculations for force field development, molecular mechanics of interfaces, molecular weight effects on mechanical properties, molecular dynamics applied to poling of polymers for electrets, Monte Carlo simulation of aromatic thermoplastics, thermal pressure coefficients of liquids, ultrasonic elastic constants, group additivity predictions, bulk consitutive models, and viscoplasticity characterization.

14. SUBJECT TERMS	15. NUMBER OF PAGES
Computational Chemistry, Molecular Mechanics, Monte Carlo Simulation, Constitutive modeling.	253
	16. PRICE CODE: A12

17. SECURITY CLASSIFICATION OF REPORT	18. SECURITY CLASSIFICATION OF THIS PAGE	19. SECURITY CLASSIFICATION OF ABSTRACT	20. LIMITATION OF ABSTRACT
Unclassifed	Unclassified		